

REFERENCE ONLY

UNIVERSITY OF LONDON THESIS

Degree phd

Year 2007

Name of Author HELEN EVELYN
MARIE
LAW

COPYRIGHT

This is a thesis accepted for a Higher Degree of the University of London. It is an unpublished typescript and the copyright is held by the author. All persons consulting the thesis must read and abide by the Copyright Declaration below.

COPYRIGHT DECLARATION

I recognise that the copyright of the above-described thesis rests with the author and that no quotation from it or information derived from it may be published without the prior written consent of the author.

LOAN

Theses may not be lent to individuals, but the University Library may lend a copy to approved libraries within the United Kingdom, for consultation solely on the premises of those libraries. Application should be made to: The Theses Section, University of London Library, Senate House, Malet Street, London WC1E 7HU.

REPRODUCTION

University of London theses may not be reproduced without explicit written permission from the University of London Library. Enquiries should be addressed to the Theses Section of the Library. Regulations concerning reproduction vary according to the date of acceptance of the thesis and are listed below as guidelines.

- A. Before 1962. Permission granted only upon the prior written consent of the author. (The University Library will provide addresses where possible).
- B. 1962 - 1974. In many cases the author has agreed to permit copying upon completion of a Copyright Declaration.
- C. 1975 - 1988. Most theses may be copied upon completion of a Copyright Declaration.
- D. 1989 onwards. Most theses may be copied.

This thesis comes within category D.

This copy has been deposited in the Library of _____

This copy has been deposited in the University of London Library, Senate House, Malet Street, London WC1E 7HU.

Tools for Analysis and Evaluation of Biocatalytic Processes

Helen Evelyn Marie Law MEng (Hons) AMIChemE

A thesis submitted for the degree of
Doctor of Philosophy
to the University of London

Department of Biochemical Engineering
University College London
Torrington Place
London
WC1E 7JE
UK

UMI Number: U593057

All rights reserved

INFORMATION TO ALL USERS

The quality of this reproduction is dependent upon the quality of the copy submitted.

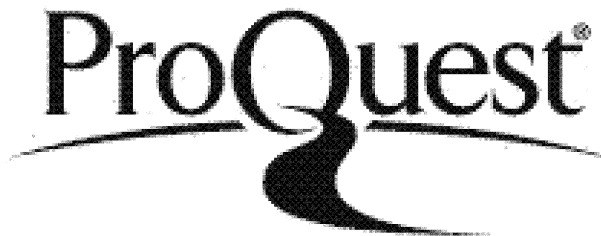
In the unlikely event that the author did not send a complete manuscript and there are missing pages, these will be noted. Also, if material had to be removed, a note will indicate the deletion.



UMI U593057

Published by ProQuest LLC 2013. Copyright in the Dissertation held by the Author.
Microform Edition © ProQuest LLC.

All rights reserved. This work is protected against
unauthorized copying under Title 17, United States Code.



ProQuest LLC
789 East Eisenhower Parkway
P.O. Box 1346
Ann Arbor, MI 48106-1346

ABSTRACT

Recently interest in biocatalysis, the use of enzymes as catalysts, has been growing. This is due in part to the ability to achieve new and interesting chemistry, but also more sustainable, milder, aqueous processes producing less waste. With these advantages though, come new process bottlenecks. Many methods of overcoming such disadvantages have been proposed. However, key to the designer is the ability to discriminate between them at an early stage. To date several methods of early identification of bioprocess bottlenecks have been presented, though none of these has enabled the easy identification of the biocatalyst requirement in the reactor with regard to integrating upstream and downstream requirements. To this end a tool by which biocatalytic processes can be analysed and evaluated, based in part on regime analysis has been presented. The method identifies biocatalyst concentrations at which limitations that control chosen process metrics become dominating. The tool has been demonstrated by the use of a model system, the biocatalytic production of S,S-ethylenediamine-N,N'-disuccinic acid by two enzymes, EDMSase and EDDSase. The reaction is characterised by fumarate inhibition, an exotherm, competition for fumarate not least by the two half reactions, equilibria close to unity and currently an unproductive wild type fermentation. Key bottlenecks were determined to be a severe limitation by the enzyme catalysing the first step, a fumarase limitation and an equilibrium limitation. Proposal of metric hurdles enabled analysis of the dominating regimes and led to determination of the feasible operating region at 232 g.l⁻¹ fumarate, 30 g.l⁻¹ ethylenediamine, 900 g_{dcw}.l⁻¹ EDDSase and 300 g_{dcw}.l⁻¹ EDMSase, enzyme concentrations unachievable by current methods. Possible processes and research to overcome these limitations were proposed and analysed for their effect on the metrics indicating that in the absence of fumarase, use of *in-situ* product removal would improve process yield 2-fold and product concentration 3-fold.

ACKNOWLEDGEMENTS

First of all I would like to thank my supervisor Prof. John M Woodley for all his support, encouragement, advice and inspiration.

I would also like to gratefully acknowledge the grants provided to me by the BBSRC, the SCI and the UCL Graduate School. Furthermore I would like to thank John Ward, Ian Fotheringham, Nick Shaw and Paul Dalby for stimulating discussions and gratefully received help.

I have had the privilege of working with many people over the course of my project, in particular Bing Chen, Al Sayar, Martina Micheletti, Preben Krabben, Colin Jacques, Chris Baldwin, Sarah Fish, Christine Ingram, Clive Whitcher, Ian Buchanan and Billy Doyle. I would also like to thank my colleagues throughout the Department for their friendship not least Supti Sarkar, Brenda Parker, Claudia Ferreira-Torres, Nigel Jackson and the whole of the Colonnades office.

I would like to thank my family for their support, both emotional and financial and apologise to my sister Maggie for her dedication being usurped. I would also like to thank my friends, notably the Greenacre Girls and Dani for their confidence in me. Finally, last but far from least I would like to thank Declan for his boundless patience, encouragement and unerring support though the rough patches.

**Dedicated to the memory of my Grandmother,
Evelyn May (Babs) Emmerson (1920 – 2006)
who never got to see this finished.**

TABLE OF CONTENTS

Abstract	2
Acknowledgements	3
Table of Contents	5
List of Figures	10
List of Tables	15
Notation	17
1 Introduction	19
1.1 Biocatalysis	19
1.1.1 Biocatalytic Process Bottlenecks.....	20
1.2 Process Analysis.....	21
1.2.1 Knowledge Accumulation.....	23
1.2.2 Methods of Acquiring Process Knowledge	25
1.2.2.1 Experiment	25
1.2.2.2 Modelling.....	25
1.3 Bottleneck Identification	34
1.3.1 Sensitivity Analysis	35
1.3.2 Blackman Kinetic Analysis	35
1.3.3 Regime Analysis	36
1.4 Process Evaluation	38
1.5 Conclusion	40
2 Aims	41
2.1 Strategy and Scope	41
3 Model System	43
3.1 Biodegradability	46
3.2 Routes to the Production of S,S-EDDS	48
3.2.1 Synthetic Pathways to S,S-EDDS	48
3.2.1.1 Ramsey, Downey and Kerzerian Route.....	48
3.2.1.2 Neal and Rose Route	48
3.2.2 Biocatalytic Routes to S,S-EDDS.....	50

3.2.2.1	Secondary Metabolite Route	50
3.2.2.2	EDDS Lyase Route	50
3.3	Choice of Process Route	55
3.3.1	Reaction Bottlenecks and Strategies to Overcome Them	55
3.3.2	Possible Downstream Processing Routes.....	59
3.4	Reactant Properties	61
3.4.1	ED	61
3.4.2	Fumarate	61
3.4.3	EDMS	61
3.5	Choice of S,S-EDDS as a Model Product.....	63
3.6	Conclusion	64
4	Biocatalyst Production	65
4.1	Introduction	65
4.2	Methods.....	65
4.2.1	Analytical Methods.....	65
4.2.1.1	Spectrophotometric Analysis of Cell Concentration	65
4.2.1.2	HPLC analysis.....	66
4.2.1.3	Glucose Assay	67
4.2.1.4	Glycerol Assay	68
4.2.1.5	Ammonium Ion Assay.....	69
4.2.1.6	Bradford Assay for Free Protein	69
4.2.2	Biocatalyst Production	69
4.2.2.1	Initial Isolation and Characterisation	69
4.2.2.2	Preparation of Master Stocks	70
4.2.2.3	Shake Flask Fermentation.....	71
4.2.3	Enzymatic Assays.....	73
4.2.3.1	Enzyme Production	73
4.2.3.2	Typical Reaction.....	74
4.2.3.3	EDMSase	75
4.2.3.4	Kinetics	76
4.2.3.5	Equilibrium Position.....	76
4.2.4	Chemical Reaction to EDMS.....	76
4.2.4.1	Temperature Dependence of EDMS Chemical Reaction	76
4.2.4.2	Determination of EDMS Chemical Reaction Constants	77
4.2.5	Solubility	77

4.3	Results.....	79
4.3.1	Biocatalyst Production	79
4.3.1.1	Strain Selection	79
4.3.1.2	Media Selection.....	82
4.3.1.3	Growth Characteristics	85
4.3.2	Reaction Characterisation.....	87
4.3.2.1	Reactant and Product Properties.....	87
4.3.2.2	Side Reactions	87
4.3.2.3	Reaction System	91
4.3.2.4	Enzymatic Properties.....	94
4.4	Discussion	102
4.4.1	Increasing the Cell Titre	102
4.4.1.1	Selection of Strains	102
4.4.1.2	Impact of Medium Composition on EDDSase Concentration	103
4.4.2	Defining the Reaction System.....	106
4.4.2.1	Competition for Reactant.....	107
4.4.2.2	A Further Side Reaction	108
4.4.2.3	EDMSase	108
4.4.2.4	Characterisation of EDDSase.....	109
4.5	Conclusions	111
5	Process Modelling	112
5.1	Models	114
5.1.1	Fumarase Kinetic Model	116
5.1.2	EDMSase Kinetic Model	119
5.1.3	EDDSase Kinetic Model.....	121
5.1.4	EDMS Chemical Kinetic Model	123
5.1.5	Energy Balance	123
5.1.5.1	Rates as a Function of Temperature	124
5.1.6	Overall Mass Balance	126
5.2	Methods.....	128
5.2.1	Experimental Determination of Kinetics.....	128
5.2.2	Determination of Model Constants	129
5.2.3	Component Model Testing	130
5.2.4	Validation.....	130
5.3	Results.....	131
5.3.1	Parameter Fitting	131

5.3.1.1	Fumarase Reaction	131
5.3.1.2	Fumarase Dependence on Temperature	134
5.3.1.3	EDDSase Reaction	136
5.3.1.4	EDDSase Dependence on Temperature	138
5.3.1.5	EDMSase Reaction	140
5.3.1.6	EDMSase Dependence on Temperature	142
5.3.1.7	EDMS Chemical Reaction	142
5.3.1.8	Temperature dependence of EDMS Chemical Kinetics	143
5.3.2	Integration and Component Testing	145
5.3.3	Validation	146
5.4	Discussion	149
5.4.1	Reaction Models	149
5.4.1.1	Error	151
5.4.1.2	Fumarase	153
5.4.1.3	EDMSase	154
5.4.1.4	EDDSase	155
5.4.2	Energy Balance	156
5.4.3	Overall Model	156
5.5	Conclusion	157
6	Process Analysis and Evaluation	158
6.1	Introduction	158
6.2	Bottleneck Identification	160
6.2.1	Identification of Process Limitations	160
6.2.2	Process Metrics	165
6.2.3	Effect of Increasing Catalyst Concentration on Process Metrics	167
6.3	Sensitivity Analysis	171
6.4	Process Evaluation	181
6.4.1	The Ideal Batch Process	181
6.4.2	Process Alternatives	186
6.5	Discussion	196
6.5.1	Metrics	196
6.5.2	Identification of Limiting regimes	197
6.5.2.1	Sensitivity Analyses	197
6.5.3	Windows of Operation can Guide Possible Process Routes	198
6.5.3.1	The Ideal Batch Process	199

6.5.3.2	Process Routes	201
6.6	Conclusion	203
7	Conclusions	204
8	Future Work.....	206
9	References	208
10	Appendices	223
10.1	Numerical Methods for Solution of ODEs.....	223
10.2	Determination of Errors	226
10.3	NCIMB Characterisation Report.....	227
10.4	X ² Goodness of Fit Test	231
10.5	Calculation of Maximum Heat Transfer Area.....	232
10.6	Sensitivity Analysis Programs	234
10.6.1	EDDSase Isothermal and Adiabatic Models.....	234
10.6.1.1	Constants	234
10.6.1.2	Isothermal Model.....	235
10.6.1.3	Adiabatic Model.....	236
10.6.2	EDDSase-Process Variable-Metric Surfaces	238
10.6.3	Window Construction	239

LIST OF FIGURES

Figure 1-1 – Generic strategy for the optimisation of integrated biocatalytic processes	24
Figure 1-2 – General reaction schematic	27
Figure 1-3 – Enzymatic reaction scheme for a unireactant reaction	28
Figure 1-4 – Blackman kinetics	37
Figure 2-1 – Schematic describing a generic method of process development.....	42
Figure 3-1 – Structure of Ethylenediaminetetraacetic acid (EDTA), a structural isomer of EDDS	45
Figure 3-2 - Hexadentate EDTA complexing with a tetracoordinate metal ion.....	45
Figure 3-3 – Reaction scheme for the production of mixture EDDS, adapted from (Ramsey <i>et al</i> , 1963)	49
Figure 3-4 – Reaction scheme for the synthetic production of S,S-EDDS using the chiral pool	49
Figure 3-5 – S,S-EDDS degradation according to Takahashi <i>et al</i> , 1999 and Witschel and Egli, 1998.....	52
Figure 3-6 – Schematic showing all process routes to S,S-EDDS.....	56
Figure 3-7 – Possible Downstream Processing Route for purification of S,S-EDDS....	60
Figure 4-1 – Reaction schematic for glycerol UV assay	68
Figure 4-2 - Maximum Specific EDDSSase Activity of Varying Strains. Fermentation batch 1, fed on S,S-EDDS as sole carbon source, biocatalyst concentrated by centrifugation (white), fermentation batch 2, fed on S,S-EDDS as sole carbon and nitrogen source, biocatalyst concentrated by centrifugation (grey) and <i>Pseudomonas putida</i> and <i>Chelatococcus asaccharovorans</i> reactions, fed on S,S-EDDS as sole carbon source, biocatalyst concentrated by centrifugation and sonicated to produce a crude enzyme isolate (hatched)	81
Figure 4-3 – Fermentation productivity and Maximum EDDSSase specific activity for <i>Chelatococcus asaccharovorans</i> on various different media.....	84

Figure 4-4 – Typical <i>Chelatococcus asaccharovorans</i> fermentation on EDDS minimal media. S,S-EDDS (g.l ⁻¹) (●), EDMS (g.l ⁻¹) (▲), cell concentration (gdcw.l ⁻¹)(■), carbon dioxide evolution rate (mmol.l ⁻¹ .h ⁻¹) (___), oxygen uptake rate (mmol.l ⁻¹ .h ⁻¹) (- -) and respiratory quotient (-..)	86
Figure 4-5 – <i>Chelatococcus asaccharovorans</i> fermentation on EDDS minimal media that failed to consume EDMS. S,S-EDDS (g.l ⁻¹) (●), EDMS (g.l ⁻¹) (▲), cell concentration (gdcw.l ⁻¹)(■), carbon dioxide evolution rate (mmol.l ⁻¹ .h ⁻¹) (___), oxygen uptake rate (mmol.l ⁻¹ .h ⁻¹) (—) and smoothed respiratory quotient (-..)	86
Figure 4-6 – Solubility of S,S-EDDS (■) and fumaric acid (▲) correlated with solution pH when provided with a large excess of solid	88
Figure 4-7 – Specific activity of EDDSase and Fumarase from <i>Chelatococcus asaccharovorans</i> produced by the same fermentation with two different catalyst formats: where catalyst in the control was concentrated by centrifugation prior to addition to the reaction and Sonicated indicates where the same centrifuged and concentrated catalyst suspension was sonicated and clarified prior to use.	88
Figure 4-8– Inhibition of EDDSase and Fumarase initial rates by increasing concentrations of 2-hydroxy-3-nitropropionate, a known reactant analog inhibitor of fumarase	90
Figure 4-9 – Maximum specific activities of the three main activities found in S,S-EDDS grown <i>Chelatococcus asaccharovorans</i> (white) Fumarase, (grey) EDMSase and (hatched) EDDSase	90
Figure 4-10 – Initial rate of production of EDMS by chemical means. Reaction of ethylenediamine and fumaric acid in aqueous solution with reaction temperature, initial fumaric acid concentration was varied whilst holding initial concentration of ED constant at 6 g.l ⁻¹ .	92
Figure 4-11 – Initial rate of production of EDMS by EDMSase, determined by summing the free concentration of EDMS and a mass balanced concentration of EDMS determined from S,S-EDDS concentration	95
Figure 4-12 - R,S-EDDS peak against typical standards	95
Figure 4-13 – EDDSase activity as a function of reaction temperature and pH	99
Figure 4-14 – EDDSase reaction pH profile	99

Figure 4-15 – Initial EDDSase activity as a function of initial fumarate concentration at varying levels of initial EDMS.....	101
Figure 4-16 –Conversion of fumaric acid to malic acid by fumarase.....	107
Figure 4-17–Conversion of ED and fumaric acid to <i>meso</i> -EDMS.....	108
Figure 4-18 –Conversion of ED and fumaric acid to S-EDMS by EDMSase.....	109
Figure 4-19 - Conversion of EDMS and fumaric acid to EDDS by EDDSase	110
Figure 5-1 - Overall Reaction scheme, showing main reaction to S,S-EDDS in the boxed area	113
Figure 5-2 – Structure of the model used to predict concentration and temperature at time t	115
Figure 5-3 – Fumarase reaction scheme	117
Figure 5-4 – EDMSase Reaction Schematic.....	120
Figure 5-5 – EDDSase reaction schematic	122
Figure 5-6 - Fumarase kinetic parameter determination where (■), represents experimental data, (▲), represents residuals, solid line, represents the fitted model and dotted lines represent the upper and lower confidence intervals.....	132
Figure 5-7 - Polynomial regression of Fumarase maximum specific activity against temperature, line representing fitted polynomial and ■, experimental data.....	135
Figure 5-8– Kinetic fit for EDDSase parameter determination.....	137
Figure 5-9 - Fumarate inhibition of EDDSase at varying initial EDMS concentrations	137
Figure 5-10 – EDDSase maximum rate as a function of reaction temperature (□) Model (■) Experimental data.....	139
Figure 5-11 - Fitting EDMSase forwards reaction kinetic parameters by weighted non-linear least squares regression. Thick lines represent model, points as described by the legend represent experimental data. Faint dotted lines represent the confidence interval in the fitted parameters.....	141
Figure 5-12 – Initial chemical rate of production of EDMS against initial fumarate concentration at constant ED.....	144

Figure 5-13a – Validation of overall kinetic model by comparison of experimental data	147
Figure 5-14b – Validation of overall kinetic model by comparison of experimental data	148
Figure 5-15 – Sensitivity of final EDDS concentration to 2-order of magnitude changes to the model parameters.....	150
Figure 6-1 – Method for identification and assessment of limiting biocatalyst regimes	161
Figure 6-2 – Progress curve using typical <i>Chc asacc</i> fermentation enzyme concentrations and initial conditions used in the typical reaction described in Chapter 4.....	162
Figure 6-3 – Schematic showing EDMSase and fumarase limitations for Figure 6-2.	164
Figure 6-4 – Key limitations to the EDDSase process and their effects on the progress curve	164
Figure 6-5 – Metric-catalyst concentration plot for fumarase and EDMSase at concentrations achievable by fermentation of <i>Chelatococcus asaccharovorans</i> and typical reaction conditions (Chapter 4).....	168
Figure 6-6 – Change in metrics when fumarase concentration is reduced to zero.....	170
Figure 6-7 – Change in metrics when EDMSase is provided to the reaction in large excess in the presence of fumarase	170
Figure 6-8 – Effect of increasing EDMSase on the metrics	172
Figure 6-9 – Effect of increasing fumarase concentration on the metrics	174
Figure 6-10 – Effect of increasing reaction temperature on the metrics.....	176
Figure 6-11 – Effect of increasing <i>meso</i> -EDMS. concentration on the metrics	178
Figure 6-12 – Effect of increasing initial concentrations of ED and fumarate on the metrics.....	180

Figure 6-13 – Operable catalyst concentrations for a reaction run at 30°C at 232 g.l ⁻¹ fumaric acid and 24 g.l ⁻¹ ED. Minimum productivity: 8.3 g.l ⁻¹ h ⁻¹ , Maximum rate: 292 g.l ⁻¹ h ⁻¹ , Minimum purity: 95%, Minimum ee: 99%.	183
Figure 6-14 - Operable reactant concentrations for a reaction run at 30°C at 920 g _{dcw} .l ⁻¹ EDDSase and 330 g _{dcw} .l ⁻¹ EDMSase. Minimum productivity: 8.3 g.l ⁻¹ h ⁻¹ , Maximum rate: 292 g.l ⁻¹ h ⁻¹ , Minimum purity: 95%, Minimum ee: 99%.	183
Figure 6-15 – Windows of operation for an EDDSase process requiring a maximum rate of 15 g.l ⁻¹ .h ⁻¹	185
Figure 6-16 – Windows of operation for an EDDSase process requiring a product concentration of 150 g.l ⁻¹	185
Figure 6-17 – Schematic for the EDMSase and EDDSase catalysed batch bioconversion of ED and Fumaric acid to S,S-EDDS	187
Figure 6-18 – Schematic for the EDMSase and EDDSase catalysed fed-batch bioconversion of ED and Fumaric acid to S,S-EDDS (fumaric acid feed).....	189
Figure 6-19 – Schematic for the EDMSase and EDDSase catalysed fed-batch bioconversion of ED and Fumaric acid to S,S-EDDS (fumaric acid feed) with <i>in-situ</i> product removal.....	191
Figure 6-20 – Schematic for the EDDSase catalysed batch bioconversion of EDMS and fumaric acid to S,S-EDDS with prior production of S-EDMS by chemical or EDMSase catalysed means.....	193
Figure 6-21 – Window of operation for the optimised Fed-batch with ISPR process .	195
Figure 6-22 – Dot plot comparing product concentration and enzyme efficiency for all five possible process flowsheets.....	195

LIST OF TABLES

Table 1-1—Strategies to overcome some common biocatalytic process bottlenecks ...	22
Table 1-2 – Mole balances applicable to popular reactor types.....	33
Table 3-1 – Overall stability constants for some selected EDDS complexes. Sources: 1) (Martell and Smith RM, 1974) 2) (Orama <i>et al</i> , 2002) 3) (Day, 2005).....	47
Table 3-2 - Known EDDSase Reaction Bottlenecks.....	58
Table 3-3 – Physical properties of ethylenediamine. Sources: 1) Beilstein database, substance entry beilstein preferred RN: 107-15-3 Ethane-1,2-diamine. 2) (Cary <i>et al</i> , 1999)	62
Table 3-4 – Fumarate physical properties. Sources: 1) Beilstein database, substance entry beilstein preferred RN 110-17-8 Fumarate. 2) (Syracuse Research Corporation, 2006).....	62
Table 4-1 Optical density- dry cell weight calibration coefficients	66
Table 4-2 – Average retention time for various EDDS related compounds when analysed by HPLC	67
Table 4-3 – Absorbance - concentration calibration coefficients for HPLC analysis of EDDS related compounds	67
Table 4-4 - Media Recipes. Notes: a. (Takahashi <i>et al</i> , 1999), b. Sigma-Aldrich, Poole, Dorset, UK, c. VWR, Poole, Dorset, UK, d. Oxoid, Basingstoke, Hampshire, UK, e. Fluka, Poole, Dorset, UK, f. Octel Corp, Ellesmere Port, Cheshire, UK.....	72
Table 4-5 – Reaction of chemically produced EDMS and fumarate or ED and fumarate with or without the presence of crude enzyme isolate from <i>Chelatococcus asaccharovorans</i>	97
Table 5-1 – EDDS related Thermodynamic Data.....	125
Table 5-2 Reaction stoichiometry for compilation of individual rate equations into an overall model	127
Table 5-3 – Net rates of change of concentration for all species involved in the EDDSase bioconversion.....	127

Table 5-4 – Kinetic parameters with related standard error and 95% confidence interval values	133
Table 6-1 – Variables tested in sensitivity analysis and associated limitations	171
Table 6-2 – Hurdle values and their associated metrics.....	181
Table 6-3 – Process Metrics for possible processes for the EDDSase catalysed bioconversion of ED and fumaric acid to S,S-EDDS	186

NOTATION

Nomenclature	Description	Units
A	Arrhenius parameter	h^{-1}
APCA	Aminopolycarboxylic acid	
C_p	Specific Heat Capacity	$J.mol^{-1}.K^{-1}$
CV	Coefficient of variance	
[D]	Ethylenediamine (ED) concentration	$g.l^{-1}$
[E₁]	EDDSase containing crude enzyme concentration	$g_{dcw}.l^{-1}$
[E₃]	EDMSase containing crude enzyme concentration	$g_{dcw}.l^{-1}$
[E₅]	Fumarase containing crude enzyme concentration	$g_{dcw}.l^{-1}$
df	Degrees of freedom	
E_a	Activation energy	$kJ.mol^{-1}$
EDDS	Ethylenediaminedisuccinic acid	
EDMS	Ethylenediaminemonosuccinic acid	
EDTA	Ethylenediaminetetraacetic acid	
Er	Approximate error for taylor series	
[F]	Fumarate concentration	$g.l^{-1}$
FI	Molar flowrate	$Mol.l^{-1}.h^{-1}$
G	Gibbs free energy	$kJ.mol^{-1}.K^{-1}$
h	Stepsize	
H_{species}	Enthalpy	$kJ.mol^{-1}$
ΔH_{f(soln)}	Heat of formation of solution	$kJ.mol^{-1}$
ΔH_f^θ	Heat of formation	$kJ.mol^{-1}$
ΔH_{RX}	Heat of reaction	$kJ.mol^{-1}$
ΔH_{S(-)}}	Infinitely dilute heat of solution	$kJ.mol^{-1}$
k_{cat}	Specific activity	$g.g_{dcw}^{-1}.h^{-1}$
K_{eq, reaction no}	Equilibrium constant	
K_i	Inhibition constant	
k_{inact}	Inactivation constant	
K_{species, b, reaction no}	Backwards rate constant	
K_{species, f, reaction no}	Forwards rate constant	
Log P	Logarithmic octanol-water partition coefficient	
[M]	<i>Meso</i> -EDMS	$g.l^{-1}$
[MA]	Malic acid	$g.l^{-1}$
N	Molar concentration	M
n	Number of variables	
NTA	Nitriloacetic acid	

Nomenclature	Description	Units
Q	Heat	$\text{kJ}\cdot\text{mol}^{-1}$
[P]	S,S-EDDS	$\text{g}\cdot\text{l}^{-1}$
r	Reaction rate	$\text{g}\cdot\text{l}^{-1}\cdot\text{h}^{-1}$
R	Universal gas constant (8.314)	$\text{J}\cdot\text{mol}^{-1}\cdot\text{K}^{-1}$
[RM]	R-EDMS	$\text{g}\cdot\text{l}^{-1}$
[RP]	R,S-EDDS	$\text{g}\cdot\text{l}^{-1}$
[SM]	S-EDMS	$\text{g}\cdot\text{l}^{-1}$
T	Temperature	K or $^{\circ}\text{C}$
t	Time	h
V	Volume	l
v	Volumetric flowrate	$\text{l}\cdot\text{h}^{-1}$
$V_{b,\text{reaction no}}$	Backwards maximum reaction rate	$\text{mol}\cdot\text{l}^{-1}\cdot\text{h}^{-1}$
$V_{f,\text{reaction no}}$	Forwards maximum reaction rate	$\text{mol}\cdot\text{l}^{-1}\cdot\text{h}^{-1}$
W	Work	kJ
W_s	Shaft work	kJ
\bar{x}	Mean	

Subscripts

0	Initial Condition
1	Reaction ordinate S-EDMS + fumarate to S,S-EDDS
2	Reaction ordinate R-EDMS + fumarate to R,S-EDDS
3	Reaction ordinate Fumarate + ED to S-EDMS
4	Reaction ordinate Fumarate + ED to <i>meso</i> -EDMS
5	Reaction ordinate Fumarate + water to Malate
f	Final Condition
j	Species j subscript
x	Exit Condition subscript

Greek letters

α	Enzymatic dissociation constant
β	Enzymatic dissociation constant
σ	Standard deviation

1 INTRODUCTION

1.1 BIOCATALYSIS

Recently interest in the use of biocatalysis, the process of using enzymes as catalysts for the production of small molecules has been growing, to the extent that over 5% of fine chemical processes now use a biocatalytic or fermentation step (Bachmann, 2003; Schmid *et al*, 2001; Straathof *et al*, 2002). Biocatalysis is typically employed in the fine chemicals industry though some notable exceptions are the production of 1,3-propanediol (Nakamura and Whited, 2003), polylactic acid (Datta *et al*, 2006) and acrylamide (Tremblay, 2001). A key reason for the use of White Biotechnology in fine chemicals is the high value of the products, because at present biocatalytic processes often require much research in order to produce efficient processes. A case in point being the 1,3-propanediol process at Dupont which required intensive research. However, the main reasons why interest in biocatalysis is growing include:

1. The need for sustainable processes. Biocatalytic processes typically operate in aqueous conditions under mild reaction conditions reducing safety hazards and volatile compound use in processing. However, biocatalytic processes have also been shown to reduce process waste, not only by reducing the amount of VOCs used in processing, but also by building specificity and therefore not producing unwanted stereoisomeric products or side products (Meyer *et al*, 1997). Furthermore biocatalytic processes are characterised by specific catalytic activity (both for reactants and for chirality) (McCoy, 2001) and as such can be seen to be both more environmentally and economically sustainable.
2. The increased availability of tools such as recombinant DNA technology and directed evolution (Arnold, 2001; Walsh, 2001) have meant that biocatalytic processes can be employed in more situations as enzymes evolved in nature for the specific use of the host organism. These activities can now be harnessed and improved by 'evolving' enzymes towards industrial processes.

3. The ability to achieve new and interesting chemistry. For example the use of the Baeyer-Villiger monooxygenase cyclohexanone monooxygenase produces a lactone unachievable by current methods of chemical synthesis (Alphand and Furstoss, 1992).
4. The need for alternative renewable feedstocks, such as sugar for the production of bioethanol, glycerol for the non-natural carbohydrate 5-deoxy-5-ethyl-D-xylulose, sucrose for antibiotics, cornstarch for polylactic acid at Cargill Dow and 1,3-propanediol at Dupont as oil stocks decline (Sheldon and van Rantwijk, 2004; Thayer, 2002)

1.1.1 Biocatalytic Process Bottlenecks

Conversely some of the benefits of using an enzymatic catalyst can hinder the efficiency of biocatalytic processes. Milder reaction conditions can be a disadvantage (Faber, 1997), leading processes to be operated within narrow limits to prevent denaturation or slowing of reaction rate and can often mean that condition changes typically associated with Le Chatelier's principle to improve final product titre or specificity cannot be used and correspondingly levels of process control must be high.

Though there are many and varied enzymes available in nature, for each individual process for which a biocatalyst could be used a search is required to find the enzyme with the most appropriate specificity, added to which titres of enzyme in wild type are often very low and though some isolated enzymes are available for purchase typically the catalyst has to be manufactured in house by fermentation (Hirose, 2002). Enzymes commonly require some water to be present so that they can retain their correct conformation and hence activity (Halling, 2002). Reactions carried out in aqueous conditions can complicate downstream processing as a result of low concentrations, high volumes and low solubilities of organic compounds in water (Faber, 1997). Furthermore enzymes are prone to inhibition phenomena by many compounds (Koeller and Wong, 2001), not least the product and/or reactant, resulting in lower reaction

rates and yields. As a result of the adsorption mechanism of enzymes, reaction kinetics are often complex. This often results in process design being undertaken in an empirical manner with a reliance on pilot plant studies to produce effective industrial processes. An inexhaustive list of some of the process engineering strategies that can be used to overcome these bottlenecks can be seen in Table 1-1.

1.2 PROCESS ANALYSIS

Table 1-1 reinforces the notion that there are myriad options available to the process engineer to improve a biocatalytic process. However, many of these process options carry their own specific trade-offs, for example, operating with a two-phase system may mean that mass transfer rates limit reaction rate, so an easy downstream separation may be accompanied by a slower reaction. Immobilisation of enzymes or whole cells often improves the stability of the biocatalyst allowing it to be re-used, reducing costs in the process, but this too is associated with drops in reaction rate resulting from mass transfer limitations. Use of extremophilic enzymes often means that enzymes are stable in conditions more suited to chemical processing such as higher temperatures (thermophiles), high salt concentrations (halophiles) and extremes of pH (acidophiles and alkaliphiles). However, in some situations these are not well characterised, limiting use of recombinant DNA technology, though this is changing (<http://archaea.ucsc.edu/>), due in part to the success of Taq polymerase for PCR (Saiki *et al*, 1988), but also to industrial need for enzymes stable at more extreme conditions. Substrate feeding, often used in situations where the reactant is inhibitory to the biocatalyst can be seen to reduce rate, by introducing a reactant limitation to the reaction. *In-situ* product removal, a useful tool for processes where product is inhibitory to the catalyst and equilibria are unfavourable can be applied in many methods not least; precipitation, adsorption, linked reactions or use of a gas phase. However, key to its implementation is the selection of a method by which product can be removed from solution requiring extensive process research.

Bottleneck	Strategy	Reference
Unproductive fermentation	Recombinant DNA technology	(Lodish <i>et al</i> , 1999)
Expensive fermentation	Immobilisation	(Lalonde and Margolin, 2002)
Enzyme activity low	Directed evolution	(Hibbert <i>et al</i> , 2005; May <i>et al</i> , 2002)
Reactant or Product immiscible with water	2-phase reaction	(Halling, 2002; Wubbolts <i>et al</i> , 1996)
	Ionic fluid	(Roberts and Lye, 2002)
Enzyme has low reaction stability	Immobilisation	(Lalonde and Margolin, 2002)
	Directed evolution	(May <i>et al</i> , 2002)
	Extremophilic enzyme	(Sellek and Chaudhuri, 1999)
Reactant inhibition	Reactant feeding	(Bird <i>et al</i> , 2002; Hilker <i>et al</i> , 2004)
Product inhibition	2-phase reaction	(Halling, 2002; Wubbolts <i>et al</i> , 1996)
	ISPR	(Lye and Woodley, 1999)
	Membrane bioreactor	(Biselli <i>et al</i> , 2002)
Low reactant solubility	Undissolved substrate reaction	(Erbeldinger <i>et al</i> , 1998; Ulijn <i>et al</i> , 2001)
Hydrolytic side reaction	2-phase reaction	(Halling, 2002; Wubbolts <i>et al</i> , 1996)
	Ionic fluid	(Roberts and Lye, 2002)
Equilibrium hinders high yield	Linked reactions	(Carlton, 1992)
	Use of gas phase	(Wubbolts, 2002)
	Extremophilic enzyme	(Sellek and Chaudhuri, 1999)
Side Reactions	Metabolic Engineering	(Nakamura and Whited, 2003; Stephanopoulos <i>et al</i> , 1998)

Table 1-1—Strategies to overcome some common biocatalytic process bottlenecks

Key to the fully optimised process therefore, is that the entire process from upstream of the reaction to final isolation of product via downstream operations is considered when optimising a biocatalytic reaction (Bogle *et al*, 1996; Hoeks *et al*, 1996; Wai and Bogle, 1996). Several authors have proposed methodologies for the integrated optimisation of bioprocesses. This requires, first a process of accumulation of knowledge about a given reaction involving the initial characterisation of reactant, product and enzyme, followed by an investigation into reaction and reactor kinetics (Biselli *et al*, 2002; Lilly and Woodley, 1996). This knowledge can then be used to identify process constraints (Lilly, 1994), evaluate the process options available and therefore guide process selection (Figure 1-1).

1.2.1 Knowledge Accumulation

Initial characterisation of the reaction is necessary covering physical properties of reactants and products such as solubilities, state of matter under reaction conditions, phases involved, standard states, health and safety guidelines and pKa values as these will represent a set of reaction limitations within which all other process limitations must be assessed (Caygill *et al*, 2006; Woodley and Lilly, 1994). Furthermore reaction parameters need to be determined ie temperature, pH and pH change over the course of the reaction (Lilly and Woodley, 1996) to provide a further set of limits within which the enzyme can be characterised in terms of the dependence of catalyst activity, stability and selectivity under process conditions (Biselli *et al*, 2002) and cofactors (Kula, 2002).

The characteristics of the overall reaction system are also required including the deduction of the reaction system pathway (Wouwer and Bogaerts, 2005), identification of transport limitations such as heat generation over the course of reaction or mass transfer between phases and characterisation of the reaction thermodynamics (Tewari, 1990; von Stockar and van der Wielen, 1997). However, though these reaction system characteristics are able to be found experimentally, often

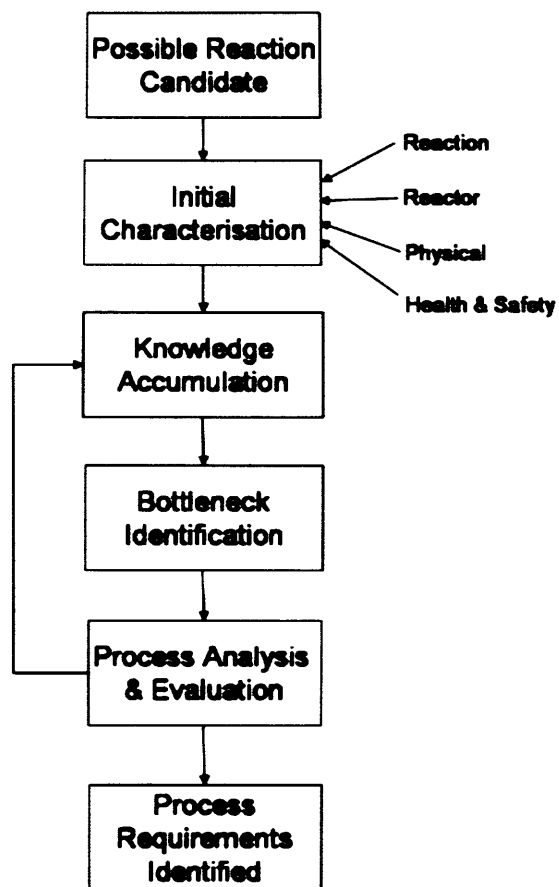


Figure 1-1 – Generic strategy for the optimisation of integrated biocatalytic processes

this is time and material intensive, therefore modelling is often used to describe these phenomena to reduce the effort required to identify the reaction system characteristics.

1.2.2 Methods of Acquiring Process Knowledge

1.2.2.1 Experiment

The collection of the above data can be a major task both time and cost intensive. As such several areas of the literature have set out to address this, by gaining more information from fewer experiments using techniques such as factorial experimentation (Hunter *et al*, 1998) or by using automation and/or miniaturisation to increase the amount of experiments achievable with less reagent in a shorter period of time (Doig *et al*, 2002; Kumar *et al*, 2004; Lye *et al*, 2003).

1.2.2.2 Modelling

Even with employment of modern methods of experimental design some of the data required may be missing and therefore some of the literature has focussed on the use of qualitative and semi-quantitative models and minimal data (Obenndip and Sharratt, 2006; Shaeri *et al*, 2006; Sharratt *et al*, 2003). The knowledge gained is commonly built into a model so as to collate and share the information, which can later be used to investigate process limitations, suggest possible designs and optimise both the chosen process and its control systems for cost and other chosen performance indicators whilst minimising further experimentation (Brass *et al*, 1997). Modelling can reduce the time and materials required in order to gain the same knowledge. It achieves this by reducing the requirement for experimental data, as the application of a model enables the interpolation of data. Furthermore, by their nature, models tend to simplify process problems to less complex systems. This can clarify the key variables, characteristics or processes in a system.

Almost every process engineering situation can be modelled, such as rate kinetics, thermodynamics, unit operations through mass and energy balancing, and heat and mass transfer. Key to the modelling process is the use of the simplest possible model

for current purpose. For example relatively crude models will suffice for initial discrimination of process routes (Brass *et al*, 1997; Marquardt, 1996). However, as a process becomes progressively more defined, increasingly complex models are required. The more complex models are often built up by the use of flowsheeting programs, such as Aspen ® or Superpro Designer ®, which are relatively user friendly containing built-in models of each unit operation. However, these are limited to the built-in functions that were supplied with the software often having no function for building in user-specific models. In particular, Superpro Designer, a biochemical process specific software package uses simplified kinetics which may not be applicable to all reactions. User-written code is an alternative, which whilst labour intensive is extremely flexible, particularly when employing a programming language such as Matlab ® which comes with many built in mathematical functions all of which can be edited. Other approaches forming hybrids of these techniques can also be used (Lohmann and Marquardt, 1996; Marquardt, 1996).

1.2.2.2.1 Reaction Modelling

There are many and varied methods of forming reaction models. They can be created piecemeal by separating out the individual components and building up an overall process model from these components (Biselli *et al*, 2002) or for example by using grey-box approaches for complicated reaction systems using combinations of techniques such as artificial neural networks together with mass balances or reaction rate models to bypass the need for large mechanistic models (Chen and Woodley, 2002; Chen *et al*, 2000).

1.2.2.2 Chemical Reactions

Chemical reaction models are well established and vary in complexity dependent on the reaction system present. Typically chemical reaction rates can be described by Equation 1-1 for the elementary reaction in Figure 1-2.

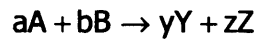


Figure 1-2 – General reaction schematic

$$r = k[A]^a[B]^b \quad (1.1)$$

Where r = rate, k = rate constant, $[A]$ is concentration of A, $[B]$ concentration of B, a is reaction order with respect to component A and b is reaction order with respect to component B (Connors, 1990b). For more complex reactions the rate equation must be determined experimentally as the stoichiometric coefficients cannot be used to determine the form of the rate-concentration relationship. It cannot be determined from first principles whether a reaction is elementary or complex and as such all chemical reaction rates require experimental determination (Fogler, 1999a).

1.2.2.3 Enzymatic Reactions

Enzyme models are typically based on the Michaelis-Menten model as a base case. However, simpler methods to model enzymatic reactions do exist. For example, Blackman kinetics assume a linear relationship of reactant concentration and maximum rate until a reactant limitation is reached and can therefore be modelled simply with linear equations and inequality constraints (Dabes *et al*, 1973; Hoeks *et al*, 1996). However, the point at which this limitation comes into effect needs to be determined experimentally. In cases where there are several side reactions or competing limitations the initial determination of the relevant limiting factor can be hard to achieve without more meaningful information on the reaction system and its kinetics. Michaelis and Menten postulated that a complex of enzyme and reactant (ES complex) was formed in a reversible and fast reaction, that the dissociation of the ES complex to E

and P (product) was the rate-limiting step and as such k_{-m} was approximately zero (Figure 1.3). Therefore it could be said that E, S and ES were in equilibrium and therefore unaffected by the production of P. This is termed the rapid-equilibrium assumption (Biselli *et al*, 2002; Segel, 1993b). The reaction eventually reduces down to the standard Michaelis-Menten equation (Equation 1.2) where r represents the rate of reaction, $[S]$, reactant concentration, K_M , the Michaelis constant and V_f denotes maximum rate of reaction and is equal to the turnover number (k_{cat}) multiplied by the initial enzyme concentration ($[E]_0$)



Figure 1-3 – Enzymatic reaction scheme for a unireactant reaction

$$r = \frac{V_f[S]}{K_m + [S]} \quad (1-2)$$

The Michaelis constant, K_m is defined as the reactant concentration at which the reaction rate is exactly half that of V_{max} and describes the binding of the enzyme reactant complex. The turnover number, K_{cat} is a measure of activity of the enzyme and describes the net number of reactant molecules per catalyst site per unit time. A measure of the effectiveness of an enzyme is the use of the specificity constant, or K_{cat}/K_m , this has units of $l.mol^{-1}.s^{-1}$ (for a bireactant system) and gives a ratio of the rate of catalysis to the rate of binding and provides a method of comparison between different enzymes. Enzymatic perfection is achieved with superoxide dismutase, which removes free radicals from the cellular environment and has a specificity constant of 2×10^9 . Briggs and Haldane proposed a further extension to Michaelis-Menten kinetics in that they assumed that the ES complex reached equilibrium very rapidly and therefore $d[ES]/dt = 0$ (Briggs and Haldane, 1925). This is termed the

quasi-steady state assumption whereas Michaelis-Menten kinetics are described by the rapid equilibrium assumption.

Michaelis-Menten kinetics assume that enzyme and reactant can bind in any order (ie the systems are random), however, a situation exists where enzyme and reactant have to bind in a pre-determined order dependent on the stoichiometry of the enzyme, these are termed ordered systems. A separate approach to the derivation of reaction kinetics is required in these situations as the equations are typically quite complex comprising many constants. King and Altman in their paper describe a method whereby all relevant terms can be found for a particular system, so none are forgotten (King and Altman, 1956). Whether an enzyme and reactant complex has a random or ordered binding system is usually found either by derivation of an initial model usually following a random order as the derivation of the equation is simpler and produces less parameters and testing the level of fit (Bauer *et al*, 1999).

1.2.2.2.4 Methods of Parameter Estimation

Chemical and enzymatic rate equations can be easily derived. However, the kinetic parameters must be determined from experimental data. As can be imagined the larger the number of parameters in a reaction rate model the easier it is to fit the data to the model. However, as models increase in complexity, parameters become less indicative of the mechanism (Gonçalves *et al*, 2002), when these situations arise it may be more rigorous to use a grey-box hybrid approach (Chen *et al*, 2000).

There are three main methods of parameter estimation; 1) integrating the rate equation and fitting the integrated rate equation to the progress curve, 2) fitting initial rate data to the rate equation when reduced down to its initial form (ie substituting reactant with initial reactant concentration and reducing any backwards reaction to zero) and 3) reducing the rate equation to a linear equation and fitting experimental data on non-linear scales by linear regression. All three methods have their advantages and disadvantages.

With the former, a key part of the solution is the derivation of the integrated rate equation, a time-consuming task particularly when the reaction system is complex and much work has been undertaken to minimise the effort required (Boeker, 1984; Duggleby, 1995; Duggleby and Wood, 1989). The integrated rate equation must then be solved typically by numerical methods such as a fourth order Runge Kutta algorithm (Biselli *et al*, 2002) and then fitting the progress curves so produced by the model with experimental data. Once again several computer programs have been written to mechanise the whole procedure (Duggleby, 2001; Goudar *et al*, 1999; Straathof, 2001). The benefit of using progress curve analysis is that the entire timescale of the reaction is taken into account in the process of parameter determination. However, for complex systems the derivation of the integrated rate equation is time consuming and for complex systems with multiple reactions the entire reaction system must be included in order for the model to have any value. Many of the current computer programs in the literature cannot accept more than individual reactions in the absence of other rate phenomena such as mass transfer or competing reactions (Straathof, 2001).

Linear regression though very simple to undertake is inherently inaccurate since by taking the logarithm of the experimental data, the errors are magnified and weighted incorrectly (Cornish-Bowden and Eisenthal, 1974; Eisenthal and Cornish-Bowden, 1974).

Non-linear regression has several benefits, not least that it is comparatively easy to determine the kinetic parameters but also that the curve fitting procedure when undertaken by a computer produces error terms. Experimental data can be weighted to account for errors (NIST/SEMATECH, 2005). The method itself produces a best estimate of the kinetic parameter and avoids the pitfalls of linear regression. However, the regression tends to produce parameters with high levels of decimal places, this can tend to mean that the method is considered to be more accurate than is the reality (Duggleby, 1991) and therefore confidence in the resultant parameters should be considered carefully. When nonlinear regression and progress curve analysis are used

to produce the kinetic parameters for the same system, good agreement between the models has been reported (Bauer *et al*, 1999). Nonlinear regression has the added benefit that by taking initial rates (ie less than 5% of reaction progress), theoretically reactions in series and running parallel do not affect the initial rate, enabling the simplification of complex reaction systems. However, by taking initial rate, the backwards reaction has to be studied separately increasing the amount of experimental work required or decreasing confidence in the model if simulation is used to provide the backwards kinetic parameters.

1.2.2.2.5 Reactor Modelling

For every reactor system, once the boundaries of the system have been defined, it is possible to derive a rate based mass balance as in Equation 1-3 below:

$$\begin{array}{ccccccccc} \text{In} & + & \text{generation} & - & \text{out} & = & \text{accumulation} & & \\ & & & & & & & & \\ F_{i,j_0} & + & \text{Gen}_j & - & F_{i,j} & = & dN_j/dt & & \end{array} \quad (1-3)$$

Where N_j represents the moles of species j in the system at time t , F_{i,j_0} represents flow of species j into the system, $F_{i,j}$, flow of j out and Gen_j , the rate of generation of j . If the system can be described as homogenous, then the rate of generation is the product of the reaction volume and rate of formation of species j , ie:

$$\text{Gen}_j = r_j \cdot V \quad (1-4)$$

Commonly used reactor types for biocatalysis include the plug flow reactor (PFR) which operates on a plug flow basis and is commonly used for immobilised enzyme reactions. Gradients form within the reactor and product concentration increases with column length. However, mixing is negligible and as such for pH or heat labile enzymes plug flow reactors maybe inadvisable. Continuous stirred tanks (CSTR) provide good mixing by use of impellers and retain catalyst. However, because the outlet stream is the same as that in the tank, reactant will always be present in the product stream and tank in order for the reaction to proceed and therefore yields are

lower than would be the case in an equivalent batch reaction. Finally, batch stirred tank reactors (BSTRs) are most commonly used in biocatalytic processes as these provide good mixing and control and complete conversion is possible. However, downtime for batch processes is high and the level of the conversion in the reactor is dependent on reaction kinetics. Mole balances for these reactors can be seen in Table 1-2. Reactions are often more complex than the situation presented above and involve side and sequential reactions. In these cases stoichiometric balances are required for each species, which together with the rates of change of individual reactions create an overall rate of change for the species. Particularly when these reaction systems are complex a computer is required to solve the system of equations numerically.

1.2.2.2.6 Energy Balances

Heat can be treated in a similar manner to form energy balances by making use of equation 1-5 together with the systems defined boundaries:

Rate of accumulation of energy with the system	=	Rate of flow of heat from surrounding to the system	-	Rate of work done by the system on the surrounding	+	Rate of energy added to the system by mass flow in	-	Rate of energy removed from the system by mass flow out	(1-5)
---	---	---	---	---	---	--	---	---	-------

$$\frac{d\hat{E}_{sys}}{dt} = \dot{Q} - \dot{W} + F_{in}E_{g,in} - F_{out}E_{g,out}$$

For systems at steady state such as continuous reactors, the rate of accumulation will reduce to zero. By neglecting changes in potential and kinetic energy as for any chemical reaction changes in the internal energy will predominate, the energy of the system can be evaluated in terms of enthalpy and integrated, so that when the system is considered well mixed and variations in pressure and volume are neglected Equation 1-5 can be stated as:

$$\sum N_i \frac{dH_i}{dt} + \sum H_i \frac{dN_i}{dt} = \dot{Q} - \dot{W}_s + \sum F_{i0}H_{i0} - \sum F_iH_i \quad (1-6)$$

Reactor	Mole Balance
BSTR	$\frac{dN_j}{dt} = r_j V$
CSTR	$V = \frac{F_{j0} - F_j}{-r_j}$
PFR	$\frac{dF_j}{dV} = r_j$

Table 1-2 – Mole balances applicable to popular reactor types

Because H is a function of temperature and each individual species specific heat capacity (Equation 1-6) and dN_i/dt a function of reaction rate, the change in temperature can be described by Equation 1-7 (Fogler, 1999b).

$$H_i = H^\circ(T_R) + \int_{T_R}^T C_{pi} dT \quad (1-7)$$

$$\frac{dT}{dt} = \frac{\dot{Q} - \dot{W}_s - \sum_{i=1}^n F_{i0}(H_i - H_{i0}) + (-\Delta H_{RX})(-r_a V)}{\sum N_i C_{pi}} \quad (1-8)$$

It can immediately be seen that the flow terms reduce to zero for a well-mixed batch reactor.

1.2.2.2.7 Solving Ordinary Differential Equations

Ordinary differential equations (ODEs) are commonly used to describe situations of change particularly in engineering applications. Often though an analytical solution is hard to come by and since the advent of the computer the use of numerical methods for the solution of ODEs have become far more prevalent. All methods of numerically solving ODEs are based on the Taylor Series which states that any function can be described in terms of its derivatives, therefore if the derivative is known the original function can be found (Appendix 10-1).

1.3 BOTTLENECK IDENTIFICATION

On development of a validated reaction model, whether this is simplistic, or detailed, modelling all aspects of side reactions, mass and heat transfer the model can then be used to assess where bottlenecks applying to the relevant reaction system lie. This can be achieved by several means: sensitivity analysis of the variables used in a process model, analysis of limiting regimes by assessment of characteristic times or on a case-by-case identification of process bottlenecks dependent on experimentally observed limitations. Identification of the bottlenecks affecting the reaction under investigation then leads the process designer to be able to assess individual limitations,

identify those limitations most critical to the success of scale-up and assess the potential process if the limitation were to be lifted guiding both process design and future experimental work. At this point it may be determined that a process would be unfeasible on the large scale as a result of unmovable limitations.

1.3.1 Sensitivity Analysis

The use of sensitivity analysis of the reaction or reactor parameters is well established for guiding the process development of reaction parameters (Blayer *et al*, 1996; Zimmermann *et al*, 2006), reactor configurations (Bühler *et al*, 2006; Pilgrim *et al*, 2006; Willeman *et al*, 2002a) and full flowsheets (Biber and Heinzle, 2004; Wingren *et al*, 2003),. However, models often have many variables and therefore visualisation of the process interactions is made difficult. As a result sensitivity analyses are frequently undertaken by changing one variable at a time and studying the impact on chosen process performance indicators, such as yield on reactant or overall rate, rather than studying interactions. Mainly because methods for studying interactions are complex and too time-consuming at a very early stage of process development when confidence in the model is low (Saltelli *et al*, 2005). Furthermore, the sensitivity analysis and therefore identification of process limitations will only be as good as the model, though at early stages of process development, crude models will suffice to indicate if a process option is worth investigating. It is noted that although sensitivity analysis of process models is a useful method for bottleneck identification, it has rarely been carried out in a formalised manner leaving the possibility that an important limitation may be left unanalysed.

1.3.2 Blackman Kinetic Analysis

Blackman kinetics (Figure 1-4) describe how below a critical concentration of reactant, rate increases linearly with reactant, with other mechanisms or reactants controlling the rate above the critical concentration. However, as with all kinetics this critical concentration has to be determined experimentally, a substantial task in that the actual

relationship between rate and reactant concentration is not linear and the limit subsequently not well defined. Furthermore there is a reliance on experiment to identify the controlling mechanism. To date, Blackman kinetics have most often been employed with already established processes, for which the analytical method is satisfactory (Brass *et al*, 1997; Dabes *et al*, 1973; Hoeks *et al*, 1996). However, use of linearised kinetics at an early stage could mean a key bottleneck at large scale remains unidentified.

1.3.3 Regime Analysis

Analysis of regimes was established in the study of mass transfer with definition of flow regimes by Reynolds in the 1870s, has been extended to many mass transfer situations and is still applied today (Bhole and Joshi, 2005; Link *et al*, 2005). Commonly, analysis of regimes in biochemical processes is restricted to investigation of characteristic times, such as mixing, reactant consumption and mass transfer, though concentration, temperature and other reactor conditions can be used (Kossen and Oosterhuis, 1985; Wolff *et al*, 1999). Characteristic times in particular enable theoretical assessment indicating where a process is fast or slow and an extension of analyses of rate controlling steps (Sweere *et al*, 1987). However, a process has to be fixed in order for regime analysis to be employed, reducing its use as a method of initial bottleneck identification.

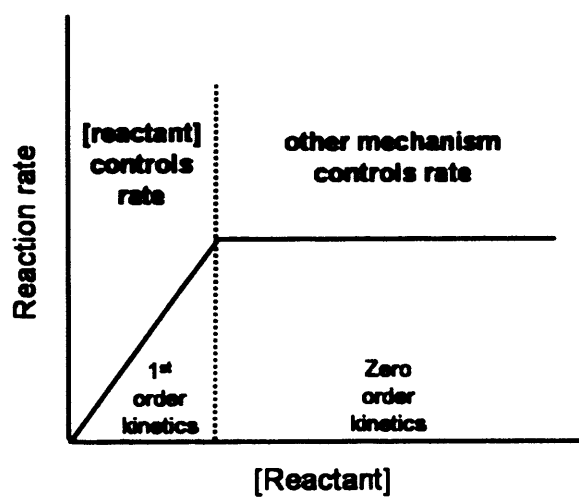


Figure 1-4 – Blackman kinetics

1.4 PROCESS EVALUATION

The initial characterisation of the factors limiting the process will guide scale-up and design of processes. This stage is typically undertaken by skilled designers, producing many possible process routes either by use of expert knowledge or by use of a hierarchical approach to process design (Sirola, 1996). Each potential process will then be assessed for its suitability for purpose and process robustness. This can be achieved by many means including: experimentally through scale-up and scale-down studies, semi-quantitative scoring methods (Shaeri *et al*, 2006), proprietary methods (www.britest.co.uk) or assessment of key process indicators from detailed process models (Wingren *et al*, 2003). However, the importance of high level initial assessment of processes cannot be understated here if every process alternative is not to be modelled in extensive detail and/or tested at pilot plant scale. With the potential process routes narrowed down, optimisation will then be required to identify the best case process and therefore future process requirements. Optimisation can be carried out in a mathematically formal manner, by making use of objective functions and constraints (Rao, 1996b) (Equation 1-9). Where X is the design vector describing a set of variable conditions involved in an engineering system, which needs to be optimised for $f(X)$, the objective function describing the criterion for that design and $g_j(X)$ and $l_j(X)$ inequality and equality constraints respectively, which describe the restrictions placed on those variables involved in the design vector (Equation 1-9).

$$\text{Find } X = \begin{Bmatrix} x_1 \\ x_2 \\ \vdots \\ x_n \end{Bmatrix} \text{ which minimises } f(X)$$

(1-9)

subject to the constraints

$$g_j(X) \leq 0, \quad j = 1, 2, \dots, m$$

$$l_j(X) = 0, \quad j = 1, 2, \dots, p$$

Optimisation problems can be based on linear, non-linear, geometric or quadratic objective functions, which can be multiple for multiobjective problems. The objective function is often based on economics, but can involve environmental and other constraints. There can be many solutions to a multiobjective optimization with inequality constraints and hence a Pareto optimum is formed, this is a set of X, that satisfies all the objective functions (Rao, 1996a). These Pareto optima can be large and as such a method to distinguish between the solutions is required, this can be done by means of grouping, by the rough sets methods (Greco *et al*, 2001) or recently by drift group analysis (Yanofsky *et al*, 2006), ranking (Steffens *et al*, 1999) or searching (Cavin *et al*, 2005). There are many methods of solving optimisation problems, including use of derivatives and searches for more complex problems which can use genetic algorithms amongst other methods as can be seen in Biegler and Grossman in their review (Biegler and Grossmann, 2004).

Optimal processes can also be found by sensitivity analysis of flowsheets (Biwer and Heinzle, 2004; Wingren *et al*, 2003; Zhou *et al*, 1997) or creation of overall flowsheets and then applying optimisation procedures to design the optimal process (Samsatli and Shah, 1996a; Samsatli and Shah, 1996b). A useful tool to visualise the competing process parameters, such as cost, environmental and safety aspects, process, scheduling, reactor, mass and heat transfer constraints is the window of operation (Blayer *et al*, 1996; Chen *et al*, 2002; Hogan and Woodley, 2000; Woodley and Titchener-Hooker, 1996; Zhou and Titchener-Hooker, 2002) in which the larger the window the more robust the process, the window itself is analogous to the Pareto domain discussed above produced by multiobjective optimisation, whilst the production of the window can be seen as analogous to the simpler more straight-forward methods of optimization, without the need for searching or derivation.

1.5 CONCLUSION

It has been noted by several groups that key to the assessment of any possible biochemical process are several steps to undertake including: initial identification of a possible reaction candidate, initial characterisation, knowledge accumulation and process analysis and evaluation to determine whether the possible reaction is feasible on the large scale and if so what process research is required prior to its possible implementation. Knowledge accumulation is often carried out by means of modelling to reduce time and material expense in experimentation by means of interpolation.

It can be concluded that though there are several methods of analysing and evaluating biochemical processes, to date there has been little widespread application of these techniques to biocatalytic processes, in the main due to the complexity of enzymatic processes, but also as a result of problems inherent in the methods themselves. Regime analysis requires a process to be fairly well defined initially, an unstructured sensitivity analysis of a process model may miss process bottlenecks and requires much work to then optimise the process and Blackman kinetics though able to identify at least one bottleneck easily, the method of finding that limitation is subjective and may mask other process limitations whilst relying heavily on experimental evidence. As a result this thesis aims to provide a tool for the analysis and evaluation of biocatalytic processes that relies on a modelled process to reduce experimental effort, is capable of defining all reaction bottlenecks and is simple enough for widespread use so as to guide the designer towards applicable process routes and necessary process research.

2 AIMS

This thesis aimed to develop simple, robust tools and strategies for assessing the potential of biocatalytic processes whilst minimising experimental effort prior to possible major investment in further process research.

2.1 STRATEGY AND SCOPE

Tools for the assessment of the possible scope of a future biocatalytic process will be tested for a model system, the production of S,S-ethylenediamine-N,N'-disuccinic acid by a carbon-nitrogen lyase, EDDSase from ethylenediamine and fumaric acid. It is clear from the preceding chapters that there are three distinct stages of process development: identification and characterisation, knowledge accumulation and design, but that the design process is often iterative and early elimination of possible process routes is crucial to reduce the number of iterative steps on route to a successful design (Figure 2-1).

The characterisation of a process is a key step in its design and so it is here, with the literature presenting some of the characterisation information required in Chapter 3 and the remainder being provided by further experimental work described in Chapter 4. Knowledge accumulation is the next step towards a process design, this is where assessment of process bottlenecks is most useful and often a model of some description will aid the understanding of the process, Chapter 5 describes the development of a reaction model to this end. Finally in Chapter 6, a novel and rapid method by which biocatalytic process bottlenecks can be identified and assessed for their potential to be removed is presented, resulting in a window of operation for the S,S-EDDS process. Potential bioprocesses then follow from the identification of bottlenecks and several possible processes are tested *in-silico* to verify the initial assessment. Finally a suggested process and future work required for the large-scale production of S,S-EDDS by bioconversion are presented in Chapters 7 and 8.

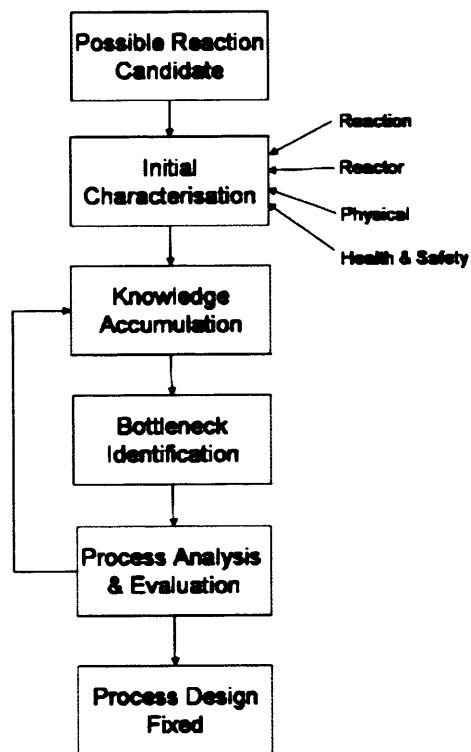


Figure 2-1 – Schematic describing a generic method of process development

3 MODEL SYSTEM

[S,S]-ethylenediamine-N,N'-disuccinic acid ([S,S]-EDDS) is a biodegradable hexadentate metal chelator (Schowanek *et al*, 1997), the structure of which can be seen below in Figure 3-1. S,S-EDDS is highly water soluble (Octaquest® E30 (2002), MSDS, Octel Corp) and has a very low log P (below -4.7) (Proctor and Gamble, 2002; Proctor and Gamble, 2003; Syracuse Research Corporation, 2003). Where log P or the octanol-water partition coefficient, describes the ratio of solubility of S,S-EDDS in octanol over its solubility in water. A negative log P indicates better solubility in water and therefore a high degree of polarity. EDDS can exist as several species, many of which are very soluble in water, however, the solubility product of $[\text{EDDS}^4][\text{H}^+]_4$, is very low at $1.8 \times 10^{-26} \text{ mol.l}^{-1}$ (Matthews and Williams, 2003), meaning that at low pH, EDDS is almost completely insoluble in water. Logarithmic acid dissociation constant (pKa) values for S,S-EDDS are 2.43 for pKa₁, 3.93 for pKa₂, 6.83 for pKa₃ and 9.83 for pKa₄ (Vandevivere *et al*, 2001b).

[S,S]-EDDS is used mainly in laundry detergents (Hartman and Perkins, 1987) in order to stabilise the oxygen bleach system from decomposition by transition metal ions (Proctor and Gamble, 2002) but is also used in photographic supplies (Takahashi *et al*, 1999), personal care products, cleaning, water treatment, metal treatment, textiles, agriculture (www.octel-corp.com (2002)), some drug formulations as a 'Trojan Horse' (Pennsylvania State University, 2003; Wittman *et al*, 2002) and paper and pulp manufacture (Jones and Williams, 2002). [S,S]-EDDS has been manufactured by Octel Corp by a method of chemical synthesis under the brand name Octaquest® since 1996 (Octel, 2002) and could compete with ethylenediaminetetraacetic acid (EDTA), a popular hexadentate chelant, a structural isomer of EDDS (Figure 3-2) on the basis of chelation ability. EDTA, however, is cheaper than S,S-EDDS, £6 versus £0.75-£1 per kilo (Patel, 2003) and was produced to a scale of 32,000 tonnes in Europe in 1997 (Oviedo and Rodriguez, 2003) from formaldehyde, ethylenediamine and a source of cyanide. This annual tonnage is large (possibly extending to 100,000

tonnes *per annum* worldwide) and causes some concern as EDTA is poorly biodegradable and its applications mainly water based causing a build up of heavy metal ions in the environment (Egli, 1988; Nowack, 2002; Witschel and Egli, 1998). Furthermore because of the large quantities consumed and its lack of biodegradability EDTA is found in European surface waters at background levels of 10-50 µg/l (Jaworska *et al*, 1999). Experiments with activated sludge have indicated while S,S-EDDS degrades without acclimation, EDTA remains recalcitrant even after 100 days of acclimation (Takahashi *et al*, 1997)). However, some bacterial strains have been isolated that do degrade EDTA, but these do not appear to be well spread throughout the natural populations (Witschel *et al*, 1997). Because S,S-EDDS is biodegradable it can be used as a method by which soil is remediated (Finžgar N *et al*, 2004; Kos and Leštan, 2004; Meers *et al*, 2005; Vandevivere *et al*, 2001b; Vandevivere *et al*, 2001a).

EDDS chelates with ligands in a similar manner to EDTA (Figure 3-3), the stability of the complex being described by a stability constant. When a chelation complex is formed by the reaction of a ligand (L) with a metal (M) the reaction can be described by equation 3.1 (Kettle, 1996):



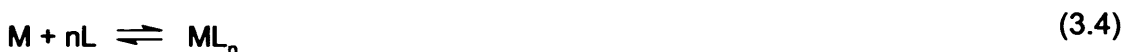
The equilibrium constant for this reaction is therefore:

$$K_1 = [ML]/[M][L] \quad (3.2)$$

Further addition of ligands can be described by the general formula for the stepwise stability constant

$$K_n = [ML_n]/[ML_{n-1}][L] \quad (3.3)$$

An overall equilibrium constant β can be formed from the product of all these stepwise constants describing the overall reaction:



$$\beta = [ML_n]/[M][L]^n \quad (3.5)$$

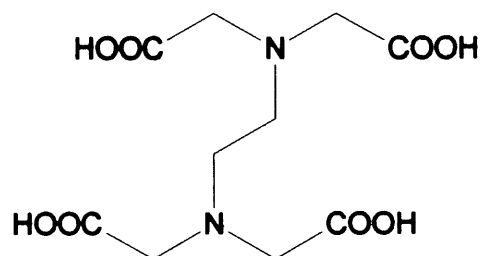


Figure 3-1 – Structure of Ethylenediaminetetraacetic acid (EDTA), a structural isomer of EDDS

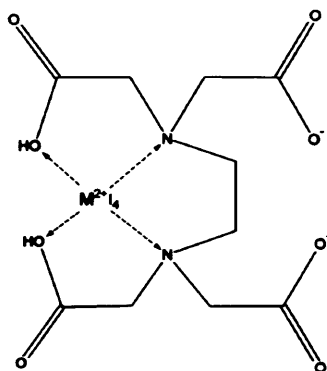


Figure 3-2 - Hexadentate EDTA complexing with a tetracoordinate metal ion

Some such stability constants for EDDS and some selected ions can be seen in Table 3-1. These clearly indicate that EDDS forms strong complexes with copper, cobalt and iron (III), but relatively weak complexes with calcium and magnesium. The similarity between complexation of EDTA and EDDS can also be seen. These constants are pH dependent, progressively becoming less stable as pH decreases (Day, 2005).

S,S-EDDS can act as a complexone type siderophore a natural chelant (Carrano *et al*, 1996) expressed by bacteria to scavenge insoluble iron (III) from the environment often produced by *Pseudomonad* bacteria (Meyer, 2000). S,S-EDDS is thought to be involved in the uptake of zinc in *Amycolatopsis japonica* (Cebulla, 1995) because of its production in zinc-limited conditions. The organism being discovered as part of an antibiotic screening program (Nishikiori *et al*, 1984) because of its ability to inhibit the zinc dependent phospholipase C (Bucheli-Witschel and Egli, 2001). As can be seen in Table 3-1, zinc does not form the strongest chelates with S,S-EDDS and in fact appears to make stronger chelates with copper, nickel, iron (III) and cobalt (Bucheli-Witschel and Egli, 2001; Neal and Rose, 1968). S,S-EDDS is likely involved in the uptake of zinc ions as a siderophore in the actinomycete with the lower zinc stability constant enabling the dissociation of zinc from the chelation complex once it has entered the cell. Furthermore, S,S-EDDS production was totally inhibited at concentrations above 2.5 μ M in the growth media (Bucheli-Witschel and Egli, 2001)

3.1 BIODEGRADABILITY

In several studies of ethylenediaminedisuccinic acid biodegradation, it has been found that the R,R isomer does not biodegrade and the R,S isomer only degrades partially leading to an intermediate, N-(2-aminoethyl)-aspartic acid (or ethylenediamine-monosuccinate) most likely the d-isomer that did not degrade any further (Bucheli-Witschel and Egli, 2001; Schowanek *et al*, 1997; Takahashi *et al*, 1997). This has led to companies such as Proctor and Gamble using only S,S isomer in their products (Jaworska *et al*, 1999; Proctor and Gamble, 2002). S,S-EDDS exhibits low toxicity to

	S,S-EDDS (mol ⁻¹ .l)		EDTA (mol ⁻¹ .l)	
	20°C	25°C	20°C	25°C
Cu (II)	18.4 ²	18.36 ¹	18.80 ¹	18.70 ¹
Fe (II)	10.7 ³		14.32 ¹	14.27 ¹
Fe (III)	22.0 ²	22.0 ³	25.1 ¹	25.0 ¹
Mn (II)	8.57 ²		13.87 ¹	13.81 ¹
Ca (II)	4.72 ³	4.23 ³	10.69 ¹	10.61 ¹
Mg (II)	6.09 ³	5.82 ³	8.79 ¹	8.83 ¹
Co (II)	14.02 ³	14.06 ¹	16.31 ¹	16.26 ¹
Hg (II)	-	17.50 ¹	21.7 ¹	21.5 ¹
Pb (II)	12.7 ¹	12.3 ³	18.04 ¹	17.88 ¹
Zn (II)	13.4 ²			

Table 3-1 – Overall stability constants for some selected EDDS complexes. Sources: 1) (Martell and Smith RM, 1974) 2) (Orama *et al*, 2002) 3) (Day, 2005)

fish and *Daphnia* (Jaworska *et al*, 1999), but does exhibit toxicity to algae, although this is most likely a result of the chelation of trace metals in the environment and resultant trace metal limitations (Schowanek *et al*, 1996). The photodegradation of EDDS has also been studied within the ultraviolet range (UV) range, which concluded that the rate of degradation due to light of an iron-EDDS complex was pH dependent, and faster than the rate of similar concentrations of EDTA under the same conditions (Metsärinne *et al*, 2001).

3.2 ROUTES TO THE PRODUCTION OF S,S-EDDS

3.2.1 Synthetic Pathways to S,S-EDDS

3.2.1.1 Ramsey, Downey and Kerzerian Route

Ramsey, Downey and Kerzerian developed several methods to create polyaminocarboxylic acids in the early 1960s (Ramsey *et al*, 1963) which are described in their patent. The route to many polyaminocarboxylic acids is via a *bis*-adduction reaction of the nitrogen atoms of an amine and the double bond of an acid, ester or salt, chosen in relation to the product desired (Figure 3-4). The drawback of this method of synthesis lies mainly within the production of all three conformations of EDDS, which since only the S,S isomer is demanded is wasteful. The process for the production of EDDS from maleic anhydride and ethylenediamine has the potential to react with near explosive violence on neutralisation with NaOH if sodium hydroxide is allowed to accumulate at all. Furthermore, some ethylenediamine monosuccinate (EDMS) is produced by this route.

3.2.1.2 Neal and Rose Route

Neal and Rose developed a method in the late 1960s that utilised the chiral pool by the use of L-aspartate reacted with 1,2-dibromoethane (Neal and Rose, 1968) (Figure 3-5). This is the process by which S,S-EDDS is currently manufactured as the tri-sodium salt by Octel Corp. This process requires the use of the expensive feedstock L-aspartic acid and results in a product costing approximately 10 times that of EDTA.

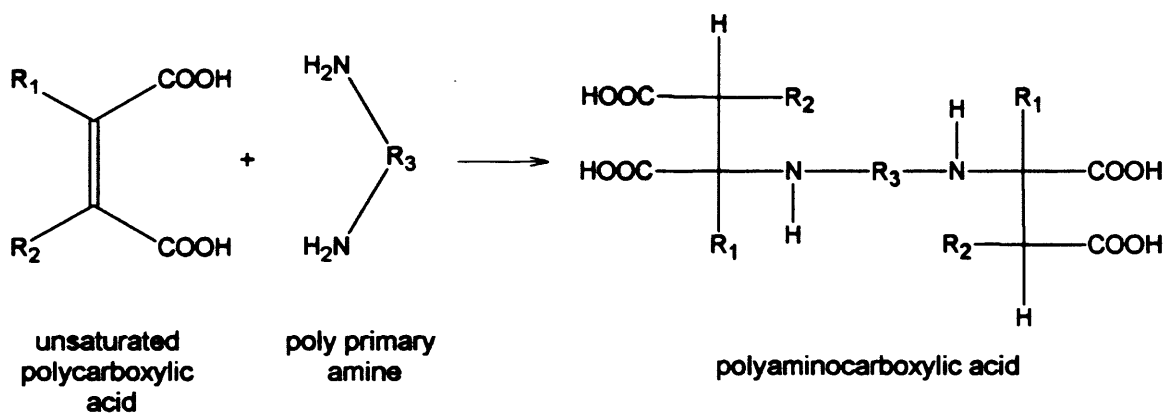


Figure 3-3 – Reaction scheme for the production of mixture EDDS, adapted from (Ramsey *et al*, 1963)

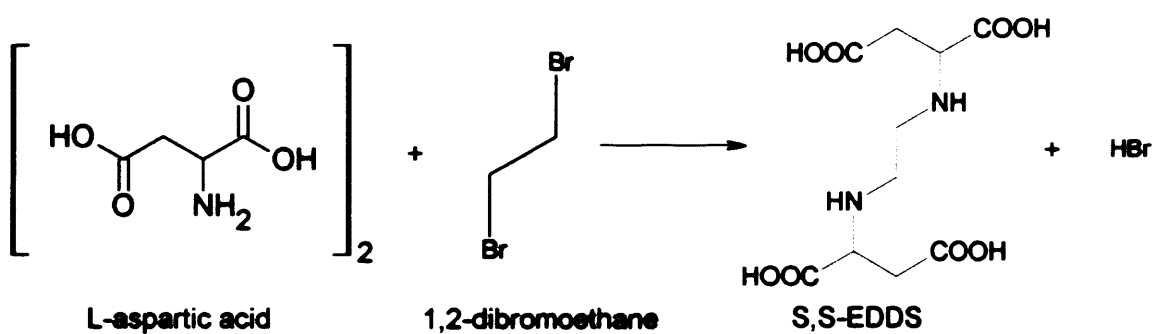


Figure 3-4 – Reaction scheme for the synthetic production of S,S-EDDS using the chiral pool

3.2.2 Biocatalytic Routes to S,S-EDDS

Following the discovery that *Amycolatopsis japonica* produced S,S-EDDS naturally (Nishikiori *et al*, 1984) under zinc limited conditions (Zwicker *et al*, 1997) several other organisms have been found able to produce S,S-EDDS following their isolation from soil samples with S,S-EDDS as the sole carbon source. Some such bacteria are *Paracoccus sp* and *Brevundimonas diminuta* (Endo *et al*, 1998; Kato *et al*, 2000; Kato *et al*, 2001).

3.2.2.1 Secondary Metabolite Route

The secondary metabolite route uses *Amycolatopsis japonica* as the host for the enzyme responsible production of EDDS (Hartman and Perkins, 1987) under zinc limited growth conditions (Zwicker *et al*, 1997). *Amycolatopsis japonica* is a gram positive actinomycete that is aerobic, non-motile and produces a reactant mycelium that fragments into squarish subunits. The actinomycete also forms sterile aerial hyphae, and is resistant to penicillin, but not neomycin sulphate or rifampicin (Goodfellow *et al*, 1997). Work has been undertaken to improve the fermentation titre even so S,S-EDDS concentration only reached approximately 20 g.l⁻¹ following an 800 hour fermentation (Zwicker *et al*, 1997). The molecular genetics of *Amycolatopsis japonica* are not particularly well defined and there exists a lack of cloning vectors, methods of transformation and marker genes all of which make the cloning of the strain difficult although recent work has sought to rectify this (Stegmann *et al*, 2001) .

3.2.2.2 EDDS Lyase Route

A carbon-nitrogen lyase capable of degrading S,S-EDDS has been found to exist in several species of bacteria: *Sphingomonas* (Takahashi *et al*, 1999), *Brevundimonas* (Kato *et al*, 2000; Takahashi *et al*, 1999) , *Pseudomonas* (Takahashi *et al*, 1999), *Acidovorax* (Takahashi *et al*, 1999), *Paracoccus* (Kato *et al*, 2000), *Chelatococcus asaccharovorans* (Witschel and Egli, 1998) and *DSM9103*, an unclassified bacterial strain (<http://www.dsmz.de/microorganisms/html/strains/strain.dsm009103.html>)

(Witschel and Egli, 1998) that is likely representative of a new branch of the *Mezorhizobia* family (Weilenmann *et al*, 2004). This lyase is termed EDDS lyase or EDDSase and appears to function in a similar manner to aspartase type enzymes, that is they catalyse the splitting of a carbon-carbon double bond and form a carbon-nitrogen bond with one of the carbons of the original double bond. There is some dispute in the literature as to the extent of the degradation of S,S-EDDS by the EDDS lyase enzyme, in some instances S,S-EDDS being broken down to two fumaric acid molecules (Endo *et al*, 1998; Kaneko *et al*, 1999; Kato *et al*, 2001; Takahashi *et al*, 1999) and in others to a fumaric acid molecule and ethylenediamine monosuccinate (Witschel and Egli, 1998), this may be due to a difference in methods employed, or additionally that the enzymes involved in the differing strains are dissimilar. Both proposed reaction mechanisms are shown below in Figure 3-6. Since S,S-EDDS and EDTA are structural isomers it could be assumed that the degradation pathway for both is similar though this appears not to be true as EDTA and nitriloacetate (NTA) another aminopolycarboxylate is broken down by a monooxygenase and a dehydrogenase, but the strain *DSM9103* can degrade both EDDS and EDTA (Egli *et al*, 1988; Egli, 2001; Satroutdinov *et al*, 2000; Wehrli and Egli, 1988; Witschel *et al*, 1997; Xun *et al*, 1996). The EDDSase gene has been found, sequenced (Mizunashi, 2001) and cloned into *Escherichia coli* JM109 via the plasmid pEDS020.

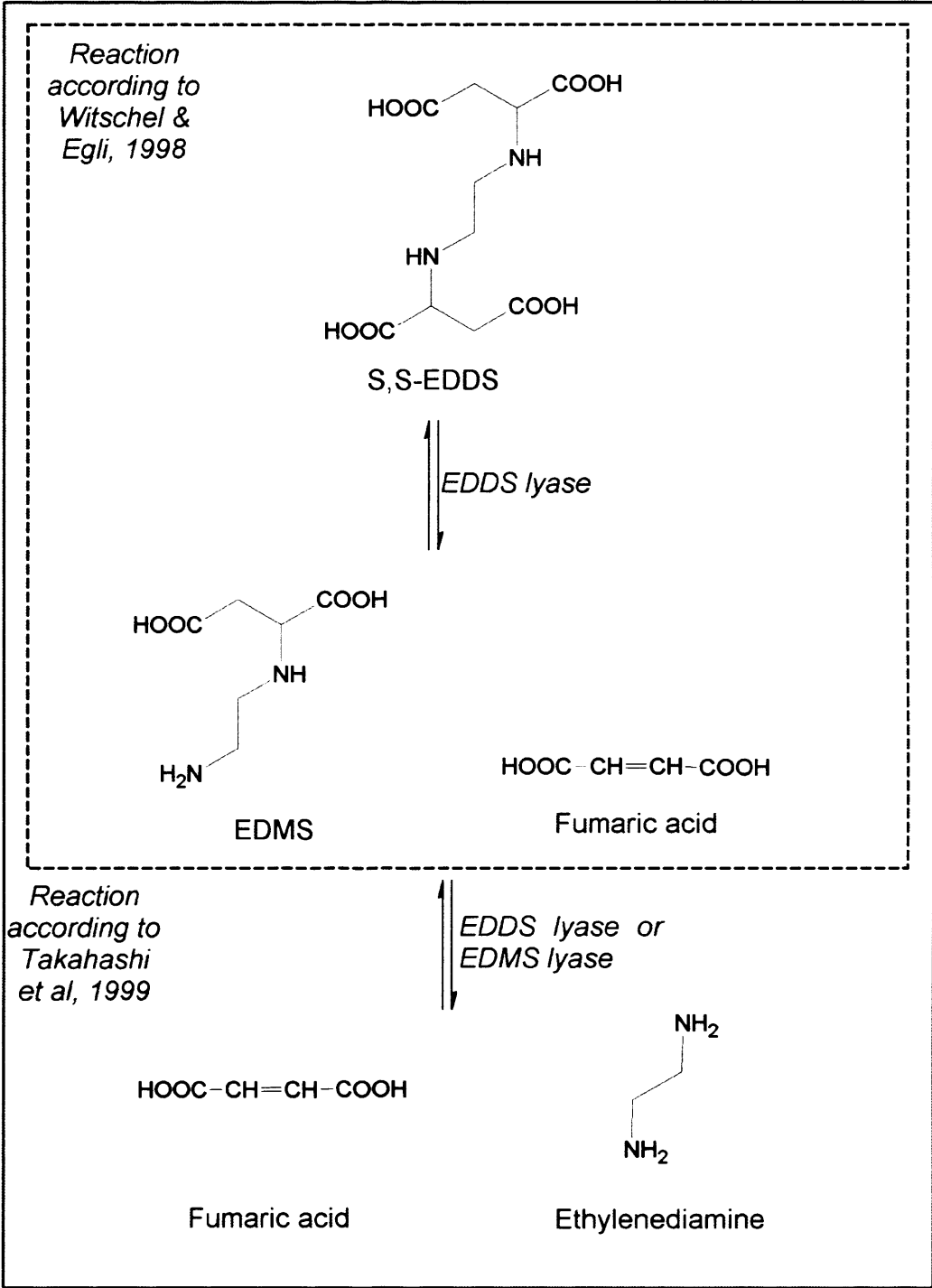


Figure 3-5 – S,S-EDDS degradation according to Takahashi et al, 1999 and Witschel and Egli, 1998

3.2.2.2.1 Typical Organisms Producing EDDSase

Several organisms other than *Amycolatopsis japonica* have the ability to create S,S-EDDS and/ or to degrade it, some of these microorganisms are discussed in further detail below.

3.2.2.2.1.1 *Chelatococcus asaccharovorans*

The gram negative obligate aerobe *Chelatococcus asaccharovorans* was first isolated by Egli (Egli, 2001) as a bacteria that degrades aminopolycarboxylic acids (APCAs), these include nitriloacetate (NTA) and S,S-EDDS although both by differing mechanisms. *Chc. asaccharovorans* has been found across much of the environment and has been found to be present in activated sludge from sewage treatment plants, in eutrophic rivers both containing and not containing NTA and in soil (Egli, 2001) and therefore can be assumed to be fairly prevalent in nature.

3.2.2.2.1.2 DSM 9103

DSM 9103 was first isolated by Witschel *et al* (Witschel *et al*, 1997) as an EDTA degrading bacteria. DSM 9103 is a gram-negative strain that grew on EDTA as its sole source of carbon, nitrogen and energy, which it broke down in a series of steps through first a monooxygenase reaction and then further redox type reactions. DSM 9103 is flexible with regards to the APCAs it can use as its energy source, these include NTA, EDTA, N,N'-EDDA and S,S-EDDS (Egli, 2001).

3.2.2.2.1.3 *Paracoccus*

Paracoccus sp is a non-fermenting gram-negative facultative anaerobe that can respire aerobically on carbon using the carbon cycle or anaerobically on nitrate and is commonly found in soil and sewage sludge (White, 1995). The bacterium is a small coccus approximately 1.1 to 1.3 μ m in diameter and an alphaproteobacteria. *Paracoccus* can grow singly, in pairs or short chains and are non motile. The colonies

formed are white to cream and contain no carotenoid pigments (Aragno and Schlegel, 1981). When respiring anaerobically *Paracoccus* uses hydrogen as the electron donor and nitrate as its electron acceptor (Madigan *et al*, 2003b), since *Paracoccus* uses nitrogen as its electron acceptor when respiring anaerobically it has a key role in the nitrogen cycle in that it denitrifies NO_3^- to N_2 removing fixed nitrogen from the environment (Madigan *et al*, 2003a), this can be both detrimental in agriculture if fields become waterlogged and anoxic, *Paracoccus* growth can increase and nitrate be leached out, conversely this is useful in water treatment as nitrates are removed and when released into the environment prevents algal overgrowth (Madigan *et al*, 2003a). Strains related closely to *Paracoccus* that also denitrify have been shown to degrade dimethylmalonate (Kniemeyer *et al*, 1999) and several other organic acids in anaerobic conditions in the presence of nitrate and only two of the strains tested in these conditions grew on sugars.

3.2.2.2.1 *Brevundimonas diminuta*

Brevundimonas diminuta is gram negative strain that will undergo oxidative fermentation on glucose and is positive for oxidase. The cells are typically small rods, form cream coloured colonies on nutrient agar and are capable of metabolising ammonia as a nitrogen source. *Brevundimonas diminuta* grows most efficiently at 30°C and requires some growth factors for adequate growth, such as pantothenate, biotin, cyanocobalamin and cystine and growing very slowly on mineral media (Stolp and Gadkari, 1981). *Pseudomonads* as *Brevundimonas* was initially classified are capable of metabolising a vast range of compounds as carbon and energy source and contain numerous inducible operons so that enzymes required for growth on an unusual reactant is readily accomplished (Madigan *et al*, 2003b).

3.3 CHOICE OF PROCESS ROUTE

It can be seen that there are four potential routes to S,S-EDDS: two synthetic and two biocatalytic routes. It was decided to focus on the EDDSase biocatalytic route as this provided a method by which fumarate, a cheaper reactant than L-aspartic acid could be employed (Figure 3-7). Furthermore S,S-EDDS would be produced in high enantiomeric excess in comparison with the Neal and Rose synthetic route. The secondary metabolite route has shown low productivity even after optimisation and efforts to improve productivity would be great requiring not only cloning and metabolic engineering but also detailed sequencing of the *Amycolatopsis japonica* genome so that cloning was possible.

3.3.1 Reaction Bottlenecks and Strategies to Overcome Them

Several process bottlenecks exist for the biocatalytic production of S,S-EDDS on the large scale. Not least the competition of fumarase for the reactant fumarate, to this end patents have described methods by which fumarase can be reduced by heat and borate buffer treatment (Kato *et al*, 2000). This requires an additional step between fermenter and reactor involving a change in cell suspension medium through either diafiltration or centrifugal harvest and resuspension, providing the ability to adjust biocatalyst concentration prior to reaction. A further reaction step can be included so as to provide the reaction with the cheaper feedstock maleic anhydride or maleic acid, making use of a further enzyme found in many microorganisms typically referred to as maleate isomerase and then using the resultant fumarate produced *in-situ* (Kato *et al*, 2001). However since the isomerisation of maleic anhydride is a further equilibrium led bio-reaction there will be further problems with yield as the equilibrium would tend towards fumaric acid.

Patents have been lodged covering the use of a heat exchanger for external cooling of the EDDSase reaction (Shigeo *et al*, 2004), indicating that the reaction is not only exothermic, but produces substantial amounts of heat, requiring careful control so

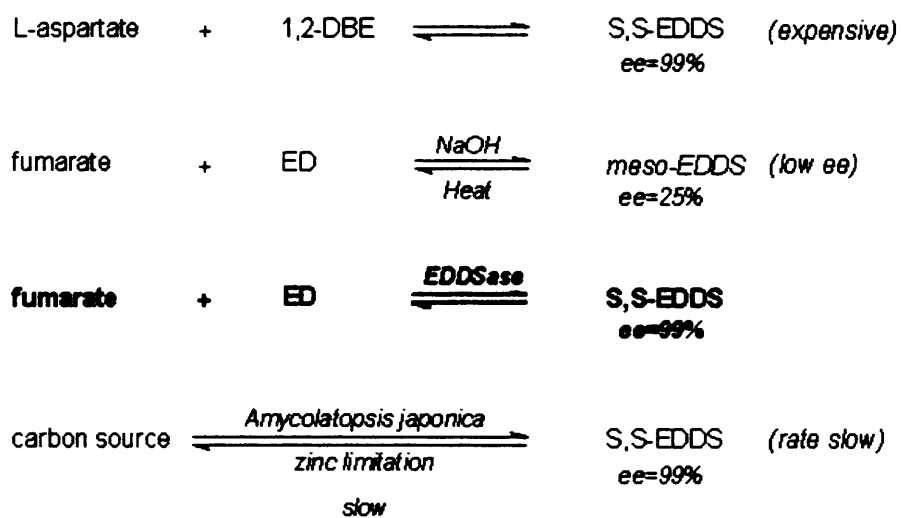


Figure 3-6 – Schematic showing all process routes to S,S-EDDS

as to avoid denaturing the required biocatalyst, but also to keep the temperature at an optimum. Further patents have covered the use of immobilised and isolated enzyme which would not only address the fumarase side reaction, but also improve the longevity of the catalyst (Kaneko *et al*, 1999; Kaneko *et al*, 2000). However, isolation and immobilisation are rarely undertaken in an industrial process because of the number of intermediate steps required such as harvest, immobilisation and resuspension which are typically not balanced by the additional increase in stability of activity. Furthermore, immobilisation of a biocatalyst onto certain types of support introduces a mass transfer limitation as reactant has to be able to reach the biocatalyst, as such there will often be a large amount of research required to find a suitable support for an individual biocatalyst.

Successful attempts have been made to increase EDDSase expression by cloning the EDDSase gene into recombinant hosts with the added benefit of proportionally reducing fumarase concentration (Kato *et al*, 2000; Mizunashi, 2001). Biocatalytic processes typically all require some form of cloned enzyme, as enzymes in nature are not required in the same concentration as in industrial processes, however, cloning requires a suitable enzyme candidate, a skilled workforce and the time in which the cloned biocatalyst and host can be produced. A later patent suggested preparing the reaction solution prior to catalyst addition at low temperature in order to prevent the production of *meso*-EDDS (Hiroyasu *et al*, 2000b), indicating a side reaction requiring careful control of reaction temperature so as not to affect product purity. Work has also been undertaken to investigate the effect of metal ions in the reaction so as to complex S,S-EDDS thereby increasing productivity by moving the equilibria towards the product. (Kaneko *et al*, 1999). This requires a careful choice of metal ion as stronger chelates will remove greater amounts of S,S-EDDS from solution, but also be harder to disassociate from the S,S-EDDS eventually. Particularly as at present S,S-EDDS is sold as a 30% w/v tri-sodium salt solution, removal of the metal ions may become a hindrance downstream. These bottlenecks are summarised in Table 3-2.

Bottleneck	Possible Solutions	Reference
Fumarase	Inhibit	(Kato <i>et al</i> , 2000)
	Isolated enzyme	(Kaneko <i>et al</i> , 1999)
	Up-regulate EDDSase	(Kato <i>et al</i> , 2000; Mizunashi, 2001)
Production of R,S-EDDS	Low temperature	(Hiroyasu <i>et al</i> , 2000a)
Back reaction	Excess fumarate	(Kaneko <i>et al</i> , 1999)
	ISPR: Complex formation	(Kaneko <i>et al</i> , 1999)
Heat Production	External heat exchanger	(Shigeo <i>et al</i> , 2004)

Table 3-2 - Known EDDSase Reaction Bottlenecks

3.3.2 Possible Downstream Processing Routes

Currently S,S-EDDS is produced by means of calcium-aspartate and 1,2-dibromoethane, the calcium-aspartate has a natural buffering capacity and with careful pH maintenance, calcium-EDDS is produced which crystallises readily and can therefore be removed from the reaction broth by centrifugation or filtration (Figure 3-8). Furthermore as can be seen in Table 3-1 above the use of the calcium salt with a low overall stability constant provides an easy route to other metal-salts of EDDS or to sodium-EDDS by neutralisation of the Ca-EDDS by sodium hydroxide (Layman *et al*, 1996). Since EDDS as a free acid is very insoluble in water, EDDS can be removed from reaction liquors as a solid following acidification to a range in which other contaminating substances remain soluble (St George and Wilson, 1998). However acid precipitation methods commonly have problems with co-precipitation which must be overcome (Lin *et al*, 1996).

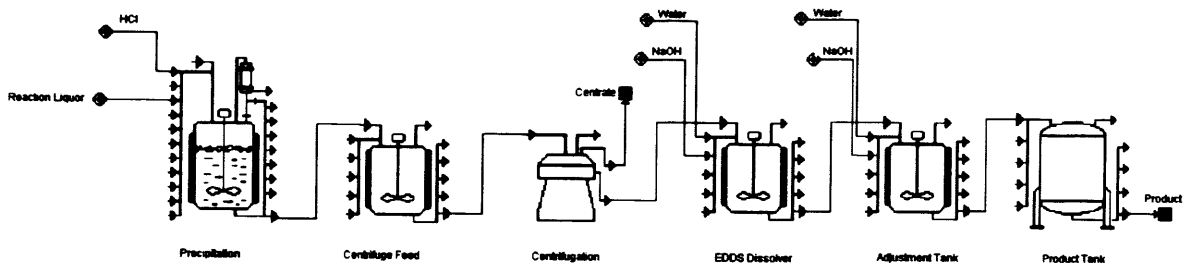


Figure 3-7 – Possible Downstream Processing Route for purification of S,S-EDDS

3.4 REACTANT PROPERTIES

3.4.1 ED

Ethylenediamine or ethane-1,2-diamine is a liquid at normal temperature and pressure, strongly alkaline (Table 3-3) and very soluble in water and alcohol. Ethylenediamine is not volatile in aqueous solution, but is expected to be volatile from soils or peat and in fact can be explosive if a vapour/air mixture forms above 34°C. Since ethylenediamine is a bidentate chelant, chelation is expected, but it breaks down rapidly in the environment, most likely by biodegradation. However, ethylenediamine is a known irritant, corrosive when undiluted and a skin sensitiser. It has not currently been tested for mutagenicity.

ED has the capability of inducing respiratory tract sensitivity and can be a cause of occupational asthma, although the mechanism by which this happens is not yet known. As a result occupational exposure limits have been set at 100ppm as a time weighted average threshold limiting value (TLV). Care must be taken in handling, good ventilation and full personal protective clothing is required (Cary *et al*, 1999).

3.4.2 Fumarate

Fumaric acid is a solid at standard temperature and pressure, and creates a weakly acidic solution in water (Chemfate, 2003), pKas in Table 3-4 below and has a log P_{ow} of 0.25 (Syracuse Research Corporation, 2006). Fumarate is not particularly soluble in water with the free acid having a solubility of 6.3 g.l⁻¹, however the di-sodium salt is soluble to 220g.l⁻¹.

3.4.3 EDMS

There is very little physical property information for EDMS (Beilstein database, 2006), however it is known that EDMS is very soluble in water and makes an alkaline solution (pH 13-14) (Ethylenediamine monosuccinate MSDS (2002), Octel Corp).

Ethylenediamine property	Value
<i>pKa</i> ¹	9.72
<i>pKa</i> ²	6.92
<i>Log P_{ow}</i> ¹	-1.2
<i>Vapour pressure</i> ²	1.2 kPA at 20°C
<i>Flash point of vapour/air mixture</i> ²	34°C
<i>Occupational exposure limit</i>	100ppm TLV

Table 3-3 – Physical properties of ethylenediamine. Sources: 1) Beilstein database, substance entry beilstein preferred RN: 107-15-3 Ethane-1,2-diamine. 2) (Cary et al, 1999)

Fumarate Property	Value
<i>pKa</i> ¹	3.01
<i>pKa</i> ²	4.31
<i>Log P_{ow}</i> ²	0.25
<i>Solubility free acid</i> ¹	6.3 g.l ⁻¹
<i>Solubility di-sodium salt</i> ¹	220 g.l ⁻¹

Table 3-4 – Fumarate physical properties. Sources: 1) Beilstein database, substance entry beilstein preferred RN 110-17-8 Fumarate. 2) (Syracuse Research Corporation, 2006)

3.5 CHOICE OF S,S-EDDS AS A MODEL PRODUCT

S,S-EDDS was chosen as a target product on the basis of several factors including:

1. An established chemical process. As there was an already established industrial chemical process, benchmarks were available against which to assess any possible alternative process routes. Interestingly, there were more than two possible process route alternatives.
2. A wide range of literature was available. The literature covered a great deal of the required knowledge of the physical properties of EDDS, though there were still some small areas in which information was hard to discover. Physical properties and health and safety issues of reactants were available though very little was known about EDMS. Furthermore, while there was a large amount of EDDSase related literature, this was mainly focussed on biodegradation work rather than large-scale processes. What process literature there was tended to be published in patents suggesting possible processing strategies, but it was unknown if this information represented a best process or otherwise as industry is often unwilling to publish best experimental data for competition reasons. However, the reaction pathway is not well defined and there is no information on the method by which EDDSase is induced in the wild type.
3. A method of producing biocatalyst was identified in the biodegradation and patent literature and possible microbes with EDDSase activity were suggested in the absence of a recombinant.
4. The system was complex enough to provide a challenge for possible process analysis tools. The bottlenecks suggested by the review of the patents such as side reactions, the necessity for the correct stereoisomer, solubility issues, health and safety considerations and non-advantageous equilibria, suggested that the EDDSase process would be an ideal candidate on which to test process analysis

tools as these were realistic processing problems and any method of process analysis and evaluation needed to be able to identify and assess these factors.

3.6 CONCLUSION

The biocatalytic production of S,S-EDDS by EDDSaase was chosen to be the model system as this provided a complex reaction system with the potential to reduce the cost of S,S-EDDS on which process analysis and evaluation tools could be tested. Particularly as the established industrial route provided benchmarks for any possible process. Whilst the knowledge of the biocatalytic production of S,S-EDDS is growing, much is still unknown, including a definitive reaction pathway, mechanism of induction in wild type strains, whether the process requires one or two enzymes and reactant properties at optimal reaction conditions. Furthermore, reaction kinetics have been defined on an isolated enzyme basis, but what information there is on the use of whole cell biocatalyst derives from patents, which are notoriously difficult to examine in any detail. As such initial characterisation of the biocatalytic route to S,S-EDDS was required to start with the accumulation of the missing data.

4 BIOCATALYST PRODUCTION

4.1 INTRODUCTION

As can be seen from the previous chapter much work has been undertaken on EDDSase. However, much of the literature takes the form of patents providing little basis for understanding or scope for assessment of the size and position of process limitations. Reaction characterisation commonly covers several areas, not least the reaction but also the reactor, reaction system, enzymes and physical characteristics. Therefore this chapter sets out to complete the characterisation of the EDDSase reactions. Before this was possible however, a source of enzyme and a method of producing it was required. As such this chapter contains initial sourcing and selection of wild type strains as well as some fermentation data, so that an effective characterisation of the reaction system, enzyme and physical properties could be carried out

4.2 METHODS

4.2.1 Analytical Methods

4.2.1.1 Spectrophotometric Analysis of Cell Concentration

Cell growth was monitored by spectrophotometric analysis (Uvikon 922, Kontron, Watford, Herts, UK) of the absorbance of cells in culture media at 600 nm. The absorbance of the cells at 600 nm was related to dry and wet cell masses for all six strains, 1-5 and 17 and *Chelatococcus asaccharovorans*. The mass of dry 1.5 ml eppendorf tubes was determined and filled with 1ml cell broth at varying concentrations for 1-5 and 17. For *Chelatococcus* the dry and wet cell weights were determined in 50 ml falcon tubes using 10 ml samples in triplicate. 1.5ml micro test-tubes were centrifuged at 13,000 rpm for 4 minutes (16060g Heraeus Biofuge 13, Kendro Laboratory Products, Bishops Stortford, Herts, UK) and 50 ml falcon tubes centrifuged at 3,500 rpm for 30 minutes (1989 g, Beckman GS6 tabletop (GH-3.8 rotor), Fullerton, CA, USA) and supernatant discarded. Triplicate wet cell weights were taken

immediately and then dry cell weights after drying overnight in an 80°C oven (Heraeus, Kendro Laboratory Products, Bishops Stortford, Herts, UK). Coefficients produced by taking the linear portion of the calibration curve (below optical densities of 1) can be seen in Table 4-1.

	Coefficient $A_{600\text{nm}} \cdot \text{g}_{\text{dcw}}^{-1}$	R²	σ
Strain 1 – not identified (pit strain)	0.7164	0.9855	0.48
Strain 2 – not identified (pit strain)	0.6985	0.9892	0.47
Strain 3 – not identified (pit strain)	1.0171	0.9823	0.29
Strain 4 – not identified (pit strain)	0.8364	0.9702	0.23
Strain 5/ <i>Brevundimonas diminuta</i>	1.38	0.9828	0.07
Strain 17/ <i>Paracoccus sp.</i>	0.4002	0.9559	0.02
<i>Chelatococcus asaccharovorans</i>	1.71	0.9995	0.03

Table 4-1 Optical density- dry cell weight calibration coefficients

4.2.1.2 HPLC analysis

S,S-EDDS, R,S-EDDS, EDMS, fumaric acid and malic acid were analysed by reverse phase HPLC (Beckman Gold Chromatograph, Beckman-Coulter, High Wycombe, Bucks, UK) on a C8 column (Spherisorb, S5C8, Waters, Elstree, Herts, UK). Analysis was by ultraviolet absorption at 254nm. Eluent was used as sample diluent and consisted of 1 g Cu(CH₃COO)₂, 1.99 g tetrabutylammonium hydroxide (TBAH), 45ml methanol (HiPerSolv for HPLC, VWR, Poole, Dorset, UK) in 1 litre 18MΩ resistivity water, so as to ensure the eluent was consistent between batches and water born impurities that could affect the chromatography were avoided. The eluent was adjusted to pH 3.10 ± 0.02 with orthophosphoric acid (HPLC grade, VWR, Poole, Dorset, UK) and filtered through a 474 Filter paper (VWR, Poole, Dorset, UK). Samples were prepared by dilution in eluent, mixed, centrifuged at 13,000 rpm for 2 minutes (16060g Heraeus Biofuge 13, Kendro, Bishops Stortford, Herts, UK) to remove precipitates and 0.2 µm filtered (Minisart NML, Vivascience, Epsom, Surrey, UK) prior to injection at 20 µl onto the column. Standards were prepared at approximately 1 g.l⁻¹ for each acid in 18 MΩ water, with sufficient 12.5 M NaOH added dropwise to create

sodium salts of fumarate and S,S-EDDS and enable complete dissolution. Standard curves were typically prepared using 5 separate dilutions of the prepared standard solution, the resulting retention times and concentration-absorbance calibration coefficients can be seen below in Table 4-2 and Table 4-3 respectively.

Species	All retention times (min)			Retention time single batch eluent (min)		
	\bar{x}	σ	CV	\bar{x}	σ	CV
S,S-EDDS	15.1	2.5	16.9%	16.4	0.1	0.6%
R,S-EDDS	12.1	0.1	0.5%	12.1	0.1	0.5%
fumarate	12.6	2.0	15.9%	13.9	0.1	0.7%
malic	4.7	0.2	4.8%	4.9	0.1	2.0%
succinic	3.8	0.1	1.5%			
EDMS	2.6	0.1	2.3%	2.6	0.1	4.5%

Table 4-2 – Average retention time for various EDDS related compounds when analysed by HPLC

Species	Calibration coefficient single batch ($A_{254nm} \cdot g^{-1}l$)		
	\bar{x}	σ	CV
S,S-EDDS	250.9	7.707153	3.1%
fumarate	222.6	13.53258	6.1%
malic	249.9	20.83076	8.3%
EDMS	287.5	1.487228	0.5%

Table 4-3 – Absorbance - concentration calibration coefficients for HPLC analysis of EDDS related compounds

4.2.1.3 Glucose Assay

Glucose concentration was measured by a method which assays for the presence of free carbonyl groups, the reducing sugars (Dubois *et al*, 1956). The assay oxidises the aldehyde group of glucose and the ketone group in fructose by the reduction of 3,5-dinitrosalicylic acid (DNS) to 3-amino,5-nitrosalicylate in alkaline conditions which absorbs at 540 nm. Alkaline DNS reagent was prepared from 16 g NaOH, 10 g dinitrosalicylic acid and 300 g sodium potassium tartrate in 1 litre distilled water.

Glucose standards were prepared by serial dilution of an approximately 1.8 g.l⁻¹ solution of glucose.

Fermentation samples, standard or water for referencing of the spectrophotometer were 0.2 µm filtered. 50 µl of filtered test sample was then taken and mixed with 100 µl of DNS reagent in a 1.5 ml boiling eppendorf tube (Eppendorf, Hamburg, Germany) and incubated at 80 °C for 5 minutes. This was then cooled on ice and 1ml of distilled water was then added to the microtube. The resulting solution was then tested for absorbency on a spectrophotometer at 540 nm (Uvikon 922 Spectrophotometer, Northstar Scientific, Bedford, Beds, UK)

4.2.1.4 Glycerol Assay

Glycerol was assayed by an enzyme linked UV assay kit (Glycerol UV method (Cat no 0148270), R-Biopharm, Darmstadt, Germany). This proceeded by reaction of glycerol and ATP by glycerolkinase to produce glycerol-3-phosphate and ADP. ADP was then reacted with phosphoenolpyruvate by pyruvate kinase to produce pyruvate and further ATP. This pyruvate was then reduced to L-lactate by lactate dehydrogenase with the corresponding oxidation of NADH to NAD⁺ (Figure 4-1). The reaction could be followed by following the drop in absorbance as NADH absorbs in the UV light region at 340 nm (922, Northstar Scientific, Watford, Herts, UK). The assay was checked by means of the use of the glycerol assay control solution provided with the assay kit.

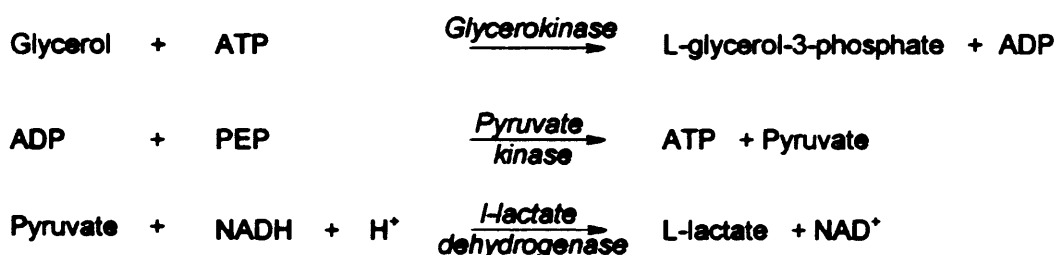


Figure 4-1 – Reaction schematic for glycerol UV assay

4.2.1.5 Ammonium Ion Assay

The concentration of ammonium was measured by the use of a modified indophenol blue method (Chemical Co-ordinating Centre of EMEP, 2004; Weatherburn, 1967). Phenol nitroprusside was made up by the addition of 3.5 g of phenol (Riedel de Haen, Poole, Dorset, UK) and 0.04 g sodium nitroprusside (Sigma-Aldrich, Poole, Dorset, UK) in 100 ml and stored in the dark below 4 °C. Alkaline hypochlorite was made up by the addition of 1.8 g NaOH and 4ml of sodium hypochlorite solution to 100 ml of distilled water, this was also stored below 4°C and in the dark. Standards were prepared by serial dilution from a 150 mg.l⁻¹ solution of NH₄Cl. 40 µl of sample, standard or water blank were taken, to which was added 0.5 ml of alkaline hypochlorite and 0.5 ml of phenol nitroprusside and well mixed. The reaction was left at room temperature for 30 minutes to incubate, following which the samples were transferred to a cuvette and absorbency tested by spectrophotometry (Uvikon 922, Northstar Scientific, Watford, Herts, UK) at 630 nm.

4.2.1.6 Bradford Assay for Free Protein

The Bradford assay for free protein uses the binding of the stain Coomassie blue with free protein to be able to elucidate the concentration of free protein by UV spectrophotometry. Serial dilutions of 1 g.l⁻¹ bovine serum albumin (Sigma-Aldrich, Poole, Dorset, UK) were used as standards. To test for concentrations of protein 20 µl of fermentation broth, standard or water for the reagent blank were taken and mixed with 1 ml of Biorad Coomassie blue reagent (Biorad, Hercules, California) in a 1 to five dilution in a 1.5 ml cuvette and well mixed. The absorbency of which was measured on a spectrophotometer at 595 nm (Uvikon 922, Kontron, Watford, Herts, UK).

4.2.2 Biocatalyst Production

4.2.2.1 Initial Isolation and Characterisation

Initially soil samples taken and purified from the waste pits at Octel's Ellesmere Port plant by Westlakes Ltd (Moor Row, Cumbria, UK) were streaked onto an agar medium

with S,S-EDDS as the sole carbon source, this consisted of EDDS Minimal Media and 20 g agar (VWR, Poole, Dorset, UK), which had been sterilised at 121 °C for 20 minutes. The strains were then purified on EDDS GYP agar plates consisting 2 % w/v agar (VWR, Poole, Dorset, UK) and was sterilised at 121 °C for 20 minutes. Cells from GYP slopes of strains 5 and 17 were streaked onto Petri dishes containing a minimal agar medium with S,S-EDDS as the sole carbon source, consisting of 21.8 mg K₂HPO₄, 8.5 mg KH₂PO₄, 44.6 mg Na₂HPO₄.12H₂O, 1.7 mg NH₄Cl, 22.5 mg MgSO₄, 116.3 mg CaCl₂, 0.3 mg FeCl₃.6H₂O, 2.0 g S,S-EDDS (Octel Corp, Ellesmere Port, Cheshire, UK), and 20g agar (agar agar, VWR, Poole, Dorset, UK), which had been sterilised at 121 °C for 20 minutes (Takahashi *et al*, 1999).

Colonies were then grown up for 5 days in an incubator at 28 °C, a colony was then picked from these plates and then streaked onto full strength nutrient broth (Oxoid, Basingstoke, Hampshire, UK) and 2% w/v agar (agar agar, VWR, Dorset, Poole, UK) slopes, which were then incubated at 28 °C for 3 days. These nutrient broth slopes were sent to NCIMB (Aberdeen, UK) for 16s rRNA sequencing and strain determination by comparison with Microseq and EMBL databases.

A further bacterial strain with the ability to degrade S,S-EDDS was obtained from DSMZ, the German Culture collection, this being *Chelatococcus asaccharovorans* (Egli *et al*, 1988; Witschel and Egli, 1998). *Pseudomonas putida* KT2440 and *Escherichia coli* JM109 were obtained from Professor John Ward of the Biochemistry Department, University College London.

4.2.2.2 Preparation of Master Stocks

Spread EDDS Minimal Media Agar plates of each strain were grown for 4 days at 28 °C to achieve pinhead sized individual colonies. The colonies on each plate were then dissolved in 3 ml of 25 % v/v glycerol/ water solution (Sigma-Aldrich, Poole, Dorset, UK), collated and then aliquoted into 1 ml eppendorfs and stored at -80°C.

4.2.2.3 Shake Flask Fermentation

Liquid culture media was prepared according to Table 4-4, with components likely to precipitate out such as magnesium, calcium and iron autoclaved separately. For EDDS minimal media, sodium and potassium phosphates, S,S-EDDS and ammonium chloride were autoclaved together in 989 ml in masses that would provide the correct concentration when additional concentrated components were added. Magnesium and calcium due to their propensity to precipitate particularly with a chelating agent present were autoclaved separately as an acidified 100-fold concentrated solution. Iron was also autoclaved separately as an acidified 1000 fold concentrated solution. When the basic media lacking Ca, Mg and Fe had cooled to approximately 50 °C, 10 ml of the concentrated calcium and magnesium solution and 1 ml of the concentrated iron solution were added to the EDDS minimal media under aseptic conditions. The resulting solution was adjusted to pH 7.5 by dropwise addition of 4 M KOH by sterile transfer and aseptic removal of samples for testing to verify pH of final media was 7.5. For GYP media $MgCl_2$, $MnSO_4$, $ZnSO_4$, $CaCl_2$ and $FeCl_3$ were autoclaved as an acidified 200 fold concentration solution.

Inocula were either from streaked minimal media agar plates or varying concentrations of glycerol stock inoculated directly into a 20 ml McCartney bottle containing 10 ml of the media to be used for that experiment and incubated at 28 °C with shaking. Once cells in the McCartney were seen to have entered the exponential phase they were then inoculated into 500 ml baffled shake flasks (polycarbonate, Nalgene, Hereford, UK) of 20 % working volume. Incubation was at 28 °C with ellipsoidal shaking at 200 rpm. This meant inoculum concentration from McCartney onwards was 10 %.

	GYP (Glucose, yeast and Peptone)	EDDS Minimal Media ^a	EDDS Minimal Media + glucose	EDDS Minimal Media + glycerol	EDDS Minimal Media, glycerol and NH4	Tryptone T or Nutrient Broth
$K_2HPO_4^b$ (g.l ⁻¹)		0.0218	0.0218	0.0218	0.0218	
$KH_2PO_4^b$ (g.l ⁻¹)	2.72	0.0085	0.0085	0.0085	0.0085	
$Na_2HPO_4 \cdot 12H_2O^b$ (g.l ⁻¹)	10.74	0.0446	0.0446	0.0446	0.0446	
NH_4Cl (g.l ⁻¹) ^c		0.0017	0.0017	0.0017	0.1	
$MgSO_4^b$ (g.l ⁻¹)	0.8307	0.0225	0.0225	0.0225	0.0225	
$CaCl_2^b$ (g.l ⁻¹)	0.0389	0.1163	0.1163	0.1163	0.1163	
$FeCl_3 \cdot 6H_2O^b$ (g.l ⁻¹)	0.0006	0.0003	0.0003	0.0003	0.0003	
S,S-EDDS ^f (g.l ⁻¹)	2	2	2	2	2	2
Glucose ^b (g.l ⁻¹)	2		1			
Glycerol ^e (g.l ⁻¹)				1	5	
Yeast extract ^d (g.l ⁻¹)	1					
Peptone ^d (g.l ⁻¹)	0.5					
$MgCl_2 \cdot 6H_2O^c$ (g.l ⁻¹)	0.4006					
$MnSO_4 \cdot 4H_2O^c$ (g.l ⁻¹)	0.0038					
$ZnSO_4^c$ (g.l ⁻¹)	0.0003					
NB or TT ^d (g.l ⁻¹)						10
PPG 2000 ^e (drop.l ⁻¹)	Drop	Drop	Drop	Drop	Drop	Drop
pH	7	7.5	7	7	7	7

Table 4-4 - Media Recipes. Notes: a. (Takahashi *et al*, 1999), b. Sigma-Aldrich, Poole, Dorset, UK, c. VWR, Poole, Dorset, UK, d. Oxoid, Basingstoke, Hampshire, UK, e. Fluka, Poole, Dorset, UK, f. Octel Corp, Ellesmere Port, Cheshire, UK

4.2.3 Enzymatic Assays

4.2.3.1 Enzyme Production

Catalyst was produced by means of a 2 l Fermentation. Cultures were started from 1 ml frozen 20 % glycerol stock, defrosted and inoculated into 9 ml sterile EDDS minimal media in a 50 ml Falcon tube (20 % working volume) and incubated at 28 °C with shaking at 200 rpm (Kühner, Birsfelden, Switzerland) for 2 days until the optical density at 600 nm reached 0.7 absorbency units (Measured on a Uvikon 922 Spectrophotometer, Northstar Scientific, Bedford, Beds, UK). EDDS minimal media consisted of 2 g S,S-EDDS as Na₃-S,S-EDDS (6.5 g, Octaquest E30, Associated Octel, Ellesmere Port, Cheshire, UK), 21.8 mg K₂HPO₄, 8.5 mg KH₂PO₄, 44.6 mg Na₂HPO₄.12H₂O, 1.7 mg NH₄Cl, 22.5 mg MgSO₄, 116.3 mg CaCl₂ and 0.3 mg FeCl₃.6H₂O (Takahashi *et al*, 1999) in 1 litre reverse osmosis water and at pH 7.5. Media was tested for sterility following sterilisation by taking 1 ml samples of broth which were spread onto nutrient agar plates. Once A_{600nm} had reached 0.7, the starter cultures were inoculated into 500 ml baffled shake flasks (Nalgene polycarbonate, Nalge (Europe) Ltd, Hereford, UK) also containing EDDS minimal media (working volume 20 %, inoculum 10 %, 28 °C incubation with shaking) and monitored twice daily until the A_{600nm} reached 0.7, typically 5 days, and samples removed for HPLC analysis confirmed that growth was on S,S-EDDS. A 10% inoculum was then taken from these shake flasks and used to inoculate a 2 l Bioreactor (Inceltech, Toulouse, France) containing EDDS minimal media and operating at 75 % working volume. pH was controlled at 7.5 by metered addition of 4 M KOH and 4 M H₃PO₄ as required. Temperature control kept the vessel at 30 °C by the use of an external heating jacket. Aeration was by submerged sparger with airflow set at 0.67 vvm and stirrer speed controlled manually at 500 rpm. Samples were withdrawn at regular intervals and analysed for S,S-EDDS and EDMS concentrations by HPLC and optical density. Cells were harvested once EDMS concentration had reduced to below 0.02 g.l⁻¹. Typical cell concentration was 0.5 g_{dcw}.l⁻¹ (coefficient of variance = 23 %), where cell concentration

is related to optical density by the following relation: cell concentration ($\text{g}_{\text{dcw}} \cdot \text{l}^{-1} \pm 3\%$) = $1.72 A_{600\text{nm}} + 0.25$, $R^2 = 0.9995$.

Cells were harvested by centrifugation, typically at 10,000 rpm (17649 g, Beckman JA10 bowl, Fullerton, CA, USA) at 4 °C for 30 minutes, the supernatant discarded, the pellet washed twice and then resuspended in approximately 10ml of cold 50mM phosphate buffer at pH 7.5. For whole cell assays these resuspended cells were used directly, but for experiments using crude enzyme isolate, the cell suspension was sonicated (Soniprep, MSE, London, UK) on ice in 10 pulses of 10 seconds with 10 second rests between pulses. The sonicated cell suspension was then clarified by centrifugation at 13,000 rpm for 30 minutes at 4°C (15588 g, Microcentrifuge 5415R, Eppendorf, Hamburg, Germany) and then sterile filtered (0.2 μm Minisart NML, Vivascience, Epsom, Surrey, UK) to remove any remaining bacterial cells.

4.2.3.2 Typical Reaction

Reactions were typically carried out at 30 °C and at 10 ml in a heated, shaken waterbath (200 rpm orbital, Grant Scientific, Cambridge, UK) or 1ml in a heated micro-test-tube mixer (1000 rpm, orbital, Thermomixer, Eppendorf, Hamburg, Germany). For every set of reactions at least one reaction was carried out as typical to be able to compare between batches of enzyme, this typical reaction used a reaction solution as described below.

Reaction solution was produced by mixing 250 mM fumaric acid, 100 mM ethylenediamine and 50 mM phosphate ions (as $\text{K}_2\text{HPO}_4 \cdot 3\text{H}_2\text{O}$) in 1 litre of reverse osmosis water, pH adjusted to 7.5 ± 0.05 with 10 M KOH. This solution was autoclaved in order to produce R- and S-EDMS. The resultant concentration of mixture-EDMS in this solution was 0.6 % w/v, fumarate, 2.4 % and ethylenediamine, 0.4 %. Some R,S- and S,S-EDDS were also produced during the autoclaving process, these amounted to 0.07 % w/v of the solution.

Reaction solution was brought to temperature prior to the start of reaction and reactions were started by the addition of a 1:10 ratio of enzyme isolate to reaction solution. Samples were removed at regular intervals and the reaction stopped in these samples by the addition of 1 M HCl totalling a tenth of the sample volume. These samples were then diluted appropriately with copper acetate/TBAH diluent, prepared as described above and analysed by HPLC for concentrations of mixture-EDMS, R,S-EDDS, S,S-EDDS, fumaric and malic acids. For initial rate experiments reactions were stopped after an hour, for full reaction profiles, reactions were commonly sampled for at least 36 hours to ensure reactions had reached equilibrium. Fumarase rates were calculated from these data by calculation of initial rates so competing reactions could be considered negligible. Errors were calculated as described in Appendix 10-2.

4.2.3.3 EDMSase

EDMS lyase activity was assayed by following the production of EDMS by whole cell or crude enzyme isolate by HPLC. The synthetic reactant mixture consisted of varying proportions of ethylenediamine and fumaric acid with one or another in excess in 50 mM phosphate buffer at pH 7.5 and 0.2 μ m filter sterilised (0.22 μ m cellulose acetate disposable sterile filter, cat no 430767, Corning, Acton MA, USA). 1 ml of cell resuspension or enzyme isolate was added to 9 ml reactant mixture, incubated with shaking for 60 hours at 30 °C. Reaction samples were taken at time intervals and diluted according to the linear region of the HPLC calibration curve with the copper acetate and TBAH HPLC diluent and mixed well. The samples were then centrifuged at 13,000 rpm for 2 minutes (16060 g Heraeus Biofuge 13, Kendro Laboratory Products, Bishops Stortford, Herts, UK), and the supernatant filtered through a 0.2 μ m syringe filter (Minisart NML, Sartorius, Epsom, Surrey, UK) to be analysed by HPLC. Errors were calculated as described in Appendix 10-2.

4.2.3.4 Kinetics

Sensitivity of catalyst activity to reaction conditions was determined by changing various reaction conditions such as temperature, pH, PO₄ concentration independently and monitoring the effect on enzyme activity when provided with the standard reaction solution and all other conditions remained the same. Typically reactions were carried out in triplicate, when analysis was a bottleneck, several samples at the beginning, middle and end of the time course were taken in triplicate and the standard reaction triplicated. The inhibitor of fumarase 2-hydroxy-2-nitropropionate was synthesised from glyoxylate and nitromethane by the method of (Shechter and Conrad, 1953). Reaction kinetics were determined both by providing enzyme with mixture EDMS, ED and fumarate for reactions assessing EDDSase activity or ED and fumarate for reactions assessing all activities in varying proportions in the presence of 50mM phosphate ions and at pH 7.5. All other reaction conditions were kept as described in 4.1.2.3.

4.2.3.5 Equilibrium Position

Reaction equilibrium position was determined for the second half reaction to EDDS from EDMS by providing catalyst with varying concentrations of EDMS, fumarate and ethylenediamine at constant phosphate ion concentration (50 mM) and pH (7.5 ± 0.2). Reaction solutions were autoclaved prior to addition of catalyst to produce an equilibrium mixture of R- and S-EDMS, fumarate and ethylenediamine. Reactions were carried out as stated in 4.2.3.2 using the above solutions and left until equilibrium had been reached. To verify the equilibrium position additional enzyme was provided to the reaction after 36 hours at which point samples were removed for analysis. The reactions were then left to equilibrate for a further 36 hours before sampling further.

4.2.4 Chemical Reaction to EDMS

4.2.4.1 Temperature Dependence of EDMS Chemical Reaction

To determine if there was a significant side reaction to EDMS, ethylenediamine and fumarate were added to universal tubes (10 ml volume, 30% w/v) in varying proportions

at pH 7.5 in the presence of 50mM phosphate buffer, mixed by vortex and run at several different temperatures, 4 °C (refrigerator), 19 °C (room temperature) and 50 °C (Waterbath, Grant Scientific, Cambridge, UK) without further mixing. Triplicate 20 µl samples were removed at intervals over 3 weeks and analysed for EDMS and fumarate concentrations by HPLC.

4.2.4.2 Determination of EDMS Chemical Reaction Constants

The kinetic constants of the chemical half reaction to EDMS were determined by the initial rate method together with isolation of one component, thereby reducing the kinetics to apparent first order. Reactions were provided with four different concentrations of ethylenediamine in at least 100-fold excess over fumarate at varied concentrations at pH 7.5 in 50 mM phosphate buffer, so it could be said that the concentration of ethylenediamine remained constant over the course of the reactions. Reactions were carried out at 50 °C, in 10 ml Rohre tubes (Sarstedt, Numbrecht-Rommelsdorf, Germany) to provide enough sample for analysis and mixed at 200 rpm in a shaking waterbath (Grant Scientific, Cambridge, UK). Samples were removed daily over a week, diluted 10-fold and analysed for fumarate and EDMS by HPLC. Samples at beginning, middle and end of the reactions were taken in triplicate to determine sampling and analysis error.

4.2.5 Solubility

Fumarate solubility was determined in 1 ml reaction tubes, held at 30 °C, the temperature at which reactions were typically carried out and mixed by shaking at 1000 rpm (Thermomixer comfort, Eppendorf, Hamburg, Germany). A large excess of fumaric acid (0.5 g free fumarate, equivalent to 500 g/l and 100-fold greater than the literature solubility of free acid in reverse osmosis water) was added to each reaction tube and mixed with varying proportions of reverse osmosis water and 10 M KOH, to make up 900 µl of liquid component at varying pHs. Samples were taken daily until it could be confirmed that equilibrium was reached by spinning reaction tubes by

centrifugation at 2,000 rpm for 1 minute (400 g, Heraeus Biofuge 13, Kendro, Bishop Stortford, Herts, UK), 20 μ l of the supernatant was removed for pH analysis and 10 μ l removed and diluted 10,000-fold for duplicate HPLC analysis of soluble fumarate concentration. pH was analysed by the use of pH sticks accurate in the range pH 0-14 \pm 1 (Fisher, Loughborough, UK) and when pH was in the range 6-8 was checked with pH paper accurate in the range pH 6-8 \pm 0.2 (Whatman, Brentford, Middlesex, UK).

EDDS solubility with respect to pH was determined in a similar manner. 10 ml of Na₃-EDDS solution (30.9 % w/v, Octaquest E30, Associated Octel, Ellesmere Port, Cheshire, UK) was placed in a 50 ml beaker and mixed by magnetic stirrer bar, pH was monitored by pH probe (VWR, Lutterworth, Leicestershire, UK) and meter (Hanna, Leighton Buzzard, Beds, UK). pH was altered by the metered addition of 1 M HCl by burette and 1 ml samples removed at intervals, spun at 13,000 rpm for 1 minute (16060 g Heraeus Biofuge 13, Kendro, Bishop Stortford, Herts, UK) and supernatant diluted ready for analysis of EDDS concentration by HPLC.

4.3 RESULTS

4.3.1 Biocatalyst Production

4.3.1.1 Strain Selection

Strains 1-5 and 17 were isolated by Westlakes Ltd from Ocel Corp's Ellesmere Port S,S-EDDS plant waste pit. These strains were grown on arrival on glucose, yeast and peptone agar containing S,S-EDDS (EDDS GYP) at 2% w/v and incubated at 28°C as recommended by Westlakes. The growth on the GYP agar did not produce any individual colonies due to the formation of a large amount of capsular material from the bacteria. The strains were then purified by inoculation of one loopful of bacterial colony from the EDDS GYP onto a minimal agar containing 2% w/v S,S-EDDS as sole carbon source (EDDS MA) and incubated at 28°C, taking approximately 6 days to produce colonies the size of a pin head. Strains grown on this minimal agar produced far less capsular material and enabled the inoculation of an individual colony of each strain into 10 ml (50% w/v) of minimal liquid media also containing 2% w/v S,S-EDDS as the next step in an inoculum train to produce 100 ml of culture at an optical density of at least 0.5 absorbency units measured at 600 nm, which could then be laid down as master stocks using glycerol at 20% v/v as a cryopreservant, this process took approximately 12 days from inoculation into the Falcon.

Chelatococcus asaccharovorans (*Chc. asacc*) was obtained from DSMZ (DSMZ 6461) as a freeze dried pellet and reconstituted according to the instructions. A loop of reconstituted culture was inoculated both onto selective EDDS minimal agar and the plate count agar and incubated at 28°C, taking 11 days for pin head sized colonies to form on the plate count agar and 15 days on EDDS MA. Masters of *Chc. asacc* were then laid down as 20% glycerol stocks and stored at -80 °C.

A BLAST search on the sequence published by Mitsubishi (Kato *et al*, 2000) indicated that several strains carried Argininosuccinate lyase (ASL) with 30% homology to EDDSease, including *Lactococcus lactis* and *Pseudomonas putida* KT2440. With this in

mind, *Pseudomonas putida* was obtained from Professor John Ward (UCL Biochemistry and molecular biology) and plated out on EDDS MA to test for growth on S,S-EDDS. Pinhead sized colonies were obtained after 5 days of incubation at 28°C and master stocks prepared as described above.

Studies of strains 1-5 and 17 growth curves and corresponding pH profiles, indicated that strains 1 and 17 and strains 2-4 were similar, with strains 1 and 17 dropping in pH during fermentation and strains 2-4 increasing in pH in the absence of pH control. This was further confirmed by inspection of pellets resulting from centrifugation of culture, with strains 2-4 being a cream colour and strains 1 and 17 creamy white. Inspection under a microscope at 1000x magnification (10x eyepiece and 100x oil immersion lens) (Leica, Milton Keynes, Bucks, UK) indicated that all strains were very small cocci. As a result of these similarities it was decided to send strains 5 and 17 for 16S ribosomal DNA (rDNA) sequencing (Appendix 10-3), which returned that strain 5 was a *Brevundimonas diminuta* and strain 17 *Paracoccus* sp. determined only to the species level.

Initial assays to test for EDDSase activity were undertaken following growth of all strains to 100 ml of culture each on EDDS minimal media. Since cell titre was low typically less than $0.5 \text{ g}_{\text{dcw}} \cdot \text{l}^{-1}$, cells were concentrated 10-fold by centrifugation, washing and resuspension in pH 7.5 50mM phosphate buffer. Cells were then provided with a 50mM phosphate based reaction solution at pH 7.5 containing 40mM fumarate and 40mM ethylenediamine and sampled over the course of 24 hours for S,S-EDDS concentration by HPLC analysis. Maximum specific activity can be seen in Figure 4-3 where fermentations batch 1 (S,S-EDDS as sole carbon source) and 2 (S,S-

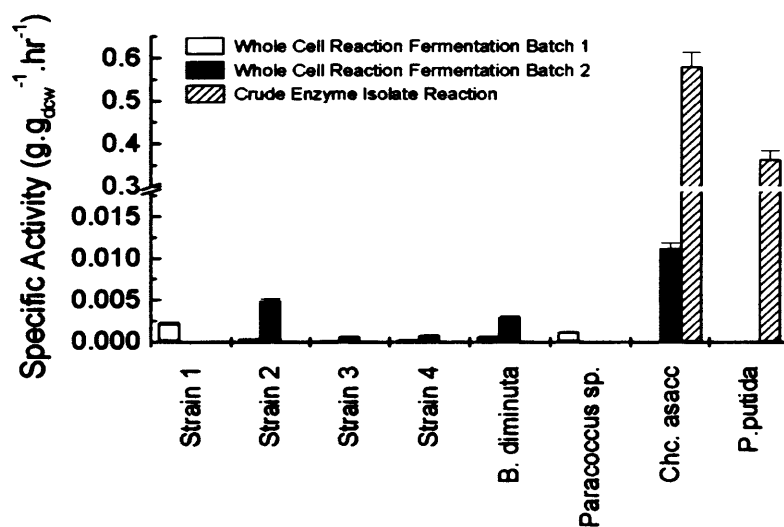


Figure 4-2 - Maximum Specific EDDSase Activity of Varying Strains. Fermentation batch 1, fed on S,S-EDDS as sole carbon source, biocatalyst concentrated by centrifugation (white), fermentation batch 2, fed on S,S-EDDS as sole carbon and nitrogen source, biocatalyst concentrated by centrifugation (grey) and *Pseudomonas putida* and *Chelatococcus asaccharovorans* reactions, fed on S,S-EDDS as sole carbon source, biocatalyst concentrated by centrifugation and sonicated to produce a crude enzyme isolate (hatched)

EDDS as sole carbon and nitrogen source) were carried out as whole cell reactions, indicating that where fermentations didn't fail, of the strains 1-5 and 17, strain 2, a suspected *Brevundimonas diminuta* and the identified *Brevundimonas diminuta* had the highest specific activity, but also that *Chelatococcus asaccharovorans* under the same conditions had a higher specific activity approximately 2x the rate of strain 2. Error (Appendix 10-2) in the measurement of these specific rates was approximately 6% and dependent mostly on sampling error and error in the determination of the dry cell weight calibration coefficient ran at an average of 5%. *Chelatococcus asaccharovorans* and *Pseudomonas putida* KT2440 were compared at a later date, with the EDDSase reactions being carried out using concentrated and sonicated crude enzyme isolate as the source of enzyme to minimise metabolic side reactions. It was assumed that most of the 10-fold increase in specific activity was a result of sonication. However, together with previous results *Chelatococcus asaccharovorans* was consequently chosen to be the strain with which to proceed. Interestingly Figure 4-3 indicates that activity from fermentations on S,S-EDDS as sole carbon and nitrogen source had greater specific activity than those provided with a small amount of NH₄Cl, though these fermentations are not comparable to those in Figure 4-4 due to the assay method having changed. These sole carbon and nitrogen fermentations were more prone to failure and doubling times typically 2-fold higher than media containing NH₄Cl.

4.3.1.2 Media Selection

Chelatococcus asaccharovorans (*Chc. asacc*) on EDDS minimal media had fermentations with doubling times typically between 4 and 20 hours, dependent on carbon source and doubling times of 16 hours when growing on S,S-EDDS. Final cell concentrations were typically $0.6 \text{ g}_{\text{dcw}} \cdot \text{l}^{-1} \pm 5\%$, resulting in low fermentation productivities of approximately $6.0 \times 10^{-3} \text{ g}_{\text{dcw}} \cdot \text{l}^{-1} \cdot \text{h}^{-1} \pm 2.0 \times 10^{-3}$. As a result, other fermentation media were tested both for their productivity (overall rate of production of biomass ie final cell concentration over the time taken for the fermentation to reach the

stationary phase) and resultant maximum EDDSase specific activity in comparison to EDDS minimal media.

These media sources were chosen to be:

1. EDDS minimal media plus glucose to boost initial growth, assuming that once the glucose had been consumed the EDDSase would be forced to be induced.
2. Inocula grown on nutrient broth to produce a strong inoculum with cells growing rapidly. Inoculated into EDDS minimal media, it was assumed that starvation of all other carbon sources would induce the EDDSase enzyme.
3. Nutrient broth with and without the addition of 2% w/v S,S-EDDS to encourage EDDSase expression.
4. Tryptone T broth with and without addition of 2% w/v S,S-EDDS. Tryptone T had particularly low concentrations of iron and zinc (3 and 11 ppm respectively compared to 50 ppm iron and 94 ppm zinc in nutrient broth). Literature had indicated a link between zinc limitation and S,S-EDDS production ((Cebulla, 1995; Goodfellow *et al*, 1997; Nishikiori *et al*, 1984).
5. EDDS GYP, a media first designed by Takahashi *et al* (Takahashi *et al*, 1999), which with the inclusion of small concentrations of complex components was expected to produce better cell titres whilst inducing EDDSase expression.

As can be seen in Figure 4-4 below in all fermentations except those fed on EDDS GYP and EDDS MM, no EDDSase was induced.

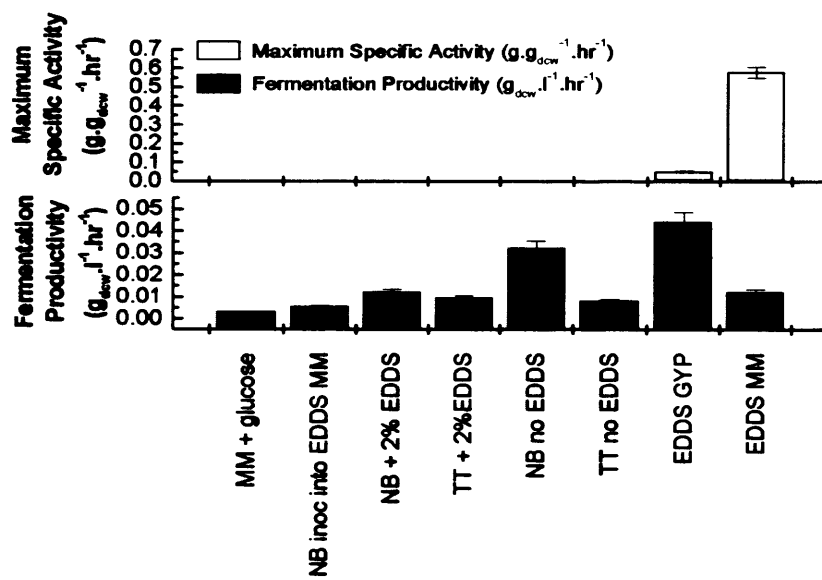


Figure 4-3 – Fermentation productivity and Maximum EDDSase specific activity for *Chelatococcus asaccharovorans* on various different media.

4.3.1.3 Growth Characteristics

Biocatalyst was typically produced by 2 l fermentation of *Chelatococcus asaccharovorans* on EDDS minimal media at 30°C, pH was controlled at 7.5 by metered addition of 4 M phosphoric acid or 4 M potassium hydroxide on demand. Seed cultures were provided to the fermentation following a two step inoculum train, in which cells were provided to the next stage at 10% inoculum, in the exponential phase of growth and consuming S,S-EDDS as carbon source and typically at a concentration of 0.2 g_{dcw}.l⁻¹ or an optical density of 0.5 Abs at 600nm. Figure 4-5 shows that there are three distinct phases of growth, an initial growth phase from the point of inoculation for 6 hours, attributable to growth on glycerol from the master stock, glycerol was found to be at 0.4 g.l⁻¹ in the inoculum, however, concentrations in the 2 l fermenter were below the 0.04 g.l⁻¹ detection limit of the glycerol assay, with a doubling time of 1.8 hours, a region of growth from 6 hours to 32 hours with a doubling time of 14 hours, accompanying a corresponding consumption of S,S-EDDS, finally in the last phase, growth is stationary, but EDMS undergoes consumption at this point after having accumulated during the second phase of growth. Interestingly when *Chelatococcus asaccharovorans* was consuming S,S-EDDS the doubling time was consistently 16 hours ± 2 hours. Typical cell titre was 0.5 g_{dcw}.l⁻¹ ± 0.1. Respiratory quotient during the initial growth phase was 1, rising during the S,S-EDDS growth stage to rest at 2.5 when growth entered the stationary phase and EDMS consumption started. The data that can be seen in Figure 4-5 for respiratory quotient was smoothed using all 950 data points in the adjacent averaging algorithm provided with Microcal Origin, graph plotting software as a result of noise inherent in the collection of the gas data by mass spectrophotometer.

Interestingly there were fermentations that accumulated EDMS, but did not consume any of the produced EDMS in the third phase of growth and entering the decline phase instead (Figure 4-6), indicating that though EDDSase was present the necessary induction or expression for consumption or breakdown of EDMS had not occurred.

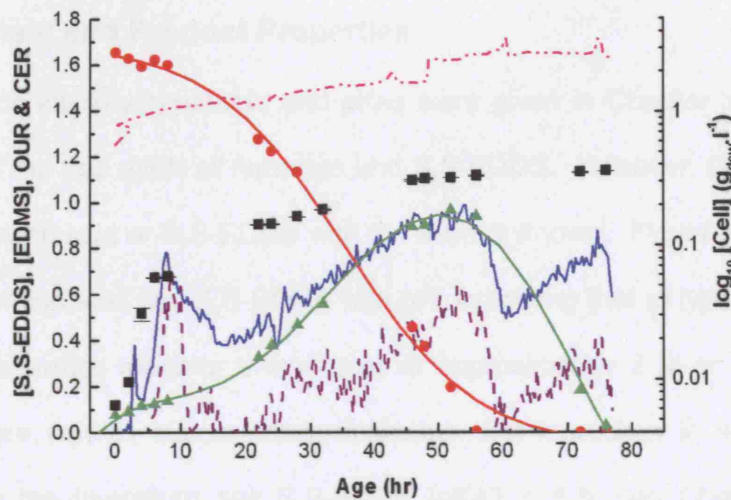


Figure 4-4 – Typical *Chelatococcus asaccharovorans* fermentation on EDDS minimal media. S,S-EDDS (g.l⁻¹) (●), EDMS (g.l⁻¹) (▲), cell concentration (gdcw.l⁻¹)(■), carbon dioxide evolution rate (mmol.l⁻¹.h⁻¹) (—), oxygen uptake rate (mmol.l⁻¹.h⁻¹) (---) and respiratory quotient (-..)

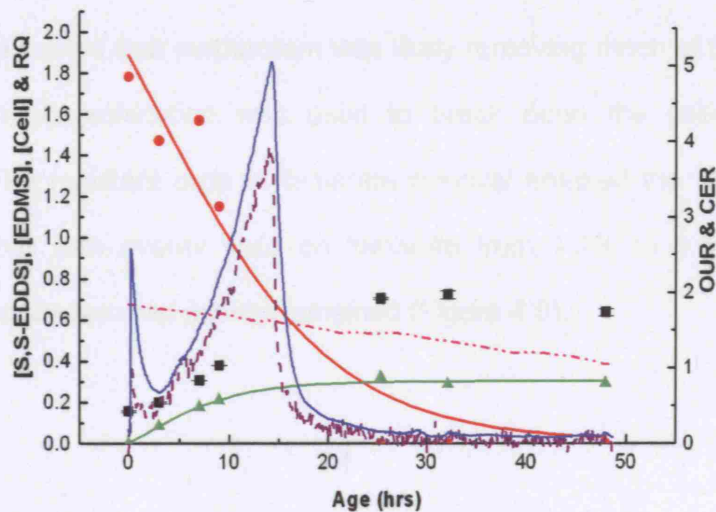


Figure 4-5 – *Chelatococcus asaccharovorans* fermentation on EDDS minimal media that failed to consume EDMS. S,S-EDDS (g.l⁻¹) (●), EDMS (g.l⁻¹) (▲), cell concentration (gdcw.l⁻¹)(■), carbon dioxide evolution rate (mmol.l⁻¹.h⁻¹) (—), oxygen uptake rate (mmol.l⁻¹.h⁻¹) (---) and smoothed respiratory quotient (-..)

4.3.2 Reaction Characterisation

4.3.2.1 Reactant and Product Properties

Typical chelation stability constants and pKas were given in Chapter 3, together with the solubility of the free acids of fumarate and S,S-EDDS. However, the correlation of solubility of fumaric acid or S,S-EDDS with pH were unknown. Figure 4-7 displays the solubility of Fumaric acid and S,S-EDDS with pH, indicating that at typical reaction pH, fumarate concentration reaches a maximum at approximately 2 M or 250 g.l⁻¹. S,S-EDDS as a free acid is almost totally insoluble, but increases in solubility as pH increases. As the tri-sodium salt S,S-EDDS (pKa3 = 6.8, see Chapter 3) is very soluble, to the extent that data was not collected due to lack of reagents. These data compare favourable to the literature values noted in Chapter 3.

4.3.2.2 Side Reactions

Initial reactions of concentrated *Chelatococcus asaccharovorans* as a whole cell catalyst had very low yields on fumarate, indicating that over 98% of the fumarate was being consumed by other reactions. Since fumaric acid is known to be citric acid cycle compound it was noted that metabolism was likely removing much of the reactant. To test the hypothesis sonication was used to break open the cells and minimise metabolism. The resultant drop in fumarate removal enabled the EDDSase rate to increase together with overall yield on fumarate from 1.2% to 3.5% even though substantial fumarate removal activity remained (Figure 4-8).

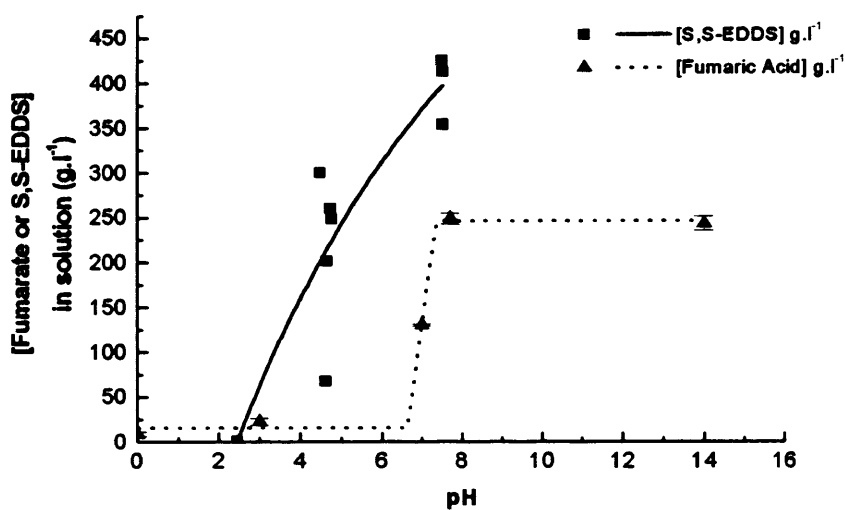


Figure 4-6 – Solubility of S,S-EDDS (■) and fumaric acid (▲) correlated with solution pH when provided with a large excess of solid

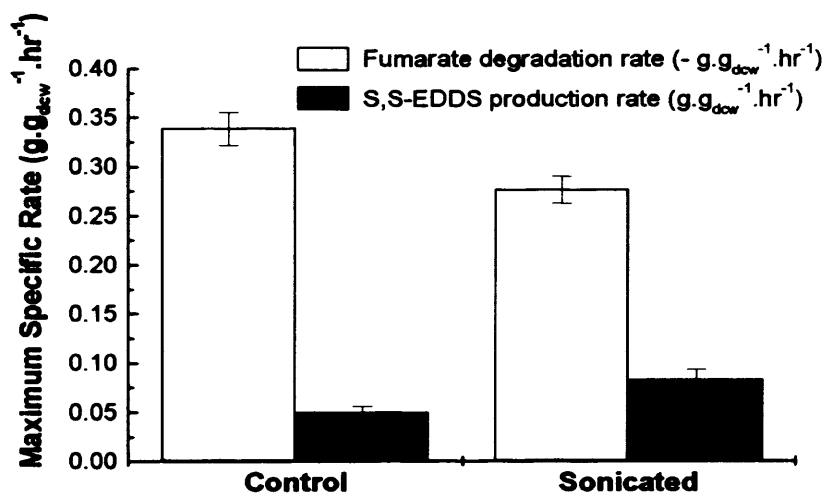


Figure 4-7 – Specific activity of EDDSase and Fumarase from *Chelatococcus asaccharovorans* produced by the same fermentation with two different catalyst formats: where catalyst in the control was concentrated by centrifugation prior to addition to the reaction and Sonicated indicates where the same centrifuged and concentrated catalyst suspension was sonicated and clarified prior to use.

Figure 4-8 indicated a further substantial side reaction since the maximum molar yield had still not exceeded 4%. Study of reaction profiles highlighted a substantial increase in a peak at 4.7 minutes, so several possible candidate reaction products were tested by spiking the compound to be tested into a standard on the HPLC. The candidates were succinic acid and malic acid, both TCA compounds and maleic acid, the *cis*-isomer of fumaric acid. As can be seen in Table 4-2, this peak corresponded to malic acid production, but also responded to addition of 2-hydroxy-3-nitropropionate a known inhibitor of fumarase (Figure 4-9) (Porter and Bright, 1980). Unfortunately as can be seen in Figure 4-9, 2-hydroxy-3-nitropropionate also inhibited EDDSase rate. Calculation of the equilibrium constant for fumarase ie malic acid over fumaric acid at equilibrium assuming water to be in large excess and therefore constant, at a value of 2, corresponded to those in the literature at K_{eq} of approximately 4 in the direction of malic acid (Flint, 1994). Finally, a *Chelatococcus asaccharovorans* reaction with the biocatalyst used in a crude enzyme isolate format was run and production of EDMS, S,S-EDDS and Malic acid formation studied, Figure 4-10 indicates that fumarase $5.3 \pm 1.9 \text{ g.g}_{dcw}^{-1} \cdot \text{h}^{-1}$ had far higher specific activity than either EDDSase $0.57 \pm 0.23 \text{ g.g}_{dcw}^{-1} \cdot \text{h}^{-1}$ or EDMSase $0.29 \pm 0.11 \text{ g.g}_{dcw}^{-1} \cdot \text{h}^{-1}$ with an approximately 10-fold higher maximum specific activity.

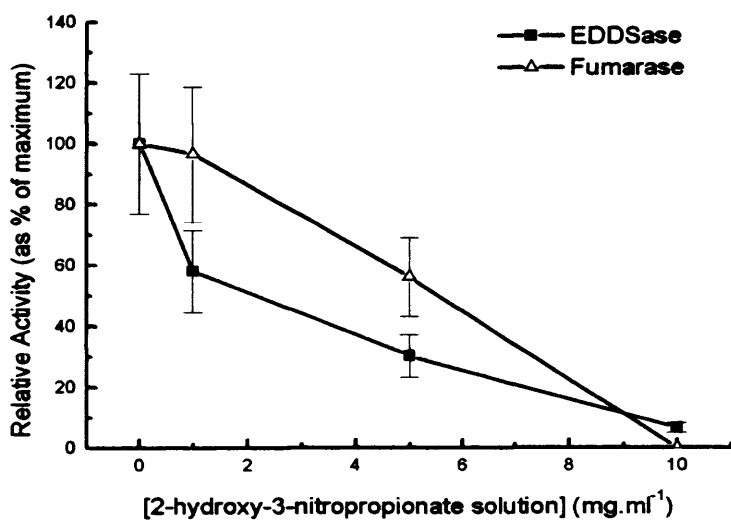


Figure 4-8– Inhibition of EDDSase and Fumarase initial rates by increasing concentrations of 2-hydroxy-3-nitropropionate, a known reactant analog inhibitor of fumarase

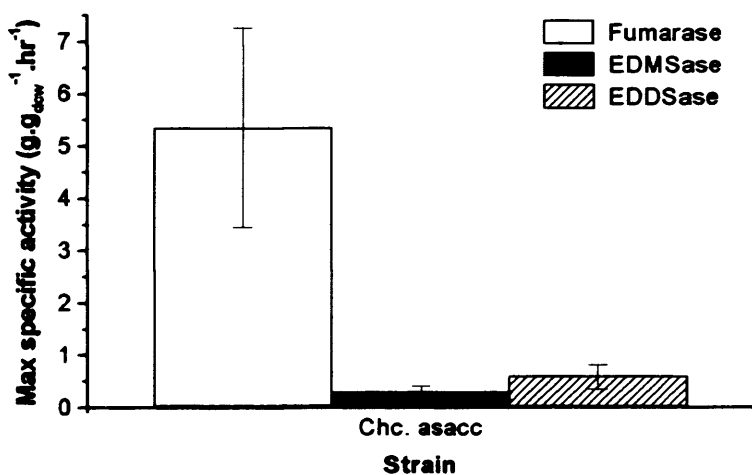


Figure 4-9 – Maximum specific activities of the three main activities found in S,S-EDDS grown *Chelatococcus asaccharovorans* (white) Fumarase, (grey) EDMSase and (hatched) EDDSase.

4.3.2.3 Reaction System

4.3.2.3.1 EDMS Chemical Reaction Characterisation

During reactions commonly some increase in optical density would be observed (an increase of 0.03 ± 0.005 absorbency units at 600nm – corresponding to an increase of $0.01 \pm 0.002 \text{ g}_{\text{dcw}}\cdot\text{l}^{-1}$), to this end it was decided to run reactions aseptically, with sterile reaction solutions and $0.2\mu\text{m}$ filtered crude enzyme isolate. Therefore it was required to establish if the reaction solution underwent change during sterilisation. Initial results indicated that it did. HPLC analysis determined that approximately $5 \text{ g}\cdot\text{l}^{-1}$ of EDMS had been created from a solution containing $29 \text{ g}\cdot\text{l}^{-1}$ fumaric acid and $6 \text{ g}\cdot\text{l}^{-1}$ ethylenediamine and the colour of the solution changed from clear to yellow-brown. To determine if this chemical side reaction was substantial an experiment was run varying concentrations of fumaric acid, whilst keeping ethylenediamine constant at $6 \text{ g}\cdot\text{l}^{-1}$ at differing temperatures. Reaction profiles were taken over the course of a fortnight and initial rates calculated by applying a tangent to the reaction curve over the first 5% of the time profile (approximately 1 day). As can be seen in Figure 4-11, as reaction temperature increases, initial rate of the chemical reaction to EDMS increases as would be expected for an exothermic reaction. Furthermore, increase in initial rate when provided with additional reactant was observed. It was interpolated from this data, that the chemical rate of *meso*-EDMS at typical reaction conditions was $0.006 \text{ g}\cdot\text{l}^{-1}\cdot\text{h}^{-1}$.

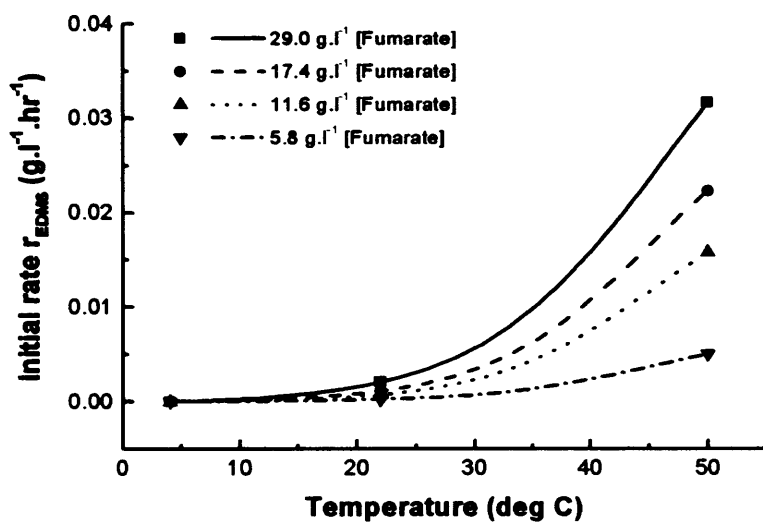


Figure 4-10 – Initial rate of production of EDMS by chemical means. Reaction of ethylenediamine and fumaric acid in aqueous solution with reaction temperature, initial fumaric acid concentration was varied whilst holding initial concentration of ED constant at 6 g.l^{-1} .

4.3.2.3.2 Equilibria

Equilibrium positions for each reaction were initially determined by the use of the sum of Gibbs energies for each bond made and broken in each individual reaction (Mavrovouniotis, 1990), however, since the error involved in the calculations was of the order 2-3 kcal.mol⁻¹ and this was the same size as the typical Gibbs energies of formation of each of the compounds of interest it could only be assumed that all the reactions appeared to have equilibrium constants close to 1. As a result of these inaccuracies, equilibrium constants were determined experimentally by the addition of crude enzyme isolate from an EDDS minimal media fermentation to several pre-prepared mixtures of different concentrations of ethylenediamine, fumaric acid and equilibrium concentration of mixture-EDMS. The relevant equilibrium constants calculated below are:

$$K_{\text{eq,Fum}} = \frac{[\text{Mal}]}{[\text{Fum}]} \quad (4.1)$$

$$K_{\text{eq,EDMS}} = \frac{[\text{EDMS}]}{[\text{Fum}][\text{ED}]} \quad (4.2)$$

$$K_{\text{eq,EDDS}} = \frac{[\text{EDDS}]}{[\text{Fum}][\text{EDMS}]} \quad (4.3)$$

The resultant equilibrium constants for each reaction were determined by taking an average over a series of 9 reactions run at differing initial concentrations to produce an overall equilibrium constants within the 95% confidence interval: $K_{\text{eq,Fum}} = 2.0 \pm 0.5$, $K_{\text{eq,EDMS}} = 1.0 \pm 0.3$ and $K_{\text{eq,EDDS}} = 29.1 \pm 4.1$. Literature values of $K_{\text{eq,Fum}} = 4.2$ (Gajewski *et al*, 1985)

4.3.2.4 Enzymatic Properties

4.3.2.4.1 EDMSase

Specific activity of EDMSase containing cells was particularly low ($0.29 \text{ g.g}_{\text{dcw}}^{-1}.\text{h}^{-1}$) (Figure 4-9), however this specific activity was consistently found to be in this region but only when EDMS had been consumed during the fermentation. As a result of the low titre assays on EDMSase were both long and expensive in terms of reagents and analysis. Furthermore, because EDDSase was always present in the crude enzyme isolate, it was decided that to determine the rate of production of EDMS only, S,S-EDDS could be mass balanced backwards to determine the total amount of EDMS formed by the EDMSase enzyme (Figure 4-11). Triplicate samples were taken at three time points and averages and standard deviation calculated, hence the average coefficient of variance at 10% was obtained. Since the range of coefficient of variance was spread evenly over all time points, it was assumed this 10% error was global and independent of sample concentration but more relevant to dilution and sampling error. Time measurements were accurate to the nearest second and error assumed negligible over the time scale of reactions (typically 60 hours) as such initial rate measurement errors were determined to be at 10% also. Due to the complexities of dissociating EDMSase and EDDSase rates, pH and temperature effects on EDMSase rates were not assessed.

An unrecognised HPLC peak was present at 12.84 minutes (Figure 4-12) (coefficient of variance 7%) in samples from enzymatic reactions provided with chemically produced EDMS, this was of a similar size to the S,S-EDDS peak and grew at a similar rate. It was hypothesised that this peak was R,S-EDDS and was being produced by EDDSase when the reaction was provided with *meso*-EDMS. Initially to confirm that this unrecognised peak occurred only in reactions provided with chemically produced EDMS, two sets of reactions either with catalyst or without were carried out with either pre-produced EDMS or an ED and fumarate solution prepared shortly before that had been kept cool at approximately 4°C and $0.2 \mu\text{m}$ filter sterilised.

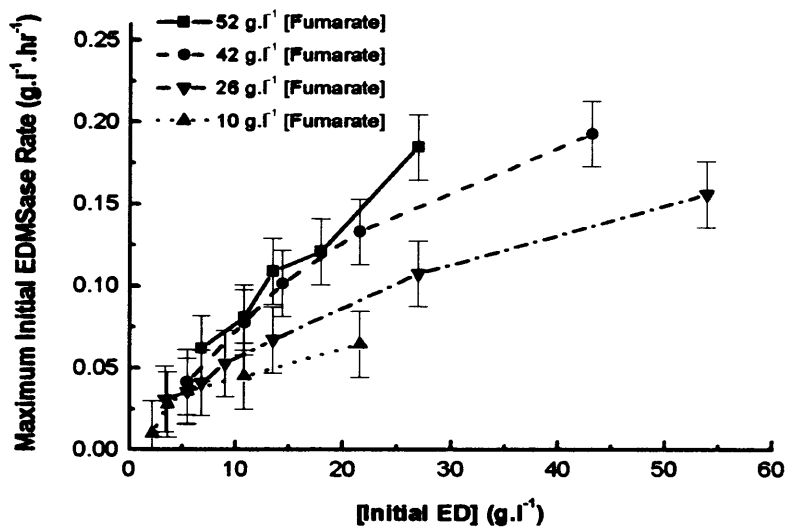


Figure 4-11 – Initial rate of production of EDMS by EDMSase, determined by summing the free concentration of EDMS and a mass balanced concentration of EDMS determined from S,S-EDDS concentration

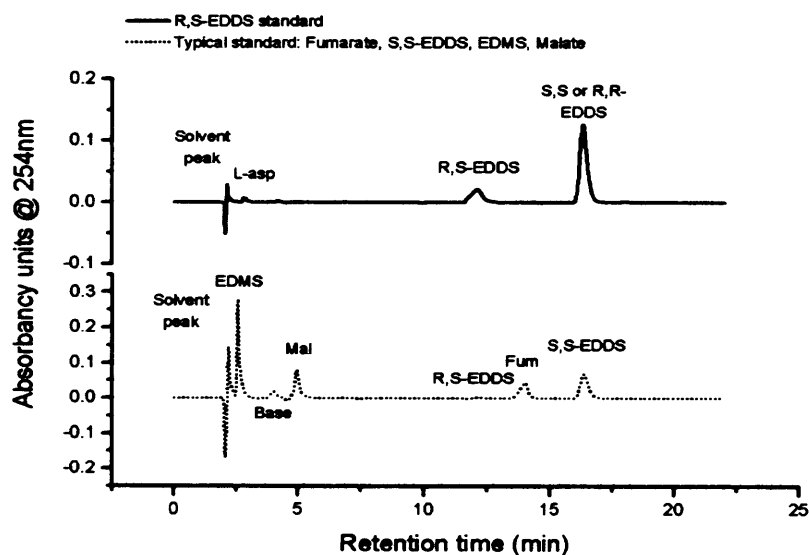


Figure 4-12 - R,S-EDDS peak against typical standards

In Table 4-5 it can be seen that almost none of the unrecognised peak was produced in the absence of chemically produced EDMS. S,S-EDDS was produced in both reactions but when provided with chemically produced EDMS, rate of production was higher. From this it was concluded that mixture-EDMS was produced by the chemical reaction, which was confirmed by the identification of the unrecognised peak as R,S-EDDS (Octel Corp) (Figure 4-12) following the sourcing of a standard of R,S-EDDS (Octel). Figure 4-12 shows that R,S-EDDS produces a peak at approximately 12.2 minutes, when standards of R,S-EDDS were run against samples containing the unrecognised peak when all other conditions were constant the retention times of standard and sample (13.5 min) varied only within 0.1 minute in either direction which was typical for the HPLC method used. The difference in retention time between the above Figure 4-13 and retention times of the reaction samples run at a later date are likely due to small changes in pH of the eluent, since from previous work it was known that an increase in eluent pH of 0.05 could increase retention time of S,S-EDDS by 0.7 minutes. It was noted from experiments where several reactions were run concurrently that the concentrations of S,S and R,S-EDDS were not equal, whereas peak sizes were when reactions were provided with *meso*-EDMS initially. In the main this is believed to be due to the R,S-EDDS standard having contained 2 strains of fungal nature and three microbial and therefore being of lesser concentration than stated. It could therefore be concluded that EDMSase was specific for the production of S-EDMS, whereas EDDSase showed no specificity for either R or S-EDMS as reactants.

		Initial Reactant Concentrations (mM)						Final Concentrations (mM)						
		ED	Fum	EDMS	Mal	S,S-EDDS	R,S-EDDS	ED	Fum	EDMS	Mal	S,S-EDDS	R,S-EDDS	Fumarate Mass
<i>Initial meso-EDMS Enzymatic Reaction</i>		75	109	+++ (mixture)	+	+	+	61	25	++	+++	++	++	71%
<i>Initial meso-EDMS Chemical Reaction</i>		75	109	+++ (mixture)	+	+	+	66	118	+++	+	+	+	107%
<i>No initial EDMS Enzymatic Reaction</i>		100	147	0	+	-	-	93	40	+	+++	+	-	64%
<i>No initial EDMS Chemical Reaction</i>		100	147	0	+	-	-	98	145	+	+	-	-	99%

Table 4-5 – Reaction of chemically produced EDMS and fumarate or ED and fumarate with or without the presence of crude enzyme isolate from *Chelatococcus asaccharovorans*

4.3.2.4.2 EDDSase

The kinetics of EDDSase were determined individually by fixing all but the relevant variable. For each experiment one set of conditions, typically the standard conditions of 30°C and pH 7.5 were run in triplicate, with all other sets of conditions data points at the beginning, middle and end of the progress curve were sampled and then analysed in triplicate to determine the size of the analytical error, which was typically the source of the variation in the triplicate reactions. As can be seen in Figure 4-13 below, the temperature at which EDDSase activity was found to be highest prior to denaturation rate being greater than the increase in rate was 51°C (324K) \pm 1°C and pH was 7.6 \pm 0.01. Reactions could be run both in the presence and absence of phosphate buffer, without any detriment to enzyme activity as maximum initial rates of triplicate crude enzyme isolated reactions run with and without phosphate buffer were within 20% of each other, the same size as the error produced by the replication.

The production of EDDS follows an acid-base reaction and as a result the reaction mixture is essentially a buffer as a result of the salt formed by the addition of ED and fumaric acid at pH 7.5, however, as the enzyme was known to be highly sensitive to pH, the pH change over the course of reaction was determined. pH increased during the first hour of reaction by 0.04 pH units and in proportion to the increase in both enantiomers of EDDS and the corresponding decrease in EDMS and fumaric acid (Figure 4-14).

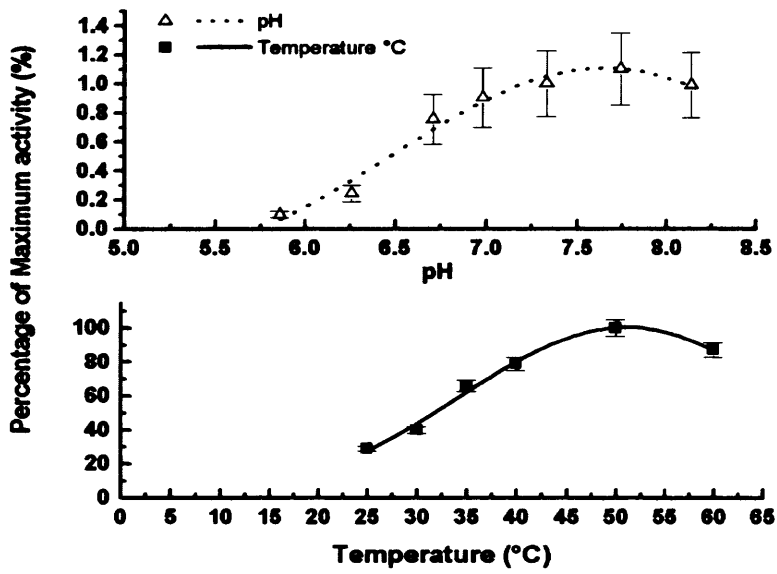


Figure 4-13 – EDDSase activity as a function of reaction temperature and pH

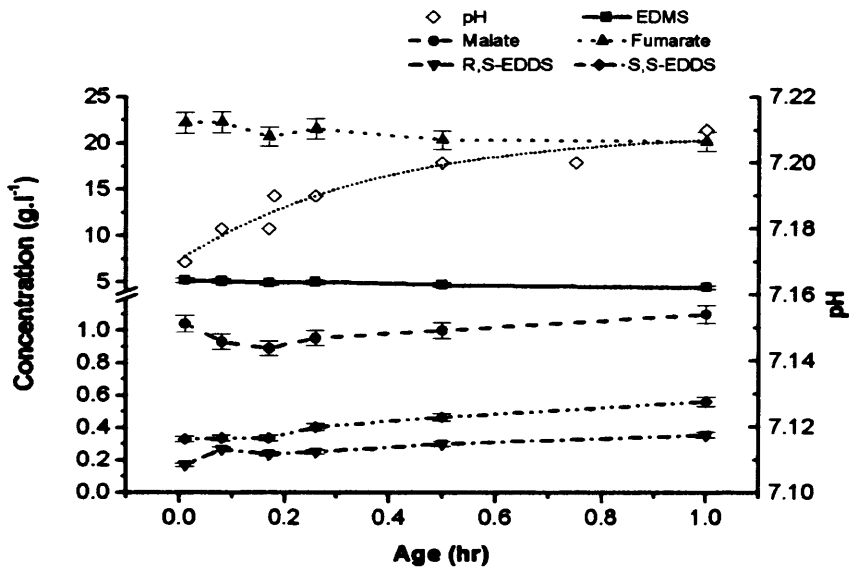


Figure 4-14 – EDDSase reaction pH profile

Reactant concentrations, as would be expected, affected the initial rate of reaction, with increases in EDMS concentration increasing the EDDSase activity (Figure 4-15). One set of reaction conditions and several samples of each of the other reaction conditions were run in triplicate and confirmed that the error in sampling accounts for the error in the initial rate in this case $0.03 \text{ g.l}^{-1}.\text{h}^{-1}$. Figure 4-15 also indicates that as fumarate concentration increased EDDS production rate decreased indicative of reactant inhibition though the data were insufficient to define the optimal initial fumarate concentration. EDDSase reactions were run for up to 60 hours and no significant drop in activity other than that attributable to the reaction approaching equilibrium was observed.

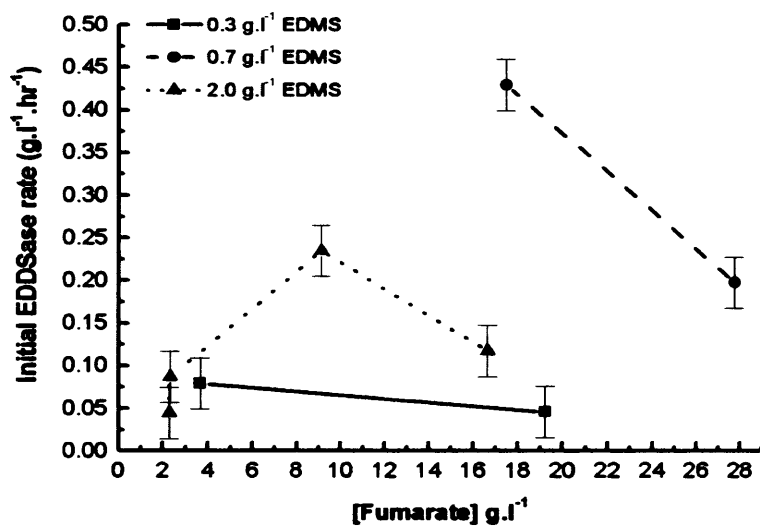


Figure 4-15 – Initial EDDSase activity as a function of initial fumarate concentration at varying levels of initial EDMS.

4.4 DISCUSSION

4.4.1 Increasing the Cell Titre

4.4.1.1 Selection of Strains

Literature indicated several strains had wild type EDDSase activity so initially work was undertaken to find an effective strain. Strains were procured from several sources: Octel Corp's Ellesmere Port S,S-EDDS waste pit, The Biochemistry and Molecular Biology Department at UCL and The DSMZ Culture Collection as a result of study of the literature. Strains 1-5 and 17 (Octel strains) were initially isolated by Westlakes Limited but neither purified or characterised and except in one case (strain 17) proof of production of S,S-EDDS had not been gained. *Pseudomonas putida* KT2440 was obtained from Professor John Ward (UCL Biochemistry and Molecular Biology) as a result of a BLAST search (NCBI PSI-BLAST) that determined that the argininosuccinate lyase from *P. putida* KT2440 had a 30% homology to EDDSase, though this is not particularly high. The BLAST search indicated that enzymes with greater homology (over 40% homology) were *Methanogen Archea*, many of which are able to assimilate amines into methane. *Chelatococcus asaccharovorans* (DSM 6461) was obtained from the German Culture Collection, DSMZ, as a result of its description by Witschel and Egli in their paper on a similar strain, DSM 9103 (Witschel and Egli, 1998) for comparison purposes. Since strains 1 and 17 and 2-5 were determined to be very similar strain 17 and strain 5 were sent for 16S ribosomal sequencing (Appendix 10-3), this returned that strain 17 was a *Paracoccus* sp. and that strain 5 was a *Brevundimonas diminuta*. It is interesting that both *Brevundimonas* and *Paracoccus* are mentioned in the literature as strains carrying the EDDSase activity (Kaneko *et al*, 1999), both are very small cocci (Aragno and Schlegel, 1981), have interesting metabolisms (Madigan *et al*, 2003a; Madigan *et al*, 2003b; White, 1995) and both have been shown to degrade many different organic acids in aerobic conditions (Kniemeyer *et al*, 1999; Madigan *et al*, 2003a). In particular *Brevundimonas* has a vast amount of inducible operons and has been found in freshwater sources (Jasper and Overmann,

2004), perhaps indicating that its prevalence is related to its ability to consume varying organic acids and the increasing concentrations of APCA chelants in European waters. Certainly, these strains were not unexpected considering they have been mentioned in the literature as containing EDDSase activity (Mizunashi, 2001; Takahashi *et al*, 1999)

Initial enzyme assays indicated that *Chelatococcus asaccharovorans* had a higher specific activity $0.6 \text{ g.g}_{\text{dcw}}^{-1} \cdot \text{h}^{-1}$ than the strains obtained from Octel Corp (Figure 4-3), and in a later assay performed with crude enzyme isolates rather than concentrated whole cells, *Chelatococcus asaccharovorans* (*Chc. asacc*) was confirmed to be the most productive of the EDDSase enzyme producers studied.

4.4.1.2 Impact of Medium Composition on EDDSase Concentration

Though several medium formulations were tested, none except EDDS minimal media in which S,S-EDDS was provided to the cells as sole carbon source or EDDS GYP (Glucose, Yeast and Peptone) media produced cells that showed EDDSase activity and between the two media formulations that did produce activity, that gained from bacterial growth on EDDS minimal media (EDDS MM) was 10-fold higher than that of cells grown on EDDS GYP (Figure 4-4) though the cell concentration was higher when *Chc. asacc* was grown on the glucose, yeast and peptone media. From the results it could be concluded that EDDSase could not be induced by merely including S,S-EDDS in the media, a form of limitation was required as all fermentations that had EDDSase activity had consumed S,S-EDDS over the course of the fermentation. Inclusion of more accessible carbon sources to the bacteria were tested to increase the initial growth. However, these cells would go into a decline phase of the cells lasting approximately 50 hours before consumption of S,S-EDDS was started which negated any of the initial strong growth. Later work has indicated that *Chelatococcus* generally does not accept sugars other than glycerol (Egli and Auling, 2005) both justifying the long death phase prior to induction when provided with glycerol and reinforcing the notion that the initial growth on EDDS minimal media was glycerol based. This 50 hour induction time was particularly long and may indicate that induction of some form of

transport was also necessary to transport EDDS into the cell as is the case with EDTA, a structural homolog to S,S-EDDS which required the calcium chelate of EDTA to be taken up in the presence of an inducible energy dependent transport carrier in DSM9103 (Witschel *et al*, 1999). It is interesting to note that previous work on a similar strain to *Chelatococcus asaccharovorans*, *Chelatobacter heintzii* described a similar long lag of 25 hours between growth on glucose and induction of the NTA degrading monooxygenase pathway (Bally and Egli, 1996), perhaps indicating that induction of some form of active transport is necessary for all APCAs.

S,S-EDDS is a hexadentate chelant. Minimal media often require a chelant, typically EDTA at concentrations between 0.5 to 2.0 mg.l⁻¹ to ensure metal ions are solubilised (Cote, 1999), whereas 2 g.l⁻¹ of a very similar chelant was in use here. Therefore it would be expected that it would chelate with any of the metal ions available to the cell during fermentation, particularly iron and zinc, which are known to bind strongly to EDDS (Chapter 3). Furthermore since the stability constants of EDTA and EDDS are similar it would also be likely that EDDS would chelate calcium and magnesium out of the *Chc. asacc* gram negative cell walls, releasing lipopolysaccharide in the process (Hardaway and Buller, 1979). EDTA has been used as a cell weakener to increase the effectiveness of antibiotic treatment for gram negative bacterial infections (Foster and DeBoer, 1998) and EDTA has been proven to damage the outer membrane of *Escherichia coli*, *Pseudomonas aeruginosa* and *Salmonella typhimurium* by increasing the permeability of the cell to hydrophobic substances (Helander and Mattila-Sandholm, 2000). This would account for the large amount of capsular material produced by the cells on solid culture media and wall growth in the 2 l vessel and may be indicative of weak permeable cells. The capsular material could also have been a result of the nitrogen limitation, though this was not investigated since the literature implies there is sufficient nitrogen available in agars, chemicals and glassware (Cote, 1999). Particularly since reverse osmosis water was used rather than high resistivity water it was deemed more likely that chelation was responsible. The effects of S,S-

EDDS as a chelant would need to be considered on scale up as it was noted that culture media stored in polycarbonate shake flasks underwent no change over several weeks, however, culture media sterilised in the same stages as that in polycarbonate shake flasks, but in a glass vessel with stainless steel impeller and baffles tended to go a grey colour when left sterile and under positive pressure overnight. Sterility tests proved negative.

Variation in doubling time for *Chc. asacc* on EDDS MM could be accounted for by the growth of *Chc. asacc* on glycerol from the working stocks, stored as 20% w/v glycerol stocks. Where 2 stocks were used as a 20% inoculum for the initial growth in 10ml McCartney bottles, glycerol assays determined that there was at least 0.4 g.l⁻¹ of glycerol in the shake flasks used to inoculate the 2 l fermenter, however, once these were inoculated into a 2 l fermentation, the dilution was sufficient to be below the detection limit of the glycerol assay, ie below 0.04 g.l⁻¹ (Boehringer Mannheim/ R-Biopharm, 2004). Inocula were inoculated whilst in the exponential phase of growth to prevent shocking the cells by rapid change of conditions from famine to feast (Gershater, 1999). Initial growth of this fermentation had a doubling time of 4 hours. However, when working stocks were centrifuged and the cells washed prior to inoculation at the same volume into the McCartney, no initial growth phase was present. Growth on S,S-EDDS was consistently found to have doubling times in region of 16 hours (\pm 2 hours) indicating that there was some metabolic limitation restricting lower doubling times, likely to be related to the maximum expression of EDDSe in wild type *Chelatococcus asaccharovorans*.

Interestingly the distinct growth of *Chc. asacc* (Figure 4-5) on EDMS after EDDS had been consumed with a corresponding drop in OUR and CER indicated cell death prior to expression of some mechanism whereby EDMS could be consumed. This was further demonstrated by later fermentations (Figure 4-6) which for an unknown reason would not consume EDMS once EDDS had been consumed. This fermentation had an EDMS production rate equivalent to that of the chemical rate at the same temperature

(0.002 g.l⁻¹.h⁻¹). Furthermore, though incomparable with *Chc. asacc* fermentations, early fermentations of the Octel strains were carried out on two different minimal media, one using S,S-EDDS as sole carbon source, the other using the same concentration of S,S-EDDS as sole carbon and nitrogen source (Figure 4-3). In these shake flask experiments, specific activities on the media that used S,S-EDDS as sole carbon and nitrogen source were higher than those provided with a small amount of an alternative nitrogen source (NH₄Cl). These shake flask fermentations were particularly slow and as can be seen in Figure 4-3 several failed. However, this may indicate that the nitrogen limitation had forced a further induction step such as the induction of an EDMSase, as the breakdown of EDDS to fumarate and EDMS does not provide the cells with a directly available nitrogen source, thereby increasing the rate of EDDSase by reducing the EDMS reactant limitation. It also appeared there was no correlation between final EDDSase and EDMSase activity, with induction of both being dependent solely on whether the respective compound was consumed during fermentation. This evidence all pointed towards EDMSase being a separate enzyme. It is interesting to note that previous work on a similar strain to *Chelatococcus asaccharovorans*, *Chelatobacter heintzii* described a long lag of 25 hours between growth on glucose and induction of the NTA degrading monooxygenase pathway (Bally and Egli, 1996)

4.4.2 Defining the Reaction System

Solubility of fumaric acid as a function of pH was determined as the literature provided values of the solubility of free acid, which were known to be below those typically used in reactions. The experimental data seen in Figure 4-7 showed that fumarate solubility reached a maximum at pH 7.5, which coincided with the optimum reaction pH, at a concentration of approximately 250g.l⁻¹ or approximately 2 molar. This solubility limit represented an absolute maximum concentration at which reactions could be run. Furthermore at concentrations of fumaric acid above 1 molar (116 g.l⁻¹), slurries had to be formed prior to addition of base to produce reaction mixtures at the correct pH, making mixing and preparation of the reaction solution difficult. Interestingly at pH 7.5,

concentrations of ED in the region of 1M with and without the presence of fumaric acid tended to crystallise, offering a further reactant concentration limit related to saturation, though this was not a phenomenon noted in the literature. In agreement with the literature it was determined that S,S-EDDS at low pH and in the form of free acid was almost completely insoluble in water in contrast to very high solubilities.

4.4.2.1 Competition for Reactant

Figure 4-8 shows that on sonication, the rate of fumarate degradation was decreased 1.5-fold and accompanied by an increase in the EDDSase rate of the same amount. It can be concluded from this that some of the fumarate degradation was prevented by stopping metabolism and growth, leaving more fumaric acid available for production of S,S-EDDS, this was unsurprising since fumarate is a citric acid cycle compound and by preventing the energy requiring steps of the TCA cycle, less fumarate should be used. Even so it can be seen in Figure 4-8, that there was still a significant side reaction removing fumarate from solution. Further evidence in the form of an HPLC peak that grew over the course of the reaction and corresponded to malic acid was indicative of that side reaction being the fumarase catalysed hydration of fumaric acid to malic acid (Figure 4-18). Fumarase would be expected to be present in an obligate aerobe such as *Chc. asacc* particularly as the strain had consumed fumaric acid during the fermentation from the breakdown of S,S-EDDS.

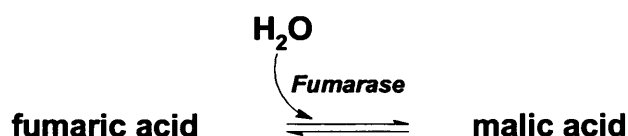


Figure 4-16 –Conversion of fumaric acid to malic acid by fumarase

Fumarase is a well characterised enzyme, due to its simple uni-uni reaction mechanism. Literature equilibrium constants are around 4, in comparison to the experimentally determined equilibrium constant of 2. As expected, rate of production of

malic acid increased with initial concentration of fumaric acid. No reduction in rate at higher reactant concentrations was observed. Both half reactions from ED to EDMS and from EDMS to EDDS use fumarate as a reactant signifying that there will be some competition for fumarate from both half reactions dependent on relative enzyme concentrations.

4.4.2.2 A Further Side Reaction

As described in section 4.3.2.3.1 above, a thermal chemical reaction to produce EDMS was discovered as a result of an experiment to determine if reaction solutions could be autoclaved without changing the reactants (Figure 4-19). Further investigation determined that the EDMS chemical reaction produced both R and S-EDMS as reaction of the autoclaved solution with crude enzyme isolate from a fermentation that had not induced EDMSase produced both R,S and S,S-EDDS in the second half reaction. At low temperature the chemical reaction was fairly insignificant (Figure 4-11). However at higher temperatures, the side reaction became significant when enzyme concentration was low enough that reactions took 60 hours to reach completion. The above provided a method of easily preparing EDMS by use of an autoclave and meant assays could then be performed on this chemically created EDMS, thereby isolating the individual rates and characteristics of the two half reactions



Figure 4-17–Conversion of ED and fumaric acid to *meso*-EDMS

4.4.2.3 EDMSase

Evidence for the presence of a second enzyme, nominated EDMSase extended beyond the fermentation evidence in section 4.3.1.3 to the production of only S,S-EDDS at a low rate when reactions were provided with ED, fumarate and biocatalyst from a fermentation that consumed EDMS in comparison to reactions provided with

ED, fumarate, *meso*-EDMS and catalyst from a fermentation that had not consumed EDMS which produced both R,S and S,S-EDDS at a far higher rate ($0.2 \text{ g.g}_{\text{dcw}}^{-1} \cdot \text{h}^{-1}$ versus $0.002 \text{ g.g}_{\text{dcw}}^{-1} \cdot \text{h}^{-1}$) (Figure 4-20). Together with the evidence above it was proposed that EDMSase is specific for the production of S-EDMS. So as to produce S,S-EDDS only, it is therefore obvious that EDMSase is required in far higher titres than currently achieved so as not to limit the second half reaction. The EDMSase reaction was found to have an equilibrium constant of unity, and no reactant or product inhibition (Figure 4-12) even up to reactant concentrations bordering on the solubility limits.



Figure 4-18 –Conversion of ED and fumaric acid to S-EDMS by EDMSase

4.4.2.4 Characterisation of EDDSase

As noted in section 4.4.2.3 EDMSase showed specificity, therefore indicating that EDDSase did not (Figure 4-21) as R,S and S,S-EDDS were produced in equal amounts within error. This error was related to the concentration of the R,S-EDDS standard, which was made by reaction of D-Asp and 1,2-dibromoethane, however at least three bacterial species and two fungal species were found in the sample provided so the standard would likely have had a lower concentration than stated. The EDDSase reaction had an equilibrium constant of 29 and rate was found to be a function of initial ED concentration. However, EDDSase appeared to be inhibited by fumarate although the data produced (Figure 4-16) was insufficient to determine the point at which this occurred. EDDSase rate increased with temperature until at 51°C the rate of denaturation due to heat predominated providing an optimum. Reactions were typically carried out at 30°C as a result of that temperature being set in early experiments and requiring a basis for comparison. These reaction conditions appear to be similar to those of a thermostable aspartase from *Bacillus* sp (Kawata *et al*, 1999).

The high optimum temperature may indicate that the enzyme responsible for the EDDSase function in *Chelatococcus asaccharovorans* is also thermostable to a degree.

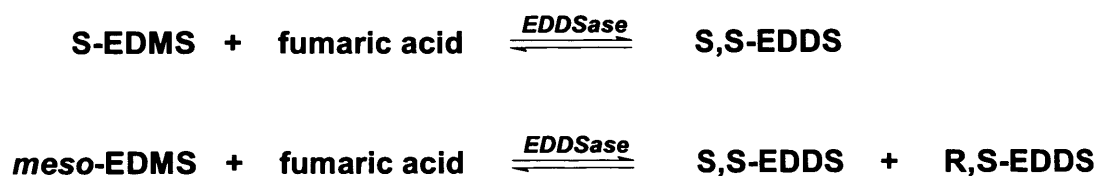


Figure 4-19 - Conversion of EDMS and fumaric acid to EDDS by EDDSase

EDDSase activity was at a maximum at pH 7.5 (Figure 4-13). The pH results agreed with fermentation data in that fermentations operated at around pH 7.5 tended to grow faster than those at pH 7.0. Interestingly, EDDSase activity had dropped to less than 10% of its maximum at pH 6.0, indicating the necessity of good control in the reactor, though this could also be a function of fumarate solubility and thermodynamic equilibrium, effectively reactant limiting the reaction. However, pH increased during EDDSase reactions (Figure 4-15), demanding control more specifically to lower pH. Moreover, the reaction system was a buffer in its own right, produced from a weak acid and weak base most likely forming the salt ethylenediammonium fumarate, as result addition of phosphate buffer made little difference to the activity. The reaction system however was typically high in salt as the amount of acid or base required to produce a reaction mixture at pH 7.5 with either ethylenediamine or fumaric acid in excess was high. Systems high in ionic strength are known to increase protein and cell aggregation (Boonaert *et al*, 1999) and as such the ionic strength of the system may indicate a potential process bottleneck and a potential reduction in activity as mass transfer limitation increases into the aggregate.

4.5 CONCLUSIONS

It can be concluded therefore that the production of S,S-EDDS by *Chelatococcus asaccharovorans* is catalysed by two enzymes, EDDSase and EDMSase in aqueous conditions at pH 7.5 and 30 °C. These enzymes so far have only been produced from fermentations that have consumed their respective products. In the wild type fumarase activity is high and competes with EDMSase and EDDSase for fumaric acid, but furthermore in a whole cell catalyst format cellular metabolism is a strong competitor for fumaric acid also.

The further characterisation of EDDSase has been accomplished confirming temperature and pH optima and providing some data for kinetic modelling. EDMSase has to some extent been characterised and a chemical reaction to *meso*-EDMS identified.

5 PROCESS MODELLING

Studies described in Chapter 4 identified several reactions competing for fumarate in the bioconversion of ED and fumarate by enzyme isolate from *Chelatococcus asaccharovorans*. It has therefore been proposed that the overall EDDS reaction in the presence of a crude enzyme isolate follows the pathway shown in Figure 5-1.

There are thought to be four reactions in this system:

1. Ethylenediamine and fumarate producing S-EDMS catalysed by EDMSase
2. Ethylenediamine and fumarate producing mixture-EDMS chemically
3. Fumaric acid hydration to malic acid catalysed by fumarase
4. Mixture-EDMS and fumaric acid producing R,S, S,R and S,S-EDDS dependent on reactant catalysed by EDDSase

In order for process analysis to be satisfactorily completed, a method by which process or reaction efficiency can be assessed at far higher biocatalyst concentrations than achievable at present is required. In order to achieve this, it seems reasonable to employ a reaction model, comprised of the kinetics of each reaction and an overall energy balance so as to produce a cohesive model of the overall reaction system.

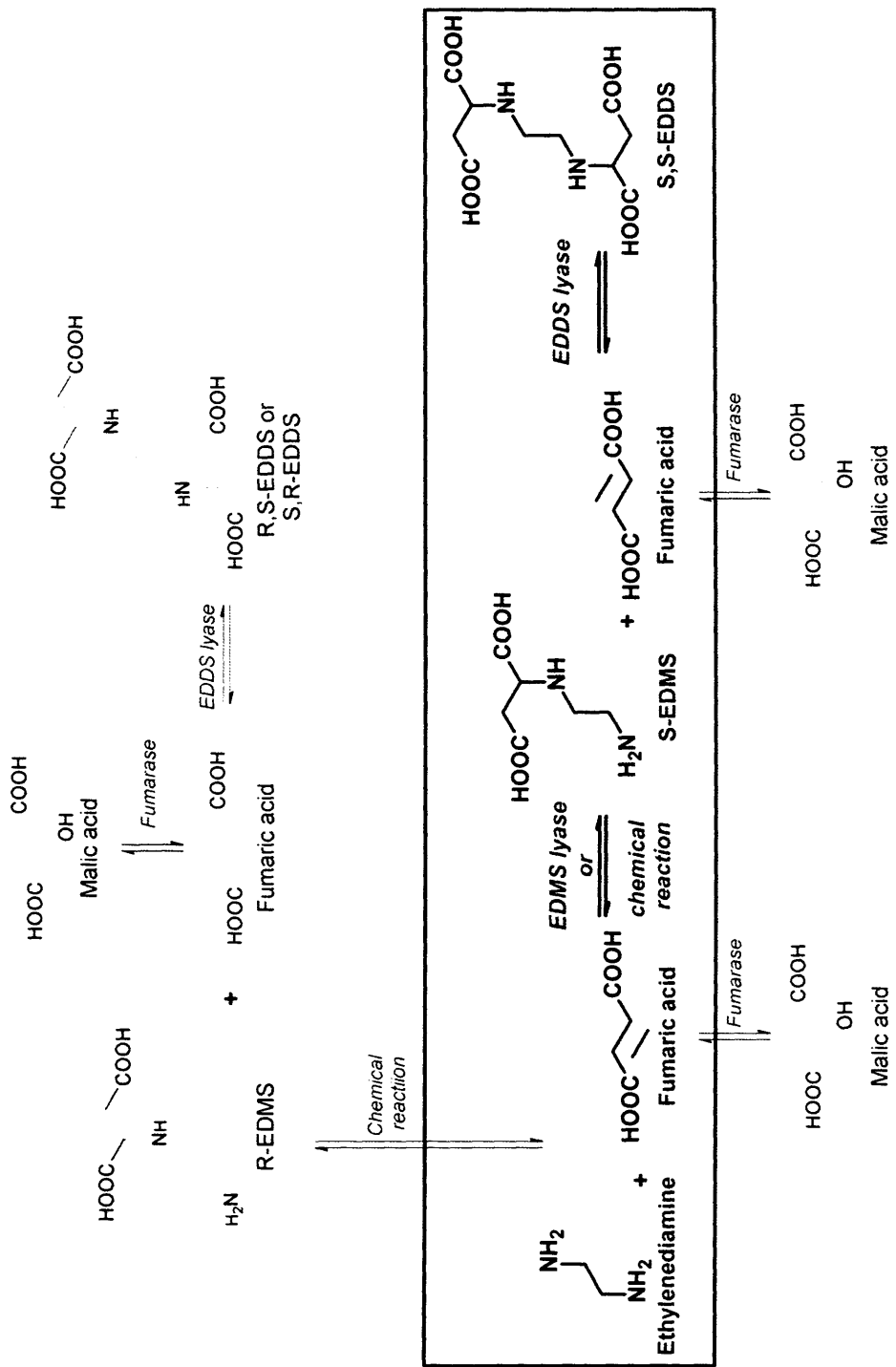


Figure 5-1 - Overall Reaction scheme, showing main reaction to S,S-EDDS in the boxed area

5.1 MODELS

Modelling of the process was undertaken in a bottom up manner, with individual modelling components being tested for functionality prior to their overall integration , testing of this integration and then validation of the whole (Rakitin, 1997). The individual components comprised kinetic models, both chemical and enzymatic, an energy balance and an overall mass balance which fulfilled the function of integrating the individual components to provide concentrations and temperatures with respect to time (Figure 5-2).

Kinetic models were derived on the assumption that rapid equilibrium kinetics applied in which the second step (ie the reactant-enzyme complex reacting to product-enzyme complex) was rate limiting. Because of the low equilibrium constant found both experimentally and in the literature for all the reactions, it was assumed reactions were readily reversible.

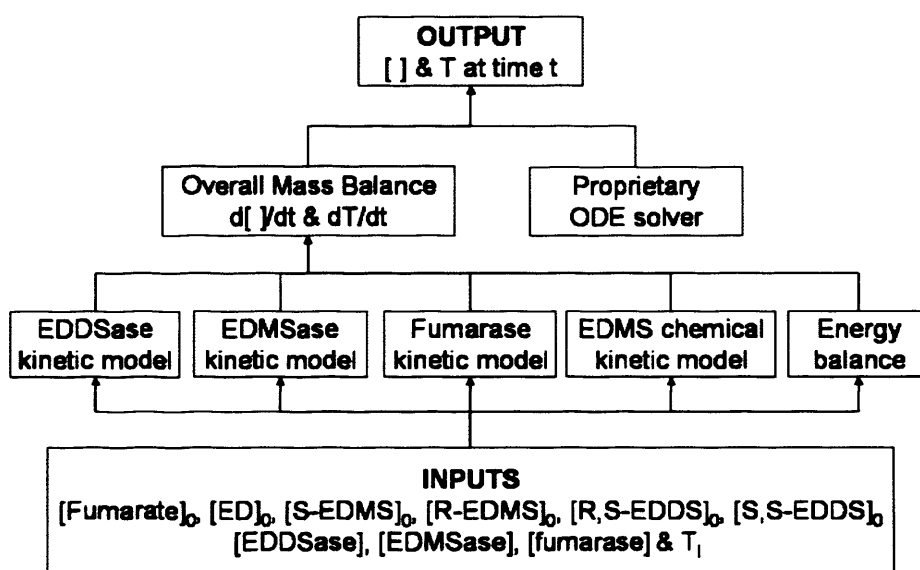


Figure 5-2 – Structure of the model used to predict concentration and temperature at time t

5.1.1 Fumarase Kinetic Model

The reaction schematic (Figure 5-3) and derivation for the fumarase rate equations can be seen below, where:

- F, represents fumarate ([F], fumarate concentration)
- MA, malic acid ([MA], malate concentration)
- E₅, fumarase,
- V_{f5}, forwards maximum rate for fumarase,
- V_{b5}, backwards maximum rate for fumarase (towards fumarate),
- K_{Ff5} the forwards fumarate rate constant and
- K_{Mab5}, the backwards rate constant

Following Michaelis-Menten kinetics (Biselli *et al*, 2002; Segel, 1993a) the uni-uni reversible reaction can be derived to be:

$$\frac{-d[F]}{dt} = \frac{d[MA]}{dt} = \frac{\frac{V_{f5}[F]}{K_{Ff5}} - \frac{V_{b5}[MA]}{K_{Mab5}}}{1 + \frac{[F]}{K_{Ff5}} + \frac{[MA]}{K_{Mab5}}} \quad (5-1)$$

At t₀, ie initial conditions [MA] = 0, therefore the rate equation reduces to:

$$\frac{d[MA]}{dt} = \frac{V_{f5}[F]}{K_{Ff5} + [F]} \quad (5-2)$$

The Haldane equation for the fumarase reaction can be found by equating the numerator of Equation 5-1 to zero, since at equilibrium the forward and backwards reaction rates are equal. The Haldane equation can be seen in Equation 5-3 and 5-4:

$$\frac{V_{f5}[F]}{K_{Ff5}} - \frac{V_{b5}[MA]}{K_{Mab5}} = 0 \quad (5-3)$$

$$K_{eq,5} = \frac{[MA]}{[F]} = \frac{\frac{V_{f5}}{K_{Ff5}}}{\frac{V_{b5}}{K_{Mab5}}} \quad (5-4)$$

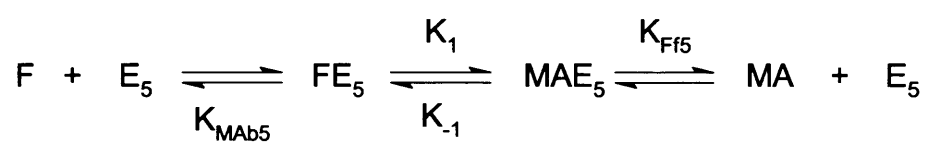


Figure 5-3 – Fumarase reaction scheme

By substituting Equation 5-3 into Equation 5-1 and multiplying through by K_{f5} the overall rate equation can be simplified to:

$$\frac{d[\text{MA}]}{dt} = \frac{V_{f5}[\text{F}] - K_{eq,5}V_{f5}[\text{MA}]}{K_{FF5} + [\text{F}] + \frac{K_{FF5}}{K_{MAb5}}[\text{MA}]} \quad (5-5)$$

V_{f5} can also be seen as the resultant product of enzyme concentration (E , $\text{g}_{\text{dcw}} \cdot \text{l}^{-1}$) and specific activity (A , $\text{g}_{\text{dcw}}^{-1} \cdot \text{h}^{-1}$) (Equation 5-6) enabling cross-referencing between sets of data and an indication of levels of enzyme expression.

$$A = V_{\text{max}} / E \quad (5-6)$$

5.1.2 EDMSase Kinetic Model

The overall EDMSase rate equation (Equation 5-7) and EDMSase forward equation (Equation 5-8) were derived from the schematic below assuming a random order reversible bi-uni mechanism and rapid equilibrium kinetics in the absence of reactant or product inhibition with the EDMSase enzyme being specific for the production of S-EDMS. (Figure 5-4) Where:

- E_3 represented EDMSase,
- V_{f3} , maximum forward rate,
- V_{b3} , maximum backwards rate,
- F, fumarate ($[F]$, fumarate concentration)
- D, ethylenediamine, ($[D]$, ED concentration)
- SM, S-EDMS, ($[SM]$, S-EDMS concentration)
- α_3 , dissociation exponent,
- K_{Ff3} , forwards fumarate rate constant for EDMSase,
- K_{Df3} , forward ethylenediamine rate constant for EDMSase and
- K_{Mb3} , backwards EDMSase rate constant).

$$\frac{d[SM]}{dt} = \frac{V_{f3} \left([F][D] - \frac{[SM]}{K_{eq3}} \right)}{K_{Ff3} \alpha_3 K_{Df3} \left(1 + \frac{[SM]}{K_{Mb3}} \right) + \alpha_3 K_{Df3} [F] + K_{Ff3} \alpha_3 [D] + [F][D]} \quad (5-7)$$

At t_0 , ie initial conditions $[EDMS] = 0$, therefore the rate equation reduces to:

$$\frac{d[SM]}{dt} = \frac{V_{f3} [F][D]}{K_{Ff3} \alpha_3 K_{Df3} + \alpha_3 K_{Df3} [F] + K_{Ff3} \alpha_3 [D] + [F][D]} \quad (5-8)$$

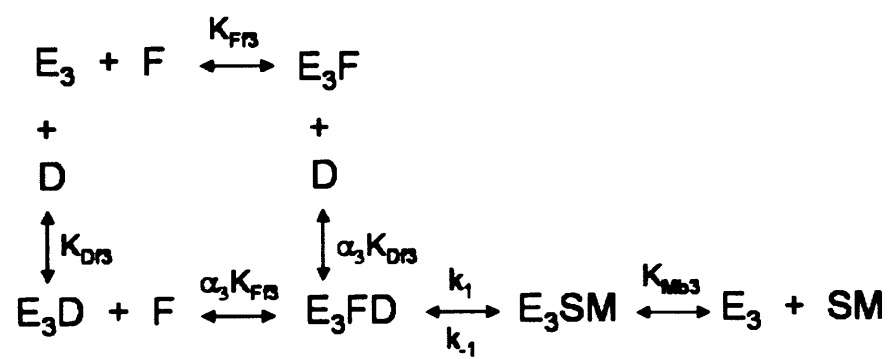


Figure 5-4 – EDMSase Reaction Schematic

5.1.3 EDDSase Kinetic Model

The overall EDDSase rate equation (Equation 5-9 below) was derived by assuming a random bi-uni mechanism and rapid equilibrium kinetics with the third step (ie bond making and breaking) being rate limiting. The experimental data in Chapter 4 indicated reactant inhibition and therefore the model included two dead-ends. The schematic can be seen in Figure 5-5 where:

- E_1 represented EDDSase,
- V_{f1} , maximum forward rate,
- V_{b1} , maximum backwards rate,
- F , fumarate ($[F]$, fumarate concentration)
- P , S,S-EDDS, ($[P]$, S,S-EDDS concentration)
- SM , S-EDMS, ($[SM]$, S-EDMS concentration)
- α_1 and β_1 , dissociation exponents,
- K_{Mf1} , forwards S-EDMS rate constant for EDDSase,
- K_{Ff1} , forward fumarate rate constant for EDDSase,
- K_i , EDDSase inhibition constant for fumarate substrate inhibition and
- K_{pb1} , backwards EDDSase rate constant,

From previous experiments it was noted that R,S-EDDS increased at a similar rate to S,S-EDDS in the presence of mixture-EDMS and in the absence of true R,S-EDDS calibration coefficients it was decided to model R,S-EDDS using the S,S-EDDS model.

$$\frac{d[P]}{dt} = \frac{V_{f1} \left([SM] - \frac{[P]}{K_{eq,1}[F]} \right)}{\alpha_1 K_{Mf1} \left(\frac{K_{Ff1}}{[F]} + 1 + \frac{K_{Ff1}}{K_{i1}} + \frac{[F]}{\beta_1 K_{i1}} + \frac{K_{Ff1}[P]}{K_{pb1}[F]} \right) + [SM] \left(\frac{\alpha_1 K_{Ff1}}{[F]} + 1 \right)} \quad (5-9)$$

At t_0 , ie initial conditions $[EDDS] = 0$, therefore the rate equation reduces to:

$$\frac{d[P]}{dt} = \frac{V_{f1}[SM]}{\alpha_1 K_{Mf1} \left(\frac{K_{Ff1}}{[F]} + 1 + \frac{K_{Ff1}}{K_{i1}} + \frac{[F]}{\beta_1 K_{i1}} \right) + [SM] \left(\frac{\alpha_1 K_{Ff1}}{[F]} + 1 \right)} \quad (5-10)$$

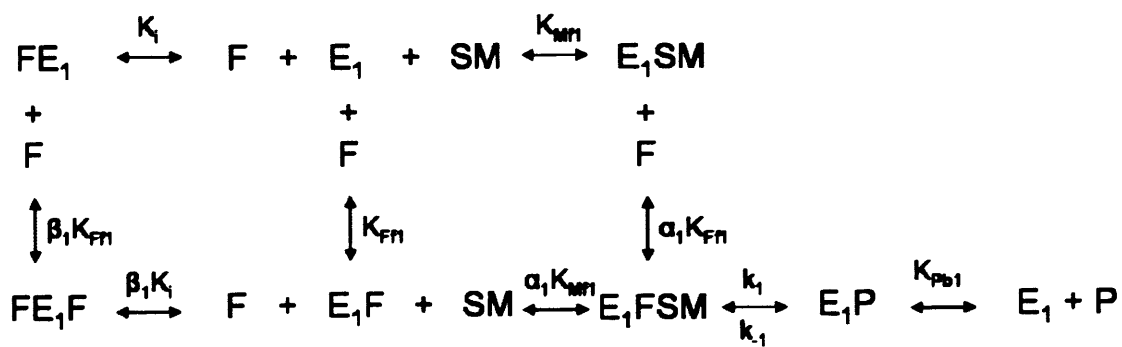


Figure 5-5 – EDDSase reaction schematic

5.1.4 EDMS Chemical Kinetic Model

The chemical rate equation (Equation 5-11) could be derived simply by application of standard chemical kinetics in solution (Connors, 1990b), where:

- v_0 represented initial rate,
- K_{f4} , forward rate constant,
- $[F]_0$, initial fumarate concentration,
- $[D]_0$, initial ethylenediamine concentration,
- f , fumarate reaction order and
- d , ethylenediamine reaction.

$$v_0 = K_{f4}[F]_0^f[D]_0^d \quad (5-11)$$

5.1.5 Energy Balance

In Chapter 4, it can be seen that most experimental reactions were carried out with temperature control. However, one reaction was run adiabatically to assess the level of heat production in the reaction and models were produced to reflect both of these situations. Generally, it was assumed that temperature control was possible and therefore the isothermal assumption was implemented, modelled by the dT/dt equal to zero. However the adiabatic assumption required a different energy balance. For an adiabatic batch reactor of 1 litre working volume with negligible shaft work the typical batch reactor energy balance (Chapter 1, Equation 1-8) reduced to Equation 5-12.

$$\frac{dT}{dt} = \frac{\dot{Q} - \dot{W}_s - \sum_{i=1}^n F_{i0}(H_i - H_{i0}) + (-\Delta H_{RX})(-r_a V)}{\sum N_i C_{pi}} \quad (1-8)$$

$$\frac{dT}{dt} = \frac{(-\Delta H_{RX})(-r_a)}{\sum N_i C_{pi}} \quad (5-12)$$

The reaction rate used was that of the sum of production of S,S and R,S-EDDS. The $\sum N_i C_{pi}$ term used the molar concentrations of all species present in solution at the

current temperature to form a specific heat capacity of the solution. Heat of reaction was calculated from the heats of formation of the aqueous ions of ED, fumarate and EDDS and specific heat capacities of the standard state on the assumption that this was the predominant reaction in the reactor. Where data was not available, interpolations based on related reactions were used. Based on stoichiometry, heat of reaction could therefore be calculated to be:

$$\Delta H_{RX}(T) = \Delta H_{RX}(298.15K) + \int_{298.15K}^T Cp.dT \quad (5-13)$$

$$\Delta H_{RX}(T) = \left(\frac{H_{EDDSaq,298.15K}}{2} - \frac{H_{EDaq,298.15K}}{2} - H_{Fumaq,298.15K} \right) + \dots \quad (5-14)$$

$$\int_{298.15K}^T \left(\frac{Cp_{EDDS}}{2} - \frac{Cp_{ED}}{2} - Cp_{Fum} \right).dT$$

Heat of formation of ions was calculated by use of heats of solution on the assumption that water was in such excess that infinitely dilute heats of solution could be used, the calculation for EDDS can be seen in Equation 5-15. Relevant data can be seen in Table 5-1.

$$H_{EDDSaq,298.15K} = \Delta H_{f,EDDS,298.15K}^{\circ} + \Delta H_{s(\infty),EDDS,298.15K} \quad (5-15)$$

5.1.5.1 Rates as a Function of Temperature

The temperature dependence of rate could be modelled for both enzymatic and chemical reactions by use of the Arrhenius equation (Equation 5-16), where A [h⁻¹] represents the Arrhenius parameter, E_a [kJ.mol⁻¹], activation energy, k represents k_{cat} or specific activity for enzymatic reactions and the forward rate constant for the chemical reaction [mol.l⁻¹.h⁻¹], R was the universal gas constant [8.314 J.mol⁻¹.K⁻¹] and T, temperature [K].

$$k = Ae^{\frac{-E_a}{RT}} \quad (5-16)$$

Data	Value	Source
$\Delta H_{f,EDDS(s),298.15K}^{\circ}$	-1950 kJ.mol ⁻¹	(Kulagina <i>et al</i> , 2000)
$\Delta H_{s(\infty),EDDS,298.15K}$	-35 kJ.mol ⁻¹	Estimate on the basis of $\Delta H_{s(\infty),ED,298.15K}$ and $\Delta H_{s(\infty),Fum,298.15K}$
$\Delta H_{f,ED(l),298.15K}^{\circ}$	-63.01±0.54 kJ.mol ⁻¹	(Good and Moore, 1970)
$\Delta H_{s(\infty),ED,298.15K}$	-31.80±0.01 kJ.mol ⁻¹	(Nichols <i>et al</i> , 1976)
$\Delta H_{f,Fum(s),298.15K}^{\circ}$	-811.80 kJ.mol ⁻¹	(Wilhoit and Shiao, 1964)
$\Delta H_{s(\infty),Fum,298.15K}$	-36.3±0.2 kJ.mol ⁻¹	(Dallos <i>et al</i> , 2000)
C_{pFum}	0.3846(T)+27.635 J.mol ⁻¹ .K ⁻¹	(Parks and Huffman, 1930)
C_{pED}	0.1633(T)+127.31 J.mol ⁻¹ .K ⁻¹	(Hough <i>et al</i> , 1950)
C_{pH2O}	0.0184(T)+65.936 J.mol ⁻¹ .K ⁻¹	¹ Gmelin Database
C_{pEDDS}	1.6019(T)-80.433 J.mol ⁻¹ .K ⁻¹	(Kulagina <i>et al</i> , 2000)
C_{pEDMS}	0.4287(T)+27.182 J.mol ⁻¹ .K ⁻¹	Based on C_{pL-asp} (Huffman and Borsook, 1932)

Table 5-1 – EDDS related Thermodynamic Data.

¹ Gmelin Database: Substance entry Gmelin Registry Number: 117 Water (2006)

With the enzymatic reactions however, there was an implied temperature optimum as a result of Arrhenius related increases in rate and biocatalyst denaturation by heat. Biocatalyst denaturation as a function of temperature was also modelled by the Arrhenius equation by modelling the enzyme concentration as a function of temperature rather than specific activity (Daniel *et al*, 2001; Peterson *et al*, 2004; Willeman *et al*, 2002b), having the overall effect of reducing V_{max} (Equations 5-17-19).

$$V_{max} = A.E \quad (5-17)$$

$$V_{max} = A_A e^{\frac{-E_A}{RT}} . E_{inact}.t \quad (5-18)$$

Where:

$$kinact = A_{inact} e^{\frac{-E_{inact}}{RT}} \quad (5-19)$$

Since this was a complex expression some cases of the temperature-specific activity relationship were modelled with a 2nd order polynomial. Specific activity for each enzyme was determined by division of the V_{max} term produced by non-linear regression by the dry weight of cells used to prepare the concentration of crude enzyme isolate used in the experiment on which that V_{max} was found. Also affecting the rate of reaction were the equilibrium constants, the variation of these with temperature were modelled with Equation 5-20 following determination of the Gibbs Energy of reaction at 30°C based on the experimentally determined equilibrium constants.

$$K_{eq} = e^{\frac{-\Delta_r G^\circ}{RT}} \quad (5-20)$$

5.1.6 Overall Mass Balance

In order to compile the overall model, net rates needed to be determined for all species present in the overall reaction and based on the reaction stoichiometry. The full list of reactions and associated equation numbers and subscripts can be seen in Table 5-2. Table 5-3 summarises the net rate of change for each species.

Reaction	Stoichiometry			Eqn		
1	S-EDMS (SM)	+	Fumaric acid (F)	EDDSase \Leftrightarrow	S,S-EDDS (P)	5-9
2	R-EDMS (RM)	+	Fumaric acid (F)	EDDSase \Leftrightarrow	R,S-EDDS (RP)	5-9
3	ED (D)	+	Fumaric acid (F)	EDMSase \Leftrightarrow	S-EDMS (SM)	5-7
4	ED (D)	+	Fumaric acid (F)	Chemical \Leftrightarrow	$\frac{1}{2}$ (R-EDMS + S-EDMS) $\frac{1}{2}$ (SM+RM)	5-11
5	H₂O (H)	+	Fumaric acid (F)	Fumarase \Leftrightarrow	Malic acid (MA)	5-1

Table 5-2 Reaction stoichiometry for compilation of individual rate equations into an overall model

Species	Net rate
F	$r_F = -r_{1F} - r_{2F} - r_{3F} - r_{4F} - r_{5F}$
SM	$r_{SM} = -r_{1SM} + r_{3SM} + r_{4SM}$
RM	$r_{RM} = -r_{2RM} + r_{4RM}$
D	$r_D = -r_{3D} - r_{4D}$
P	$r_P = r_{1P}$
RP	$r_{RP} = r_{2RP}$
MA	$r_{MA} = r_{5MA}$

Table 5-3 – Net rates of change of concentration for all species involved in the EDDSase bioconversion

5.2 METHODS

5.2.1 Experimental Determination of Kinetics

The kinetics of enzymatic reactions were determined by the use of crude enzyme isolate from *Chelatococcus asaccharovorans* prepared as described in Chapter 4. Reactions were typically carried out at 30°C, pH 7.5 in 50 mM phosphate buffer and at 10ml in a heated, shaken waterbath (200rpm orbital, Grant Scientific, Cambridge, UK) or 1ml in a heated micro-test-tube mixer (1000rpm, orbital, Thermomixer, Eppendorf, Hamburg, Germany). For every set of reactions at least one reaction was carried out as a control (Chapter 4 – Section 4.2.3.2) to be able to compare between batches of enzyme. Reaction solution was brought to temperature prior to the start of reaction and reactions were started by the addition of a 1:10 ratio of enzyme isolate to reaction solution. Samples were removed at regular intervals and the reaction stopped in these samples by the addition of 1 M HCl totalling a tenth of the sample volume. These samples were then diluted appropriately with copper acetate/TBAH diluent, prepared as described above and analysed by HPLC (Chapter 4) for concentrations of mixture-EDMS, R,S-EDDS, S,S-EDDS, fumaric and malic acids.

When assessing kinetics of EDDSase and fumarase full progress curves (36 hours) were taken for varying initial concentrations of *meso*-EDMS, ED and fumarate in the presence of crude enzyme isolate. Initial rates of malic acid, S,S-EDDS and R,S or S,R-EDDS and EDMS production were calculated by fitting hyperbolae to the progress curves in Microcal Origin ® and taking tangents to these hyperbolae at time zero over not more than 5% of the progress curve. Kinetics of EDMSase were determined by providing crude enzyme isolate with ED and fumarate in varying initial concentrations and analysing both initial rates of production of EDMS, S,S-EDDS, R,S and S,R-EDDS, malic acid and the full progress curves taken over 60 hours. In order to find the true initial rate of EDMS production all stereoisomers of EDDS were assumed produced from EDMS and mass balanced backwards.

The kinetic constants of the chemical half reaction to EDMS were determined by the initial rate method together with isolation of one component, thereby reducing the kinetics to apparent first order. Reactions were provided with four different concentrations of ethylenediamine in at least 100-fold excess over fumarate at varying concentrations at pH 7.5 in 50mM phosphate buffer, so it could be said that the concentration of ethylenediamine remained constant over the course of the reactions. Reactions were carried out at 50 °C, in 10 ml Rohre tubes (Sarstedt, Numbrecht-Rommelsdorf, Germany) to provide enough sample for analysis and mixed at 200rpm in a shaking waterbath (Grant Scientific, Cambridge, UK). Samples were removed daily over a week, diluted 10-fold and analysed for fumarate and EDMS by HPLC (section 3.1.1.1). Several samples taken in triplicate to determine sampling and analysis error.

5.2.2 Determination of Model Constants

The constants in the models described in Section 5.1 were determined by either non-linear regression for enzymatic models or linear regression for models that could be reduced to linear form by use of logarithms, such as the Arrhenius parameters and the chemical rate equation using kinetic data gained in Chapter 4. Non-linear regression was carried out using the Levenberg-Marquardt algorithm in Microcal Origin ® (Marquardt, 1963) after manually inputting the relevant model form. Different weighting methods were used dependent upon the experimental data and its associated errors, for example for the regression of the fumarase reaction parameters, equal weighting was employed since at least four data points for each set of variables was available. However, for the regression of other kinetic parameters error related to the data was used in the absence of knowledge of the data variability.

5.2.3 Component Model Testing

Once model constants were found, individual model components were tested for functionality by testing against similar data to that used to produce the constants. These were analysed by means of the use of the chi-squared goodness of fit hypothesis test and parity plots when the chi-squared goodness of fit returned meaningless values.

5.2.4 Validation

On integration of the constituent parts of the model by the use of the overall mass balance and reaction stoichiometry, the model was validated by the assessment of experimental data run at varying temperatures and at varying initial concentrations of *meso*-EDMS and/or ED and fumarate at a wide range of those tested. When the model being tested was that using the adiabatic assumption for the energy balance a stiff ode solver, ode23s based on Rosenbrock methods from Matlab ® was used (Press *et al*, 1992). However, when the isothermal assumption was made ode45, a 4th order Runge-Kutta method was employed, code for both these situations can be seen in Appendix 10-6. Chi² (Appendix 10-4) or parity plot comparison of concentration-time curves produced experimentally and *in-silico* were then made.

5.3 RESULTS

5.3.1 Parameter Fitting

5.3.1.1 Fumarase Reaction

Using data generated from a series of progress curves described in Chapter 4 at varying initial concentrations of fumarate in the presence of crude enzyme isolate. Initial rates over less than the first 5% of conversion were determined by fitting the progress curves with hyperbolae and taking the tangent to the curve at time zero. The series of initial rates were then plotted against the initial concentration of fumarate present in the reaction and fitted to the initial rate model in Equation 5-2 by non-linear regression of all data points, under the assumption that all data points had equal weighting using the Levenberg-Marquardt algorithm in Microcal Origin™. The resultant plot and fit can be seen in Figure 5-6. The V_{f5} and K_{FF5} found by the fitting were $0.19 \pm 0.015 \text{ mmol.l}^{-1}.\text{min}^{-1}$ (ie $0.0114 \text{ mol.l}^{-1}.\text{h}^{-1}$) and $51 \pm 21.6 \text{ mM}$ (0.051 mol.l^{-1}) (Table 5-4). The 95% confidence intervals were 0.03 and 45 respectively, indicating a good fit of V_{f5} but not such a good fit of K_{FF5} . Figure 5-6 demonstrates residuals are relatively evenly balanced above and below the $y=0$ line. In order to validate the fumarase kinetic model and simulate K_{MAb5} , the ordinary differential equation in Equation 5-1 was substituted with the initial conditions $[F]=[F]_i$ and $[MA]=0$ and mass balance 5-21, so that malic acid concentration could be predicted with time using Equation 5-22.

Mass balancing for fumarate:

$$[F]_i = [F] + [MA] \quad (5-21)$$

$$\frac{d[MA]}{dt} = \frac{V_{f5} \left(\frac{([F]_0 - [MA]) - [MA]}{K_{eq,5}} \right)}{K_{FF5} + ([F]_0 - [MA]) + \frac{K_{FF5}}{K_{MAb5}} [MA]} \quad (5-22)$$

Equation 5-22 was simulated with ode45 (a Matlab® solver) with K_{MAb5} between 0.001 and 1.0 M. As a result the best fit was determined to be provided by $K_{MAb5} = 0.2 \text{ M}$.

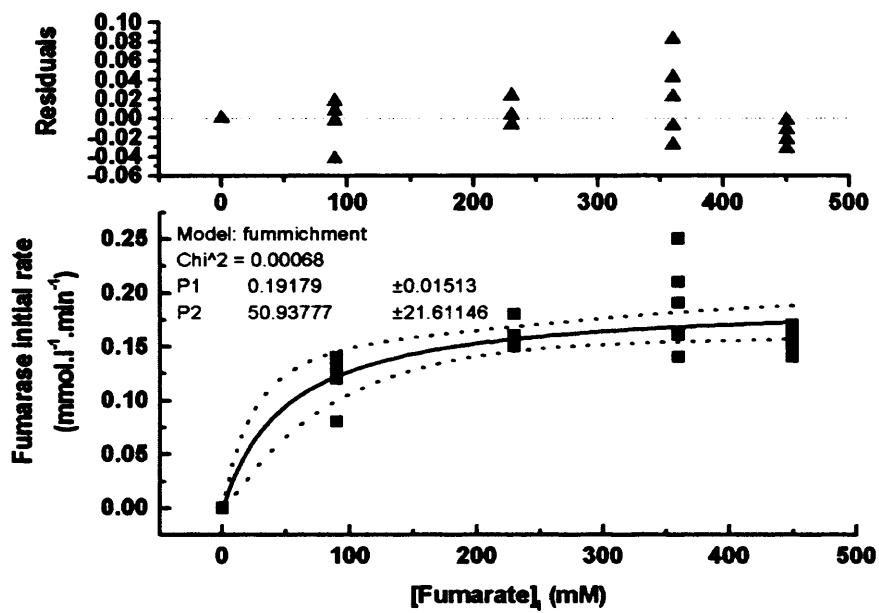


Figure 5-6 - Fumarase kinetic parameter determination where (■), represents experimental data, (▲), represents residuals, solid line, represents the fitted model and dotted lines represent the upper and lower confidence intervals.

Parameter	Value	Standard error	95% Confidence Interval	Units
<u>EDDSase</u>				
V_{f1}	65.0	3079	8549	mmol.l ⁻¹ .h ⁻¹
α_1	1	n/a - fixed		
β_1	0.67	n/a - fixed		
K_{Mf1}	102	8230	22850	mmol.l ⁻¹
K_{Ff1}	63	6266	17398	mmol.l ⁻¹
K_i	59	5945	16506	mmol.l ⁻¹
K_{Pd1}	0.1	n/a - simulated		mmol.l ⁻¹
<u>EDMSase</u>				
V_{f5}	0.061	0.011	0.023	mmol.l ⁻¹ .min ⁻¹
α_3	1	n/a - fixed		
K_{Ff3}	330	91	190	mmol.l ⁻¹
K_{Df3}	576	91	191	mmol.l ⁻¹
K_{Mb3}	100	n/a - simulated		mmol.l ⁻¹
<u>EDMS Chemical</u>				
K_{f4}	7.59 e ⁻⁴	0.008	1.1 e ⁻⁴	
f	1	n/a - fixed		
d	0.4	0.03	0.26	
<u>Fumarase</u>				
V_{f5}	0.19	0.015	0.03	mmol.l ⁻¹ min ⁻¹
K_{Ff5}	51	21.6	44	mmol.l ⁻¹
K_{MAb5}	200	n/a - simulated		mmol.l ⁻¹

Table 5-4 – Kinetic parameters with related standard error and 95% confidence interval values

5.3.1.2 Fumarase Dependence on Temperature

Fumarase rate dependence on temperature was modelled by a 2nd order polynomial relationship between A_5 (maximum fumarase specific activity in $\text{mol.g}_{\text{dcw}}^{-1}\text{h}^{-1}$) and temperature in Kelvin. The polynomial was fitted to the data in Figure 5-7 using the polynomial regression tool in Microcal Origin. The resultant polynomial can be seen in Equation 5-23, for which R^2 was 0.704. In the process of checking the fit of the model it was determined that though the constants were very small, they were very sensitive to computer related rounding errors. However, the maxima of the polynomial does agree with literature values stating optima between 20 and 35°C (293 to 308K) for a non-thermostable fumarase (Rhee and Sohn, 2003).

$$A_5 = -0.09766 + 6.71819 \times 10^{-4} (T) - 1.13706 \times 10^{-6} (T)^2 \quad (5-23)$$

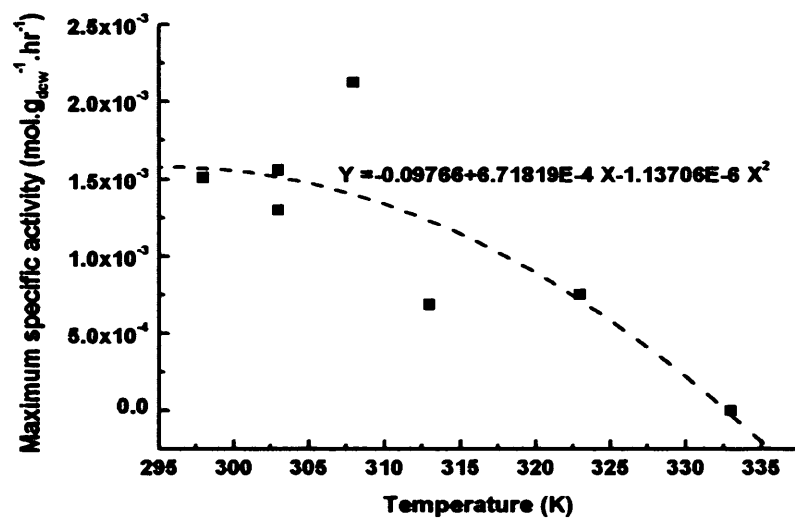


Figure 5-7 - Polynomial regression of Fumarase maximum specific activity against temperature, line representing fitted polynomial and ■, experimental data

5.3.1.3 EDDSase Reaction

The rate constants for Equation 5-9 were found by non-linear regression using the Levenberg-Marquardt routine in Microcal Origin. Initial rate data was obtained from a previous experiment in which *meso*-EDMS was reacted with fumarate in the presence of ED and crude enzyme isolate containing fumarase and EDMSase (Chapter 4, Figure 4-16). Initial rates were taken over less than 5% of the progress curve, by fitting hyperbolae and taking the tangent at close to zero, therefore the effect of EDMSase and fumarase on EDDSase initial rates was assumed to be negligible. The plot was weighted using error bars relevant to the data, where the standard deviation of the initial rate for all data (within the 60% confidence interval) was 0.042 mmol.l⁻¹.h⁻¹. This constant error was applied to the data due to the predominance of dilution and sample preparation error, which was consistently in this region. The fitting procedure shared the parameters: V_{f1} , K_{Ff1} , K_{Mf1} , K_{i1} , α_1 and β_1 fixed the initial fumarate concentration to that determined by HPLC analysis and α_1 at unity because the lines of constant initial fumarate intersected above the x-axis in double reciprocal plots. Parameters were constrained by inequalities $K_{Ff1} > 0$, $K_{Mf1} > 0$, $K_{i1} > 0$, $\beta_1 > 0$. The parameters so produced were: V_{f1} , 67 ± 3079 mmol.l⁻¹.h⁻¹, K_{Ff1} , 63 ± 6266 mM, $K_{Mf1} = 102 \pm 8230$ mM, $K_i = 59 \pm 5945$ mM & $\beta_1 = 0.7$ (Figure 5-8 & Table 5-4) with the 95% confidence interval in the region of 5 orders of magnitude indicating very low confidence in the fitted parameters. K_i indicated a peak in activity around 0.06 M (7 g.l⁻¹) with steady decrease in activity to 10% of the maximum rate at 1.8 M (210 g.l⁻¹) (Figure 5-9). The EDDSase reaction model was verified by ODE (Equation 5-24) and K_{b1} found by simulation of Equation 5-24 with K_{b1} in the range 0.00001 to 0.1M K_{b1} was determined to be 0.0001 M.

$$\frac{d[P]}{dt} = \frac{V_{m1} \left(([SM]_0 - [P]) - \frac{[P]}{K_{eq,1}([F]_0 - [P])} \right)}{\alpha_1 K_{Mf1} \left(\frac{K_{f1}}{[F]_0 - [P]} + 1 + \frac{K_{Ff1}}{K_{i1}} + \frac{[F]_0 - [P]}{\beta_1 K_{i1}} + \frac{K_{Ff1}[P]}{K_{bp1}([F]_0 - [P])} \right) + ([SM]_0 - [P]) \left(\frac{\alpha_1 K_{Ff1}}{[F]_0 - [P]} + 1 \right)} \quad (5-24)$$

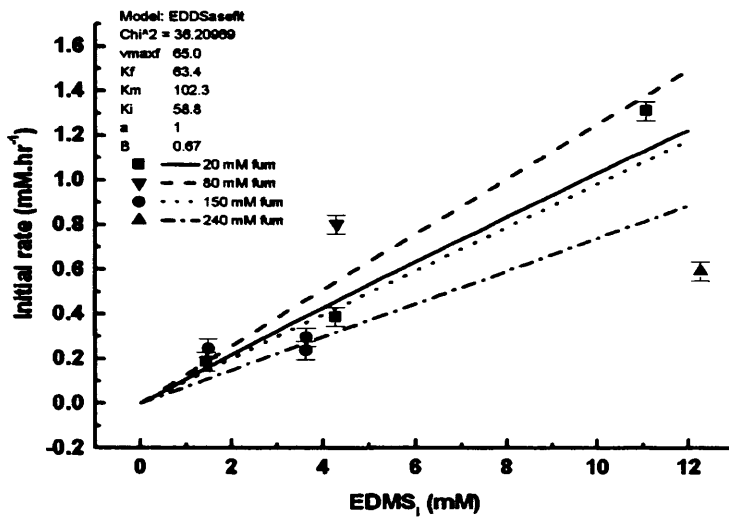


Figure 5-8– Kinetic fit for EDDSase parameter determination

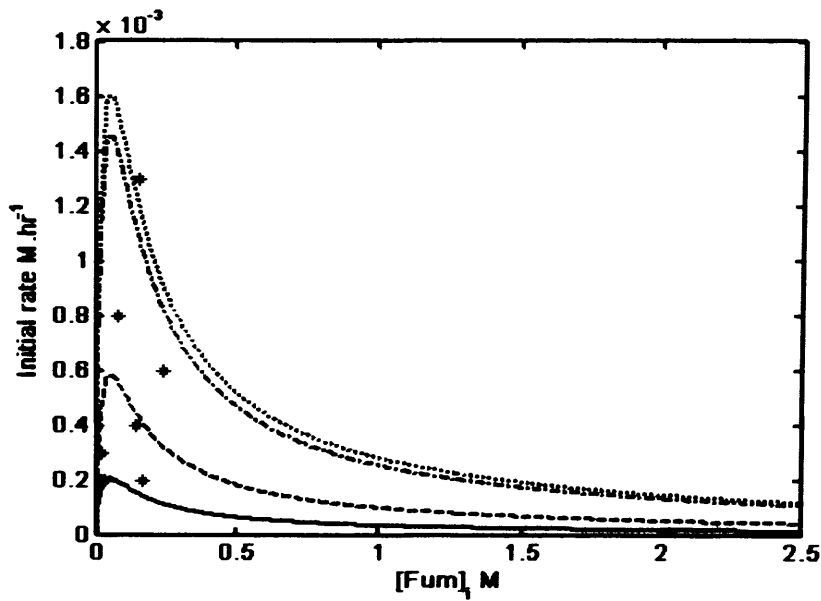


Figure 5-9 - Fumarate inhibition of EDDSase at varying initial EDMS concentrations

On verification most reactions followed the model quite closely with chi-squared values ranging between 11 and 33 for 40 degrees of freedom (required test statistic in the 5% significance level was 55.8), including one situation in which fumarate concentration was particularly low which after initial increase in EDDS concentration, then decreased the S,S-EDDS concentration presumably a result of fumarase competition for reactant.

5.3.1.4 EDDSase Dependence on Temperature

EDDSase was assessed for its initial rate at varying temperatures (Figure 4-14, Chapter 4). The variation in this initial rate with temperature could be described by the Arrhenius equation (Equations 5-17 and 5-18). Arrhenius parameters for increase in specific activity with temperature and decrease in enzyme concentration with heat denaturation were determined by linear regression of either the logarithm of specific activity or enzyme concentration against the reciprocal temperature. The time term in Equation 5-17 was set to 60 hours due to no evidence of enzymatic instability (Equations 5-25 & 5-26). Model and experimental data can be seen in Figure 5-10.

$$V_{m1} = 4.2712 \times 10^7 e^{\frac{-6477}{T}} \cdot E_1 \cdot^{-kinact.t} \quad [\text{mol.l}^{-1}\text{h}^{-1}] \quad (5-25)$$

$$kinact = 8.6328 \times 10^{11} e^{\frac{-10455}{T}} \quad [\text{g}_{dcw} \cdot \text{l}^{-1}] \quad (5-26)$$

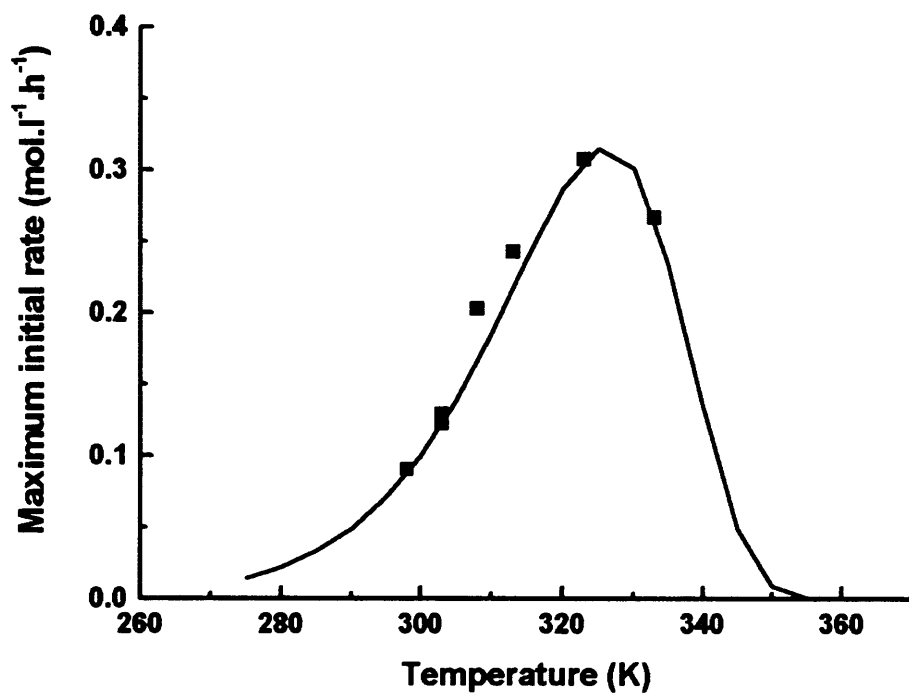


Figure 5-10 – EDDSase maximum rate as a function of reaction temperature (—) Model (■) Experimental data

5.3.1.5 EDMSase Reaction

Initial rate data was produced from a series of reactions in the presence of both EDDSase and EDMSase enzymes produced both EDDS and EDMS from ED and fumarate (Chapter 4, Figure 4-12). Since EDDS can only be formed from EDMS, a mass balance was performed to calculate the total EDMS present in the system at each individual time point. Initial rates were determined by fitting hyperbolae to the [EDMS]-time plots and taking the gradient of the tangent to these lines at time zero. Equation 5-11 above was written in Microcal Origin™ in the non-linear curve fitting program using the Levenberg-Marquardt algorithm to fit curves by non-linear least-squares regression minimising the X^2 parameter. The plot was weighted using error bars relevant to the data, where the standard deviation of the initial rate for all data (within the 60% confidence interval) was $0.0029 \text{ mmol.l}^{-1}.\text{min}^{-1}$. This error was applied to the data as constant due to the predominance of dilution and sample preparation error, which was consistently in this region. The fitting procedure shared the parameters: V_{f3} , K_{Ff3} , K_{Df3} and α_3 as would be expected and constrained the parameters with the inequalities $K_{Ff3} > 0$, $K_{Df3} > 0$ and $0 < \alpha_3 < 1$. α_3 was constrained because the lines of constant initial fumarate intersected above the x-axis in double reciprocal plots. Initial fumarate concentration was also used as a parameter and fixed at the concentrations shown in the legend of Figure 5-11. As can be seen in Figure 5-11, the kinetic parameters returned by the fit were: $V_{f3} = 0.06 \pm 0.011 \text{ mmol.l}^{-1}.\text{min}^{-1}$, $K_{Ff3} = 330 \pm 91 \text{ mM}$, $K_{Df3} = 580 \pm 91 \text{ mM}$ and $\alpha_3 = 1$ (Table 5-4). The 95% confidence intervals were a similar size to the parameters, indicating reasonable confidence in the model. Experimental data indicated that backwards rate parameters were likely small, however an ordinary differential equation was formed (Equation 5-27) and used to simulate values of K_{Mb3} in the range 0.0001 to 1, from this $k_{Mb3} = 0.1$ was determined.

$$\frac{d[M]}{dt} = \frac{V_{f3} \left(([F]_0 - [M])([D]_0 - [M]) - \frac{[M]}{K_{eq,3}} \right)}{K_{Ff3} \cdot \alpha_3 \cdot K_{Df3} \left(1 + \frac{[M]}{K_{Mb3}} \right) + ([F]_0 - [M]) \alpha_3 \cdot K_{Df3} + ([D]_0 - [M]) \alpha_3 \cdot K_{Ff3} + ([F]_0 - [M])([D]_0 - [M])} \quad (5-27)$$

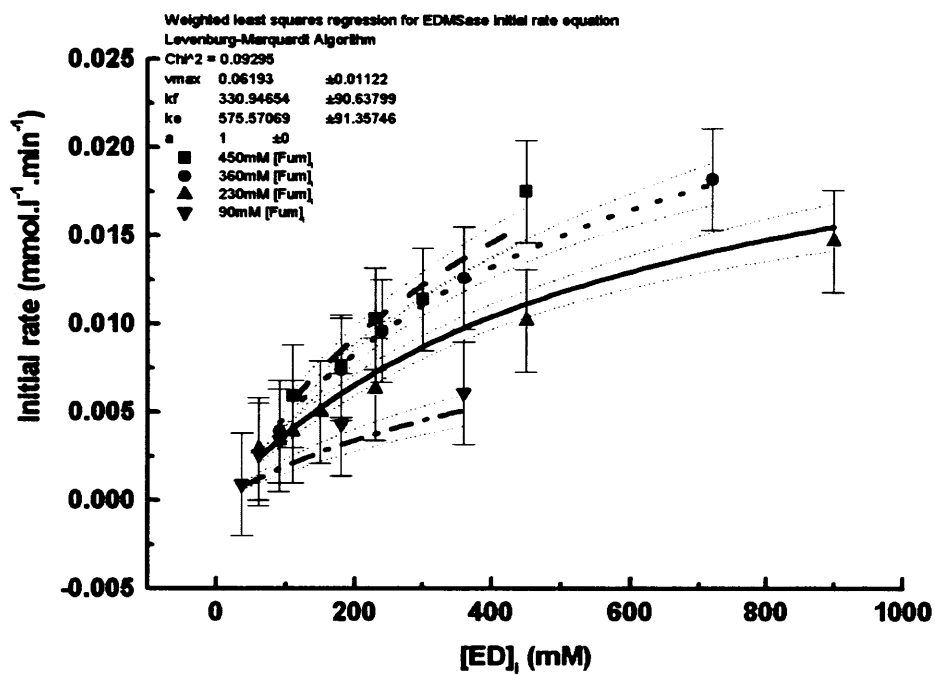


Figure 5-11 - Fitting EDMSase forwards reaction kinetic parameters by weighted non-linear least squares regression. Thick lines represent model, points as described by the legend represent experimental data. Faint dotted lines represent the confidence interval in the fitted parameters.

5.3.1.6 EDMSase Dependence on Temperature

In the absence of experimental evidence it was decided to use the same temperature optima as EDDSase for EDMSase adjusted for the lower specific activity in the absence of experimental evidence, this was more easily achieved by means of a polynomial (Equation 5-28).

$$A_3 = - 0.1091 + 6.7611 e^{-4} (T) - 1.0380 e^{-6} (T)^2 \quad (5-28)$$

5.3.1.7 EDMS Chemical Reaction

The rate equation for the chemical reaction of ED and fumarate was determined by isolating fumarate, a process by which ED is added to the reaction in massive excess (at least 100x) and can therefore be assumed constant throughout the reaction. Isolation reduced equation 5-11 to 5-29, where K'_{f4} was the observed reaction rate with respect to ethylenediamine.

$$v_o = K'_{f4} [F]_o^f \quad (5-29)$$

Where

$$K'_{f4} = K_{f4} [D]_o^e \quad (5-30)$$

The rate constants were determined by linear regression of the logarithm of initial rate data against the logarithm of the controlling concentration. Initial rates were found by fitting hyperbolae to the progress curve and taking tangents over the first 5% of the progress curve. From the literature it has been determined that providing reaction has not exceeded 5% conversion that error related to estimating the initial rate from a tangent to a progress curve is unimportant (Connors, 1990a) in comparison to other sources of error. The gradients so produced were then replotted against the logarithm of the relevant ethylenediamine concentration (Equations 5-31 & 5-32)

$$\text{Log } v = \quad = \text{log } K'_{f4} + f \text{ log } [F]_o \quad (5-31)$$

$$\text{Log } K'_{f4} \quad = \text{log } K_{f4} + e \text{ log } [D]_o \quad (5-32)$$

Initially the logarithm of initial fumarate concentration was plotted against the log of reaction rate in $\text{mol.l}^{-1}.\text{h}^{-1}$. Within error this produced fumarate orders of approximately 1. However, as a result of taking logarithms, errors in the y-intercept were amplified and large. Since the order of reaction was close to one, it was determined the reaction was first order in fumarate and as such initial rate was plotted against initial fumarate concentration on normal scales at constant ethylenediamine concentration (Figure 5-12). These were fitted to a linear relationship by linear regression and forced through the origin, due to the assumption that in the absence of fumarate there is no reaction to EDMS following stoichiometry. The linear regression procedure was used in the absence of weighting, on the assumption that errors were of the same order and related in the main to sampling and analytical error. The scatter of the residuals in Figure 5-12 confirmed that the residuals so produced by this fitting procedure were random and small. The gradients so obtained were replotted and therefore provided the rate constant K_{f4} ($7.59 \text{ e}^{-4} \text{ mol.l}^{-1}.\text{h}^{-1}$) and ED reaction order (0.4) (Table 5-4).

5.3.1.8 Temperature dependence of EDMS Chemical Kinetics

The temperature dependence of the EDMS chemical reaction was determined by linear regression of the Arrhenius relationship. Arrhenius parameter and activation energy were $1.43\text{e}^{-1} \text{ mol.l}^{-1}.\text{h}^{-1}$ and 8.6 kJ.mol^{-1} respectively.

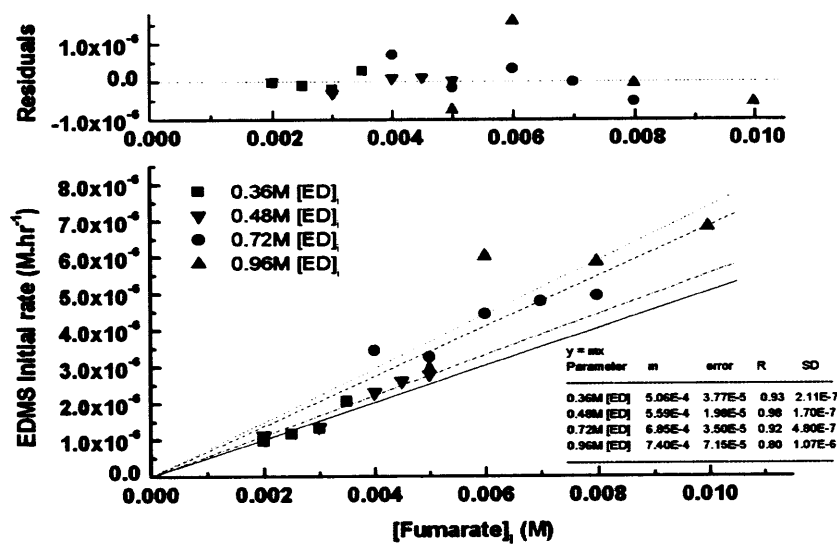


Figure 5-12 – Initial chemical rate of production of EDMS against initial fumarate concentration at constant ED

5.3.2 Integration and Component Testing

The overall model was set up for two assumptions:

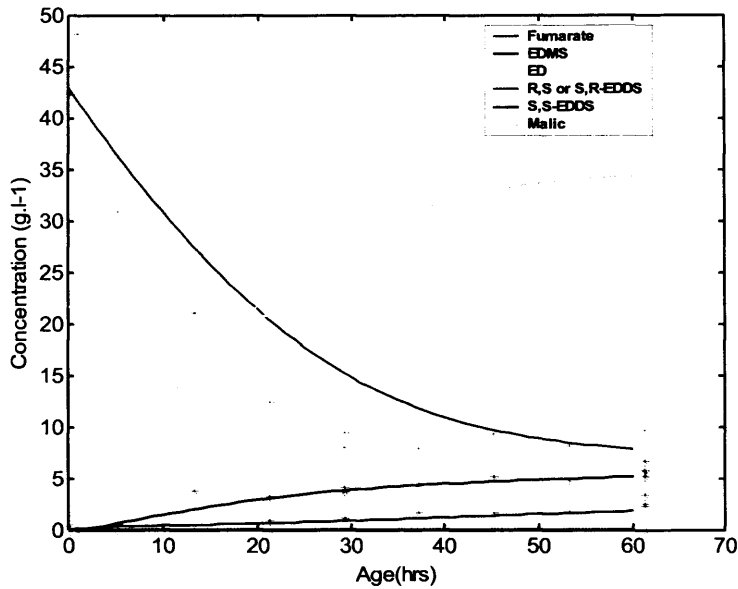
1. Isothermal reactor: Since reactions were typically carried out in the presence of temperature control, the model was verified for the situation in which temperature was assumed to be constant throughout the reaction with only composition of the reaction liquor and therefore specific heat capacities changing.
2. Adiabatic reactor: The alternative situation was that in which the reactions could be said to be run adiabatically and therefore any heat produced during the course of the reaction would affect reaction rate.

For both situations the overall mass balance and stoichiometry in Tables 5-2 and 5-3 were used to provide the change in concentration with time which when solved with a proprietary ode solver from Matlab ® provided progress curves for a wide range of initial conditions. In the first instance, the ODEs created by the use of the overall mass balance and reaction stoichiometry were solved by means of a fourth order Runge-Kutta ODE solver from Matlab ®, ode45, and therefore provide a series of computer generated progress curves in the absence of a dT/dt term as it was assumed that dT/dt was constantly zero under the isothermal assumption. However, for the adiabatic model the dT/dt term provided by the energy balance introduced some instability and therefore a stiff ode solver from Matlab ®, ode23s, was employed, together with breaks to aid the calculation process when temperature had increased to point at which V_{max} was essentially negative, ie specific activity was below zero. The above stoichiometry formed the basis of a series of ODEs, solved by ode45 in Matlab ® a 4th order Runge Kutta based algorithm. The series of ODEs for both sets of assumptions, relevant rate constants and the Matlab programs can all be seen in Appendix 10-6.

5.3.3 Validation

Validation of the overall model was carried out for both isothermal and adiabatic reactor assumptions. In the first instance, the ODEs created by the use of the overall mass balance and reaction stoichiometry were solved by means of a fourth order Runge-Kutta ODE solver from Matlab ®, ode45, and therefore provide a series of computer generated progress curves that could be compared to experimental data. The experimental data used for validation was not used in the determination of the model parameters and was produced with crude enzyme isolate from an individual batch of fermentation broth. Enzyme concentrations were found by determination of the V_{max} of each enzyme in the crude enzyme isolate and division of this by the average specific activity found in Chapter 4 to account for variations in crude enzyme isolate preparation. As can be seen in Figure 5-13 and 5-14., the model generally predicted the course of the reaction well under several sets of conditions including using both ED and *meso*-EDMS as reactants. Chi-squared values fell between 11 and 18 for 40 degrees of freedom, well below the required test statistic in the 95% confidence interval indicating the isothermal model is a valid hypothesis in situations where temperature is controlled.

$F_0 = 43 \text{ g.l}^{-1}$ $D_0 = 22 \text{ g.l}^{-1}$
 $SM_0 = 0 \text{ g.l}^{-1}$ $RM_0 = 0 \text{ g.l}^{-1}$
 $E_1 = 10.6 \text{ g.l}^{-1}$, $E_3 = 8 \text{ g.l}^{-1}$, $E_5 = 14 \text{ g.l}^{-1}$
 Chi-squared 18.83



$F_0 = 25 \text{ g.l}^{-1}$ $D_0 = 4 \text{ g.l}^{-1}$
 $SM_0 = 2 \text{ g.l}^{-1}$ $RM_0 = 2 \text{ g.l}^{-1}$
 $E_1 = 10.6 \text{ g.l}^{-1}$, $E_3 = 8 \text{ g.l}^{-1}$, $E_5 = 14 \text{ g.l}^{-1}$
 Chi-squared 11.78

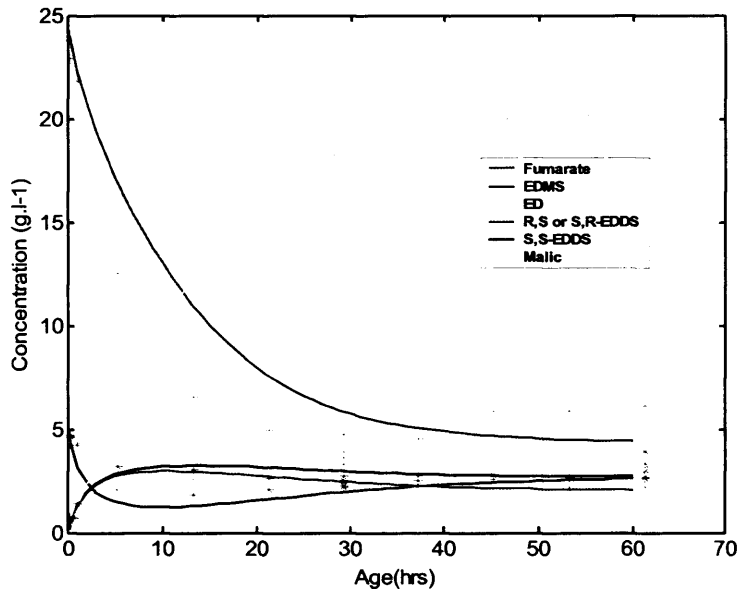
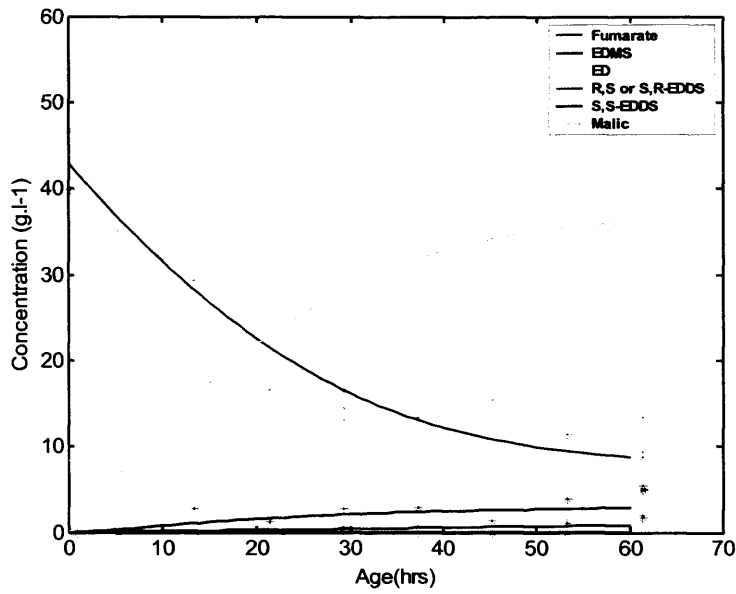


Figure 5-13 – Validation of overall kinetic model by comparison of experimental data

$F_0 = 43 \text{ g.l}^{-1}$ $D_0 = 8 \text{ g.l}^{-1}$
 $SM_0 = 0 \text{ g.l}^{-1}$ $RM_0 = 0 \text{ g.l}^{-1}$
 $E_1 = 10.6 \text{ g.l}^{-1}$, $E_3 = 8 \text{ g.l}^{-1}$, $E_5 = 14 \text{ g.l}^{-1}$
 Chi-squared 32.7



$F_0 = 12 \text{ g.l}^{-1}$ $D_0 = 2 \text{ g.l}^{-1}$
 $SM_0 = 0 \text{ g.l}^{-1}$ $RM_0 = 0 \text{ g.l}^{-1}$
 $E_1 = 10.6 \text{ g.l}^{-1}$, $E_3 = 8 \text{ g.l}^{-1}$, $E_5 = 14 \text{ g.l}^{-1}$
 Chi-squared 33.97

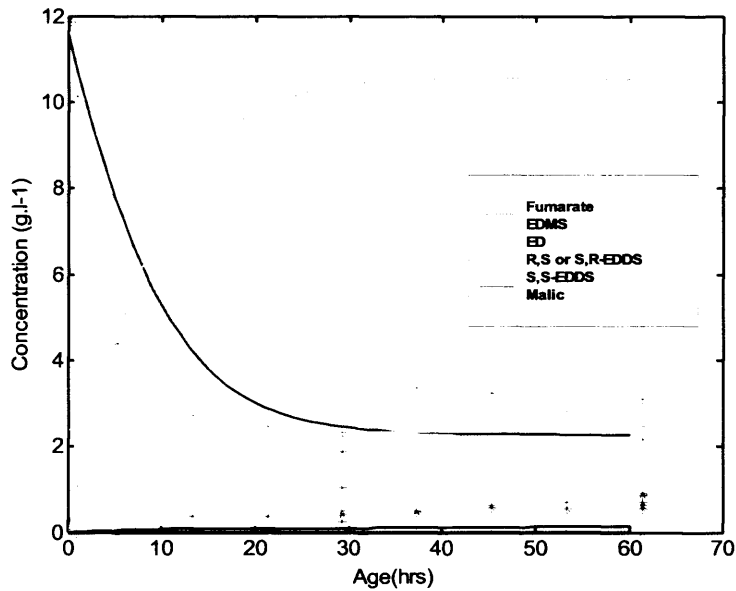


Figure 5-14 – Validation of overall kinetic model by comparison of experimental data

5.4 DISCUSSION

5.4.1 Reaction Models

The overall kinetic model was compiled by means of net rates (Table 5-3) and the reaction stoichiometry deducted in Chapter 4. The model was solved numerically using a fourth order Runge-Kutta ordinary differential equation solver built into Matlab ® for models run on the assumption of an isothermal process, however, for the adiabatic assumption a second order stiff solver also a built-in Matlab ® function was used as the solution appeared to show some stiffness. The error constraint in the solver was left at the default of 0.0001 as this was far smaller than the error involved in the elucidation of the comprising constants. The numerical solution was compared with experimental data not used to create the model. The chi-squared goodness of fit statistics returned for these models with 40 degrees of freedom were required at a significance level of 5% to be below 55 were 36 or lower and enable the overall conclusion that the models hypothesis is valid in the range for which the data was tested.

A quick sensitivity analysis was carried out on a parameter by parameter basis (Kossen and Oosterhuis, 1985). The one-by-one sensitivity analysis approach is known to not be particularly rigorous, with many groups preferring to use global sensitivity analyses to assess interactions (Saltelli *et al*, 2005). However, it does provide the modeller with a method by which Sensitivity analysis can quickly give an indication of high parameter sensitivity in the model. It can be seen in Figure 5-15 that the model is particularly sensitive to fumarase related parameters. This is understandable in that fumarase activity is substantially higher than that of EDMSase ($0.17 \text{ g.g}_{\text{dcw}}^{-1}.\text{h}^{-1}$ versus $0.08 \text{ g.g}_{\text{dcw}}^{-1}.\text{h}^{-1}$) and in many cases the low EDMSase concentration effectively substrate limits the reaction. It is however interesting to note the positive impact on final EDDS concentration with variation in the EDDS equilibrium constant, indicating that eventual assessment of methods of improving equilibrium such as use of *in-situ* product removal strategies may prove worthwhile as it has in industry for example in the production of amino acids (Ager *et al*, 2001; Carlton, 1992; Lye and Woodley, 1999).

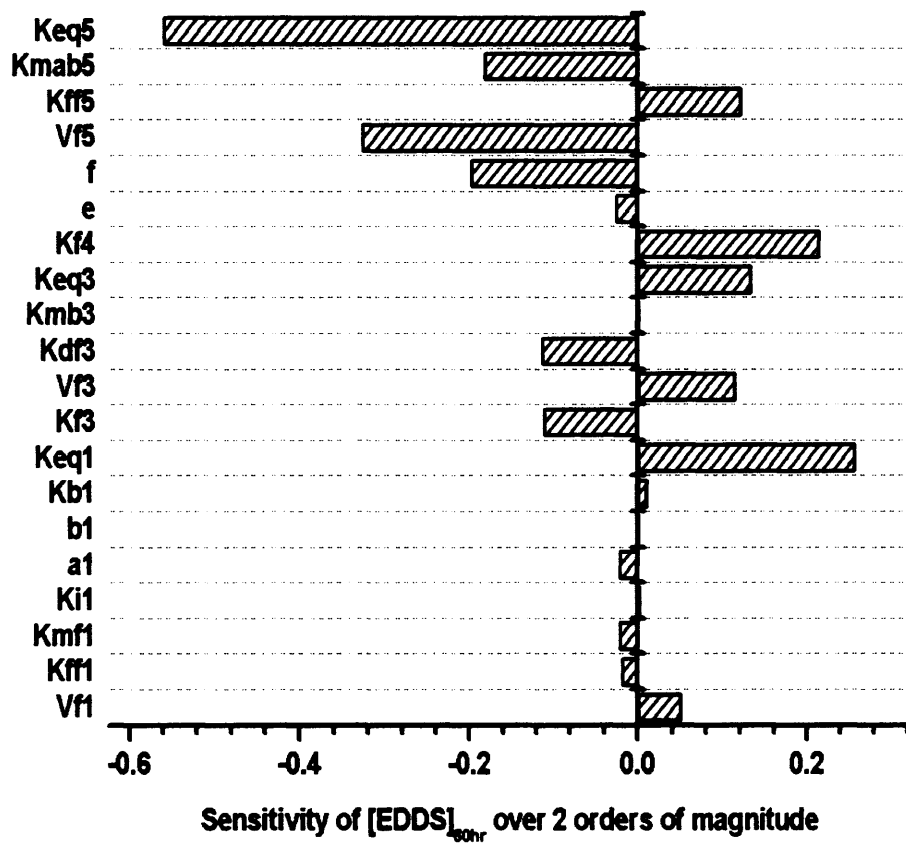


Figure 5-15 – Sensitivity of final EDDS concentration to 2-order of magnitude changes to the model parameters

5.4.1.1 Error

Error was inherent in the model from several different sources. Not least experimental error in the data used to provide the kinetic parameters, but also in the form of the models used and the fact that the overall model comprised many different parts all with associated error of their own. Several assumptions were made in the course of model development which all carry a level of uncertainty such as the existence of EDDSase, the use of the S,S-EDDS model to model the production of R,S (or S,R)-EDDS, dead-end inhibition of EDDSase by fumaric acid, stability of EDDSase under reaction conditions, use of the isothermal model in most situations and that minimal experimental data could be used to provide a basis for later extrapolation.

5.4.1.1.1 Experimental and Methodological Error

There were several sources of experimental error that affected the model including: the method for determining initial rates, sampling and analytical error and the methods themselves. Initial rates were determined by following the progress curve of a reaction by sampling at regular intervals, analysis by HPLC, fit of hyperbolae to the progress curve and then tangents to the progress curve being taken at less than 5% of reaction progress. This was a relatively consistent method producing consistent levels of error over all time points ($0.042 \text{ mol.l}^{-1}.\text{h}^{-1}$ for EDDSase and $0.0029 \text{ mmol.l}^{-1}.\text{min}^{-1}$ for EDMSase). Other methods do exist such as the use of chords for the integrated form of the Michaelis-Menten equation (Waley.SG, 1981) and creation of gradients from early sample points, based on the fact that early in an enzymatic reaction the kinetics are effectively first order. However, the chord method relies on integration of the relevant equation, a task that can be particularly time consuming for more complex enzyme reactions and assuming the early data is linear is highly reliant on the accuracy of a few sample points, when it was known for the EDDS reaction at early stages this error was often larger than the amount of EDDS produced as a result of the low and competing catalyst concentrations involved.

For EDMSase initial rate data, mass balances were used to backwards calculate the total amount of EDMS in the system. This though a valid method, does increase the amount of uncertainty as it relies on the mass balance closing and no remaining bacterial cells being able to consume the carbon. However, the mass balance on fumarate for these reactions was running at an average of 95%.

5.4.1.1.2 Model Related Error

Choice of the model for each constituent part also carried an element of error. For example the use of polynomials to represent the relationship of EDMSase rate and fumarase rate with temperature were highly sensitive to decimal places in the fitted parameters. However, polynomials were used as a result of lack of relevant data. For fumarase this was related to the temperature-rate data stopping at 30 °C, preventing the arrhenius relationship being used for the increasing side of the relationship. For the EDMSase activity-temperature relations this was related to crude enzyme isolate being used thereby preventing the isolation of temperature effects on EDMSase rate. The polynomial in this case represented the assumption that the peak of activity was similar to that of EDDSase and was in no way mechanistically correct. Though the use of the Arrhenius method is mechanistically correct describing more accurately the thermodynamics of activation and denaturation (Daniel *et al*, 2001) there are others who have employed polynomials to model temperature-activity effects (Fonchy *et al*, 1999).

Enzymatic models were chosen to be the simplest that would model the system at hand. For the EDDSase reaction system, this meant that all enzyme kinetic models used random order binding and the rapid equilibrium assumption. This is because use of ordered or steady state models would have vastly increased the amount of parameters to fit and therefore the error inherent in the fitting (King and Altman, 1956; Segel, 1993c). Since reasonable models were created though confidence in the EDDSase individual parameters was low, it seemed reasonable that the models

chosen were sufficient, but that confidence would have improved with additional initial rate data.

5.4.1.1.3 Kinetic Parameter Error

Error created in the non-linear regression of experimental initial rate data to the rate models was very variable. EDDSase standard error was high and resulted in confidence in the parameters being very low with the confidence interval being of 5 orders of magnitude, this has implications for the ability to extrapolate the model, particularly with its later reliance on EDDSase kinetics. Beneficially though, the overall model, when validated with several datasets from different fermentations, had Chi-squared values lower than the test-statistic, indicating that the model was reasonable for the range of conditions tested. Interestingly, although sensitivity to fumarase parameters was high, confidence in EDMSase and fumarase data was reasonable. It can be noted at this stage, that it would obviously be preferable to gain further EDDSase initial rate data to produce a more reliable parameter fitting.

Backwards rate constants were estimated by simulation of ODEs for all three enzymatic systems and it is noted that as a result of the mixture of enzymes in the crude, that this is not a particularly reliable method due to the variation in the progress curve at later stages. It would perhaps be more valid to rely on the backwards rate constant had initial rate data for the backwards reaction been collected and regressed to the backwards rate model.

5.4.1.2 Fumarase

Fumarase kinetic constants were determined by non-linear regression of initial rate data against fumaric acid concentration with all points assumed to have equal weighting. Sensitivity analysis of the predicted progress curves by numerical solution in Matlab and comparison of this to experimental progress curves. It is noted that this backwards rate is inaccurate and that a far better estimation of the backwards rate constant could be made by use of malic acid as a reactant and analysing the initial

rates of the backwards reaction to fumaric acid to produce the backwards parameter by non-linear regression (Segel, 1993b). The temperature information in the literature focussed mainly on thermostable fumarases (<http://www.brenda.uni-koeln.de/>) (Flint, 1994), however, the experimental evidence suggested that fumarase from *Chelatococcus asaccharovorans* had an optimum at about 30°C, so a polynomial was applied to the maximum rate over the enzyme concentration against temperature. Verification of this temperature optimum in *Chelatococcus* would be worthwhile, particularly since EDDSase appears to have a high temperature optima for a soil bacterium, but also because this could provide a method for heat inactivation of fumarase without recourse to expensive chemical agents. The polynomial adjusted V_{\max} accordingly, though mechanistically this was not correct. Validation of the fumarase kinetic model provided a X^2 value of 59.5, lower than the test statistic required for 95% confidence in the model for 60 degrees of freedom was 79.1.

5.4.1.3 EDMSase

The EDMSase model constants were determined in the same manner as those for fumarate, relying on mass balanced S,S-EDDS data to provide the actual initial rates of EDMS production. The X^2 value so produced on running the numerically solved progress curve and comparing it to experimental data was 34.0 when the test statistic was 43.8, confirming a 95% confidence in the model. The rate constants for the EDMS chemical reaction were determined by linear regression, following well established chemical techniques and could be seen to fit the data sufficiently in Figure 5-13 and 14.

The reaction model and specific activity, $0.08 \text{ g.g}_{\text{dcw}}^{-1} \cdot \text{h}^{-1}$ indicated that EDMSase titre was very low, but existed. Comparison of the model to the experimental data confirmed that the production of EDMS was not just by chemical means, as the rate of production was higher than that achievable solely by the chemical reaction. Together with the validation that R,S-EDDS was produced when the chemical reaction to EDMS dominated and the fermentation data seen in Chapter 3 indicated that EDMSase was a separate enzyme, worthwhile isolating and characterising fully. Literature appears to

back this up, with a Swiss group indicating that EDDSase does not catalyse the first half reaction when isolated (Witschel and Egli, 1998).

5.4.1.4 EDDSase

EDDSase was modelled using a typical bi-uni Michaelis-Menten model, however, data in Chapter 3, indicated the possibility of fumarate inhibition and hence a dead-end inhibition term was included in the model. It can be seen in Figure 5-8, that the regression determined a fumarate inhibition constant at approximately 7 g.l^{-1} at the fumarase concentrations used. In the process of modelling the EDDSase reaction system it was assumed initially that there was no decrease in enzyme activity due to denaturation over time. This was a result of several experiments carried out over time periods of the order of weeks in a miniature CSTR to keep reactant and reactant concentrations constant with a 30 kDa ultrafiltration membrane to ensure enzyme remained in the reactor. These experiments were inconclusive as concentrations were so low as to be within the range of the HPLC analytical error. It was expected that as the enzyme denatured the concentration of EDDS would increase over time, however, no change in product concentration was seen over the course of any of these experiments. Furthermore it was known that reactions had been run up to 60 hours in length and that product concentration was still changing in these experiments at the time when the reaction was stopped as a result of lack of remaining sample.

Interestingly though, the assumption that enzyme stability does not decrease over at least the time span of 60 hours enables the hypothesis to be tested on running the model. As can be seen in Figure 5-13 and 5-14 above that S,S-EDDS concentration predicted by the overall model could be compared favourably to the data, indicating that at least over the range of reaction conditions tested and over the course of 60 hours EDDSase activity appears to be stable. It was known however from storage stability experiments that EDDSase activity degraded by approximately 50% over 48 hours at 4°C , whether as ammonium sulphate or phosphate buffer suspension.

However following the above hypothesis, it is proposed that the crude enzyme isolate contains proteases particularly metalloproteases, that are inhibited in the presence of the chelating fumarate, ED, EDMS and EDDS.

5.4.2 Energy Balance

The energy balance was compiled with the use of the assumption of an adiabatic process, so that the maximum heat production rate could be found. Where data required to calculate the specific heat capacities or enthalpies was missing estimations were made or data used from a similar compound. Though this is not completely reliable data, the adiabatic model was not to be used for later extrapolation, but for estimation of maximum rate as related to the ability of the process equipment to remove heat. The heat of reaction was based on the reaction of fumarate and ED and did not include EDMS as this data did not exist and EDMS cancelled out in the stoichiometry.

5.4.3 Overall Model

The compilation of the model into a validated whole was achieved so that further process analysis and possibilities for scale-up could then be carried out. The model was derived on a volumetric basis and so to some extent is independent of scale, particularly with a regard to reaction rates and heat production rates. However, heat and mass transfer are scale dependent. The process being characterised as it is by fumarate inhibition and the need for good temperature and pH control all indicate that good mixing will be required in the fermenter furthermore heat removal will need to be assessed as the surface area to volume ratio decreases with increasing scale.

Overall, the model can be seen to describe the EDDSase system of reactions as they stand at present with reasonable agreement. Models have been built to enable the extrapolation of the data on the basis of scale and changes to the catalyst concentrations available, but confidence in the EDDSase reaction model particularly is low and therefore care is required when considering further analyses.

5.5 CONCLUSION

A process model has been proposed by the isolation of each separate reaction and an energy balance and compiling the resulting rate equations into a system of ordinary differential equations solvable by a fourth order Runge Kutta algorithm. The resultant model was validated using experimental data and indicated several interesting features of the reaction system, namely that EDMSase was responsible for the selective production of S-EDMS and was crucial to the overall production of S,S-EDDS by biocatalytic means, but also that EDDSase was particularly stable under reaction conditions, the result gained from the analysis of heat production during a small scale EDDSase reaction was not a result of experimental error, but a result of low rates and that the reactant fumarate was inhibitory to EDDSase.

6 PROCESS ANALYSIS AND EVALUATION

6.1 INTRODUCTION

Process analysis is an integral part of any process development. However, it can be seen in the literature that there are few methods available for the analysis of biocatalytic processes. This is mainly as a result of the complex kinetics and reaction parameters that are often inherent in enzymatic reactions such as mass transfer limitations, side reactions and low water solubility of reactants and products amongst others. As a result the literature covers many and varied biocatalytic processes often accompanied by complex and accurate mechanistic models (Bühler *et al*, 2006; Willeman *et al*, 2002a; Zimmermann *et al*, 2006). However, these models are rarely used to evaluate the likely process route or even to determine more bottlenecks than those specifically under investigation. This situation arises for several reasons not least the complexity of both biocatalytic processes and the models so created to describe them, but also the lack of generic methods for bottleneck identification applicable to all biocatalytic process. Consequently, key bottlenecks may go undiscovered until later in the design process. It can be noted at this point that in the initial stages of process development it is key that process analyses should not be too detailed, indeed since the aim at this point is to determine where additional process research should be focussed and further changes to the models are likely, detailed analyses can be a hindrance, costing too much in terms of effort for the desired result. Several methods of initial identification of bioprocess bottlenecks other than individual assessment of the biocatalytic reaction at hand have been suggested. These include:

1. Identification of limiting reactant concentrations by the use of Blackman kinetics (Brass *et al*, 1997; Dabes *et al*, 1973; Hoeks *et al*, 1996). These describe how below a critical concentration of reactant, rate increases linearly with concentration, with other mechanisms or reactants controlling the rate above the critical concentration. However, as with all kinetics this critical

concentration has to be determined experimentally, a task made harder by the assumption of linearity when enzyme kinetics are not linear. Furthermore, reliance on experiments to identify the controlling mechanism may mean a key bottleneck at large scale remains unidentified.

2. Assessment of characteristic times in regime analysis, where controlling regimes can be identified by assessment of characteristic times, reactant concentrations or reactor conditions (Kossen and Oosterhuis, 1985; Sweere *et al*, 1987; Wolff *et al*, 1999). This can be seen to be analogous to the identification of flow regimes by assessment of velocities in chemical engineering situations (Bhole and Joshi, 2005; Link *et al*, 2005). As with Blackman kinetics a certain amount of experimentation and a somewhat fixed process are required to be able to identify the controlling regimes.

Neither of these methods address the issue of biocatalyst concentration, so comparison between fermentation output and what is required in terms of biocatalyst in the bioreactor cannot be made. Knowledge of the catalyst concentration required for the reaction is key to process integration, as this can affect both the quality of the process liquor and therefore downstream unit operations, but will also affect sizing of the fermentation, whether the reaction can be carried out *in-situ* in the fermenter or whether further processing between fermenter and reactor are required to gain the desired catalyst concentration. This chapter aims to address this.

The previous chapter details and validates a kinetic model for the biocatalytic production of S,S-EDDS from a wild type biocatalyst. It would obviously have been desirable to use a simpler form of kinetics at this early stage of process design. However, the number of unknowns and competing reactions precluded this. As seen in Chapter 4, there are several key hindrances to the EDDSase process at present, not least lack of biocatalyst in process scale quantities. Therefore to be able to compare the synthetic route to S,S-EDDS and the theoretical biocatalytic route a model is

necessary to be able to extrapolate to larger enzyme concentrations. As such the model described in Chapter 5 will form the basis of a process analysis undertaken to determine the key bottlenecks or limiting regimes inherent in the process with regards to biocatalyst concentration and enable the proposal of possible design solutions.

What is presented here is a novel method for analysing and evaluating biocatalytic processes which uses the importance of biocatalyst concentration for process integration to develop a view of the potential of the overall process and enable the designer to develop methods for future biocatalyst improvement.

6.2 BOTTLENECK IDENTIFICATION

6.2.1 Identification of Process Limitations

As can be seen in Figure 6-1, in order to identify the limiting catalyst regimes product-time curves at varying catalyst concentrations were required. For the EDDSase process these were obtained by interrogation of the isothermal model described in Chapter 5. One such progress curve can be seen in Figure 6-2 run at enzyme concentrations taken from the fermentation batch from which the model was validated (i.e. 10.6 g.l⁻¹ EDDSase, 8 g.l⁻¹ EDMSase and 140 g.l⁻¹ fumarase Chapter 5, Figure 5-13) and at the concentrations used for a typical reaction: 29 g.l⁻¹ fumaric acid and 6 g.l⁻¹ ethylenediamine.

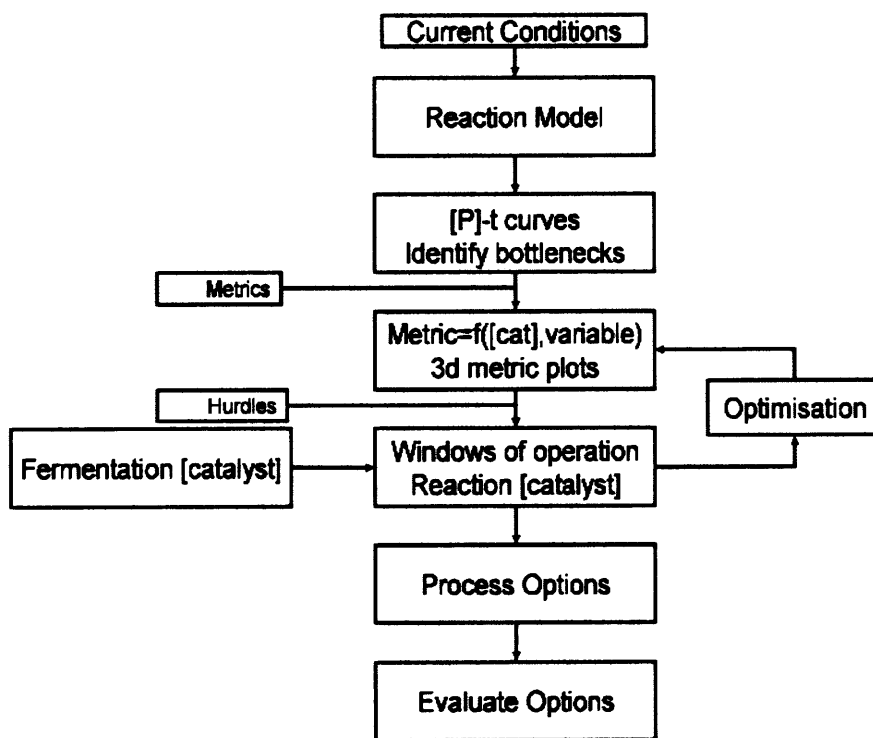


Figure 6-1 – Method for identification and assessment of limiting biocatalyst regimes

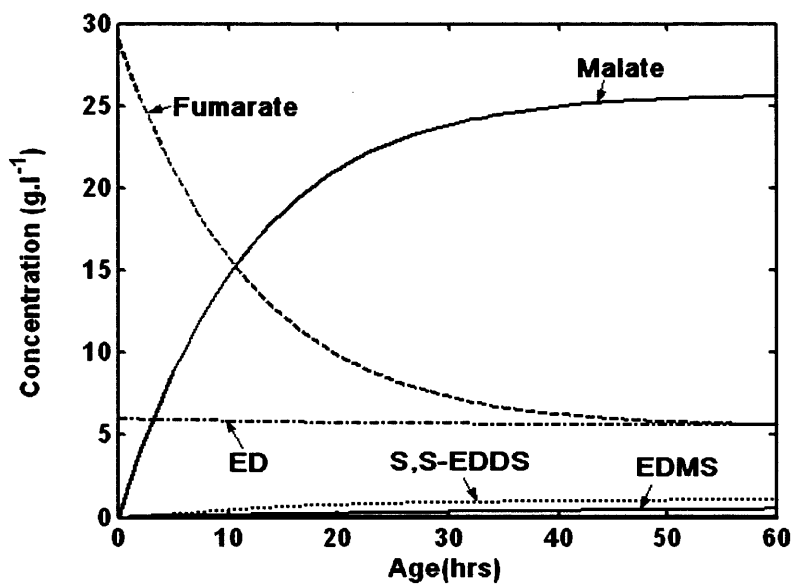


Figure 6-2 – Progress curve using typical *Chc asacc* fermentation enzyme concentrations and initial conditions used in the typical reaction described in Chapter 4

Limitations to this typical reaction were found by the use of a simple sensitivity analysis of the model described in Chapter 5, by assessing the impact of extreme changes in biocatalyst concentration other than EDDSase (e.g. reduction of fumarase to zero and 1000-fold increase of EDMSase concentration) on the S,S-EDDS concentration progress curve. By studying the variation in the progress curve in the absence of fumarase identified that a fumarase limitation existed in Figure 6-2 (Figure 6-3, line C) which was related to the fumarase reduction of fumaric acid and essentially a concentration limitation. For EDMSase, a rate limitation was identified (Figure 6-3, line B) which substrate limited the EDDSase catalysed second half reaction.

As an extension to this initial sensitivity analysis, it was possible to identify two further limitations that were masked by the EDMSase and fumarase limitations initially. This was achieved by decreasing fumarase concentration to zero and setting EDMSase concentration to be in large excess (1000x) (Figure 6-3). It can be seen therefore in Figure 6-4 that the remaining limitations that could not be changed were an equilibrium limitation (line D) which was a function of the initial concentrations fed to the reaction and a EDDSase biocatalyst limitation (line A) in which rate was limited by the concentration of EDDSase provided to the reaction. EDMSase and fumarase limitations identified in Figure 6-3 are also shown in Figure 6-4 as lines B and C respectively.

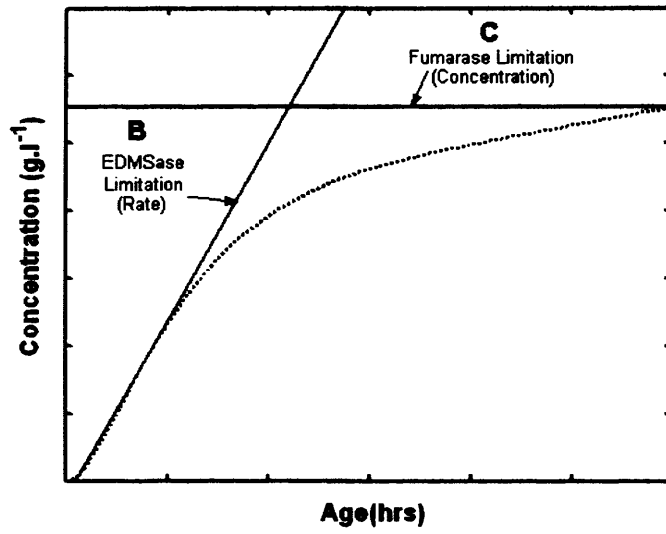


Figure 6-3 – Schematic showing EDMSase and fumarase limitations for Figure 6-2

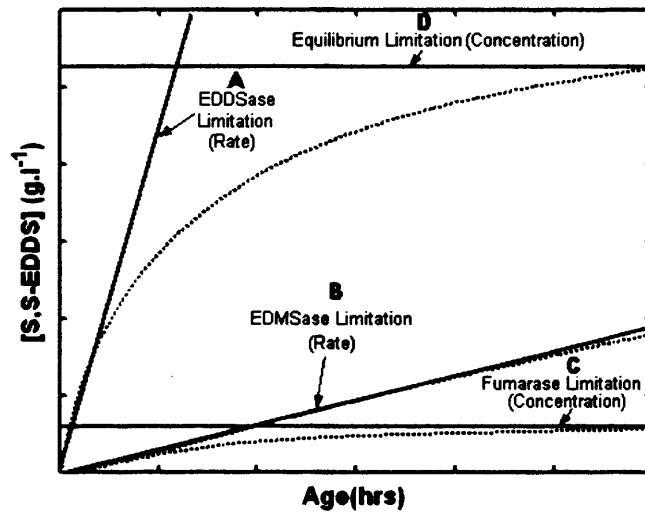


Figure 6-4 – Key limitations to the EDDSase process and their effects on the progress curve

6.2.2 Process Metrics

From Figure 6-2 together with knowledge of the current synthetic process, likely downstream processing routes and typical industrial performance indicators several process metrics could be suggested. It was known that the likely downstream processing route was to be precipitation driven as the current synthetic route employs calcium precipitation of S,S-EDDS at present and this to some extent defined the requirements of the process flowsheet, in particular the final reaction liquor was required to be in high S,S-EDDS purity and concentration. Taking this into account, the process performance indicators were chosen to be:

1. Final product concentration ($[P]_{\text{final}}$), the total amount of product produced over a 12 hour batch time, the current batch time for the synthetic process. The final product concentration indicates the size requirements of the reactor; a high product concentration requires a smaller reaction vessel and makes downstream processing easier.

$$P = \frac{[P]_{\text{final}}}{12} \quad (\text{g.l}^{-1}.\text{hr}^{-1}) \quad (6-1)$$

2. Yield ($Y_{P/F}$) of S,S-EDDS on the theoretical maximum achievable from the fumarate concentration provided to the reaction. It can be seen in Figure 6-2 that fumaric acid is used particularly inefficiently with molar yield on fumarate being approximately 3%. Yield was calculated (Equation 6-2, where 116 and 292 are the atomic masses of fumarate and S,S-EDDS respectively) based on the theoretical maximum from the quantity of fumaric acid provided to the reaction.

$$Y_{\frac{P}{F}} = \frac{[P]_{\text{final}}}{[F]_0} \times \frac{116}{292} \times 100 \quad (\%) \quad (6-2)$$

3. Enzyme efficiency (η) or the amount of product produced per gram of biocatalyst (Equation 6-3). Enzyme efficiency indicates the expense required

in fermentation, a high enzymatic efficiency indicating a small fermentation and *vice versa*.

$$\eta = \frac{[P]_{\text{final}}}{[E_1]} \quad (\text{g} \cdot \text{g}_{\text{dcw}}^{-1}) \quad (6-3)$$

4. Maximum rate of S,S-EDDS production ($r_{p,\text{max}}$) or initial rate ($\text{g} \cdot \text{l}^{-1} \cdot \text{h}^{-1}$). A high rate is indicative of a productive process; however this is dependent on stability.
5. Purity (X) of S,S-EDDS at the end of the batch in comparison to all amino acid type compounds (Equation 6-4). Purity provides a measure of the difficulty of downstream separation.

$$X = \frac{[P]_{\text{final}}}{[P]_{\text{final}} + [RP]_{\text{final}} + [RM]_{\text{final}} + [SM]_{\text{final}}} \times 100 \quad (\%) \quad (6-4)$$

6. Enantiomeric excess (ee, Equation 6-5), the ratio of S,S-EDDS to all EDDS in the process stream. As only the S,S stereoisomer is biodegradable ee provides a further measure of ease downstream processing.

$$ee = \frac{[P]_{\text{final}}}{[P]_{\text{final}} + [RP]_{\text{final}}} \quad (\%) \quad (6-5)$$

6.2.3 Effect of Increasing Catalyst Concentration on Process Metrics

In general it can be assumed that increasing biocatalyst concentration should increase reaction rate and other metrics such as product concentration. However, the situation is not so straight forward and process limitations affect this relationship. To improve the metrics an optimal catalyst concentration is required which will then determine the concentration of catalyst required to be produced by fermentation and in the EDDSase example, the ratio of the three enzymes required. To this end, metric-catalyst concentration plots were produced by generation of isothermal model progress curves at varying initial EDDSase concentrations on the assumption that temperature could be controlled adequately. The metrics so produced from each curve were collated and plotted against their respective EDDSase concentration. Figure 6-5, shows the final process metrics for a series of *in-silico* reactions in which EDMSase was set at $8 \text{ g}_{\text{dcw}}\cdot\text{l}^{-1}$, fumarase, $140 \text{ g}_{\text{dcw}}\cdot\text{l}^{-1}$, fumarate, $29 \text{ g}\cdot\text{l}^{-1}$ and ED, $6 \text{ g}\cdot\text{l}^{-1}$ at 30°C as *per* the validation batch (Chapter 5). As was seen in Figure 6-4, there are currently several limitations to the EDDSase reaction, namely lack of EDMSase, an excess of fumarase and equilibrium and as a result it can be seen in the lower half of Figure 6-5 the metrics are very low (with product concentration being less than $0.5 \text{ g}\cdot\text{l}^{-1}$ upto an EDDSase concentration of $10 \text{ g}_{\text{dcw}}\cdot\text{l}^{-1}$ and that enzymatic efficiency is excessively low. Furthermore it can also be seen that increasing EDDSase concentration to above $10 \text{ g}_{\text{dcw}}\cdot\text{l}^{-1}$ in the presence of the fumarase and EDMSase limitations appears to be futile.

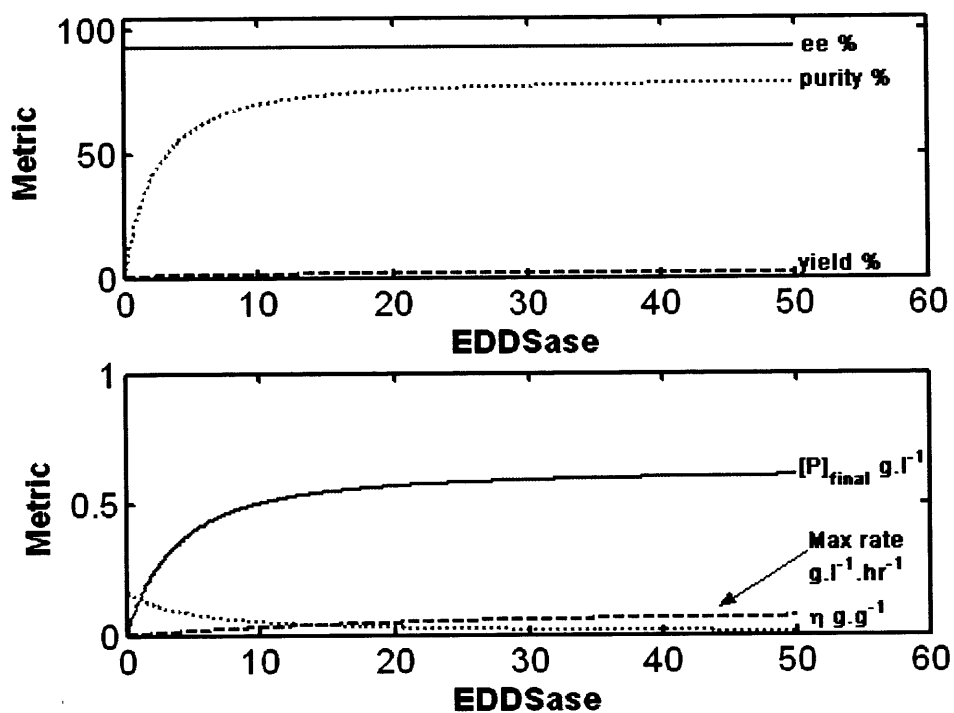


Figure 6-5 – Metric-catalyst concentration plot for fumarase and EDDSase at concentrations achievable by fermentation of *Chelatococcus asaccharovorans* and typical reaction conditions (Chapter 4)

However, as indicated in Figures 6-3 and 6-4, EDMSase and fumarase currently limit the EDDSase reaction and further interrogation of the model and in particular assessing the enzymatic efficiency of EDDSase when these limitations are reduced can indicate which limitation is currently the greater bottleneck.

By studying the metrics against initial EDDSase concentration *in-silico* for two situations in which EDMSase concentration was increased to be in large excess or fumarase was reduced to zero it was found that the key limitation to improvements in the metrics was EDMSase concentration. Reduction in fumarase concentration (Figure 6-6) had little effect on final concentration, purity or rate, whereas increasing EDMSase concentration in the presence of fumarase did (enzymatic efficiency of $0.5 \text{ g.g}_{\text{dcw}}^{-1}$ versus $0.05 \text{ g.g}_{\text{dcw}}^{-1}$ when EDMSase concentration was increased 1000-fold) (Figure 6-7). A further method for assessment and identification of limiting regimes is also presented in (Law *et al*, 2006) for a biocatalytic oxidation reaction for a simplified, linearised set of kinetics.

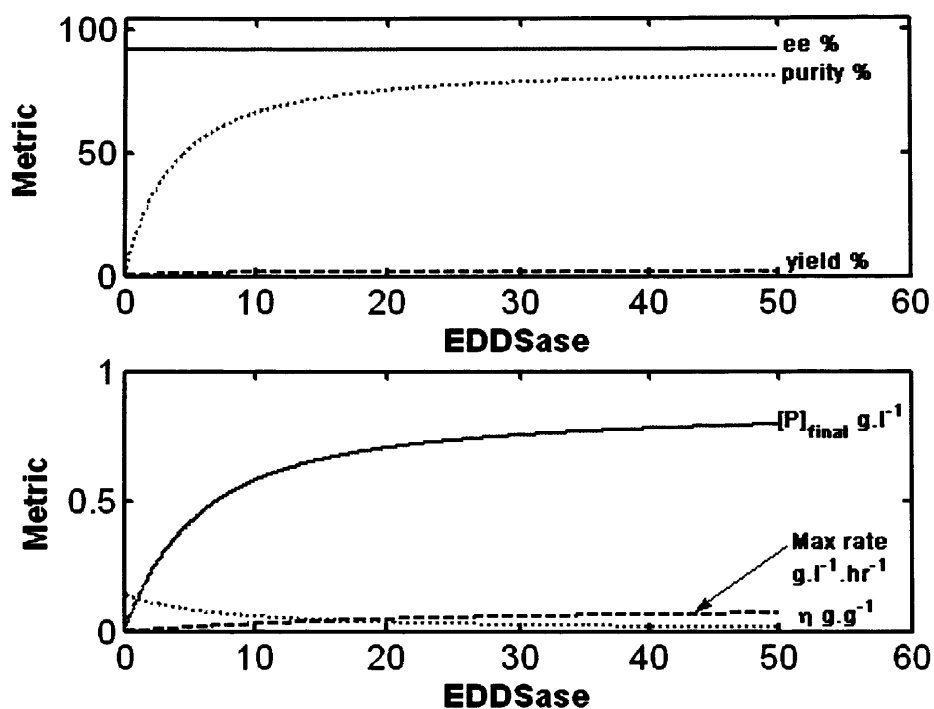


Figure 6-6 – Change in metrics when fumarase concentration is reduced to zero.

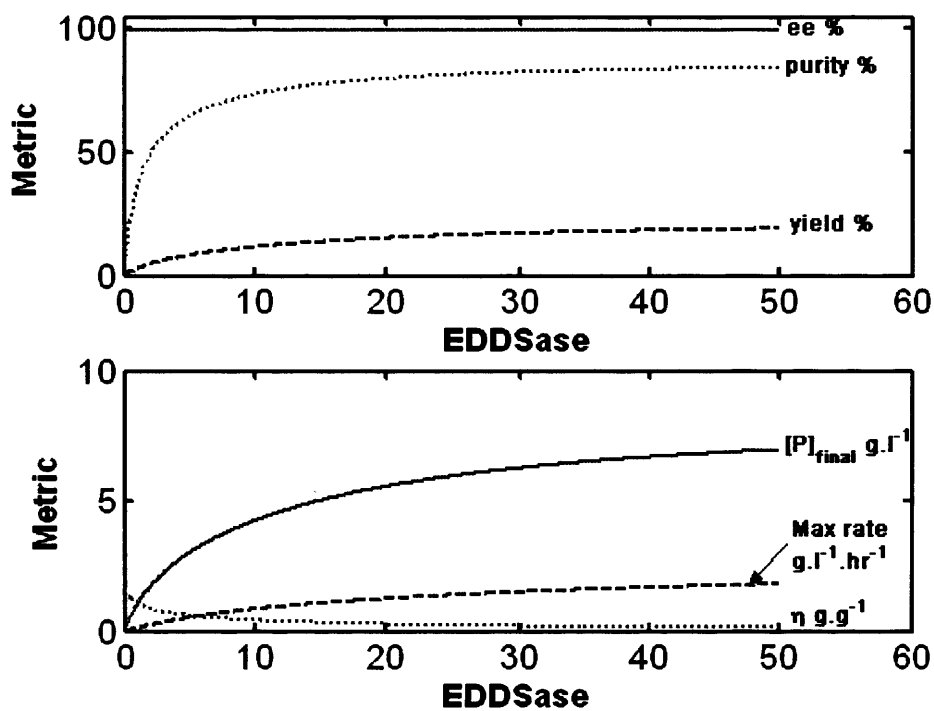


Figure 6-7 – Change in metrics when EDM5ase is provided to the reaction in large excess in the presence of fumarase

6.3 SENSITIVITY ANALYSIS

It can be seen in Figures 6-5 to 6-7, identification of the limiting variable requires comprehensive sensitivity analysis. It is instructive therefore to plot metric against catalyst concentration and one other variable, providing a method of analysing the effect of reducing an individual limitation. Matlab was used to create progress curves for each set of conditions, produce and collate the metrics and finally plot a 3d surface so analyses of the changing metrics with catalyst concentration and the limiting process variable were possible. A typical program and its constituent parts for the assessment of the effect of increasing EDMSase and the catalyst EDDSase on the metrics can be seen in Appendix 10-6. The process variables and associated limitations assessed were: EDMSase, fumarase, Initial ED, initial EDMS and initial fumarate concentrations and reaction temperature (Table 6-1). Figure 6-8 shows the change in each metric (A, maximum rate, B, final product concentration, C, yield, D, enantiomeric excess, E, enzyme efficiency and F, purity) with EDDSase to assess the effect of increasing EDMSase concentration and therefore reducing the EDMSase limitation. Initial concentrations were fumarate 29 g.l⁻¹, ED 6 g.l⁻¹, no EDMS and Fumarase 140 g_{dcw}.l⁻¹ at 30 °C as *per* standard reaction conditions. It can be seen that increasing EDMSase concentration increases rate (Figure 6-8A), product concentration (B) and yield (C). However, this quickly reaches a plateau, indicating the presence of a further limitation, related in this case to fumarate removal. Interestingly increasing EDMSase appeared to increase purity and enantiomeric excess (D and F respectively).

Variable	Associated Limitation
[EDMSase]	EDMSase (rate)
[Fumarase]	Fumarase (concentration)
[ED]	Equilibrium (concentration)
[Fumarate]	Equilibrium (concentration)
[EDMS]	Equilibrium (concentration)
Temperature	EDDSase (rate)

Table 6-1 – Variables tested in sensitivity analysis and associated limitations

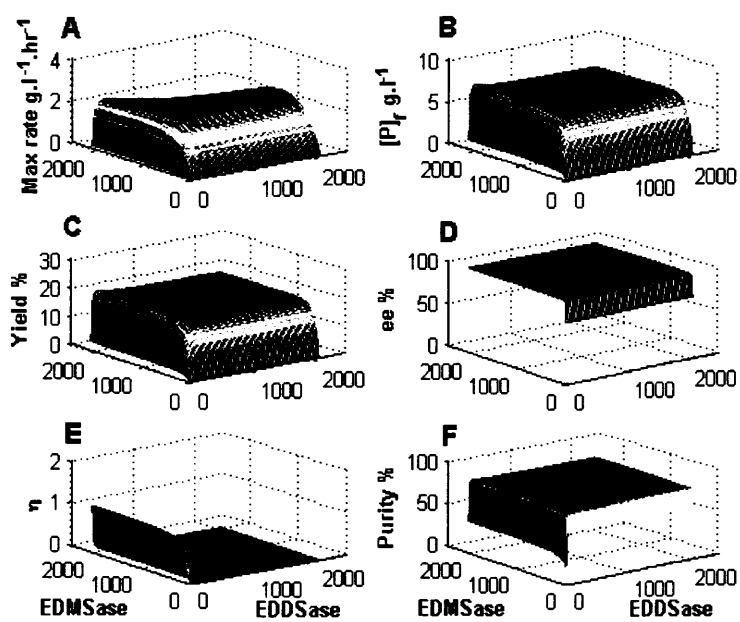


Figure 6-8 – Effect of increasing EDMSase on the metrics

Figure 6-9 shows the change in metrics with EDDSase and fumarase concentration at initial concentrations of 29 g.l⁻¹ fumarate, 6 g.l⁻¹ ED, no EDMS, 8 g_{dcw}.l⁻¹ EDMSase at 30 °C, highlighting the effect of the fumarase limitation. It can be seen in Figure 6-9 A, B and C that any increase in fumarase dramatically decreases the initial rate, product concentration and yield as the amount of fumaric acid available to EDDSase decreases and that this also affects the enzyme efficiency (E). Interestingly ee increases with increasing fumarate concentration, presumably because less fumarate is available for the chemical reaction mixture-EDMS (Figure 6-9 D). Purity initially decreased with fumarate before reaching a plateau indicating a further limitation (Figure 6-9 F), a possible consequence of fumarate unavailability to the second half reaction. Reducing fumarase concentration in the reaction could therefore be seen to be worthwhile.

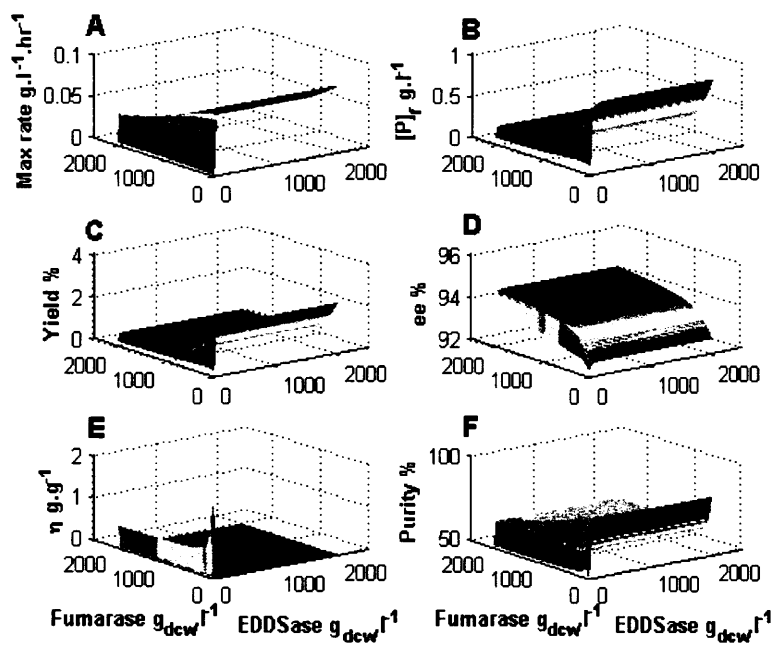


Figure 6-9 – Effect of increasing fumarase concentration on the metrics

The effect of temperature can be seen on the metrics in Figure 6-10. Initial conditions were 29 g.l⁻¹ fumaric acid, 6 g.l⁻¹ ED, no EDMS, 8 g_{dcw}.l⁻¹ EDMSase and 140 g_{dcw}.l⁻¹ fumarase. As would be expected from the model temperature increased initial rate, product concentration and yield until 50 °C was reached. At which point further increases in temperature decreased the rates according to denaturation theory (Figure 6-10 A, B and C). Interestingly though both ee and purity peaked at 30 °C and then proceeded to decrease with further increases in temperature (Figure 6-10 D and F), as a result of increased chemical reaction rates. Therefore it could be proposed that the reaction temperature should remain 30 °C.

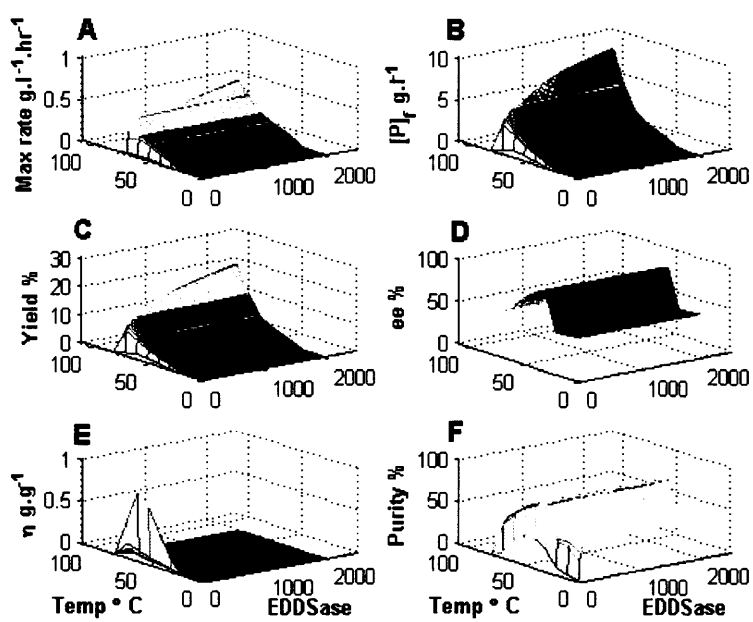


Figure 6-10 – Effect of increasing reaction temperature on the metrics

Figure 6-11 shows the effect of using *meso*-EDMS as would be the case if a chemical reaction were used to produce the intermediate with no intermediate resolution of the EDMS enantiomers. Initial conditions were 30 °C, 29 g.l⁻¹ fumarate, no ED, 8 g_{gcw}.l⁻¹ EDMS and 140 g_{dcw}.l⁻¹ fumarase. Increases in initial concentrations of *meso*-EDMS can be seen to increase rate as the lack of EDMSase becomes unimportant. Product concentration increases correspondingly as does yield on fumarate. However, ee and purity are low at less than 50 % (Figure 6-11 D and F) a result of EDDSase being unspecific for EDMS stereoisomers of the *meso*-EDMS as a reactant forming R,S-EDDS and S,S-EDDS stereoisomers, suggesting that use of *meso*-EDMS would be detrimental to the process unless an intermediate resolution was used.

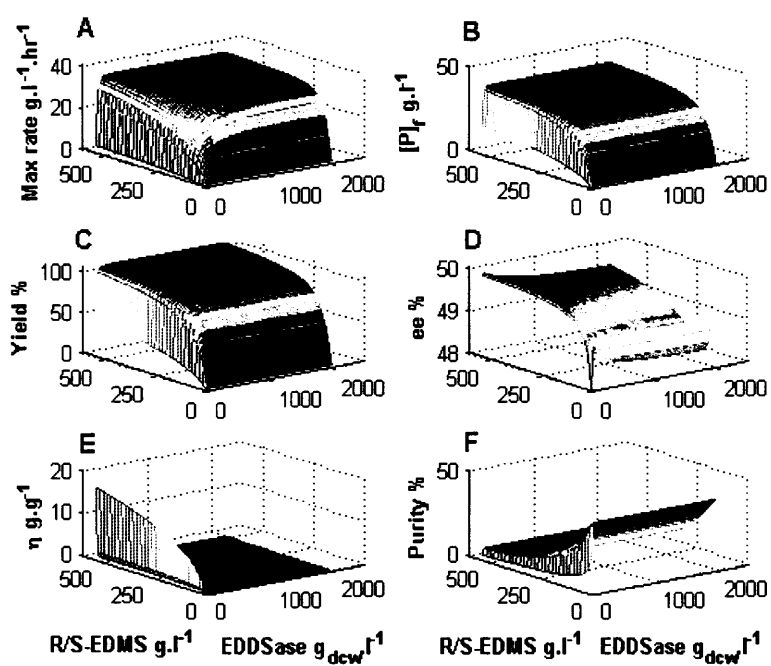


Figure 6-11 – Effect of increasing *meso*-EDMS. concentration on the metrics

The effect of both reactant concentrations on the process metrics were assessed at constant EDDSase and EDMSase concentrations as in bireactant systems the reactant not in excess has a limiting effect. It can be seen in Figure 6-12 A ($10 \text{ g}_{\text{dcw}} \cdot \text{l}^{-1}$ EDDSase, $8 \text{ g}_{\text{dcw}} \cdot \text{l}^{-1}$ EDMSase and $140 \text{ g}_{\text{dcw}} \cdot \text{l}^{-1}$ fumarase and 30°C) that initial rate and final product concentration were higher in the presence of an excess of ED. This skewing towards ED was found to be a result of a fumarate inhibition of EDDSase. Yield on fumarate was low indicating a limitation related to lack of EDMSase. Purity and yield were at a maximum at approximately $50 \text{ g} \cdot \text{l}^{-1}$ fumarate, decreasing with increasing fumarate. Furthermore, purity appeared independent of ED concentration, related to fumarate reacting to produce malate in the presence of fumarase thereby reducing the available fumarate for the EDDSase reaction. It would be logical therefore to propose that reactions were run at an excess of ED at the conditions assessed.

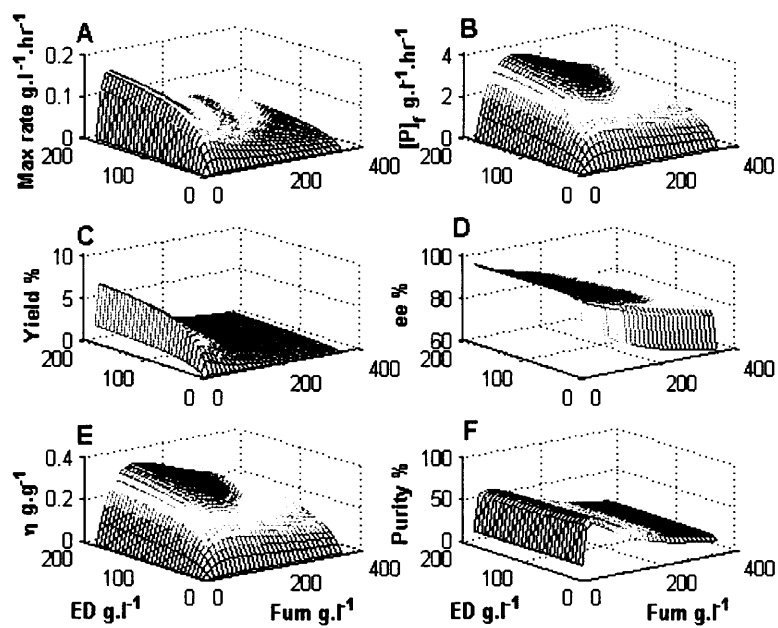


Figure 6-12 – Effect of increasing initial concentrations of ED and fumarate on the metrics

6.4 PROCESS EVALUATION

6.4.1 The Ideal Batch Process

Process metrics were chosen on the basis of typical industrial performance indicators which could be associated with hurdle values and at the same time enabled assessment of possible process economics (Table 6-2). Some such metrics were chosen to be final product concentration, which is typically over 100 g.l⁻¹.batch⁻¹ (Rozzell, 1999), yield, which for equilibrium led reactions is often low and enzyme efficiency, which is preferably at least 10 g.g_{dcw}⁻¹. Furthermore knowledge of the product currently sold by Octel as Octaquest E30, required S,S-EDDS to be 95% of all amino acid compounds and 99% of the total EDDS concentration, these were assessed as purity and enantiomeric excess respectively. It was also known from the model produced in Chapter 5 and a Mitsubishi patent (Shigeo *et al*, 2004) that the process was exothermic and rate of volumetric heat production was a function of maximum rate, described by the energy balance derived in Chapter 5 in adiabatic conditions. The maximum surface area available for heat transfer was calculated from the volume required for 1000 tonnes *per annum* of S,S-EDDS and required that temperature production had to be less than 15 K.l⁻¹.h⁻¹ (see Appendix 10-5) corresponding to a maximum rate of 292 g.l⁻¹.h⁻¹.

The key limiting regimes suggested by the sensitivity analysis and several process performance hurdles based on the chosen metrics were then used to plot two windows of operation for the process to indicate the operable region. One window was based

Metric	Hurdle
Minimum product concentration	100 g.l ⁻¹
Maximum rate	292 g.l ⁻¹ .h ⁻¹
Minimum purity	95 %
Minimum enantiomeric excess	99 %
Minimum enzymatic efficiency	10 g.g _{dcw} ⁻¹
Minimum yield	50 %

Table 6-2 – Hurdle values and their associated metrics

on the comparison of EDDSase and EDMSase concentrations and the other the comparison of ED and fumarate initial concentrations having assumed that some method of reducing fumarase/EDDSase ratio substantially was possible. The windows were formed in Matlab® by use of the isothermal model described in Chapter 5 and simple equality based search routines within while loops that located the relevant process hurdle and returned the corresponding catalyst or reactant concentrations (Appendix 10.6.3). Process related constraints could be added to these plots, for the example of the EDDSase process these were chosen to be the solubility limit of fumarate (2 M or 232 g.l⁻¹), the point at which ED tended to crystallise in solution (1 M or 60 g.l⁻¹) and the hurdles shown in Table 6-2 with the exception of η . For catalyst concentration windows the purity, ee, productivity and rate constraints were the same, however, the reactant limits were not required and an EDMS limitation line was included. This was the point at which EDMSase concentration was such that rate was at an optimum, the inoperable region being where EDMSase was limiting. These constraining catalyst or reactant concentrations were then plotted in 2d and shading applied to indicate the inoperable region (Matlab code can be seen in Appendix 10-6).

The operable region was initially located by the use of 232 g.l⁻¹ fumarate and 60 g.l⁻¹ ED, the maximum concentrations the reaction theoretically could be run at. Inspection of the resultant window indicated an area limited by two constraints rather than all six and hence provided two enzyme concentrations which formed a basis for further iterative production of windows using both reactant and enzyme concentration plots to locate the window of operation. These windows were related to the 3d plots by projection of the constraint contours onto the x-y axis. The optimised windows of operation can be seen in Figure 6-13 and 6-14. The reactant window of operation is far smaller than that produced by the enzyme ratio plot, the size of the operable region depending heavily on the equilibrium and purity. From these plots it follows that a reasonable process can be run at 920 g_{dcw}.l⁻¹ EDDSase, 330 g_{dcw}.l⁻¹ EDMSase, 24 g.l⁻¹ ED and 232 g.l⁻¹ fumarate, though this was close to the solubility limit.

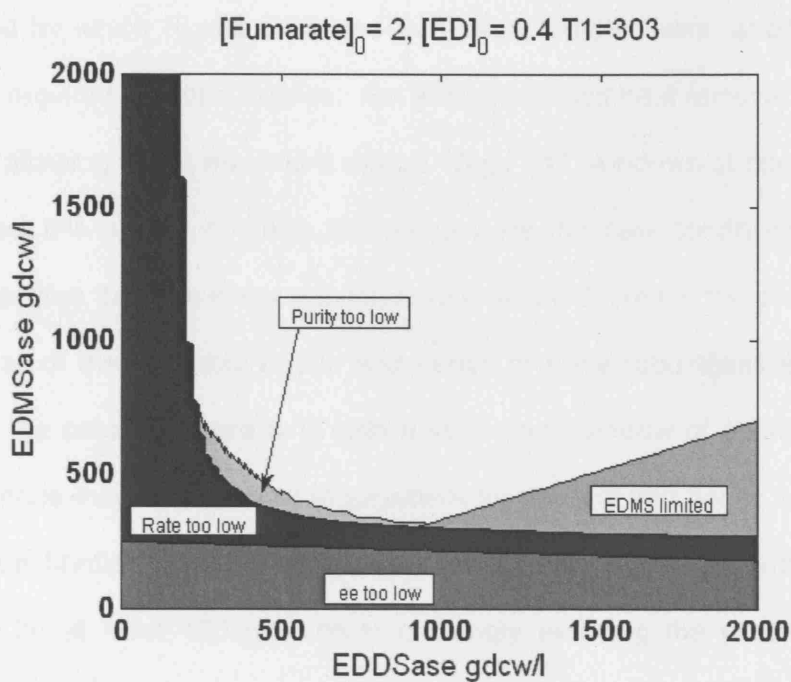


Figure 6-13 – Operable catalyst concentrations for a reaction run at 30°C at 232 g.l⁻¹ fumaric acid and 24 g.l⁻¹ ED. Minimum productivity: 8.3 g.l⁻¹h⁻¹, Maximum rate: 292 g.l⁻¹h⁻¹, Minimum purity: 95%, Minimum ee: 99%.

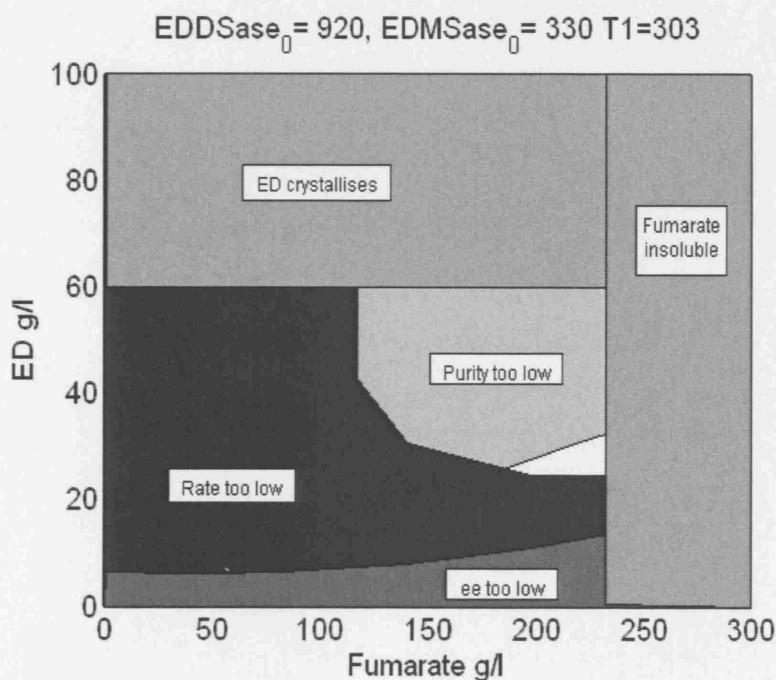


Figure 6-14 - Operable reactant concentrations for a reaction run at 30°C at 920 g_{dcw}.l⁻¹ EDDSase and 330 g_{dcw}.l⁻¹ EDMSase. Minimum productivity: 8.3 g.l⁻¹h⁻¹, Maximum rate: 292 g.l⁻¹h⁻¹, Minimum purity: 95%, Minimum ee: 99%.

The method by which Figure 6-15 and 6-16 were created was readily adaptable to changes in required process metrics. For example if less heat removal than estimated is possible allowing say a maximum rate of $15 \text{ g.l}^{-1}.\text{h}^{-1}$, windows of operation could be run to reflect this and to optimise the process for the new conditions. It would be logical to assume that this lower maximum rate would decrease the productivity of the process, size of the operable region and hence process robustness and this can be seen to be the case in Figure 6-15 with a very small window of operation. A further process change may be a greater requirement for product and hence a higher product concentration hurdle. Figure 6-16 shows such a change with product concentration required to be at least 150 g.l^{-1} , correspondingly reducing the possible size of the operable region to nil, requiring the original process flowsheet to be revisited in order to produce greater than 150 g.l^{-1} .

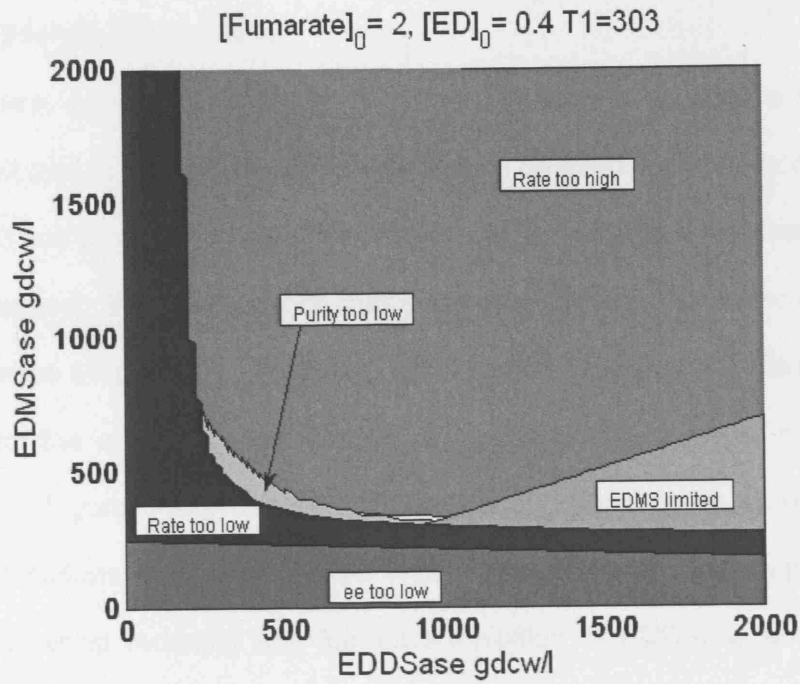


Figure 6-15 – Windows of operation for an EDDSase process requiring a maximum rate of 15 g.l⁻¹.h⁻¹

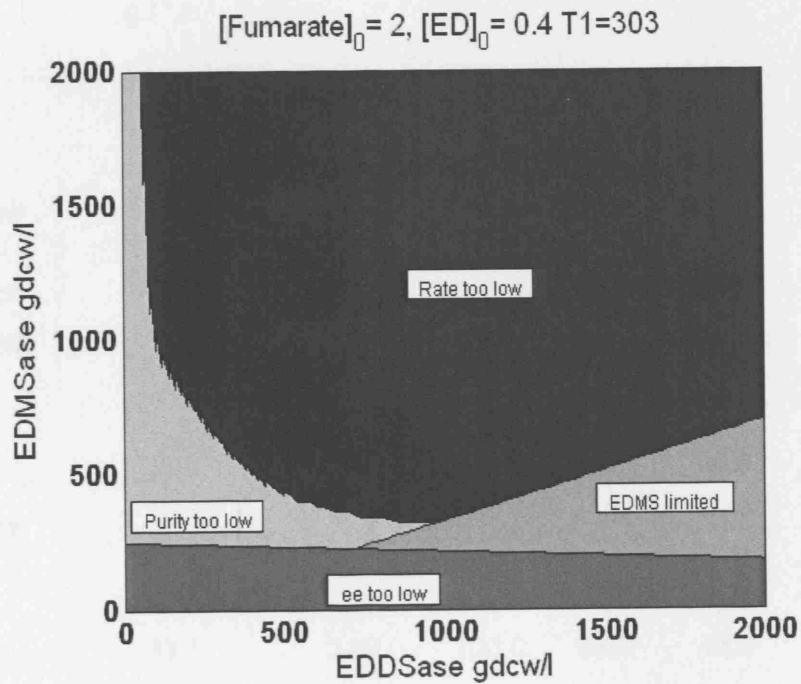


Figure 6-16 – Windows of operation for an EDDSase process requiring a product concentration of 150 g.l⁻¹

6.4.2 Process Alternatives

From the base case batch process (Figure 6-17) described above a progress curve could be run and so process metrics assessed. The metrics so produced can be seen in Table 6-3 and provided a basis from which any further possible process routes could be benchmarked. Process designs that addressed an individual or several limitations could therefore be proposed, modelled by alteration of the overall mass balance and assessed for the same process metrics as the benchmark. These included feeding fumaric acid (Figure 6-18), removing product during the process by some method of ISPR, combinations of the two (Figure 6-19) to move the equilibrium position towards the product, whilst reducing any fumarate inhibition of EDDSase and the use of a chemical reaction or a separate enzymatic reaction to produce the intermediate S-EDMS (Figure 6-20) to reduce the EDMS limitation.

Process	Maximum Rate g.l⁻¹.h⁻¹	[P]_{final} g.l⁻¹	ee %	Purity %	Yield %	Enzyme efficiency g.g_{dcw}⁻¹
Batch	13.9	96	99.3	96.1	32.9	0.10
Fed-Batch	18.4	104	99.5	99.5	50.4	0.11
Fed Batch with ISPR	8.3	385	99.9	98.9	79.1	0.42
2 pot – EDMSase & EDDSase	38.0	249	100.0	98.0	55.0	0.27
2 pot – Chemical & EDDSase	33.1	218	100.0	98.0	46.0	0.24

Table 6-3 – Process Metrics for possible processes for the EDDSase catalysed bioconversion of ED and fumaric acid to S,S-EDDS

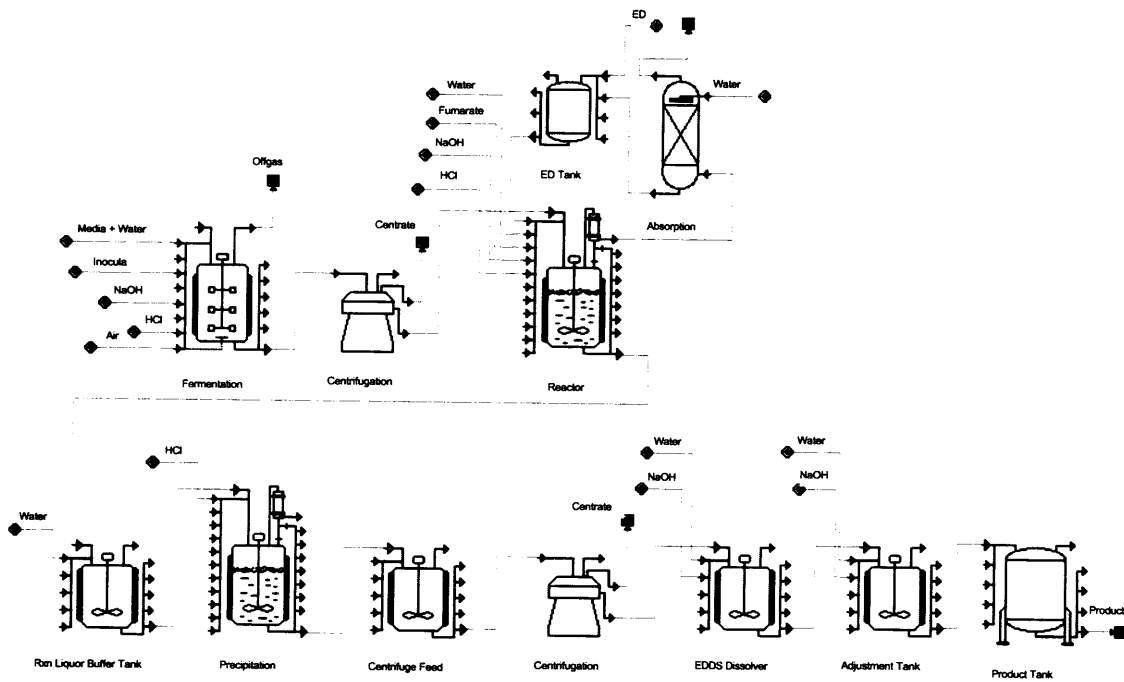


Figure 6-17 – Schematic for the EDMSase and EDDSase catalyzed batch bioconversion of ED and Fumaric acid to S,S-EDDS

Mass balances for each of these individual reactions were derived for the two situations where batch mass balances could not be used. The fumarate mass balance for a fed-batch reaction (Figure 6-18) can be seen in Equation 6-6, together with an EDDS mass balance for the same reaction altered by the volume in the tank to produce a concentration. All other mass balances were as Equation 6-7

$$\frac{d[F]}{dt} = \frac{-r_1 - r_2 - r_3 - r_4 - r_5}{V_0 + v_0 t} + F_F \quad (6-6)$$

$$\frac{d[P]}{dt} = \frac{r_1}{V_0 + v_0 t} \quad (6-7)$$

Where r_n represents rate of reaction as derived in Chapter 5, V_0 , initial volume set at 1 l, v_0 , volumetric flowrate (0.034 l.h^{-1} based on the batch rate of reaction) of the fumarate feed stream set at a concentration of 116 g.l^{-1} (1 molar) for ease of calculation and preparation and F_F was the molar flowrate of fumarate ($\text{mol.l}^{-1}.\text{h}^{-1}$) and equal to the volumetric flowrate because of the concentration of the feed. The resultant process metrics can be seen in Table 6-3.

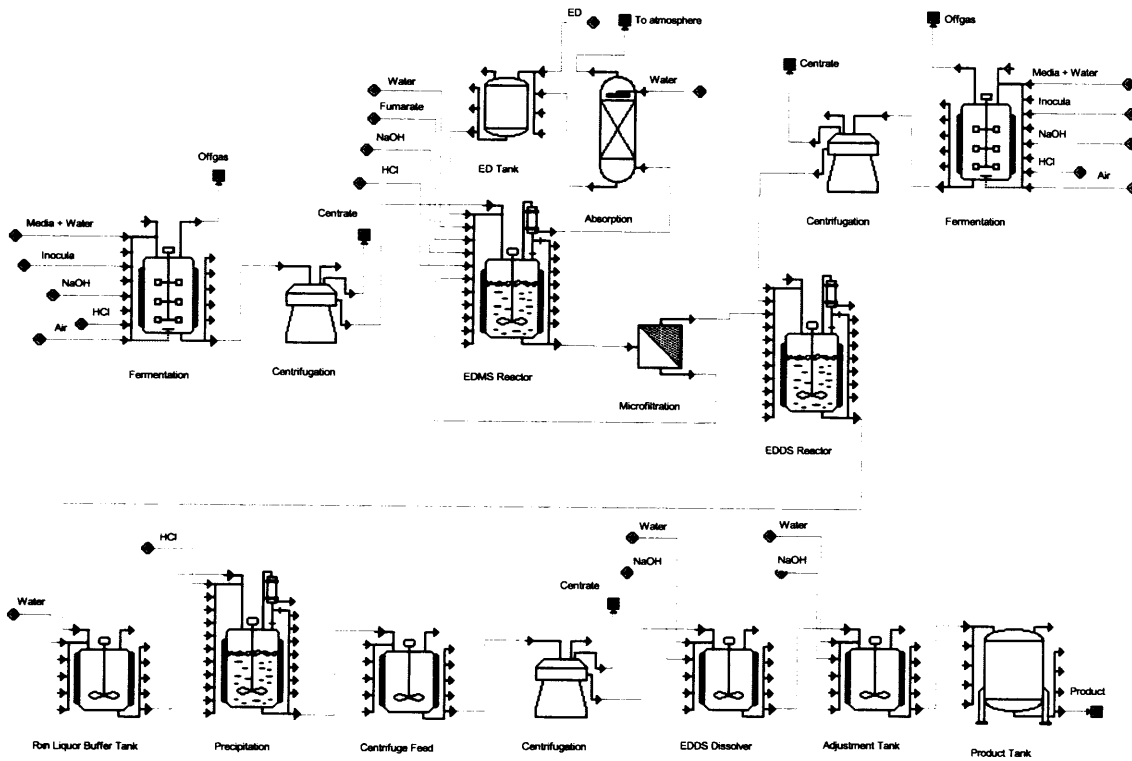


Figure 6-18 – Schematic for the EDMSase and EDDSase catalysed fed-batch bioconversion of ED and Fumaric acid to S,S-EDDS (fumaric acid feed)

For a reaction where ISPR and fumarate feeding (Figure 6-19) were implemented the fumarate mass balance, S,S-EDDS mass balance and one other component, ED, balance are shown in Equations 6-8 to 6-10.

$$\frac{d[F]}{dt} = \frac{-r_1 - r_2 - r_3 - r_4 - r_5}{V_0 + (v_0 - v_x)t} + F_F \quad (6-8)$$

$$\frac{d[P]}{dt} = \frac{r_1}{V_0 + (v_0 - v_x)t} - F_P \quad (6-9)$$

$$\frac{d[D]}{dt} = \frac{-r_1 - r_2 - r_3 - r_4}{V_0 + (v_0 - v_x)t} \quad (6-10)$$

Where v_x was the exiting flowrate of the S,S-EDDS product stream, set at 0.017 l.h^{-1} on the assumption that half the flow leaving the reactor (ie a total of 0.034 l.h^{-1}) would be recycled and removed of S,S-EDDS, thereby providing a molar exiting flowrate of S,S-EDDS of $0.017 \text{ mol.l}^{-1}.\text{h}^{-1}$. The metrics for the process can be seen in Table 6-3.

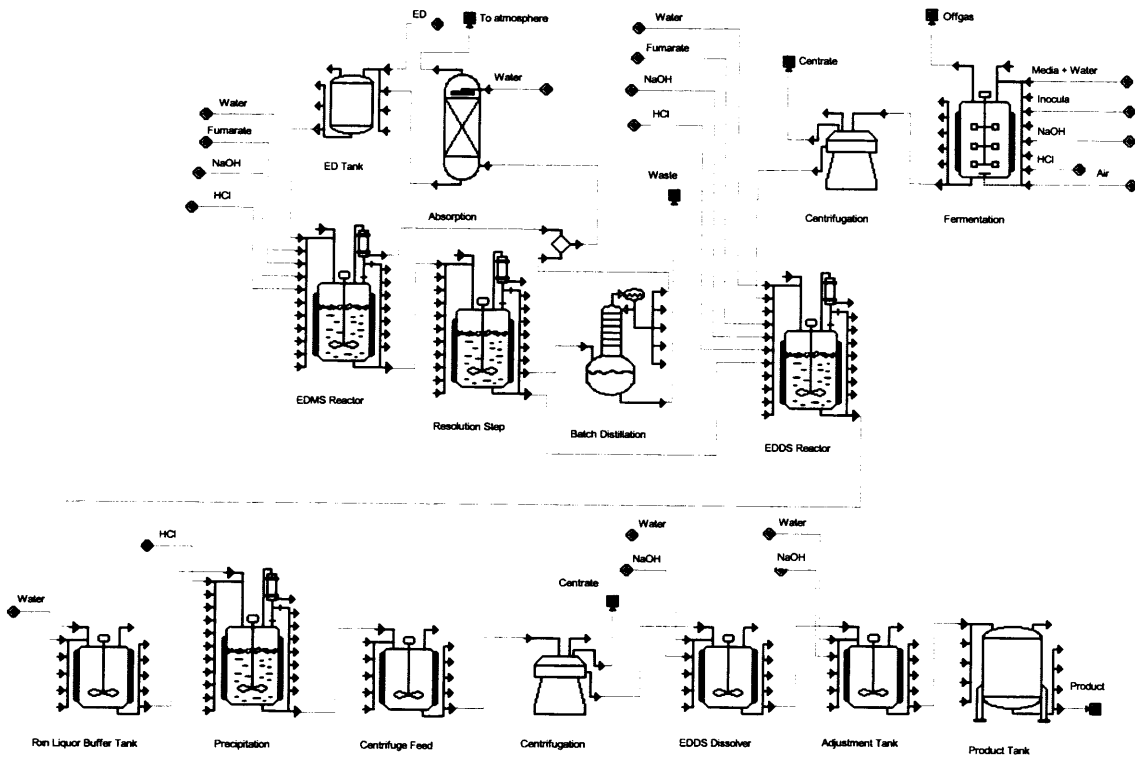


Figure 6-19 – Schematic for the EDMSase and EDDSase catalyzed fed-batch bioconversion of ED and Fumaric acid to S,S-EDDS (fumaric acid feed) with *in-situ* product removal

For reactions using 2 reactors (Figure 6-20), the batch equations based on the isothermal model described in Chapter 5 were used. The two scenarios included either a chemical batch reaction of ethylenediamine and fumarate to produce *meso*-EDMS followed by a separation step prior to biocatalytic reaction of EDDSase to produce pure S,S-EDDS or a separate biocatalytic step of fumarate and ethylenediamine in the presence of EDMSase to produce pure S-EDMS prior to the second half reaction. Process metrics for both scenarios can be seen in Table 6-3.

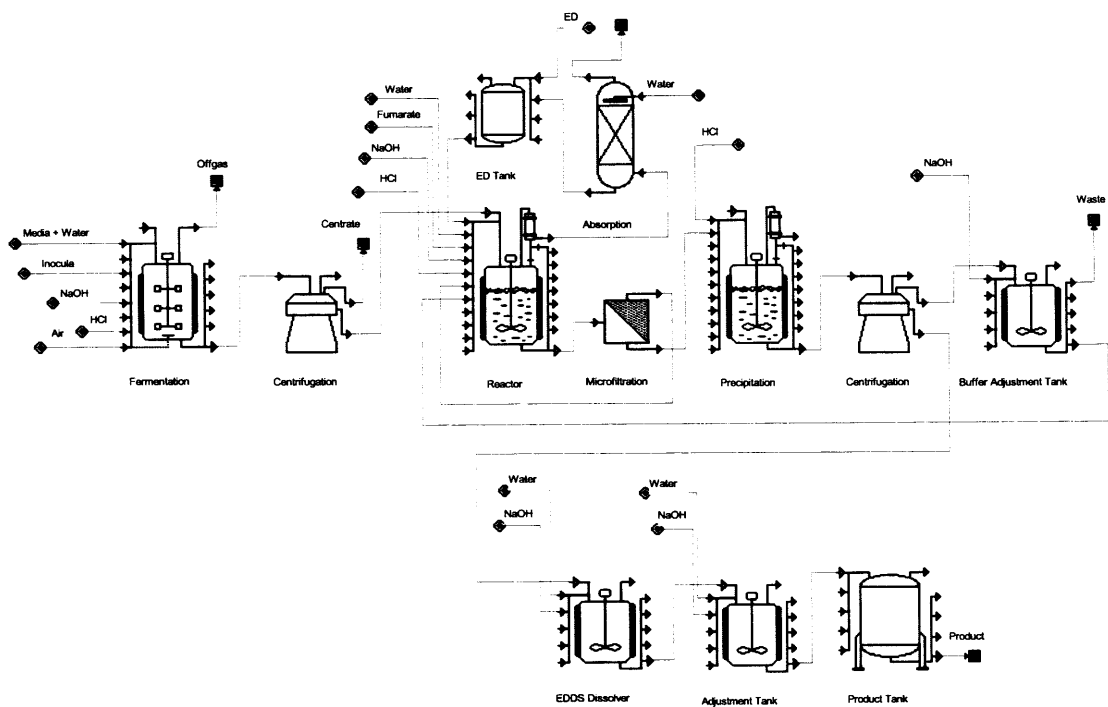


Figure 6-20 – Schematic for the EDDSase catalysed batch bioconversion of EDMS and fumaric acid to S,S-EDDS with prior production of S-EDMS by chemical or EDMSase catalysed means

It can be seen in Table 6-3 that a slight increase in product concentration, rate and yield was seen for the fed-batch process over the batch however the enzyme efficiency barely increased (Figure 6-22). The fed-batch process with ISPR had a far higher productivity (3.5-fold) than either the batch or fed-batch reaction with no ISPR, yield was higher and η increased 3-fold on the standard batch reaction though this was still lower than even a low hurdle value of $1 \text{ g.g}_{\text{dcw}}^{-1}$ (Table 6-2). This low enzyme efficiency is based on the current specific activities of catalyst produced from a minimal media *Chelatococcus asaccharovorans* fermentation and implies an expensive fermentation. The 2 pot reactions both saw 2-fold increases in enzyme efficiency and yield in comparison to the batch process, but these were still very low. However, fed-batch with ISPR and 2-pot reactions all achieved product concentrations over the hurdle value as can be seen in Figure 6-22.

Interestingly optimisation of the fed-batch with ISPR process by further use of windows of operation (Figure 6-21) meant that EDDSase concentration could be reduced approximately 10-fold to $100 \text{ g}_{\text{dcw}}^{-1}$ to produce the same product concentration, instantly increasing the enzymatic efficiency to $3.5 \text{ g.g}_{\text{dcw}}^{-1}$ (Figure 6-22).

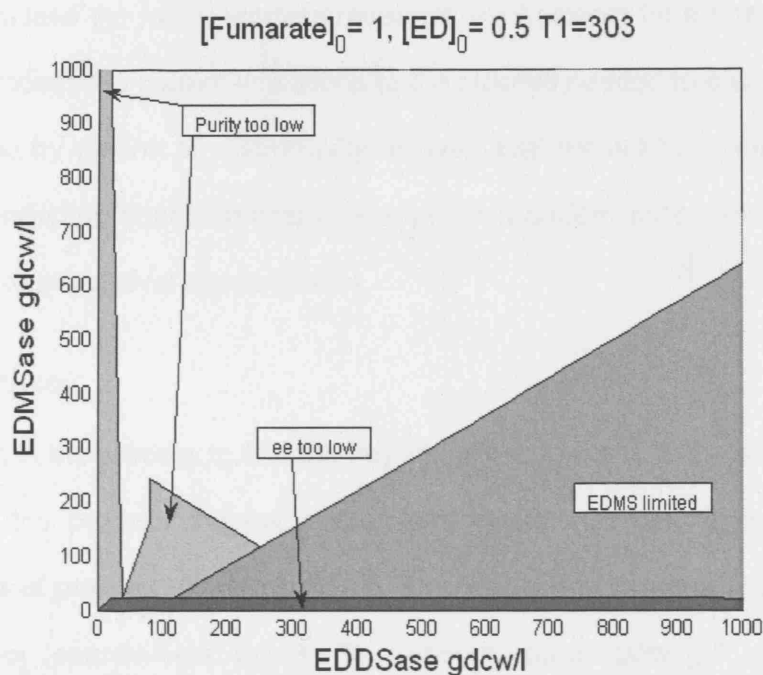


Figure 6-21 – Window of operation for the optimised Fed-batch with ISPR process

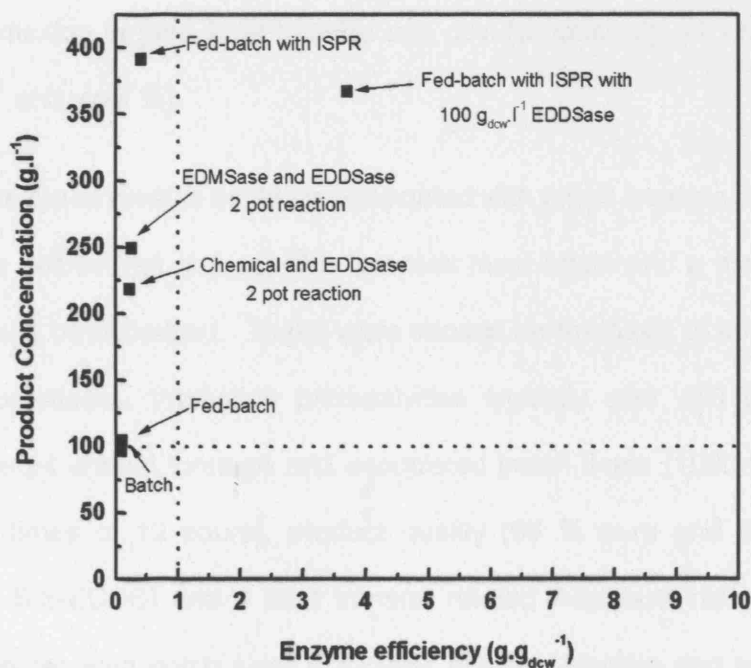


Figure 6-22 – Dot plot comparing product concentration and enzyme efficiency for all five possible process flowsheets

6.5 DISCUSSION

In order to assess the future process research requirements for a possible large scale EDDSase process the current limitations to the process needed to be determined. This was achieved by means of a sensitivity analysis that set out to assess the dominant limitations restricting improvements in key process performance indicators or metrics with respect to biocatalyst concentration.

6.5.1 Metrics

The first step in the process to find the key limitations to the EDDSase process was the selection of the process metrics, these were chosen on the basis of downstream requirements of process stream quality to enable easier separation of product from the process liquor (enantiomeric excess %, purity %, productivity $\text{g.l}^{-1}.\text{h}^{-1}$ and yield %), upstream requirements for effective fermentation impacting the size of the required fermentation to produce sufficient biocatalyst (enzyme efficiency ($\text{g.g}_{\text{dcw}}^{-1}$), maximum initial rate and productivity both $\text{g.l}^{-1}.\text{h}^{-1}$) and processing requirements for scheduling, annual production targets, heat transfer and cost (productivity $\text{g.l}^{-1}.\text{h}^{-1}$, maximum initial rate $\text{g.l}^{-1}.\text{h}^{-1}$ and yield %).

Furthermore these metrics could be associated with either maxima or minima providing both hurdle values that any possible process must attain and a method by which the process could be optimised. These were chosen on the basis of knowledge of current industrial processes, producing productivities typically over $100 \text{ g.l}^{-1}.\text{day}^{-1}$ (Rozzell, 1999), a target annual tonnage and associated batch times (1000 tonnes per annum and batch times of 12 hours), product quality (95 % pure and 99 % enantiomeric excess for S,S-EDDS) and a heat transfer related maximum rate, calculated on the basis of the required batch size, EDDSase reaction kinetics and productivity to be a maximum of $292 \text{ g.l}^{-1}.\text{h}^{-1}$ related to a heat production rate of $15 \text{ K.l}^{-1}.\text{h}^{-1}$.

6.5.2 Identification of Limiting regimes

These metrics could then be plotted against biocatalyst concentration for an individual reaction. Four key limitations to the production of a feasible process that controlled the metrics an increasing biocatalyst concentration were identified (Figure 6-4): A) an EDDSase limitation whereby increasing biocatalyst concentration increases rate and all other metrics, B) an EDMSase limitation that prevented the effective use of EDDSase, reducing rate, yield, productivity and enantiomeric excess where EDMSase was so low that the chemical reaction was significant and correspondingly pulling the equilibrium towards EDMS, C) a fumarase limitation that effectively reduced the amount of fumarate available for reaction and therefore equilibrium limiting the reaction. This affected productivity and yield but also initial rate of EDDSase production when fumarase concentration was particularly high and D) an equilibrium limitation caused by the initial reactant concentrations and the low equilibria inherent in the EDDSase and EDMSase reactions limiting rate, yield and productivity.

It was clear from the initial plots (Figure 6-5 to 6-7) that the prevailing limitation was an EDMSase limitation, which began to effect the metrics at a crude enzyme isolate concentration of $1 \text{ g}_{\text{dcw}} \cdot \text{l}^{-1}$ EDDSase. This restricted EDDS production rate to $0.005 \text{ g} \cdot \text{g}_{\text{dcw}}^{-1} \cdot \text{h}^{-1}$ at the point at which the limitation became controlling *versus* a possible specific rate of $0.1 \text{ g} \cdot \text{g}_{\text{dcw}}^{-1} \cdot \text{h}^{-1}$. It is noted however, that the point at which EDMSase concentration controls the metrics is not well defined as the relationships between metrics, EDDSase and EDMSase are not linear, hence the figures above state the point at which the EDMSase concentration begins to limit the change in metric against EDDSase concentration.

6.5.2.1 Sensitivity Analyses

The 3d plots could be seen to provide further insight not just into the metrics and their comparison with biocatalyst concentration but also an assessment of the effect of optimising or changing a process variable and its associated limitations could be seen.

So for example, increase in EDMSase titre made a worthwhile change on the metrics until fumarase began to dominate. It was clear that EDMSase was required in far greater concentrations than those currently possible from the wild type fermentation of *Chelatococcus asaccharovorans*, but furthermore that any increase in EDMSase concentration needed to be accompanied by an optimal increase in EDDSase so as to not enzyme limit the reaction. It could also be seen that some mechanism of reducing fumarase activity substantially was required as this was responsible for much reduction in yield. In this manner it could easily be seen that also reducing R-EDMS concentration in the reaction would be worthwhile whereas increasing initial fumarate concentration without also increasing initial ED concentration would bring about further limitations as a result of the equilibrium. Finally, as a result of the limiting equilibria inherent in the EDDSase process, some method of moving the equilibrium towards the product could be seen to be desirable. It can clearly be seen from these assessments however, that there is no point raising any limitation if the actual dominant limitation, in this case EDMSase concentration, is not addressed first.

6.5.3 Windows of Operation can Guide Possible Process Routes

To further assess the process for possible process research opportunities one or more of the factors controlling the dominating regimes needed to be reduced. Correspondingly these were to be the reduction of fumarase concentration to zero, but more importantly it was assumed that EDMSase concentration could increase to any concentration required on the assumption that changes could be made to the fermentation that would enable this. From this basis further change in reactant concentration and enzyme concentration ratios could be made to find the optimum process that satisfied all the process constraints. To this end, windows of operation were used as they provided a simple visual method of optimisation without the necessity for the mathematical rigour of a full optimisation procedure, furthermore biochemical processes often lead to pareto optima and windows enable this to be easily visualised. The previous sensitivity analysis provided a suitable basis for such

an analysis and it is this facility, the application of hurdle values to the metrics and employment of simple search routines to produce windows of operation which increases the utility of the method of bottleneck identification proposed. The method employed is also flexible in that changes to the process can be modelled by changing the mass balances or kinetic models and changes to hurdles can be applied easily as can be seen in Figures 6-17 and 6-18.

6.5.3.1 The Ideal Batch Process

Figures 6-13 and 6-15 show there is an operable region for the process at 232 g.l⁻¹ fumarate and 24 g.l⁻¹ ED which represents a 4-fold molar excess of fumarate. However, the fumarate concentration required is close to the solubility limit in order to avoid large build-ups of EDMS and therefore production of R,S-EDDS. A benefit of this large excess to health and safety of the process is that ED is kept to a minimum as it is a known respiratory sensitiser.

It can be seen from Figure 6-15 however, that concentrations of cells producing EDDSase and EDMSase crude enzyme isolates of approximately 920 g_{dcw}.l⁻¹ and 330 g_{dcw}.l⁻¹ respectively were needed to produce the product concentrations required. Typical high cell density fermentations can reach 100 g_{dcw}.l⁻¹ (Knorre *et al*, 1991), clearly indicating that a concentration step between fermenter and reactor would be required. Furthermore the requirement for 3-fold more EDDSase than EDMSase indicates that the enzymes could not be produced in the same host, requiring two separate fermentations, as engineering the appropriate ratios of the two enzymes *in-vivo* could be a substantial task. As a result of the increased fermentation expense it may therefore be cost effective to isolate and immobilise the enzymes with the added benefit of reducing the fumarase side reaction to zero.

The figures produced by the windows in terms of biocatalyst concentration are at least 900-fold the current cell titre achievable from the fermentation. Therefore it can be seen that a concentration step between fermentation and reaction would not be sufficient to

produce the enzyme concentrations required. Also necessary is recombinant DNA technology to increase specific activity by increasing plasmid copy number or by changing the expression system to one more readily induced in an easily fermentable host and directed evolution to increase rate and specificity in order to make the required amount of catalyst a feasibility.

Since the work described here was carried out with biocatalyst in a crude enzyme isolate format, transport and therefore mass transfer of reactant into the cell and product out of the cell have not been modelled. The EDDSase process may be a suitable candidate for an isolated enzyme reaction in light of the number and extent of metabolic side reactions present particularly if the enzyme is thermostable as results have suggested and immobilisation was employed in order to extend catalyst life. Commonly biocatalytic processes operate in a whole cell format so as to reduce processing steps and therefore costs between fermenter and reactor, further work to assess if some form of active transport is required for S,S-EDDS as it is with EDTA (Witschel *et al*, 1999) would be required, as these may produce further limiting regimes. Furthermore in a whole cell catalyst format, substantial work to reduce fumarase activity and metabolism would be required as the reactants fumarate and ED, would provide cells with both nitrogen and carbon with which to produce additional biomass. Possible strategies for limiting growth and metabolism include forcing a limitation of an essential mineral or possible use of anaerobic reaction conditions to prevent the citric acid cycle, whilst providing cells with glucose for active transport. The EDDSase process seems particularly suitable for metabolic engineering, down regulating fumarase and the citric acid cycle whilst increasing titres of EDMSase and EDDSase, the extent to which this is possible having been demonstrated by the 1,3-propanediol process at Dupont (Nakamura and Whited, 2003). A further strategy to reduce fumarase activity has been employed by Mitsubishi in their EDDSase patents, employing borate buffer and heat treatment to denature most of the enzymes in the cell, relying on the thermostability of EDDSase. However, not only does this require

yet more processing steps (harvest, resuspension, heat treatment for several hours and further harvest) prior to the addition of catalyst to the reactor but until EDMSase is characterised fully this strategy cannot be assessed as EDMSase may not be as thermostable as EDDSase. However, the chemical reaction to EDMS is still a process option so if the equilibrium could be overcome, process research into EDMSase need not be required.

Experimentally it was noted, that fermentation in stainless steel containing tanks caused some chelation, this would be reduced if the expression system was changed to one that did not require S,S-EDDS for induction. However, this also indicates that reactions may have to take chelation of S,S-EDDS with vessel material into account, making vessels more expensive, particularly if glass-lining is required. Iron II creates reasonably stable chelates with S,S-EDDS (Table 3-1), however, iron III, creates one of the strongest S,S-EDDS complexes and therefore the iron would prove hard to remove downstream.

6.5.3.2 Process Routes

On the basis of the assumption that the required changes to the fermentation could be made, several process routes were proposed in order to increase either rate, productivity and or yield by altering the equilibrium. The batch process optimised by the windows of operation was used as a benchmark producing 96 g.l^{-1} of correct quality product from a 12 hour batch, but with an enzyme efficiency of $0.1 \text{ g.g}_{\text{dcw}}^{-1}$ and a yield on fumarate of less than 50% (Table 6-3). It was known that fumarate inhibited the EDDSase reaction and that therefore reducing the actual fumarate concentration available to the biocatalyst, but providing the equilibrium with sufficient fumarate with which to minimise production of R,S-EDDS was to be achieved by means of fumarate feeding (Figure 6-18). This increased yield to just above 50% and increased productivity to 104 g.l^{-1} over the course of the batch. It was also assessed whether splitting the two half reactions would improve the metrics (Figure 6-18), using either the chemical production of *meso*-EDMS and then using some form of separation likely a

chiral chromatography step to feed the EDDSase reaction pure S-EDMS or use of a separate EDMSase catalysed reaction to produce nearly pure S-EDMS also. However, these reactions though productive and still had enzyme efficiencies below $1 \text{ g.g}_{\text{dcw}}^{-1}$ (Figure 6-22) because of the amount of EDMS fed and the equilibrium, purities were around 60%, increasing the difficulty of downstream separation as the amount of amino acid type compounds increased. Finally a fed-batch reaction with ISPR (Figure 6-22) was tested, this removed S,S-EDDS from the reaction by keeping it below 16 g.l^{-1} pulling the equilibrium further towards the product, furthermore yield was increased to 79% and enzyme efficiency increased 3-fold, though still below the hurdle (Figure 6-22). The enzyme efficiency however, could be improved optimisation (Figure 6-21) and implementation of any of the fermentation strategies described above.

It is important to note here that none of these investigated reactions were optimised for their own conditions (except Fed-batch plus ISPR – Figure 6-21), merely tested at the same conditions as the benchmark reaction with initial concentrations of ED, EDDSase and EDMSase were held constant. However, for fed-batch reactions, total fumarate concentration was reduced by half a mole or 60 g.l^{-1} in order to ensure that fumarate concentration remained reasonably constant at 116 g.l^{-1} the maximum concentration of fumarate that did not inhibit EDDSase at $600 \text{ g}_{\text{dcw}}.l^{-1}$ during feeding, suggesting that the reaction would be unsuitable for feeding fumarate at concentrations in excess of the solubility limit and allowing the dissolution process to feed fumarate.

Windows of operation have been employed in several biocatalytic situations in the past and have proved themselves useful for integration of biocatalytic processes (Blayer *et al*, 1996; Chen *et al*, 2002; Hogan and Woodley, 2000) and have to date generally been constructed from experimental data collected specifically for the purpose of that window. However, what is presented here combines the use of a generic process development strategy with a simple method directly producing windows of operation from sensitivity analysis data to assess the potential of a given biocatalytic from fairly basic kinetic data. However, it must be noted that the method here is reliant on the

model which it employs. In the EDDSase case, care must be taken when relying on the data, since confidence in the EDDSase kinetic parameters is low and extrapolation is likely to be error prone, though trends should still remain the same. What is key however, is that the method is simple and applicable to other biocatalytic systems (Law *et al*, 2006) and that at an early stage of process development truly rigorous models may actually hinder process development in the time taken to collate and process the required experimental data.

6.6 CONCLUSION

A simple sensitivity analysis for the identification of limiting bottlenecks by comparison of relevant process metrics, biocatalyst concentration and other process variables has been presented for the assessment of a biocatalytic conversion which is believed can be applied to any bioprocess including bio-oxidations (Law *et al*, 2006) provided enough information is available to be able to assess the limiting regimes, whether by means of experiment and/or modelling.

A model reaction, the bioconversion of fumaric acid and ED to S,S-EDDS by EDMSase and EDDSase was found to be dominated at almost all EDDSase concentrations by EDMSase concentration which covered a fumarase limitation. Assumptions that catalyst concentration limitations could be overcome by judicious use of genetic technologies such as gene knock-out, recombinant technology and directed evolution, produced an optimised reaction which determined that concentrations of EDDSase and EDMSase 600-fold greater than can currently be produced by wild type fermentation of *Chelatococcus asaccharovorans* were required. Furthermore, at these concentrations the dominating controller of the process metrics was found to be equilibrium, this could be altered by careful process selection. Several processes were tested by altering the mass balance produced in Chapter 5, suggesting that a possible EDDSase process would be most effective if fumarate feeding and ISPR were implemented.

7 CONCLUSIONS

1. A biocatalytic process for the production of S,S-EDDS has been defined and further characterised using a two-enzyme system of EDMSase and EDDSase from *Chelatococcus asaccharovorans* to produce S,S-EDDS from ED and fumaric acid via S-EDMS. The reaction system was determined to comprise two half reactions, the first of which was catalysed by EDMSase but could also be carried out by chemical means producing *meso*-EDMS. The reaction system was characterised by fumarase and metabolic side reactions, equilibria close to unity and an exotherm. EDDSase was found to be characterised by fumarate inhibition, thermostability to 50°C and lack of specificity for S-EDMS, indicating that EDMSase was specific for the S-enantiomer. Specific activity in wild type *Chelatococcus asaccharovorans* was found to be $0.6 \text{ g.g}_{\text{dcw}}^{-1} \cdot \text{h}^{-1}$ with typical fermentation titres of $0.5 \text{ g}_{\text{dcw}} \cdot \text{l}^{-1}$.
2. A reaction characterisation was used to split the reactions into their constituent parts and produce an isothermal reaction model. This model was built up of several enzymatic rate models, one chemical rate model and an energy balance combined by the use of an overall mass balance and solved numerically by use of in-built ordinary differential equation solvers in Matlab®. An adiabatic reaction model was also proposed to assess heat production in the reaction. Confidence in the most of the models was reasonable, though confidence in the EDDSase model was low. However, validation confirmed the models hypotheses by use of the Chi² goodness of fit test, returning test statistics consistently lower than those required for the number of degrees of freedom for 95% confidence in the hypothesis.
3. A tool for the analysis and evaluation of the potential of bioconversions based on a form of regime analysis was presented. Key to this tool was the ability to determine optimal reaction and process conditions from an initial assessment

of process bottlenecks. This tool assessed controlling limitations on enzyme concentrations and chosen process metrics using the example of the biocatalytic production of S,S-EDDS as a model system. Metrics were chosen for the analysis of the EDDSase process were productivity, maximum rate, yield, enantiomeric excess, purity and enzymatic efficiency. Process variables affecting the process included: EDMSase, fumarase and initial reactant concentrations and temperature.

4. The analysis of controlling regimes for the EDDSase process indicated a strong limitation of all process metrics by lack of the intermediate enzyme, EDMSase, controlling the process metrics at EDDSase concentrations above $1 \text{ g}_{\text{dcw}}\cdot\text{l}^{-1}$. Use of sensitivity analyses enabled further identification of limitations including a substantial fumarase limitation and an equilibrium limitation known to be a function of initial reactant concentration.
5. The analysis of the dominating regimes led to two windows of operation based on the analysis, which enabled a feasible region of process operation to be determined. A process in the feasible region would require an EDMSase concentration of $250 \text{ g}_{\text{dcw}}\cdot\text{l}^{-1}$, an initial concentration of fumarate at $232 \text{ g}\cdot\text{l}^{-1}$, a concentration at the solubility limits of fumarate in water, ED at $30 \text{ g}\cdot\text{l}^{-1}$ and an EDDSase concentration of $600 \text{ g}_{\text{dcw}}\cdot\text{l}^{-1}$, 600-fold greater than produced by wild type *Chelatococcus asaccharovorans* fermentation. The feasible operating window led to suggestions of possible process designs.
6. A possible process considering these limitations was proposed to be a fumarate fed-batch reaction with *in-situ* product removal to reduce the equilibrium limitation. The fed-batch process with ISPR was predicted to increase yield 2-fold and product concentration 3-fold over the batch process.

8 FUTURE WORK

1. It is clear from the assessment of the current process and the required process conditions which resulted from the analysis, that much work is required before a possible EDDSase process could be implemented on the large scale. Key to this would be the isolation and enzymatic characterisation of EDMSase from *Chelatococcus asaccharovorans* as this would confirm its existence, provide a basis for possible intellectual property rights, enable further refinement of any model and allow its genetic improvement. It follows from the specific activity of EDMSase ($0.08 \text{ g}_{\text{dcw}}^{-1} \cdot \text{h}^{-1}$) that recombinant technology may not be enough to increase the EDMSase titre sufficiently and that therefore some effort towards directed evolution (Arnold, 2001; Bornscheuer *et al*, 2002), may be necessary. Even so, some concentration step between fermentation and reactor may be required precluding the easier 'one-pot' operation, but correspondingly reducing fermentation impurities in the process liquor.
2. It can also be seen that some additional characterisation of EDDSase would be required, including stability studies, study of the induction mechanism of EDDSase and experimental determination of the relevant missing enthalpies for use in the energy balance. Furthermore, more EDDSase half reaction kinetic data would enable the refinement of the model and reduction of the error. Since EDDSase appears to be required in concentration 3-fold greater than that of EDMSase, it is unlikely that these enzymes could be expressed in the same host, further increasing the likelihood that reaction and fermentation would be carried out in separate vessels.
3. Process research should also be carried out into possible methods of *in-situ* product removal, it has been assumed here that S,S-EDDS can be easily removed by pH alteration, but the extent to which S,S-EDDS can be removed from solution without removing fumaric acid needs to be assessed. However

crystallisation and chelation may also prove worthwhile strategies which require additional research in order to discriminate between them for both efficiency of recovery and cost.

4. With regards to process analytical tools, testing of the regime analysis technique should be extended to more than two reactions and some method of automating the process created as at present enough knowledge (and often too much) has to be accumulated to enable initial assessment of the process limitations. This could be achieved by use of a graphical user interfaces accepting basic simulation data to make the process more 'user-friendly' as at present knowledge of some form of programming language is required. It is noted that some form of process model is required for this analysis. Current status of enzyme modelling packages requires a large degree of user input to produce sensible models and often these are limited as to the models built-in and to single enzyme reactions, so a comprehensive system based on initial rates and simple kinetic models could provide the required data, however it would require a high degree of flexibility and a number of built-in functions, indicating that perhaps the best way of automating the regime analysis technique would be as a tie-in module in a process simulation package such as Aspen Batch Plus or Superpro Designer.

9 REFERENCES

- Ager, David J, Li, Tao, Pantaleone, David P, Senkpeil, Richard F, Taylor, Paul P, and Fotheringham, Ian G (2001) Novel biosynthetic routes to non-proteinogenic amino acids as chiral pharmaceutical intermediates *Journal of Molecular Catalysis B: Enzymatic* **11**: 199-205
- Alphand, Veronique and Furstoss, Roland (1992) Microbiological transformations. 22. Microbiologically mediated Baeyer-Villiger reactions: a unique route to several bicyclic γ -lactones in high enantiomeric purity *Journal of Organic Chemistry* **57**: 1306-1309
- Aragno M and Schlegel HG (1981) The Hydrogen-Oxidising Bacteria in *The Prokaryotes, A Handbook on Habitats, Isolation, and Identification of Bacteria*, 1st edition. Springer-Verlag, Berlin pp865 - 893
- Arnold, F (2001) Combinatorial and computational challenges for biocatalyst design *Nature* **401**: 253-257
- Bachmann, R. Industrial Biotech Product Opportunities. (2003). Bio 2003, Washington, 6/23/03
- Bally, Matthias and Egli, Thomas (1996) Dynamics of Substrate Consumption and Enzyme Synthesis in *Chelatobacter heintzii* during Growth in Carbon-Limited Continuous Culture with Different Mixtures of Glucose and Nitroacetate *Applied and Environmental Microbiology* **62**: 133-140
- Bauer, Michael, Griengel, Herfried, and Steiner, Walter (1999) Kinetic Studies on the Enzyme (S)-Hydroxynitrile Lyase from *Havea brasiliensis* Using Initial Rate Methods and Progress Curve Analysis *Biotechnology and Bioengineering* **62**: 20-29
- Bhole, Manish R and Joshi, Jyeshtharaj B (2005) Stability analysis of bubble columns: Predictions for regime transition *Chemical Engineering* **60**: 4493-4
- Biegler, Lorenz T. and Grossmann, Ignacio E. (2004) Retrospective on optimization *Computers and Chemical Engineering* **28**: 1169-1192
- Biran A and Breiner M (2002) System Modelling and Simulation in *MATLAB 6 For Engineers*, 1st edition. Pearson Education Ltd, Harlow pp547 - 581
- Bird, Paul A., Sharp, D C A, and Woodley, John M. (2002) Near-IR spectroscopic monitoring of analytes during microbially catalysed Baeyer-Villiger bioconversions *Organic Process Research & Development* **6**: 569-576
- Biselli M, Kragl U, and Wandrey C (2002) Reaction Engineering for Enzyme-Catalyzed Biotransformations in *Enzyme Catalysis in Organic Synthesis*, 2nd edition. Wiley-VCH Verlag, Weinheim pp185 - 257
- Biwier, Arno and Heinzle, Elmar (2004) Process modeling and simulation can guide process development: case study α -cyclodextrin *Enzyme and Microbial Technology* **34**: 642-650
- Blayer, S, Woodley, John M., and Lilly, Malcolm D. (1996) Characterization of the Chemoenzymatic Synthesis of *N*-Acetyl-D-neuraminic Acid (Neu5Ac) *Biotechnology Progress* **12**: 758-763
- Boehringer Mannheim/ R-Biopharm. (2004) Glycerol UV-Method (Cat no: 0148270).

- Boeker, Elizabeth A (1984) Integrated rate equations for enzyme-catalysed first-order and second-order reactions *Biochemical Journal* **223**: 15-22
- Bogle, I. D. L., Cockshott, A R, Bulmer, M, Thornhill, N, Gregory, M, and Dehghani, M (1996) A Process Systems Engineering View of Biochemical Process Operations *Computers & Chemical Engineering* **20**: 943-949
- Boonaert CJ-P, Dupont-Gillain C, Dengis P, Dufrêne Y, and Rouxhet P (1999) Cell Separation, Flocculation in *Encyclopedia of Bioprocess Technology - Fermentation, Biocatalysis, and Bioseparation, Volumes 1-5*, edition. John Wiley & Sons, New York pp531 - 547
- Bornscheuer, Uwe T., Bessler, Cornelius, Srinivas, Ramiseti, and Krishna, Sajja Hari (2002) Optimizing lipases and related enzymes for efficient application *Trends in Biotechnology* **20**: 433-437
- Brass, J M, Hoeks, Frans W J M M, and Rohner, M (1997) Application of modelling techniques for the improvement of Industrial Bioprocesses *Journal of Biotechnology* **59**: 63-72
- Briggs, George Edward and Haldane, John Burdon Sanderson (1925) A Note on the Kinetics of Enzyme Action *Biochemical Journal* **19**: 338-339
- Bucheli-Witschel, Margarete and Egli, Thomas (2001) Environmental fate and microbial degradation of aminopolycarboxylic acids *FEMS Microbiology Reviews* **25**: 69-106
- Bühler, Bruno, Straathof, Adrie JJ, Witholt, Bernard, and Schmid, Andreas (2006) Analysis of Two-Liquid-Phase Multistep Biooxidation Based on a Process Model: Indications for Biological Energy Shortage *Organic Process Research & Development* **10**: 628-643
- Carlton GJ (1992) The Enzymatic Production of L-aspartic Acid in *Biocatalytic Production of Amino Acids and Derivatives*, edition. John Wiley and Sons, Inc, New York pp3 - 21
- Carrano, Carl J, Drechsel, Hartmut, Kaiser, Dietmar, Jung, Günther, Matzanke, Berthold, Winkelmann, Günther, Rochel, Natacha, and Albrecht-Gary, Anne Marie (1996) Coordination Chemistry of the Carboxylate Type Siderophore Rhizoferrin: The Iron (III) Complex and its Metal Analogs *Inorganic Chemistry* **35**: 6429-6436
- Cary R, Dobson S, and Delic J (1999) Concise International Chemical Assessment Document 15 - 1,2-Diaminoethane (Ethylenediamine), World Health Organisation, Geneva
- Cavin, L, Fischer, U, Mosat, A, and Hungerbühler, K (2005) Batch process optimization in a multipurpose plant using Tabu Search with a design-space diversification *Computers & Chemical Engineering* **29**: 1770-1786
- Caygill, G, Zanfir, M, and Gavriilidis, A (2006) Scalable Reactor Design for Pharmaceuticals and Fine Chemicals Production. 1: Potential Scale-up Obstacles *Organic Process Research & Development* **10**: 539-552
- Cebulla I (1995) Gewinnung komplexbildender Substanzen mittels *Amycolatopsis orientalis*. *PhD Thesis* Eberhard-Karls-Universität, Tübingen, Germany
- Chapra SC and Canale RP (2006) Runge Kutta Methods in *Numerical Methods for Engineers*, 5th edition. McGraw-Hill, New York pp681 - 725

Chemfate. Chemfate Search Results: Fumaric Acid. (2003)
<http://esc.syrres.com/scripts/CHFcgi.exe>

Chemical Co-ordinating Centre of EMEP. Determination of ammonium in precipitation. (2004) http://www.nilu.no/projects/ccc/manual/documents/04_4-Determination%20of%20ammonium%20in%20precipitation.htm

Chen, Bing H., Doig, Steve D., Lye, Gary J, and Woodley, John M. (2002) Modelling of the Baeyer-Villiger Monooxygenase Catalysed Synthesis of Optically Pure Lactones *Trans IChemE* **80**: 51-55

Chen, Bing H. and Woodley, John M. (2002) Wavelet shrinkage data processing for neural networks in bioprocess modeling *Computers and Chemical Engineering* **26**: 1611-1620

Chen, L, Bernard, O, Bastin, G, and Angelov, P (2000) Hybrid modelling of biotechnological processes using neural networks *Control Engineering Practise* **8**: 821-827

Connors KA (1990a) *Chemical Kinetics - The Study of Reaction Rates in Solution*, 1st edition. VCH Inc, New York

Connors KA (1990b) Introduction to Chemical Kinetics in *Chemical Kinetics - The study of Reaction Rates in Solution*, 1st edition. VCH Inc, New York pp1 - 15

Cornish-Bowden, A and Eisenthal, Robert (1974) Statistical Considerations in the Estimation of Enzyme Kinetic Parameters by the Direct Linear Plot and Other Methods *Biochemical Journal* **139**: 721-730

Cote RJ (1999) Media Composition, Microbial, Laboratory Scale in *Encyclopedia of Bioprocess Technology - Fermentation, Biocatalysis and Bioseparations Volumes 1-5*, edition. John Wiley & Sons, New York pp1640 - 1660

Coulson JM and Richardson JF (1996) *Chemical Engineering 1: Fluid flow, Heat Transfer and Mass Transfer*, 5th edition. Butterworth Heinemann, Oxford

Dabes, J N, Finn, R K, and Wilke, C R (1973) Equations of Substrate-Limited Growth: The Case for Blackman Kinetics *Biotechnology and Bioengineering* **15**: 1159-1177

Dallos, A, Hajós-Szikszay, É, Horváth, A, Liszi, J, Barczynska, J, and Bald, A (2000) Enthalpies of solution and crystallisation of fumaric acid in aqueous solution *Journal of Chemical Thermodynamics* **32**: 587-595

Daniel, Roy M, Danson, Michael J, and Eisenthal, Robert (2001) The temperature optima of enzymes: a new perspective on an old phenomenon *Trends in Biochemical Sciences* **26**: 223-225

Datta, Rathin, Tsa, Shih-Perng, Bonsignore, Patrick, Moon, Seung-Hyeon, and Frank, James R (2006) Technological and economic potential of poly(lactic acid) and lactic acid derivatives *FEMS Microbiology Reviews* **16**: 221-231

Day, M (2005) Octel Chelate-Metal Ion Stability Constant Database.

Doig, Steve D., Pickering, S C R, Woodley, John M., and Lye, Gary J (2002) The use of microscale processing technologies for quantification of biocatalytic Baeyer-Villiger oxidation kinetics *Biotechnology and Bioengineering* **80**: 42-49

- Dubois, M, Gilles, KA, Hamilton JK, Rebers, PA, and Smith F (1956) Colorimetric methods for the determination of sugars and related substances *Analytical Chemistry* **28**: 350-356
- Duggleby, Ronald G (1991) Analysis of biochemical data by nonlinear regression: is it a waste of time? *Trends in Biochemical Sciences* **16**: 51-52
- Duggleby RG (1995) Analysis of Enzyme Progress Curves by Nonlinear Regression in *Enzyme Kinetics and Mechanism. Part D: Developments in Enzyme Dynamics*, 1st edition. Academic Press, San Diego pp61 - 90
- Duggleby, Ronald G (2001) Quantitative Analysis of the Time Courses of Enzyme-Catalysed Reactions *Methods* **24**: 168-174
- Duggleby, Ronald G and Wood, Chris (1989) Analysis of progress curves for enzyme-catalysed reactions *Biochemical Journal* **258**: 397-402
- Egli, Thomas (1988) (An)aerobic breakdown of chelating agents used in household detergents *Microbiological Sciences* **5**: 36-41
- Egli, Thomas (2001) Biodegradation of Metal-Complexing Aminopolycarboxylic Acids *Journal of Bioscience and Bioengineering* **92**: 89-97
- Egli T and Auling G (2005) Genus II. Chelatococcus in *Bergey's Manual of Systematic Bacteriology*, Class I edition. Springer, New York pp433 - 437
- Egli, Thomas, Weilenmann, Hans-Ulrich, El-Banna, Tarek, and Auling, Georg (1988) Gram-Negative, Aerobic, Nitritotriacetate-utilizing Bacteria from Wastewater and Soil *Systematic and Applied Microbiology* **10**: 297-305
- Eisenthal, Robert and Cornish-Bowden, Athel (1974) The direct linear plot. A new graphical procedure for estimating enzyme kinetic parameters *Biochemical Journal* **139**: 715-720
- Endo T, Hashimoto Y, and Takahashi R (1998) Production of alkylene of phenylenediamine disuccinic acid from fumaric acid and a diamine using lyase from microbes USPTO 5,707,836 Assignees: Nitto
- Erbeldinger, Markus, Ni, Xiongwei, and Halling, Peter (1998) Enzymatic synthesis with mainly undissolved substrates at very high concentrations *Enzyme and Microbial Technology* **23**: 141-148
- Faber K (1997) Introduction and Background Information in *Biotransformations in Organic Chemistry*, 3rd edition. Springer-Verlag, Berlin pp1 - 26
- Finžgar N, Kos, B, and Leštan, D (2004) Washing of Pb Contaminated Soil using [S,S] ethylenediamine disuccinate and horizontal permeable barriers *Chemosphere* **57**: 655-661
- Flint, D. H. (1994) Initial Kinetic and Mechanistic Characterization of *Escherichia coli* Fumarase A *Archives of Biochemistry and Biophysics* **311**: 509-516
- Fogler HS (1999a) *Elements of Chemical Reaction Engineering*, 3rd edition. Prentice Hall Inc, Upper Saddle River, New Jersey

Fogler HS (1999b) Unsteady-State Nonisothermal Reactor Design in *Elements of Chemical Reaction Engineering*, 3rd edition. Prentice Hall Inc, Upper Saddle River, New Jersey pp534 - 580

Fonchy, E, Morin, A, Rodrigue, N, Müller, B, and Chalièr, P (1999) Effect of Growth Temperature on Hydrolytic and Esterifying Activities from *Pseudomonas fragi* CRDA 037 Grown on Whey *Applied and Environmental Microbiology* **65**: 3114-3120

Foster, AP and DeBoer, DJ (1998) The Role of *Pseudomonas* in Canine Ear Disease *Compendium on Continuing Education* **20**: 909-918

Gajewski, E, Goldberg, R N, and Steckler, D K (1985) Thermodynamics of the conversion of Fumarate to L-(-)-Malate *Biophysical Chemistry* **22**: 187-195

Gershater CJL (1999) Inoculum Preparation in *Encyclopedia of Bioprocess Technology - Fermentation, Biocatalysis and Bioseparations Volumes 1-5*, edition. John Wiley & Sons, New York pp1435 - 1444

Gonçalves, Luciana R B, Sousa, Ruy Jr, Fernandez-Lafuente, Roberto, Guisan, Jose M, Giordano, Raquel L C, and Giordano, Roberto C (2002) Enzymatic Synthesis of Amoxicillin, Avoiding Limitation of the Mechanistic Approach for Reaction Kinetics *Biotechnology and Bioengineering* **80**: 622-631

Good, William D and Moore, Richard T (1970) Enthalpies of Formation of Ethylenediamine, 1,2-Propanediamine, 1,2-Butanediamine, 2-methyl-1,2-propanediamine and isobutylamine *Journal of Chemical and Engineering Data* **15**: 150-154

Goodfellow, Michael, Brown, Anne B, Cai, Junpeng, Chun, Jongsik, and Collins, Matthew D (1997) *Amycolatopsis japonicum* sp. nov., an Actinomycete Producing (S,S)-N,N'-Ethylenediaminedisuccinic Acid *Systematic and Applied Microbiology* **20**: 78-84

Goudar, Chetan T, Sonnad, Jagadeesh R, and Duggleby, Ronald G (1999) Parameter estimation using a direct solution of the integrated Michaelis-Menten equation *Biochimica et Biophysica Acta* **1429**: 377-383

Greco, Salvatore, Matarazzo, Benedetto, and Slowinski, Roman (2001) Rough sets theory for multicriteria decision analysis *European Journal of Operational Research* **129**: 1-47

Halling P (2002) Enzymic Conversions in Organic and Other Low-Water Media in *Enzyme Catalysis in Organic Synthesis*, 2nd edition. Wiley-VCH Verlag GmbH, Weinheim pp259 - 285

Hardaway, K. L. and Buller, C. S. (1979) Effect of Ethylenediaminetetraacetate on Phospholipids and Outer Membrane Function in *Escherichia coli* *Journal of Bacteriology* **137**: 62-68

Hartman FA and Perkins CM (1987) Detergent Compositions containing ethylenediamine-N,N'-disuccinic acid US 4,704,233 Assignees: The Procter and Gamble Company

Helander, I. M. and Mattila-Sandholm, T (2000) Fluorometric assessment of Gram-negative bacterial permeabilization *Journal of Applied Microbiology* **88**: 213-219

- Hibbert, Edward G, Baganz, Frank, Hailes, Helen C, Ward, John M, Lye, Gary J, Woodley, John M., and Dalby, Paul A (2005) Directed evolution of biocatalytic processes *Biomolecular Engineering* **22**: 11-19
- Hilker, I, Alphand, V, Wohlgemuth, R, and Furstoss, R (2004) Microbial Transformations 56. Preparative scale asymmetric Baeyer-Villiger oxidation using a highly productive "two-in-one" resin-based in situ SFPR concept *Advanced Synthesis and Catalysis* **346**: 203-214
- Hirose Y (2002) Production and Isolation of Enzymes in *Enzyme Catalysis in Organic Synthesis*, 1st edition. Wiley VCH, Weinheim pp41 - 66
- Hiroyasu B, Shigeo T, and Kiyonobu N (2000a) Production of Highly Pure S,S-Ethylenediamine-N,N'-disuccinic acid JP 2000-300286 Assignees: Mitsubishi Rayon Co.
- Hiroyasu B, Shigeo T, and Kiyonobu N (2000b) Production of Highly Pure S,S-Ethylenediamine-N,N'-disuccinic acid JP 2000-300286 Assignees: Mitsubishi Rayon Co.
- Hoeks, Frans W J M M, Mühle, Johann, Böhlen, Lisi, and Pšenicka (1996) Process Integration aspects for the production of fine chemicals illustrated with the biotransformation of γ -butyrobetaine into L-carnitine *The Chemical Engineering Journal* **61**: 53-61
- Hogan, Matthew C and Woodley, John M. (2000) Modelling of two enzyme reactions in a linked cofactor recycle system for chiral lactone synthesis *Chemical Engineering Science* **55**: 2001-2008
- Hough, EW, Mason, DM, and Sage, BH (1950) Heat Capacities of Several Organic Liquids *Journal of the American Chemical Society* **72**: 5775-5777
- Huffman, Hugh M and Borsook, Henry (1932) Thernal Data I. The Heat Capacities, Entropies and Free Energies of seven Organic compounds containing Nitrogen *Journal of the American Chemical Society* **54**: 4297-4301
- Hunter JS, Natrella MG, Barnett H, Hunter WG, and Koehler TL (1998) Design and Analysis of Experiments in *Juran's Quality Handbook*, 5th edition. McGraw-Hill, New York pp47.1 - 47.77
- Jasper, E and Overmann, J (2004) Ecological Significance of Microdiversity: Identical 16S rRNA Gene Sequences Can Be Found in Bacteria with Highly Divergent Genomes and Ecophysologies *Applied and Environmental Microbiology* **70**: 4831-4839
- Jaworska, Joanna S, Schowanek, Diederik, and Feijtel, Tom C J (1999) Environmental Risk Assessment for Trisodium [S,S]-Ethylene Diamine Disuccinate, A Biodegradable Chelator used in Detergent Applications *Chemosphere* **38**: 3597-3625
- Jones, Paul W and Williams, David R (2002) Chemical speciation simulation used to assess the efficiency of environment-friendly EDTA alternatives for use in the pulp and paper industry *Inorganica Chimica Acta* **339**: 41-50
- Kaneko M, Endo T, Fukuda T, and Kato M (2000) Process for Producing alkali metal [S,S]-ethylenediamine-N,N'-disuccinates USPTO 6,136,573 Assignees: Mitsubishi Rayon Co.

Kaneko M, Hashimoto Y, Endo T, and Kato M (1999) Process for producing optically active aminopolycarboxylic acid US 5,981,238 Assignees: Mitsubishi Rayon Co.

Kato M, Kaneko M, and Endo T (2000) Method for removing fumarase activity, microorganisms obtainable by the method, and production of optically active aminopolycarboxylic acids using the microorganisms US 6,103,508 Assignees: Mitsubishi Rayon Co.

Kato O, Kaneko M, and Endo T (2001) Methods for producing [S,S]-Ethylenediamine-N,N'-disuccinate USPTO 6,621,798 Assignees: Mitsubishi Rayon Co.

Kawata, Y., Tamura, K., Yano, S., Mizobata, T., Nagai, J., Esaki, N., Soda, K., Tokushige, M., and Yumoto, N. (1999) Purification and Characterization of Thermostable Aspartase from *Bacillus* sp YM55-1 *Archives of Biochemistry and Biophysics* **366**: 40-46

Kettle S (1996) Stability of Coordination Compounds in *Physical Inorganic Chemistry: a coordination chemistry approach*, 1st edition. Spektrum Academic Publishers Ltd, Oxford pp73 - 94

King, Edward L and Altman, Carl (1956) A Schematic Method of Deriving the Rate Laws for Enzyme Catalysed Reactions *Journal of Physical Chemistry* **60**: 1375-1378

Kniemeyer, Olaf, Probian, Christina, Roselló-Mora, Ramon, and Harder, Jens (1999) Anaerobic Mineralization of Quaternary Carbon Atoms: Isolation of Denitrifying Bacteria on Dimethylmalonate *Applied and Environmental Microbiology* **65**: 3319-3324

Knorre, WA, Deckwer, WD, Korz, D, Pohl, HD, Riesenberger, D, Ross, A, Sanders, E, and Schulz, V (1991) High cell density fermentation of recombinant *Escherichia coli* with computer-controlled optimal growth rate *Annals of the New York Academy of Sciences* **646**: 300-306

Koeller, Kathryn M and Wong, Chi-Huey (2001) Enzymes for chemical synthesis *Nature* **409**: 232-240

Kos, B and Leštan, D (2004) Chelator induced phytoextraction and in situ soil washing of Cu *Environmental Pollution* **132**: 333-339

Kossen N and Oosterhuis N (1985) Modelling and Scale-up of Bioreactors in *Fundamentals of Biochemical Engineering*, 1st edition. VCH, Weinheim pp571 - 605

Kula M-R (2002) Introduction in *Enzyme Catalysis in Organic Synthesis*, 2nd edition. Wiley-VCH Verlag GmbH, Weinheim pp1 - 39

Kulagina, T G, Lebedev, B V, and Vasil'ev, V P (2000) The Thermodynamic Properties of Ethylenediaminedisuccinic Acid Monohydrate in the Temperature Tange 0-330K *Russian Journal of Physical Chemistry* **74**: 1937-1941

Kumar, S, Wittmann, C, and Heinzle, E (2004) Minibioreactors *Biotechnology Letters* **26**: 1-10

Lalonde J and Margolin A (2002) Immobilization of Enzymes in *Enzyme Catalysis in Organic Synthesis*, 2nd edition. Wiley-VCH Verlag GmbH, Weinheim pp163 - 184

Law, HEM, Baldwin, CVF, Chen, Bing H., and Woodley, John M. (2006) Process limitations in a whole-cell catalysed oxidation: Sensitivity analysis *Chemical Engineering Science* **61**: 6646-6652

Layman W, Kannappan C, and Lecouvé J-P (1996) Method for Producing Calcium Salts of [S,S]-Ethylenediamine-N,N'-disuccinic acid US 5,550,285 Assignees: none

Lilly, Malcolm D. (1994) Advances in biotransformation processes *Chemical Engineering Science* **49**: 151-159

Lilly, Malcolm D. and Woodley, John M. (1996) A Structured approach to design and operation of biotransformation processes *Journal of Industrial Microbiology* **17**: 24-29

Lin RW, Atkinson EE, and Balhoff DE (1996) Process for Producing [S,S]-Ethylenediamine-N,N'-Disuccinic Acid US 5,554,791 Assignees: Albemarle Corporation

Link, J M, Cuypers, L A, Deen, N G, and Kuipers, J A M (2005) Flow regimes in a spout-fluid bed: A combined experimental and simulation study *Chemical Engineering Science* **60**: 3425-3442

Lodish H, Berk A, Zipursky SL, Matsudaira P, Baltimore D, and Darnell J (1999) *Molecular Cell Biology*, 4th edition. W.H. Freeman & Company, New York

Lohmann, B and Marquardt, W. (1996) On the Systemization of the Process of Model Development *Computers & Chemical Engineering* **20**: S213-S218

Lye, Gary J, Shamlou, Parviz A., Baganz, Frank, Dalby, Paul A, and Woodley, John M. (2003) Accelerated design of bioconversion processes using automated microscale processing techniques *Trends in Biotechnology* **21**: 29-37

Lye, Gary J and Woodley, John M. (1999) Application of *in situ* product-removal techniques to biocatalytic processes *Trends in Biotechnology* **17**: 395-402

Madigan MT, Martinko JM, and Parker J (2003a) Microbial Habitats, Nutrient Cycles, and Plant/Animal Interactions in *Brock Biology of Microorganisms*, 10th edition. Prentice Hall, Upper Saddle River, NJ pp -

Madigan MT, Martinko JM, and Parker J (2003b) Prokaryotic Diversity: Bacteria in *Brock Biology of Microorganisms*, 10th edition. Prentice Hall, Upper Saddle River, NJ pp -

Marquardt, Donald W (1963) An Algorithm for Least-Squares Estimation of Nonlinear Parameters *Journal of the Society for Industrial and Applied Mathematics* **11**: 431-441

Marquardt, W. (1996) Trends in Computer-Aided Process Modelling *Computers & Chemical Engineering* **20**: 591-609

Martell A and Smith RM (1974) *Critical Stability Constants - Volume 1 Amino Acids*, Plenum Press, New York

Matthews, TD and Williams, DR (2003) Solubility products for aminopolycarboxylate ligands: determination, validation and speciation uses *Analytica Chimica Acta* **480**: 119-122

Mavrovouniotis, ML (1990) Group contributions for estimating standard gibbs energies of formation of biochemical compounds in aqueous solution *Biotechnology and Bioengineering* **36**: 1070-1082

May O, Voigt CA, and Arnold FH (2002) Enzyme Engineering by Directed Evolution in *Enzyme Catalysis in Organic Synthesis*, 2nd edition. Wiley-VCH Verlag GmbH, Weinheim pp95 - 138

McCoy, Michael (2001) Making Drugs with Little Bugs *Chemical Engineering News* **79**: 37-43

Meers, E, Ruttens, A, Hopgood, MJ, Samson, D, and Tuck, FMG (2005) Comparison of EDTA and EDDS as potential soil amendments for enhanced phytoextraction of heavy metals *Chemosphere* **58**: 1011-1022

Metsärinne, Sirpa, Tuhkanen, Tuula, and Aksela, Reijo (2001) Photodegradation of ethylenediaminetetraacetic acid (EDTA) and ethylenediamine disuccinic acid (EDDS) within natural UV radiation range *Chemosphere* **45**: 949-955

Meyer, Hans-Peter, Kiener, Andreas, Imwinkelfried, René, and Shaw, Nicholas (1997) Biotransformations for Fine Chemical Production *Chimia* **51**: 287-289

Meyer, Jean-Marie (2000) Pyoverdines: pigments, siderophores and potential taxonomic markers of fluorescent *Pseudomonas* species *Archives of Microbiology* **174**: 135-142

Mizunashi W (2001) Protein having ethylenediamine-N,N'-disuccinic acid: ethylenediamine lyase activity and gene encoding the same USPTO 6,168,940 Assignees: Nitto

Moler, C. Stiff Differential Equations in Cleve's Corner Newsletter. (2006) http://www.mathworks.com/company/newsletters/news_notes/clevescorner/may03_cleve.html

Nakamura, Charles E and Whited, Gregory M (2003) Metabolic engineering for the microbial production of 1,3-propanediol *Current Opinion in Biotechnology* **14**: 454-459

Neal, John A and Rose, Norman J (1968) Stereospecific Ligands and Their Complexes. I. A Cobalt(III) Complex of Ethylenediaminedisuccinic Acid *Inorganic Chemistry* **7**: 2405-2412

Nichols, N, Sköld, R, Spink, C, and Wadsö, I (1976) Thermochemistry of solutions of biochemical model compounds 6. α,ω -dicarboxylic acids, -diamines and -diols in aqueous solution *Journal of Chemical Thermodynamics* **8**: 993-999

Nishikiori, Takaaki, Okuyama, Akira, Naganawa, Hiroshi, Takita, Tomohisa, Takeuchi, Tomio, Aoyagi, Takaaki, and Umezawa, Hamao (1984) Production by actinomycetes of (S,S)-N,N-ethylenediaminedisuccinic acid, an inhibitor of phospholipase C *Journal of Antibiotics* **37**: 426-427

NIST/SEMATECH. *e-Handbook of Statistical Methods*, date. (2005) <http://www.itl.nist.gov/div898/handbook/pmd/section1/pmd142.htm>,

Nowack, Bernd (2002) Environmental Chemistry of Aminopolycarboxylate Chelating Agents *Environmental Science and Technology* **36**: 4009-4016

Obenndip, DA and Sharratt, PN (2006). Towards an Information-Rich Process Development. Part I: Interfacing Experimentation with Qualitative/ Semiquantitative Modelling. *Organic Process Research & Development*. DOI: 10.1021/op050236t

Octel. Corporate Website. (2002) www.octel-corp.com

Orama, Marjatta, Hyvönen, Helena, Saarinen, Heikki, and Aksela, Reijo (2002) Complexation of [S,S] and mixed stereoisomers of N,N'-ethylenediaminedisuccinic acid (EDDS) with Fe (III), Cu (II), Zn (II) and Mn (II) ions in aqueous solution *Journal of the Chemistry Society, Dalton Transactions* **24**: 4644-4648

Oviedo, C and Rodriguez, J (2003) EDTA: The Chelating Agent Under Environmental Scrutiny *Química Nova* **26**: 901-905

Parks, George S and Huffman, Hugh M (1930) Thermal Data on Organic Compounds. IX. A Study on the Effect of Unsaturation on the Heat Capacities, Entropies and Free Energies of Some Hydrocarbons and Other Compounds *Journal of the American Chemical Society* **52**: 4381-4391

Patel, RN (2003) Interview.

Pennsylvania State University. Principles and Applications Regarding Siderophores. (2003) <http://www.personal.psu.edu/users/r/d/rdr128/Siderophores.htm>

Peterson, Michelle E, Eisenthal, Robert, Danson, Michael J, Spence, Alastair, and Daniel, Roy M (2004) A New Intrinsic Thermal Parameter for Enzymes Reveals True Temperature Optima *Journal of Biological Chemistry* **279**: 20717-20722

Pilgrim, Axel, Kawase, Motoaki, Matsuda, Fumihiko, and Miura, Kouichi (2006) Modeling of the simulated moving-bed reactor for the enzyme-catalyzed production of lactosucrose *Chemical Engineering Science* **61**: 353-362

Porter, D J T and Bright, H J (1980) 3-Carbanionic Substrate Analogues Bind Very Tightly to Fumarase and Aspartase *The Journal of Biological Chemistry* **255**: 4772-4780

Press WH, Teukolsky SA, Vetterling WT, and Flannery BP (1992) Integration of Ordinary Differential Equations in *Numerical recipes in C: The Art of Scientific Computing*, 2nd edition. Cambridge University Press, Cambridge pp707 - 752

Proctor and Gamble. Ethylene Diamine DiSuccinate (SS-EDDS). (2002) http://www.scienceinthebox.com/en_UK/pdf/SS-EDDS.pdf

Proctor and Gamble (2003) S,S-(ethylenediamine N,N'-disuccinic acid) MSDS :

Rakitin SR (1997) *Software verification and validation: a practitioner's guide*, 1st edition. Artech House, Boston

Ramsey WM, Downey, and Kerzerian C (1963) Lower Alkylene and Lower Alkylene-Phenylene-Lower Alkylene Polyamine Bis N,N' Lower Alkylene Di and Tri Carboxylic Acids, Esters, Salts and Chelates 3,077,487 Assignees: none

Rao SS (1996a) Further Topics in Optimization in *Engineering Optimization. Theory and Practice*, edition. John Wiley & Sons, New York pp768 - 835

Rao SS (1996b) Introduction to Optimization in *Engineering Optimization. Theory and Practice*, edition. John Wiley & Sons, New York pp1 - 64

Rees DG (2001) *Essential Statistics*, 4th edition. Chapman & Hall, Boca Raton

Rhee, Jong Il and Sohn, Ok-Jae (2003) Flow injection system for on-line monitoring of fumaric acid in biological processes *Analytica Chimica Acta* **499**: 71-80

Roberts NJ and Lye GJ (2002) Application of room temperature ionic liquids in biocatalysis: opportunities and challenges in *Ionic Liquids. Industrial Applications to Green Chemistry.*, 1st edition. ACS Symposium Series 818. American Chemical Society, Washington pp347 -

Rozzell, J David (1999) Biocatalysis at commercial scale: Myths and realities *Chimica Oggi* **May/June**: 42-47

Saiki, RK, Gelfand, DH, Stoffel, S, Scharf, SJ, Higuchi, R, Horn, GT, Mullis, KB, and Erlich, HA (1988) Primer-Directed Enzymatic Amplification of DNA with a Thermostable DNA Polymerase *Science* **239**: 487-491

Saltelli, Andrea, Ratto, Marco, Tarantola, Stefano, and Campolongo, Francesca (2005) Sensitivity Analysis for Chemical Models *Chemical Reviews* **105**: 2811-2827

Samsatli, N J and Shah, N (1996a) Optimal Integrated Design of Biochemical Processes *Computers and Chemical Engineering* **20**: S315-S320

Samsatli, N. J. and Shah, N. (1996b) An Optimization Based Design Procedure for Biochemical Processes. Part I: Preliminary Design and Operation *Trans IChemE* **74**: 221-231

Satroutdinov, Aidar D, Dedyukhina, Emiliya G, Chistyakova, Tat'yana I, Witschel, Margarete, Minkevich, Igor G, Eroshin, Valery K, and Egli, Thomas (2000) Degradation of Metal-EDTA Complexes by Resting Cells of the Bacterial Strain DSM 9103 *Environmental Science and Technology* **34**: 1715-1720

Schmid, Andreas, Dordick, J S, Hauer, B, Kieners, A, Wubbolts, M, and Witholt, Bernard (2001) Industrial biocatalysis today and tomorrow *Nature* **401**: 258-268

Schowaneck, Diederik, Feijtel, Tom C J, Perkins, Christopher M, Hartman, Frederick A, Federle, Thomas W, and Larson, Robert J (1997) Biodegradation of [S,S], [R,R] and mixed stereoisomers of ethylene diamine disuccinic acid (EDDS), a transition metal chelator *Chemosphere* **34**: 2375-2391

Schowaneck, Diederik, McAvoy, Drew, Versteeg, Don, and Hanstveit, Arnbjörn (1996) Effects of nutrient trace metal speciation on algal growth in the presence of the chelator [S,S]-EDDS *Aquatic Toxicology* **36**: 253-275

Segel I (1993a) *Enzyme kinetics : behavior and analysis of rapid equilibrium and steady-state enzyme systems*, John Wiley, New York

Segel I (1993b) Kinetics of Unireactant Enzymes in *Enzyme kinetics : behavior and analysis of rapid equilibrium and steady-state enzyme systems*, edition. John Wiley, New York pp18 - 99

Segel I (1993c) Steady-state kinetics of multireactant enzymes in *Enzyme kinetics : behavior and analysis of rapid equilibrium and steady-state enzyme systems*, edition. John Wiley, New York pp506 - 846

Sellek, Gerard A and Chaudhuri, Julian B (1999) Biocatalysis in organic media using enzymes from extremophiles *Enzyme and Microbial Technology* **25**: 471-482

Shaeri, Jobin, Wohlgemuth, R, and Woodley, John M. (2006) Semiquantitative Process Screening for the Biocatalytic Synthesis of D-Xylulose-5-phosphate *Organic Process Research & Development* **10**: 605-610

Sharratt, P N, Wall, K, and Borland, J N (2003) Generating innovative process designs using limited data *Journal of Chemical Technology and Biotechnology* **78**: 156-160

Shechter, H and Conrad, F (1953) Orientation in Reactions of Dinitrogen Tetroxide and Methyl Acrylate *Journal of the American Chemical Society* **75**: 5610-5613

Sheldon, Roger A and van Rantwijk, Fred (2004) Biocatalysis for Sustainable Organic Synthesis *Australian Journal of Chemistry* **57**: 281-289

Shigeo T, Hiroyasu B, and Kiyonobu N (2004) Method for producing S,S-Ethylenediamine-N,N'-disuccinic acid JP 2004-236620 Assignees: Mitsubishi Rayon Co.

Sirola, Jeffrey J (1996) Strategic Process Synthesis: Advances in the Hierarchical Approach *Computers & Chemical Engineering* **20**: S1637-S1643

St George G and Wilson D (1998) Preparation of Disodium Ethylene-N,N'-disuccinate WO 98/43944 Assignees: The Dow Chemical Company

Steffens, M A, Fraga, E. S., and Bogle, I. D. L. (1999) Multicriteria process synthesis for generating sustainable and economic bioprocesses *Computers & Chemical Engineering* **23**: 1455-1467

Stegmann, Efthimia, Pelzer, Stefan, Wilken, Kerstin, and Wohlleben, Wolfgang (2001) Development of three different gene cloning systems for genetic investigation of the new species *Amycolatopsis japonicum* MG417-CF17, the ethylenediaminedisuccinic acid producer *Journal of Biotechnology* **92**: 195-204

Stephanopoulos G, Aristidou A, and Nielsen J (1998) *Metabolic Engineering Principles and Methodologies*, 1st edition. Academic Press, San Diego

Stolp H and Gadkari D (1981) Nonpathogenic Members of the Genus *Pseudomonas* in *The Prokaryotes Volume 1*, edition. Springer-Verlag, Berlin pp719 - 741

Straathof, Adrie JJ (2001) Development of a Computer Program for Analysis of Enzyme Kinetics by Progress Curve Fitting *Journal of Molecular Catalysis B: Enzymatic* **11**: 991-998

Straathof, Adrie JJ, Panke, Sven, and Schmid, Andreas (2002) The Production of fine chemicals by biotransformations *Current Opinion in Biotechnology* **13**: 548-556

Sweere, APJ, Luyben, KChAM, and Kossen, NWF (1987) Regime analysis and scale-down: tools to investigate the performance of bioreactors *Enzyme and Microbial Technology* **9**: 386-398

Syracuse Research Corporation. Online Log P Calculation. (2003)
<http://esc.syrres.com/interkow/kowdemo.htm>

Syracuse Research Corporation. Interactive LogKow (KowWin) Demo: Fumarate CAS: 110-16-7. (2006) http://www.syrres.com/esc/est_kowdemo.htm

Takahashi, Rikiya, Fujimoto, Naoshi, Suzuki, Masaharu, and Endo, Takakazu (1997) Biodegradabilities of ethylenediamine-N,N'-disuccinic acid (EDDS) and other chelating agents *Bioscience, Biotechnology and Biochemistry* **61**: 1957-1959

Takahashi, Rikiya, Yamayoshi, Kenji, Fujimoto, Naoshi, and Suzuki, Masaharu (1999) Production of (S,S)-ethylenediamine-N,N'-disuccinic acid from ethylenediamine and fumaric acid by bacteria *Bioscience, Biotechnology and Biochemistry* **63**: 1269-1273

Tewari, Yadu B (1990) Thermodynamics of Industrially-Important, Enzyme-Catalysed Reactions *Applied Biochemistry and Biotechnology* **23**: 187-203

Thayer, Ann M. (2002) Biocatalysis *Chemical Engineering News* **79**: 27-34

Tremblay, Jean-François (2001) Japan's Unique Perspective *Chemical Engineering News* **79**: 45-49

Ulijn, Rein V, Janssen, Anja E. M., Moore, Barry D, and Halling, Peter (2001) Predicting when Precipitation-Driven Synthesis Is Feasible: Application to Biocatalysis *Chem.Eur.J.* **10**: 2089-2098

Vandevivere, Philippe C, Hammes, Frederik, Verstraete, Willy, Feijtel, Tom C J, and Schowanek, Diederik (2001a) Metal Decontamination of Soil, Sediment, and Sewage Sludge by means of Transition Metal Chelant [S,S]-EDDS *Journal of Environmental Engineering* **127**: 802-811

Vandevivere, Philippe C, Saveyn, Hans, Verstraete, Willy, Feijtel, Tom C J, and Schowanek, Diederik (2001b) Biodegradation of Metal-[S,S]-EDDS Complexes *Environmental Science and Technology* **35**: 1765-1770

von Stockar, Urs and van der Wielen, Luuk AM (1997) Thermodynamics in Biochemical Engineering *Journal of Biotechnology* **59**: 25-37

Wai, PPC and Bogle, I. D. L. (1996) Process Synthesis and Simulation Strategies for Integrated Biochemical Process Design *Computers & Chemical Engineering* **20**: S357-S362-

Waley.SG (1981) An easy method for the determination of initial rates *Biochemical Journal* **193**: 1009-1012

Walsh, Christopher (2001) Enabling the chemistry of life *Nature* **409**: 226-231

Weatherburn, M W (1967) Phenol-Hypochlorite Reaction for Determination of Ammonia *Analytical Chemistry* **39**: 971-974

Wehrli, Ernst and Egli, Thomas (1988) Morphology of Nitritotriacetate-Utilizing Bacteria *Systematic and Applied Microbiology* **10**: 306-312

Weilenmann, Hans-Ulrich, Engeli, Barbara, Bucheli-Witschel, Margarete, and Egli, Thomas (2004) Isolation and growth characteristics of an EDTA-degrading member of the α -subclass of *Proteobacteria* *Biodegradation* **15**: 289-301-

White D (1995) *The Physiology and Biochemistry of Prokaryotes*, 2nd edition. Oxford University Press, New York

Wilhoit, R C and Shiao, Daniel (1964) Thermochemistry of Biologically Important Compounds *Journal of Chemical and Engineering Data* **9**: 595-599

Willeman, Wouter F, Gerrits, Pieter J, Hanefeld, Ulf, Brussee, Johannes, Straathof, Adrie JJ, van der Gen, Arne, and Heijnen, Joseph J (2002a) Development of a Process Model to Describe the Synthesis of (R)-Mandelonitrile by *Prunus anygdulus*

HYdroxynitrile Lyase in an Aqueous-Organic Biphasic Reactor *Biotechnology and Bioengineering* **77**: 239-247

Willeman, Wouter F, Straathof, Adrie JJ, and Heijnen, JJ (2002b) Reaction temperature optimization procedure for the synthesis of (*R*)-mandelonitrile by *Prunus amygdalus* hydroxynitrile lase using a process model approach *Enzyme and Microbial Technology* **30**: 200-208

Wingren, Anders, Galbe, Mats, and Zacchi, Guido (2003) Techno-Economic Evaluation of Producing Ethanol from Softwood: Comparison of SSF and SHF and Identification of Bottlenecks *Biotechnology Progress* **19**: 1109-1117

Witschel, Margarete and Egli, Thomas (1998) Purification and characterisation of a lyase from the EDTA-degrading bacterial strain DSM 9103 that catalyses the splitting of [S,S]-ethylenediaminedisuccinate, a structural isomer of EDTA *Biodegradation* **8**: 419-428

Witschel, Margarete, Egli, Thomas, Zehnder, Alexander JB, Wehri, Ernst, and Spycher, Max (1999) Transport of EDTA into cells of the EDTA-degrading bacterial strain DSM 9103 *Microbiology* **145**: 973-983

Witschel, Margarete, Nagel, Samuel, and Egli, Thomas (1997) Identification and Characterization of the Two-Enzyme System Catalysing Oxidation of EDTA in the EDTA-Degrading Bacterial Strain DSM 9103 *Journal of Bacteriology* **179**: 6937-6943

Wittman, S, Schnabelrauch, M, Scherlitz-Hofmann, I, Möllmann, U, Ankel-Fuchs, D, and Heinisch, L (2002) New Synthetic Siderophores and Their β -Lactam Conjugates Based on Diamino Acids and Dipeptides *Bioorganic and Medicinal Chemistry* **10**: 1639-1670

Wolff, A, Zhu, L, Wong, YW, Straathof, Adrie JJ, Jongejan, JA, and Heijnen, JJ (1999) Understanding the Influence of Temperature Change and Cosolvent Addition on Conversion Rate of Enzymatic Suspension Reactions Based on Regime Analysis *Biotechnology and Bioengineering* **62**: 125-134

Woodley JM and Lilly MD (1994) Biotransformation Reactor Selection and Operation in *Applied Biocatalysis*, 1st edition. Harwood Academic Publishers GmbH, Chur pp371 - 393

Woodley, John M. and Titchener-Hooker, Nigel J. (1996) The use of windows of operation as a bioprocess design tool *Bioprocess Engineering* **14**: 263-268

Wouwer, Alain Vande and Bogaerts, Phillipe (2005) Special issue on bioprocess modelling and control *Bioprocess and Biosystems Engineering* **27**: 281-282

Wubbolts MG (2002) Addition of Amines to C = C Bonds in *Enzyme Catalysis in Organic Synthesis*, 2nd edition. Wiley-VCH, Weinheim pp866 - 872

Wubbolts, Marcel G., Favre-Bulle, Olivier, and Witholt, Bernard (1996) Biosynthesis of synthons in two-liquid-phase media *Biotechnology and Bioengineering* **52**: 301-307

Xun, Luying, Reeder, Robert B, Plymale, Andrew E, Girvin, Donald C, and Bolton, Harvey JR (1996) Degradation of Metal-Nitriloacetate Complexes by Nitriloacetate Monooxygenase *Environmental Science and Technology* **30**: 1752-1755

Yanofsky, Corey, Taylor, D G, and Thibault, Jules (2006) Novel Methodology for assessing a ranked Pareto domain: Drift group analysis *Chemical Engineering Science* **61**: 1308-1316

Zhou, Yuhong H., Holwill, I. L. J., and Titchener-Hooker, Nigel J. (1997) A Study of the use of computer simulations for the design of integrated downstream processes *Bioprocess Engineering* **16**: 367-374

Zhou, Yuhong H. and Titchener-Hooker, Nigel J. (2002) Visualizing Integrated Bioprocess Designs Through "Windows of Operation" *Biotechnology and Bioengineering* **65**: 550-557

Zimmermann, Vera, Beller, Matthias, and Kragl, Udo (2006) Modelling the Reaction Course of a Dynamic Kinetic Resolution of Amino Acid Derivatives: Identifying and Overcoming Bottlenecks *Organic Process Research & Development* **10**: 622-627

Zwicker, N, Theobald, U, Zähler, H, and Fiedler, H-P (1997) Optimisation of fermentation conditions for the production of ethylene-diamine-disuccinic acid by *Amycolatopsis orientalis* *Journal of Industrial Microbiology and Biotechnology* **19**: 280-285

10 APPENDICES

10.1 NUMERICAL METHODS FOR SOLUTION OF ODES

The Taylor Series (Equations 1-9 and 1-10) describes a way in which all continuous functions can be described in terms of an infinitely termed polynomial, but furthermore means that once a function is known potentially all the derivatives of that function are also known (Biran and Breiner, 2002). Where $R_n(x)$ is the remainder accounting for the remaining terms from n to infinity. The Taylor series provides a useful method whereby once a differential is known in addition to some initial condition, the value of the dependent variable can be determined and this therefore forms the basis of many algorithms suitable for application by computer to solve ODEs.

$$f(x) = \sum_{n=1}^{\infty} a_n (x - x_0)^n \quad \text{where} \quad a_n = \frac{1}{n!} f^{(n)}(x_0) \quad (1-9)$$

ie:

$$f(x) = f(x_0) + \frac{x - x_0}{1!} f'(x_0) + \frac{(x - x_0)^2}{2!} f''(x_0) + \frac{(x - x_0)^3}{3!} f'''(x_0) + \dots \\ + \frac{(x - x_0)^n}{n!} f^{(n)}(x_0) + R_n(x) \quad (1-10)$$

As the Taylor series is infinite there will always be a remainder term involved in the series which accounts for much of the deviation from the analytical result. In particular it is common for only the first few terms of the Taylor series to be employed in the calculation of some function of x from a derivative and this truncation of the series gives rise to a truncation error. Furthermore, if there are several x for which it is desired to find the dependent variable, there will be propagation errors created in the use of each new numerically derived x_0 to find the new x (Biran and Breiner, 2002). The use of computers also creates a further source of rounding error inherent in the rounding operation employed so numbers can fit into the allocated computer memory, these errors are then propagated through further iterations.

The forwards Euler Method uses the first two terms of the Taylor series (equation 1.16), where h is step size, corresponding to the $x-x_0$ term in equation 1.15 above and $f(x_i, y_i)$ is the derivative of some function evaluated at x_i and y_i .

$$y_{i+1} = y_i + f(x_i, y_i)h \quad (1.17)$$

The use of the Euler method creates an error term that can be quite large due to the truncation of the Taylor series, assuming as it does that the derivative at the beginning of the interval applies over the entire interval. This truncation error will be nonexistent for functions that are linear in x as there will be no second order derivative and therefore the forwards Euler Method provides an exact solution. However, for higher ordered equations this truncation error can be significant (Chapra and Canale, 2006). The method could be made more accurate by inclusion of higher-order terms. However, when the ODE in question is a function of dependent and independent variables the differentiation of the higher order terms can become unmanageable.

$$Er = \frac{h^2}{2!} f''(x_i, y_i) \quad \text{or} \quad Er = Oh^2 \quad (1.18)$$

As can be seen in equation 1-18, decreasing the step-size, h , will have a significant effect on the error (Er), however, decreasing step size comes with a cost, the increased step-size increases the calculation effort and for complex equations this may be expensive with a regard to processor time.

Heun's method or the Predictor-Corrector method, estimates the derivative at the beginning and end of the interval, taking an average of the two to predict the new value improving the estimation of the next step. Both the Heun and Euler methods are forms of Runge-Kutta Methods, which combine the accuracy of the Taylor series but mean the higher derivatives need not be calculated. Runge-Kutta methods essentially calculate several derivatives over the course of each step interval and calculate a weighted average. There are many variations of these Runge-Kutta methods, taking

derivatives at different points in each incremental step and/ or weighting them differently. Runge Kutta methods make use of an increment function $\phi(x_i, y_i, h)$ such that

$$y_{i+1} = y_i + \phi(x_i, y_i, h)h \quad (1.19)$$

$$\text{Where: } \phi = a_1k_1 + a_2k_2 + \dots + a_nk_n \quad (1.20)$$

And where a's are constants and k's are:

$$\begin{aligned} k_1 &= f(x_i, y_i) \\ k_2 &= f(x_i + p_1h, y_i + q_{11}k_1h) \\ k_3 &= f(x_i + p_2h, y_i + q_{21}k_1h + q_{22}k_2h) \\ &\cdot \\ &\cdot \\ &\cdot \\ k_n &= f(x_i + p_nh, y_i + q_{n-1,1}k_1h + q_{n-1,2}k_2h + \dots + q_{n-1,n-1}k_{n-1}h) \end{aligned} \quad (1.21)$$

The Euler method is essentially a one step RK method (ie 1st order) and the Heun method a 2nd order RK method (ie 2 step), which have global truncation errors of $O(h)$ and $O(h^2)$ respectively. The RK methods most commonly use are generally fourth order with global truncation errors equivalent to $O(h^4)$ (Chapra and Canale, 2006). Higher RK methods are even more accurate; however, this will require a trade-off against the computational expense required in the increased number of calculation steps. Some differential equations can show stiffness on solution by numerical means resulting in instability in the solution often seen as an oscillation. This occurs when there are often two very different scales of the independent variable over which dependent variables are changing, (Press *et al*, 1992) stiffness can be resolved by decreasing the step size of the integration, and therefore the error term, however, this then requires longer processing times (Moler, 2006). To solve stiff ODEs, implicit methods can be used in which the unknown appears on either side of the equation. The implicit or backwards Euler method evaluates the derivative at a future time whilst others have proposed implicit Runge-Kutta methods for higher order solutions (Press *et al*, 1992).

10.2 DETERMINATION OF ERRORS

Where number of samples prohibited triplicate samples throughout an experiment, triplicate samples were taken at three time points, usually at the beginning, middle and end of an experiment. Average (Equation 10.2-1) and standard deviation (Equation 10.2-2) were then calculated and hence coefficient of variance (Equation 10.2-3) was obtained. Where coefficient of variance was within 2% for all data sets, the coefficient of variance was applied to all data as a result of this often being related to sampling and analytical error, rather than experimental error.

$$\bar{x} = \frac{\sum x}{n} \quad (10.2-1)$$

$$\sigma = \sqrt{\frac{\sum(x - \bar{x})^2}{n-1}} \quad (10.2-2)$$

$$CV = \frac{\sigma}{\bar{x}} \times 100\% \quad (10.2-3)$$

Where \bar{x} represents the mean, x , a variable, n , number of observations, σ , standard deviation, CV, coefficient of variation

10.3 NCIMB CHARACTERISATION REPORT

CONFIDENTIAL

8th April 2003

Our Ref: NCSQ 18628
Your Ref: EG420950

Client: Helen Law
Advanced Centre for
Biochemical Engineering
University College London
Department of Biochemical
Engineering
Torrington Place
London
WC1E 7JE
United Kingdom

Isolate Codes: HL5 and HL17

Date Received: 20th March 2003

Methodology: 16S rDNA sequence analysis was carried out on these samples using NCIMB Ltd internal work instructions; WI-NC-68,105, 108, 134, 136 and 138

Identification Summary:

Isolate Code	Identification	% Similarity	Match
HL5	<i>Brevundimonas species</i>	97.58	genus
HL17	<i>Paracoccus species</i>	99.53	genus

Comments:

Searching the MicroSeq database did not give a genus level match for HL17 and therefore the sequence obtained for the isolate was searched against the EMBL database (Appendix 1). HL5 appears to most closely resemble *B.diminuta*, but some new species, formerly *Caulobacter*, are not yet on the MicroSeq database for comparison.

Ref:W.R.Abraham et al Int.J.Syst.Bact 1999, 49(3) 1053-1073

Responsible Scientist: Miss Nicola Ingram
Microbial Identification

Authorized and approved on behalf of NCIMB Ltd: *Al Baxter*

This report shall not be reproduced except in full, without the approval of NCIMB Ltd., and applies only to the isolates listed.
Furthermore, nothing in this report shall be taken to imply any endorsement by NCIMB Ltd as to the fitness for purpose of any product to which the report applies.

NCSQ 18628.doc

Page 1 of 4

NCIMB Ltd., 23 St Machar Drive, Aberdeen AB24 3RY, Scotland, UK
Tel: +44 (0) 1224 273332 Fax: +44 (0) 1224 272461 E-mail enquiries@ncimb.co.uk Website: http://www.ncimb.co.uk

Registered No. SCO 78368 Registered Office: 23 St Machar Drive, Aberdeen. NCIMB Limited



NCIMB
LIMITED

P R O V I D I N G T H E S O L U T I O N

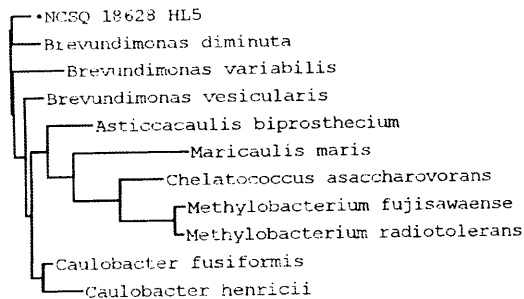


CONFIDENTIAL

HL5 TOP 20 HITS MicroSeq™ 500

Alignment: 413 •NCSQ 18628 HL5
2.42 % 471 Brevundimonas diminuta
2.66 % 471 Brevundimonas vesicularis
3.39 % 471 Caulobacter fusiformis
3.87 % 471 Brevundimonas variabilis
5.33 % 471 Caulobacter henricii
5.93 % 469 Asticcacaulis biprosthecium
10.41 % 471 Chelatococcus asaccharovorans
10.65 % 471 Maricaulis maris
10.90 % 471 Methylobacterium fujisawaense
10.90 % 471 Methylobacterium radiotolerans
10.90 % 469 Dichotomicrobium thermohalophilum
11.14 % 469 Prosthecomicrobium pneumaticum
11.86 % 469 Ochrobactrum anthropi
11.86 % 471 Aquaspirillum polymorphum
11.86 % 473 Methylobacterium zatmanii
12.11 % 471 Hyphomicrobium hollandicum
12.11 % 471 Methylobacterium mesophilicum
12.11 % 469 Xanthobacter flavus
12.11 % 471 Methylobacterium organophilum
12.35 % 473 Methylobacterium rhodinum

N Join: 6.081 %



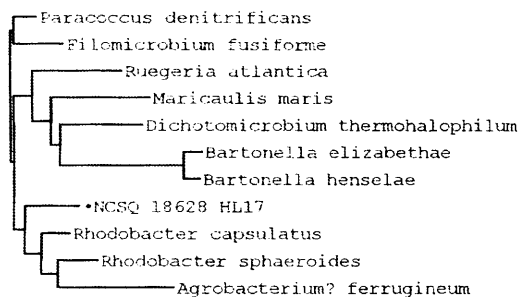
1111111223
0001122048
0474905143
•NCSQ 18628 HL5 A-GT-CAATG
Brevundimonas diminuta -TT-GGGGA

CONFIDENTIAL

HL17 TOP 20 HITS MicroSeq™ 500

Alignment: 427 •NCSQ 18628 HL17
4.22 % 471 Rhodobacter capsulatus
4.92 % 471 Paracoccus denitrificans
5.39 % 469 Filomicrobium fusiforme
6.32 % 471 Rhodobacter sphaeroides
9.13 % 469 Ruegeria atlantica
10.77 % 474 Bartonella elizabethae
11.01 % 471 Maricaulis maris
11.24 % 486 Agrobacterium? ferrugineum
11.24 % 469 Dichotomicrobium thermohalophilum
11.48 % 472 Bartonella henselae
11.48 % 472 Bartonella vinsonii vinsonii
11.48 % 469 Agrobacterium tumefaciens
11.48 % 469 Phyllobacterium myrsinacearum
11.59 % 469 Phyllobacterium rubiacearum
11.71 % 469 Labrys monachus
11.71 % 471 Aquaspirillum polymorphum
12.18 % 471 Methylobacterium radiotolerans
12.18 % 469 Agrobacterium rubi
12.18 % 469 Chelatobacter heintzii
12.18 % 469 Agrobacterium rhizogenes

N Join: 5.998 %



111111123334
458899334666712480
304534452129070825
•NCSQ 18628 HL17 TATACT-CTAGTATCTCG
Rhodobacter capsulatus GATTTTGTTCGAAAGGACCC

NCSQ 18628 doc

Page 3 of 4

CONFIDENTIAL

Appendix 1 Sequence alignment of Isolate HL17

>>EM_PRO:AB025189 AB025189.1 Paracoccus sp. MBIC4018 gen (1409 nt)
initn: 2101 initl: 1470 opt: 2105 Z-score: 965.9 bits: 189.5 E(): 9.1e-47
99.532% identity (99.765% ungapped) in 427 nt overlap (2-427:1-427)

```

      10      20      30      40      50      60
HL17, CGAACGCTGGCGGCAGGCCTAACACATGCAAGTCGAGCGAGATCTTCGGATCTAGCGGCG
      :
EM_PRO GAACGCTGGCGGCAGGCCTAACACATGCAAGTCGAGCGAGATTTTCGGATCTAGCGGCG
      10      20      30      40      50
      70      80      90     100     110     120
HL17, GACGGCTGAGTAACGCGTGGGAATATGCCCTTCTCTACGGAATAGCCCCGGGAAACTGGG
      :
EM_PRO GACGGCTGAGTAACGCGTGGGAATATGCCCTTCTCTACGGAATAGCCCCGGGAAACTGGG
      60      70      80      90     100     110
      130     140     150     160     170
HL17, AGTAATACCGTATCGCCCTTTGGGGGAAAGATTTATCGGAGAAGGATTAGCCCGGTTG
      :
EM_PRO AGTAATACCGTATACGCCCTTTGGGGGAAAGATTTATCGGAGAAGGATTAGCCCGGTTG
      120     130     140     150     160     170
      180     190     200     210     220     230
HL17, GATTAGGTAGTTGGTGGGGTAATGGCCTACCAAGCCTACGATCCATAGCTGGTTTGAGAG
      :
EM_PRO GATTAGGTAGTTGGTGGGGTAATGGCCTACCAAGCCTACGATCCATAGCTGGTTTGAGAG
```

10.4 χ^2 GOODNESS OF FIT TEST

Model hypotheses were tested by means of the χ^2 test for goodness of fit at a 5% significance level for the relevant number of degrees of freedom (df). The χ^2 statistic was calculated by Equation 10.4-1 and used with the number of degrees of freedom (Equation 10.4-2) to find the required test statistic from statistical tables (Rees, 2001). When the calculated χ^2 was less than the tabulated value, the null hypothesis (ie the model described the data) could not be rejected. It could therefore be inferred when tabulated test statistic was larger than calculated that the model did describe the observed experimental data for the data sets tested.

$$\chi^2 = \sum \frac{(O-E)^2}{E} \quad (10.4-1)$$

$$df = n - 1 \quad (10.4-2)$$

Where O is the observed value and E the expected value, ie O, experimental value, E, modelled value, df, degrees of freedom, n, number of observations.

10.5 CALCULATION OF MAXIMUM HEAT TRANSFER AREA

It was assumed that total annual tonnage was required to be 1000 tonnes, therefore producing a tonnage of 2.7 tonnes per day. At a minimum yield of 100 g.l⁻¹, this means a volume of 270 m³ working volume is required per day. It was decided to split this into 8 50m³ vessels, assumed to be 3m in diameter, 9m in height and with an impeller diameter of 1m (height: diameter ratio and diameter: impeller diameter ratio both of 3:1).

Calculation of film heat resistance in the reactor

$$Nu = 0.81 Re^{0.68} Pr^{0.34} = hD/\lambda \text{ (Coulson and Richardson, 1996)}$$

$$Re = \rho N d_i^2 / \mu = 1,600,000 \text{ (}\mu_{H_2O} = 1 \text{ cP} = 0.001 \text{ Nsm}^{-2}, \rho_{H_2O} = 1000 \text{ kgm}^{-3}\text{)}$$

$$Pr = C_p \mu / \lambda = 8.4 \text{ (}\lambda = 0.5 \text{ Wm}^{-1}\text{K}^{-1}\text{)}$$

$$\text{Therefore } Nu = 27640.2 \text{ and } \underline{h = 13820.1 \text{ W m}^{-2}\text{K}^{-1}}$$

Resistance to heat transfer (jacket assumed to be cooled with water, media assumed to be mainly aqueous with salts and vessel to be stainless steel)

$$\begin{aligned} 1/U &= 1/h_{\text{film rctr}} + 1/h_{\text{foul rctr}} + 1/h_{\text{wall}} + 1/h_{\text{foul jacket}} + 1/h_{\text{film kacet}} \\ &= 13820^{-1} + 0.2 \times 10^{-3} + 1.56 \times 10^{-4} + 0.1 \times 10^{-3} + 1 \times 10^{-3} = 1.428 \times 10^{-3} \text{ K m}^2 \text{ w}^{-1} \end{aligned}$$

$$\text{therefore } U = 700 \text{ Wm}^{-2} \text{ K}^{-1}$$

Calculation of heat load

$$dT/dt = -\Delta H_{rx} \times r_1 \times V / \Sigma NC_p_{H_2O} \text{ (values from Chapter 4 for 30°C)}$$

$$= (62 \text{ kJ/mol} \times r_1 \times V) / 4.2 \text{ kJ/kg K} = 15 \text{ K/mol}_{EDDS} \times r_1 \times V$$

So at 1 mol/l h, heat production = 861 kW and equivalent of 4.2 x 10⁻³ K/ s l

Calculation of reasonable area for heat transfer

Vessel jacket surface area assuming jacket to cover 5m of height = 47m², add 50 coils at 2.5m in diameter, pipe 5cm in diameter therefore surface area = 62 m² giving a total of 109 m².

Calculation of ability of heat transfer area to remove heat

Assume glycol can be used at -20°C, flowrate is 25 kg/s, 5K/s heat is removed

Exit temp of glycol for removal of 1000 kW work

$$\begin{aligned} Q = mC_p\Delta T \quad \text{therefore } T_x &= 1000 \text{ kW} / (25 \text{ kg/s} \times 4.2 \text{ kJ/kg K}) + 253 \text{ K} \\ &= 263 \text{ K} \end{aligned}$$

$$\text{LMTD} = 50\text{K}$$

Heat removal area required:

$$\begin{aligned} Q = hA\Delta T \quad \text{therefore } A &= 1000 \text{ kW} / 0.7 \text{ kW/m}^2 \text{ K} \times 50 \text{ K} \\ &= 28.6 \text{ m}^2 \end{aligned}$$

Therefore cooling area is more than sufficient to remove heat produced by exothermic production of 1 mol/l h S,S-EDDS (ie 292 g/l h)

10.6 SENSITIVITY ANALYSIS PROGRAMS

Programs were run using Matlab® 6.5 release 13 student version with the Symbolic Math Toolbox on a Dell Latitude C640 (Intel Pentium 4 1.70 GHz and 256 MB RAM) running Windows XP.

10.6.1 EDDSase Isothermal and Adiabatic Models

10.6.1.1 Constants

```
% EDDSCONSTANTS
%
% List of all constants for EDDS related models so same constants are used for all
% EDDS models and can be changed easily

% Temp and energy balance consts
R=0.0083145;      % Universal gas const - kJ/mol.K
Hpr=-1915;       % mid-point estimation of heat of formation of EDDS ions kJ/mol at
298K heat of soln based on fum and ed
Hdr=-94.79;      % Heat of formation of ED ions kJ/mol
Hfr=-848.1;      % Heat of formation of fumarate ions kJ/mol

% Rate constants
% Rxn1 - SM+F=P
A=42712407.08; %arrhenius const for kcat
EaR=-6476.6; %Ea/R const for kcat
kinactA=8.63276E+11; % arrhenius const for kinact – log makes v inaccurate
kinactEaR=-10455; % Ea/R const for kinact
G1=-8.49;        % gibbs free nrg edds rxn kJ/mol.K
kf1=0.063;
km1=0.102;
ki1=0.058;
kb1=0.0001;
a1=1;
b1=0.68;

% Rxn2 - RM+F=RP
%vm2=vm1;
%keq2=keq1;
kf2=kf1;
km2=km1;
ki2=ki1;
kb2=kb1;
a2=a1;
b2=b1;

% Rxn3 - F+D=SM
kf3=0.286; % Vm3 is in each program as it uses a polynomial function to model a3
kd3=0.549;
kb3=0.1;

% Rxn4 - F+D=(SM+RM)/2
A4=1.43e11;
```

```
EaR4=-10299.34;
```

```
% Rxn5 - F+H=MA
```

```
%am5=.00143; % am5 and vm5 are in individual progs as are functs of temp
```

```
kf5=0.051;
```

```
G5=-3.49; % gibbs free nrg edds rxn kJ/mol.K
```

10.6.1.2 Isothermal Model

```
function dy=eddst2(t,y,e1,e3,e5,T1);
```

```
% EDDST2
```

```
% This function describes EDDS kinetic rates
```

```
%
```

```
% Describes matrix y as a function of time t at varying initial temps
```

```
% assuming process is isothermal and well mixed
```

```
% y includes all species concs, temp is input arg
```

```
% Solver setup: (t,y)= solver(odefun,tspan,y0,options,e1,e3,e5,T1)
```

```
% Ensure F0 and either D0 or M0 initialised with values greater than 0, or answer
```

```
% is infinite and nonsense
```

```
%
```

```
% Enzs: e1=eddsase, e3=edmsase, e5=fumarase
```

```
% Species order: y=[F, SM, RM, D, RP, P, MA]
```

```
% Reaction order: 1:EDDSase, 2:RS-EDDS via EDDSase, 3:EDMSenz,
```

```
% 4:EDMSchem, 5:Fumarase
```

```
dy = zeros(7,1); % create vector dy Species order (F, SM, RM, D, RP, P, MA)
```

```
eddsconstants % loads edds related constants
```

```
% Temp and energy balance consts
```

```
% Rate constants
```

```
% Rxn1 - SM+F=P
```

```
am1=A*exp(EaR./T1); % calc of temp specific spec act
```

```
kinact=kinactA*exp(kinactEaR/T1); % calc of temp specific denat rate
```

```
vm1=e1*am1*exp(-kinact*60); % vmax calc from inact and arrhenius
```

```
keq1=exp(-G1./(R*T1)); % eqm const as a funct of temp
```

```
% Rxn2 - RM+F=RP
```

```
vm2=vm1;
```

```
keq2=keq1;
```

```
% Rxn3 - F+D=SM
```

```
if T1>=295;
```

```
am3=-0.10906+(6.76114e-4*T1)-(1.03799e-6*(T1^2));
```

```
else;
```

```
am3=0.0000001; % spec rate – nonsense when am3 is zero
```

```
end
```

```
%e3=100;
```

```
vm3=am3*e3;
```

```
keq3=1;
```

```
% not a function of temp as gibbs is zero and  
%relationship doesn't hold
```

```
% Rxn4 - F+D=(SM+RM)/2
```

```
k4=A4*exp((EaR4)./T1); % relationships here are in J/mol
```

```
keq4=keq3;
```

```

% Rxn5 - F+H=MA
am5=-0.09766+(6.71819e-4*T1)-(1.13706e-6*(T1^2)); %mol/gdcw.h
vm5=am5*e5;
keq5=exp(-G5./(R*T1));          % eqm const as a funct of temp
kb5=kf5*keq5;

%Species order
%1: F = y(1) %2: SM = y(2) %3: RM = y(3) %4: D = y(4)
%5: RP = y(5) %6: P = y(6) %7: MA = y(7) %8: T=y(8)

% reaction eqns
r1=((vm1*(y(2)-(y(6)./(keq1*y(1)))))./(((km1*a1)*((kf1./y(1))+1+(kf1./ki1)+(y(1)./(...
(b1*ki1)+(kf1*y(6)./(kb1*y(1)))))+(y(2)*(((a1*kf1)./y(1))+1)))));
r2=((vm2*(y(3)-(y(5)./(keq2*y(1)))))./(((km2*a2)*((kf2./y(1))+1+(kf2./ki2)+(y(1)./(...
(b2*ki2)+(kf2*y(5)./(kb2*y(1)))))+(y(3)*(((a2*kf2)./y(1))+1)))));
r3=((vm3*((y(1)*y(4))-(y(2)./keq3)))./(((kf3*kd3)*(1+(y(2)./kb3)))+(y(1)*kd3)+...
(y(4)*kf3)+(y(1)*y(4))));
r4=((k4*y(1)*(y(4)^0.4))-((k4./keq4)*(y(2)+y(3))));
r5=((vm5*y(1))-((vm5./keq5)*y(7)))./(((kf5+y(1))+((kf5./kb5)*(y(7))))));

% net rates
dy(1)=-r1-r2-r3-r4-r5;
dy(2)=-r1+r3+r4;
dy(3)=-r2+r4;
dy(4)=-r3-r4;
dy(5)=r2;
dy(6)=r1;
dy(7)=r5;

```

10.6.1.3 Adiabatic Model

```

function dy=eddst(t,y,e1,e3,e5);
% EDDST
% This function describes EDDS kinetic rates and unsteady state temp
% variation
%
% Describes matrix y as a function of time t at varying initial temps
% assuming process is adiabatic and well mixed -
% y includes all species concs, temp is part of matrix y
% Solver setup: (t,y)= solver(odefun,tspan,y0,options,e1,e3,e5)
% Ensure enzyme is initialised with values greater than 0, or answer
% is infinite and nonsense
%
% Enzs: e1=eddsase, e3=edmsase, e5=fumarase
% Species order: y=[F, SM, RM, D, RP, P, MA, T1]
% Reaction order: 1:EDDSase, 2:RS-EDDS via EDDSase, 3:EDMSenz,
% 4:EDMSchem, 5:Fumarase% function describes matrix y (ie matrix of all
% species concs) computed at time t

dy = zeros(8,1);          % create vector dy Species order (F, SM, RM, D, RP, P, MA, T)

eddsconstants

% temp related reaction constants not in eddsconstants.m
% Rxn3 - F+D=SM
if y(8)>=295;

```

```

am3=-0.10906+(6.76114e-4*y(8))-(1.03799e-6*(y(8)^2));
else;
    am3=0.0000001;
end
vm3=am3*e3;
keq3=1;
keq4=keq3;

% Rxn5 - F+H=MA
%am5=.00143;
am5=-0.09766+(6.71819e-4*y(8))-(1.13706e-6*(y(8)^2)); %mol/gdcw.h
vm5=am5*e5;

%Species order
%1: F = y(1) %2: SM = y(2) %3: RM = y(3) %4: D = y(4)
%5: RP = y(5) %6: P = y(6) %7: MA = y(7) %8: T=y(8)
% rxn order
% 1: SS 2: RS 3: SM 4: SM+RM 5: MA 6: temp

% reaction eqns
if y(8)>=350;
    return
elseif y(1)<0
    y(1)=0.000000001; % control loop ensuring no -ve concs as it can't handle them
elseif y(2)<0
    y(2)=0.000000001;
elseif y(3)<0
    y(3)=0.000000001;
elseif y(4)<0
    y(4)=0.000000001;
elseif y(5)<0
    y(5)=0.000000001;
elseif y(6)<0
    y(6)=0.000000001;
elseif y(7)<0
    y(7)=0.000000001;
else
r1=(((e1*exp((kinactA*exp(kinactEaR./y(8)))^60)*A*exp(EaR./y(8)))*(y(2)-(y(6))./...
((exp(-G1./R.*y(8))))*y(1)))))./(((km1*a1)*((kf1./y(1))+1+(kf1./ki1)+(y(1))./...
(b1*ki1)+(kf1*y(6))./(kb1*y(1)))))+(y(2)*((a1*kf1)./y(1))+1));
r2=(((e1*exp((kinactA*exp(kinactEaR./y(8)))^60)*A*exp(EaR./y(8)))*(y(3)-(y(5))./...
((exp(-G1./R.*y(8))))*y(1)))))./(((km2*a2)*((kf2./y(1))+1+(kf2./ki2)+(y(1))./...
(b2*ki2)+(kf2*y(5))./(kb2*y(1)))))+(y(3)*((a2*kf2)./y(1))+1));
r3=((vm3*(y(1)*y(4)-(y(2))./keq3))./(((kf3*kd3)*(1+(y(2))./kb3)))+(y(1)*kd3)+(...
y(4)*kf3)+(y(1)*y(4)));
r4=(((A4*exp((EaR4)./y(8)))*y(1)*(y(4)^0.4))-(((A4*exp((EaR4)./y(8)))/keq4)*...
(y(2)+y(3))));
r5=(((vm5*y(1))-((vm5./exp(G5./R.*y(8))))*y(7)))./((kf5+y(1))+((kf5./kf5*(exp(G5./...
(R.*y(8)))))*y(7))));

%energy balance 1 litre basis Cp edms based on heat cap of struct similar l-asp -
missing
% one aminogroup and 2 c moieties cps in kj/mol.K
% heat of rxn is overall ed + 2fum to edds, and kJ/mol
% spec heat cap of rxn mixture includes edms assuming L-asp
% heat formation Edds based on average heat of solution being approx 35 kJ/mol
Hrx=(Hpr./2)-(Hdr./2)-(Hfr)+(((0.165.*(y(8)-298.15)^2))-0.117.*(y(8)-298.15));

```



```
Cpsoln=((55.5.*((0.0184*y(8))+65.936))+y(1).*((0.3846*y(8))+27.635))+y(4).*...
((0.1633*y(8))+127.31))+((y(6)+y(7)).*((1.6019*y(8))-80.433))+((y(2)+y(3)).*...
((0.4287*y(8))+27.182)))/1000;
```

```
% net rates
dy(1)=-r1-r2-r3-r4-r5;
dy(2)=-r1+r3+r4;
dy(3)=-r2+r4;
dy(4)=-r3-r4;
dy(5)=r2;
dy(6)=r1;
dy(7)=r5;
dy(8)=(-Hrx.*(r1+r2))./Cpsoln;
end
```

10.6.2 EDDSase-Process Variable-Metric Surfaces

```
% EDDSSSENS2
%
% Plots EDDSase/EDMSase/metric meshes Sets up ode solver edds kinetic model
% Refers to EDDST2.m
%
% Form of init cond matrix = [F0 SM0 RM0 D0 RP0 P0 MA0] Odesolver syntax =
% [T, Y] = solver(odefun,tspan,y0,options,e1,e3,e5,T1) Recommend stiff
% solver, gets stuck occasionally
```

```
F0=.25;
SM0=0;
RM0=0;
D0=.1;
RP0=0;
P0=0;
MA0=0;
e1a=1:30:2100;
e3b=(1:30:2100);
e5=140;
T1=303;
```

```
% create metric matrices u=init rate, v=EDDSf, x=% purity, z=enzeff (ie
% EDDSF/e1)
q=ones(70,70);
p=ones(70,70);
u=ones(70,70);
v=ones(70,70);
x=ones(70,70);
z=ones(70,70);
```

```
b=1;
while b<=70;
    e3=e3b(b,1); % for each e3
    for a=1:70;
        e1=e1a(1,a); % for each e1
        [t,y]=ode23s(@eddst2,[0:12],[F0 SM0 RM0 D0 RP0 P0 MA0],[],e1,e3,e5,T1);
        w=diff(y); % get grads
        p(b,a)=(y(12,6))./12)*292; %overall rate
        q(b,a)=(y(12,6)*292)./((y(12,6)+y(12,5))*292)).*100; %ee
```

```

u(b,a)=w(2,6)*292; %max rate
v(b,a)=(y(12,6)./(y(1,1)./2)).*100; % yield
x(b,a)=((y(12,6)*292)./((y(12,6)*292)+(y(12,5)*292)+(y(12,3)*176)...
+(y(12,2)*176))).*100; %purity
z(b,a)=(y(12,6)*292)./e1; % g/g
end
b1=b+1;
b=b1
end

```

```

%Species order
%1:F=y(1) 2:SM=y(2) 3:RM=y(3) 4:D=y(4) 5:RP=y(5) 6:P=y(6) 7:MA=y(7)

```

```

% mesh metrics against e1 and e3

```

```

Figure

```

```

subplot(3,2,1);
mesh(e1a,e3b,u)
axis([0 2500 0 2500 0 20])
xlabel('Max rate g.l-1.h-1','Fontweight','bold')

```

```

subplot(3,2,2);
mesh(e1a,e3b,p)
axis([0 2500 0 2500 0 5])
xlabel('Overall rate g.l-1.h-1','Fontweight','bold')

```

```

subplot(3,2,3);
mesh(e1a,e3b,v)
axis([0 2500 0 2500 0 30])
xlabel('Yield %','Fontweight','bold')

```

```

subplot(3,2,4);
mesh(e1a,e3b,q)
axis([0 2500 0 2500 0 100])
xlabel('ee %','Fontweight','bold')

```

```

subplot(3,2,5);
mesh(e1a,e3b,z)
axis([0 2500 0 2500 0 50])
xlabel('EDDSase','Fontweight','bold')
ylabel('EDMSase','Fontweight','bold')
xlabel('\eta','Fontweight','bold')

```

```

subplot(3,2,6);
mesh(e1a,e3b,x)
axis([0 2500 0 2500 0 100])
xlabel('EDDSase','Fontweight','bold')
ylabel('EDMSase','Fontweight','bold')
xlabel('Purity %','Fontweight','bold')

```

10.6.3 Window Construction

```

% EDDSPRETTYPLOT1
% Plots constraint/lim window based on EDDSase and EDMSase axes
%
% Uses metric matrices from EDDSSSENS2.m and employs searches to
% find points at which metric hurdles are overcome. Can be varied

```

```

% by initial concs as these will affect rate. Polynomials or splines are
% then fitted to produce smooth lines
%
% Reaction kinetics modelled by EDDST2.m - isothermal assumption
% Constants held by EDDSCONSTANTS.m

```

```
clear
```

```

% run eddssens2 for the chosen conditions - will be a function of
% EDi and Fumi

```

```

F0=input('Initial [Fumarate]:')
D0=input('Initial [ED]:')
T1=input('Reaction Temperature:')
SM0=0;
RM0=0;
RP0=0;
P0=0;
MA0=0;
e1a=1:20:2001;
e3b=(1:20:2001);
e5=0;

```

```

% create metric matrices u=init rate, v=EDDSf, x=% purity,
% z=enzeff (ie EDDSF/e1), q=ee%, p=overall rate

```

```

q=ones(101,101);
p=ones(101,101);
u=ones(101,101);
v=ones(101,101);
x=ones(101,101);
z=ones(101,101);

```

```
b=1;
```

```
while b<=101;
```

```
    e3=e3b(b,1); % for each e3
```

```
    for a=1:101;
```

```
        e1=e1a(1,a); % for each e1
```

```
        [t,y]=ode23s(@eddst2,[0:12],[F0 SM0 RM0 D0 RP0 P0 MA0],[,],e1,e3,e5,T1);
```

```
        w=diff(y); % get grads
```

```
        p(b,a)=(y(13,6)/12)*292; %overall rate
```

```
        q(b,a)=((y(13,6)*292)/((y(13,6)+y(13,5))*292)).*100; %ee
```

```
        u(b,a)=w(2,6)*292; %init rate
```

```
        v(b,a)=(y(13,6))*292; % eddsf
```

```
        x(b,a)=((y(13,6)*292)/((y(13,6)*292)+(y(13,5)*292)+(y(13,3)*176)+...
```

```
            (y(13,2)*176))).*100; %purity
```

```
        z(b,a)=(y(13,6)*292)/e1; % g/g
```

```
    end
```

```
    b1=b+1;
```

```
    b=b1
```

```
end
```

```
save eddsprettyp1.mat
```

```
% Create min rate hurdle line
```

```
minrate=input('Minimum overall rate g/l.h? (suggested: 8.3 g/l.h - equiv of 100g/l in 12 h):')
```

```
minrate1=minrate-.5; % need leeway or will miss point all together
```

```
minrate2=minrate+.5;
```

```
rate=[0 0];
```

```

c=1;
b=1;
while b<=101;
    for a=1:101;
        if minrate1<=p(b,a)
            if p(b,a)<=minrate2
                rate(c,1)=e1a(1,a); %eddsase
                rate(c,2)=e3b(b,1); %edmsase
                c1=c+1;
                c=c1
                break % only first point found - higher pts are subst lim
            break
        else
            end
        else
            end
        end
    end
    b1=b+1;
    b=b1
end
if sum(rate,2)==0; % fill axes with patch if no rate greater than min
    yy=zeros(size(e3b));
    patchratex=[0 2000 2000 0];
    patchratey=[0 0 2000 2000];
else
    d1=sortrows(rate,[1]); % sort into ascending by e3b - 2 values of e1a causes probs
with regression
    yy=spline(d1(:,2),d1(:,1),e3b); %e3b is x value here - make sure you turn it around!
    patchratex=[yy' 0 0 2000];
    patchratey=[e3b' 2000 0 0];
end

maxrate=input('Maximum initl rate g/l.h? (suggested: 14.6 g/l.h - equiv of heat rate 7.5
K/l.h):')
maxrate1=maxrate-.5; % leeway
maxrate2=maxrate+.5;
mrate=[0 0];
c=1;
b=1;
while b<=101;
    for a=1:101;
        if maxrate1<=u(b,a)
            if u(b,a)<=maxrate2
                mrate(c,1)=e1a(1,a); %eddsase
                mrate(c,2)=e3b(b,1); %edmsase
                c1=c+1;
                c=c1
                break % only first point found - higher pts are subst lim
            break
        else
            end
        else
            end
        end
    end
    b1=b+1;
    b=b1
end
end

```

```

if sum(mrate,2)==0; % fill axes if rates are all too high
    yy2=zeros(size(e3b));
    patchmratex=[0 0 0 0];
    patchmratey=[0 0 0 0];
else
    d2=sortrows(mrate,[1]); % sort into ascending by e1a
    yy2=spline(d2(:,2),d2(:,1),e3b); %e3b is x value here - make sure you turn it around!
    patchmratex=[yy2' 2000];
    patchmratey=[e3b' 2000];
end

% create edms limitation line, find max rate and corresponding
% edmsase concentration for each eddsase conc - stopping after
% 100 gdcw/l as this is reactant limited and extrapolate
c=1;
d=diff(u,1,2);
for b=1:11;
    a=2;
    while a<=100;
        if d(b,a)<.05
            lim(c,1)=e1a(1,a);
            lim(c,2)=e3b(b,1);
            c1=c+1;
            c=c1
            break
            break
        else
            end
            a1=a+1;
            a=a1;
        end
    end
end
p1=polyfit(lim(:,1),lim(:,2),1); % linear regression
limline=polyval(p1,e1a); % points for linear regression line
patchlimx=[e1a 2000 0];
patchlimy=[limline 0 0];

% create ee line
minee=input('Minimum ee%? (suggested 99%):')
ee=[0 0];
c=1;
for a=1:101;
    b=1;
    while b<=101;
        if q(b,a)>=minee;
            ee(c,1)=e1a(1,a);
            ee(c,2)=e3b(b,1);
            c1=c+1;
            c=c1
            break
            break
        else
            end
            b1=b+1;
            b=b1;
        end
    end
end
end

```

```

if sum(ee,2)==0;
    eeline=zeros(size(e1a))*3;
    patcheex=[0 2000 2000 0];
    patcheey=[0 0 2000 2000];
else
p2=polyfit(ee(:,1),ee(:,2),1); % linear regression for ee
eeline=polyval(p2,e1a); % points for linear regression line
patcheex=[e1a 2000 0];
patcheey=[eeline 0 0];
end

% create purity line
minpur=input('Minimum purity%? (suggested 95%):')
minpur1=minpur-.1;
minpur2=minpur+.1;
pur=[0 0];
c=1;
b=1;
while b<=101;
    for a=1:101;
        if minpur1<=x(b,a)
            if x(b,a)<=minpur2
                pur(c,1)=e1a(1,a); %eddsase
                pur(c,2)=e3b(b,1); %edmsase
                c1=c+1;
                c=c1 % no break want curve
            else
                end
            else
                end
        end
        b1=b+1;
        b=b1
    end
end
if sum(pur,2)==0;
    purline=zeros(size(e3b));
    patchpurx=[0 2000 2000 0];
    patchpury=[0 0 2000 2000];
else
    d3=sortrows(pur,[2]);% sort into ascending by e1a - 2 values of e1a causes probs
with regression
    d4=sortrows(pur,[1]);
    p3=polyfit(d3(:,2),d3(:,1),2); % quadratic regression for ee
    purline=polyval(p3,e3b); % points for quadratic regression line
    patchpurx=[purline' 2000 0 0 2000];
    patchpury=[e3b' 2000 2000 0 0];
end

```

Figure

```

subplot(2,1,1);
plot(yy,e3b,e1a,limline,e1a,eeline,purline,e3b,yy2,e3b)
axis([0 2000 0 2000])
xlabel('EDDSase gdcw/l')
ylabel('EDMSase gdcw/l')
legend('minimum rate','EDMSase limitation','ee','purity','Max rate')
title(['EDDSase vs EDMSase limitations with [Fumarate]_0= ',num2str(F0),' ', [ED]_0= ',
num2str(D0),' T1=',num2str(T1)])

```

```

subplot(2,1,2);
plot(yy,e3b,e1a,limline,e1a,eeline,purline,e3b,yy2,e3b)
axis([0 2000 0 2000])
xlabel('EDDSase gdcw/l')
ylabel('EDMSase gdcw/l')
patch(patchlimx,patchlimy,'g') % edms lim patch
patch(patchpurx,patchpury,'c') % purity lim patch
patch(patchratex,patchratey,'b') % rate lim patch
patch(patchmratex,patchmratey,'m') % max rate lim patch
patch(patcheex,patcheey,'r') % ee lim patch

```

Figure

```

plot(yy,e3b,e1a,limline,e1a,eeline,purline,e3b,yy2,e3b)
axis([0 2000 0 2000])
xlabel('EDDSase gdcw/l','FontSize',14)
ylabel('EDMSase gdcw/l','FontSize',14)
title(['[Fumarate]_0= ',num2str(F0),', [ED]_0= ', num2str(D0),',
T1=',num2str(T1)],'FontSize',14)
patch(patchmratex,patchmratey,'m') % max rate lim patch
patch(patchpurx,patchpury,'c') % purity lim patch
patch(patchlimx,patchlimy,'g') % edms lim patch
patch(patchratex,patchratey,'b') % rate lim patch
patch(patcheex,patcheey,'r') % ee lim patch

```